PB86-238466

BEHAVIOR OF PILES AND PILE GROUPS UNDER LATERAL LOAD

Research, Development, and Technology

Turner-Fairbank Highway Research Center
6300 Georgetown Pike
McLean, Virginia 22101

U.S. Department of Transportation

Federal Highway Administration

Report No.
FHWA/RD-85/106

Final Report
March 1986

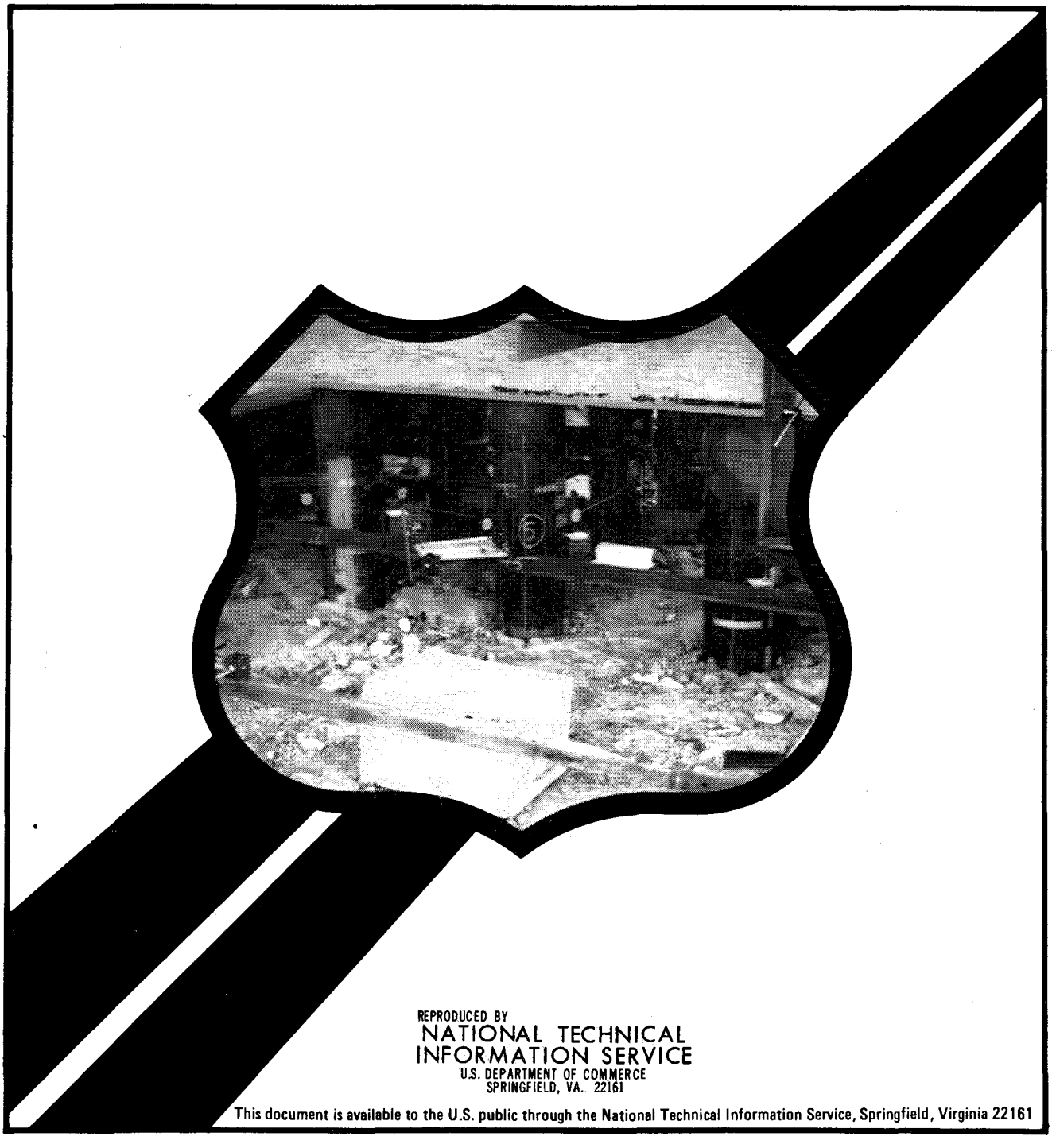

FOREWORD

This report details and describes design procedures for piles subjected to lateral loads. It will be of interest to geotechnical and bridge engineers.

This report presents the results of the University of Texas, research project, "Behavior of Piles and Pile Groups Under Lateral Load." The program was conducted for the Federal Highway Administration, Office of Engineering and Highway Operations Research and Development, Washington, D.C., under Interagency agreement DTFH61-84-Y-30005. This final report covers the period of research and development from September 28, 1982, to May 1, 1983.

Sufficient copies of the report are being distributed by FHWA Bulletin to provide a minimum of two copies to each FHWA regional office, two copies to each FHWA division, and two copies to each State highway agency. Direct distribution is being made to the division offices.

Richard E. Hay, Director
Office of Engineering
and Highway Operations
Research and Development

NOTICE

This document is disseminated under the sponsorship of the Department of Transportation in the interest of information exchange. The United States Government assumes no liability for its contents or use thereof. The contents of this report reflect the views of the contractor, who is responsible for the accuracy of the data presented herein. The contents do not necessarily reflect the official policy of the Department of Transportation. This report does not constitute a standard, specification, or regulation.

The United States Government does not endorse products or manufacturers. Trade or manufacturers' names appear herein only because they are considered essential to the object of this document.

Technical Report Documentation Page

1. Report No.	2. Government Accession No.	3. Recipient's Catalog No.
FHWA/RD-85/106		

4. Title and Subtitle	5. Report Date
Behavior of Piles and Pile Groups Under Lateral Load	March 1986
	6. Performing Organization Code
	8. Performing Organization Report No.
7. Author(s)	
L. C. Reese	
9. Performing Organization Name and Address	10. Work Unit No. (TRAIS)
The University of Texas at Austin College of Engineering Bureau of Engineering Research Austin, Texas 78712	FCP 35P2-192
	11. Contract or Grant No.
	DTFH61-84-Y-30005
	13. Type of Report and Period Covered
12. Sponsoring Agency Name and Address	Final Report Aug. 1983 - Dec. 1983
Federal Highway Administration Office of Engineering & Highway Operations Research and Development Washington, D.C. 20590	14. Sponsoring Agency Code
	CME/0158

15. Supplementary Notes

FHWA Contract Manager: Carl D. Ealy (HNR-30)

16. Abstract

Several methods of analysis and design of piles under lateral loading are in use. Presumptive values that suggest allowable loads, but very conservative ones, are included in some manuals of practice. Batter piles may be employed with an assumption, not entirely correct, that no lateral load is taken by vertical piles. Several rational methods, in which the equations of mechanics are satisfied, have been proposed. The methods of Broms and of Poulos and his coworkers are reviewed.

The rational method utilizes different equations to solve the governing differential equation along with the use of nonlinear curves to describe the soil response. Curves showing soil resistance p as a function of pile deflection y have been recommended for several types of soil and pile loading.

Case studies are presented where results from analysis are compared with those from experiment. Design recommendations are made and needed research is outlined.

17. Key Words	18. Distribution Statement
Piles, lateral loading, analysis, design soil response p-y curves, deflection, bending, group effects, static loading, cyclic loading, difference-equation methods, nondimensional curves	No restrictions. This document is available to the public through the National Technical Information Service, Springfield, VA 22161

19. Security Classif. (of this report)	20. Security Classif. (of this page)	21. No. of Pages	22. Price
Unclassified	Unclassified	311	

Form DOT F 1700.7 (8-72) Reproduction of completed page authorized

METRIC CONVERSION FACTORS

APPROXIMATE CONVERSIONS FROM METRIC MEASURES

SYMBOL	WHEN YOU KNOW	MULTIPLY BY	TO FIND	SYMBOL
	LENGTH			
in	inches	2.5	centimeters	cm
ft	feet	30	centimeters	cm
yd	yards	0.9	meters	m
mi	miles	1.6	kilometers	km
	AREA			
in^2	square inches	6.5	square centimeters	cm^2
ft^2	square feet	0.09	square meters	m^2
yd^2	square yards	0.6	square meters	m^2
mi^2	square miles	2.6	square kilometers	km^2
	acres	0.4	hectares	ha
	MASS (weight)			
oz	ounces	28	grams	g
lb	pounds	0.45	kilograms	kg
	short tons(2000lb)	0.9	tonnes	t
	VOLUME			
tsp	teaspoons	5	milliliters	ml
tbsp	tablespoons	15	milliliters	ml
fl oz	fluid ounces	30	milliliters	ml
c	cups	0.24	liters	l
pt	pints	0.47	liters	l
qt	quarts	0.95	liters	l
gal	gallons	3.8	liters	l
ft^3	cubic feet	0.03	cubic meters	m^3
yd^3	cubic yards	0.76	cubic meters	m^3
	TEMPERATURE (exact)			
°F	Fahrenheit temperature	5/9 (after subtracting 32)	Celsius temperature	°C

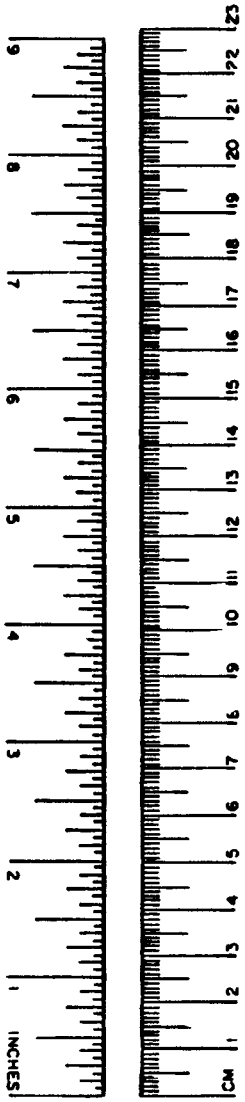

APPROXIMATE CONVERSIONS FROM METRIC MEASURES

SYMBOL	WHEN YOU KNOW	MULTIPLY BY	TO FIND	SYMBOL
	LENGTH			
mm	millimeters	0.04	inches	in
cm	centimeters	0.4	inches	in
m	meters	3.3	feet	ft
m	meters	1.1	yards	yd
km	kilometers	0.6	miles	mi
	AREA			
cm^2	square centimeters	0.16	square inches	in^2
m^2	square meters	1.2	square yards	yd^2
km^2	square kilometers	0.4	square miles	mi^2
ha	hectares(10,000m^2)	2.5	acres	
	MASS (weight)			
g	grams	0.035	ounces	oz
kg	kilograms	2.2	pounds	lb
t	tonnes (1000kg)	1.1	short tons	
	VOLUME			
ml	milliliters	8.03	fluid ounces	fl oz
l	liters	2.1	pints	pt
l	liters	1.06	quarts	qt
l	liters	0.26	gallons	gal
m^3	cubic meters	36	cubic feet	ft^3
m^3	cubic meters	1.3	cubic yards	yd^3
	TEMPERATURE (exact)			
°C	Celsius temperature	9/5 (then add 32)	Fahrenheit temperature	°F

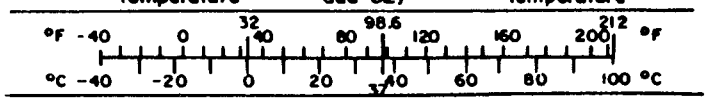

PREFACE

In 1977, the Implementation Division of the Federal Highway Administration sponsored the writer and colleagues in the preparation of a two-volume work entitled, "Design Manual for Drilled Shafts." Volume 2 of that work presented design procedures for drilled shafts subjected to lateral loads. This present volume, a manual for highway engineers, is related to piles and drilled shafts and updates and enlarges on the 1977 work. This manual is sponsored by the Research Division of the Federal Highway Administration.

The objectives of the manual are to present background material, design procedures, and methods of verifying computations for deep foundations under lateral load. Emphasis is placed on the use of nonlinear curves for soil response and the use of numerical procedures to solve the governing differential equation. An Executive Summary of this work includes recommendations for further research and the means of carrying out that research.

A companion work is under preparation for the Implementation Division of FHWA and is entitled, "Handbook on Design of Piles and Drilled Shafts under Lateral Load." A draft of that work was employed in two two-day workshops, the first in Austin, Texas in June, 1983, and the second in Albany, New York in July, 1983.

TABLE OF CONTENTS

TABLE OF CONTENTS (continued)

TABLE OF CONTENTS (continued)

TABLE OF CONTENTS (continued)

TABLE OF CONTENTS (continued)

TABLE OF CONTENTS (continued)

Note: Appendixes are available upon request from Materials Division, Office of Engineering and Highway Operations Research and Development, 6300 Georgetown Pike, McLean, Virginia 22101

LIST OF FIGURES

LIST OF FIGURES (continued)

LIST OF FIGURES (continued)

LIST OF FIGURES (continued)

LIST OF FIGURES (continued)

LIST OF FIGURES (continued)

LIST OF FIGURES (continued)

LIST OF FIGURES (continued)

LIST OF FIGURES (continued)

LIST OF FIGURES (continued)

LIST OF FIGURES (continued)

LIST OF TABLES

LIST OF TABLES (continued)

LIST OF TABLES (continued)

LIST OF TABLES (continued)

LIST OF NOTATIONS

a_i	horizontal coordinate of global axis system in pile group analysis
a_y, a_s, a_m, a_v, a_p	nondimensional coefficients, same as A-coefficient except for rigid-pile theory
A	coefficient used to define the shape of the p-y curve, unified criteria for clay
A_c	empirical coefficient used in equations for p-y curves for stiff clays below water surface, cyclic loading
A_s	empirical coefficient used in equations for p-y curves for stiff clays below water surface, static loading
A_y, A_s, A_m, A_v, A_p	nondimensional coefficients in elastic-pile theory relating to an applied force P_t, for deflection, slope, moment, shear and soil reaction, respectively
$\overline{A}_c$	empirical coefficient used in equations for p-y curves for sand, cyclic loading
$\overline{A}_s$	empirical coefficient used in equations for p-y curves for sand, static loading
A_o, A_1, ...A_m	coefficients in solutions for the difference equation method
A_{1t}	deflection coefficient for long pile with pile top restrained against rotation
A_1, B_1, C_1, D_1	nondimensional coefficients for piles of infinite length and finite length, constant pile stiffness, constant soil stiffness, no axial loading
b	pile diameter or width of foundation (L)
b_i	vertical coordinate of global axis system in pile group analysis (L)
b_y, b_s, b_m, b_v, b_p	nondimensional coefficients same as B-coefficients, except for rigid-pile theory
b_1,b_2,...b_5	coefficients in solutions for the difference equation method
B_c	empirical coefficient used in equations for p-y curves for sand, cyclic loading

B_s	empirical coefficient used in equations for p-y curves for sand, static loading
B_y, B_s, B_m, B_v, B_p	nondimensional coefficients in elastic-pile theory relating to an applied moment M_t for deflection, slope, moment, shear and soil reaction, respectively
B_o, B_1, ...B_m	coefficients in solutions for the difference equation method
c	undrained shear strength (F/L^2)
c_a	average undrained strength of clay from ground surface to depth (F/L^2)
c_{avg}	average undrained shear strength (F/L^2)
$\overline{C}$	coefficient related to stress level used in p-y curves for stiff clay above water surface
$\overline{C}_1$, $\overline{C}_2$, $\overline{C}_3$, $\overline{C}_4$	coefficient to be determined by use of boundary conditions for case of constant pile stiffness and constant soil stiffness, no axial loading
C	coefficient used in equations for p-y curves for sand
C_y	nondimensional deflection coefficient assuming $E_s = k_c$
C_1^*, C_2^*, C_3^*	coefficients in solutions for the difference equation method
D_E	degradation parameters for soil modulus
D_p	degradation parameters for yield pressure
D_R	rate factor
e	eccentricity of lateral load
e	Napierian base
E	Young's modulus (F/L^2)
E	term used in difference equation solution
E_{cp}	soil modulus after cyclic loading (F/L^2)
E_s	soil modulus (secant to p-y curve)(F/L^2)

E_{si} or $E_{s(max)}$	initial or maximum soil modulus (F/L^2)
E_{sm}	soil modulus at node m (F/L^2)
E_{sP}	soil modulus (values suggested by Poulos) (F/L^2)
EI_c	pile stiffness of combined pile and jacket leg (F/L^2)
EI	flexural rigidity of pile (F/L^2)
E_M	the Menard modulus of deformation (F/L^2)
f	parameter in Broms method for computing pile load (L)
f_b	bending stress on pile (F/L^2)
F	coefficient used to define deterioration of soil resistance at large deformations, unified criteria for clay, static loading
F_{h_i}	horizontal component of force on any "i-th" pile (F)
F_{mt}	moment coefficient at top of pile for fixed-head case
F_p	force against a pile in clay from wedge of soil (F)
F_p	rate coefficient (limited data suggest a range of from 0.05 - 0.3)
F_{pt}	force against a pile in sand from a wedge of soil (F)
F_{v_i}	vertical component of force on any "i-th" pile (F)
F_y	deflection coefficient for fixed head pile
g	parameter in Broms method for computing pile load (L)
G_m	shear modulus from pressuremeter (F/L^2)
G_1, G_2, G_3, G_4	terms used in difference equation solution
h	$= \frac{X}{L}$, depth coefficient in rigid-pile theory

h	increment length in difference-equation method (L)
Δ_h	horizontal translation in global coordinate (L)
h_i	pile increment length (L)
H	specific depth below ground surface (L)
H_j	lateral load on pile j (F)
H_k	the lateral load on pile k (F)
H_G	total lateral load on pile group (F)
H_1, H_2, H_3	terms used in difference equation solution
i	$= \sqrt{-1}$
I	moment of inertia (L^4)
I_{sM}	influence coefficient for computing pile-head rotation for applied moment at groundline
I_{sP}	influence coefficient for computing pile-head rotation for applied shear at groundline
I_{yF}	influence coefficient for computing pile-head deflection for a pile with fixed head
I_{yM}	influence coefficient for computing pile-head deflection for applied moment at groundline
I_{yP}	influence coefficient for computing pile-head deflection for applied shear at groundline
I_ρ	surface displacement influence value
$I_{\rho F}$	elastic influence coefficient for fixed-head pile
$I_{\rho H}$	elastic influence coefficient for deflection caused by horizontal load
$I_{\rho M}$	elastic influence coefficient for deflection caused by moment
$I_{\rho P}$	elastic influence coefficient for deflection caused by horizontal load
J	factor used in equation for ultimate soil resistance near ground surface for soft clay

J	a constant having the same dimensions as the soil modulus for rigid pile analysis (F/L^2)
J_m	$= M_t/y_t$ modulus for computing M_t from y_t (F)
J_x	$= P_x/x_t$ modulus for computing P_x from x_t (F/L)
J_y	$= P_t/y_t$ modulus for computing P_t from y_t (F/L)
J_1, J_2, J_3, J_4	coefficients used in difference equation solution
k	constant giving variation of soil modulus with depth (F/L^3)
k_c	coefficient used in equations for p-y curves for stiff clays below water surface, cyclic loading (F/L^3)
k_s	initial slope of p-y curve for sand (F/L^3)
k_0, k_1, k_2, ...	constants of soil modulus variation in $E_s = k_0 + k_1X + k_2X^2$
k_M	slope of initial portion of Menard's soil response curve (F/L^3)
k_θ	$= M_t/S_t$, spring stiffness of restrained pile head (FL)
K	reduction factor used in expression for force against pile from wedge of soil
K_a	minimum coefficient of active earth pressure
K_0	coefficient of earth pressure at rest
K_p	Rankine coefficient of passive pressure
K_R	pile flexibility factor
L	length of pile (L)
LI	liquidity index for clay
m	number of piles in group
m	pile node number
m	slope used in defining portion of p-y curve for sand

LIST OF NOTATIONS (continued)

M	bending moment (F-L)
M_c	bending moment at pile top (F-L)
M_m	bending moment at node m (F-L)
M_{max}	maximum bending moment in pile (F-L)
M_{max}^{pos}	maximum positive bending moment (F-L)
M_{pos}, $M+$	positive moment (F-L)
M_t	bending moment at pile head (F-L)
M_{t_i}	bending moment at "i-th" pile head (F-L)
M_t/S_t	rotational restraint constant at pile top (F-L)
M_y, M_{yield}	yield moment of pile (F-L)
M_y^+, M_y^-	positive yield moment and negative yield moment of pile (F-L)
n	exponent used in equations for p-y curves for sand
n	exponent in $E_s = kx^n$, $\phi(Z) = Z^n$ or $\phi(h) = h^n$
N	tensile force active on beam-column (F)
N	number of cycles of load application used in p-y curves for stiff clay above water surface
O_R	overconsolidation ratio for clay
p	soil resistance (F/L)
p_c	ultimate soil resistance for pile in stiff clay below water surface (F/L)
p_{cd}	ultimate soil resistance at depth for pile in stiff clay below water surface (F/L)
p_{cR}	residual resistance on cyclic p-y curves, unified criteria for clay (F/L)
p_{ct}	ultimate soil resistance near ground surface for pile in stiff clay below water (F/L)
p_f	the initial volume of the cavity (L^3)

p_f	pressure at the point where there is no longer a straight-line relationship between pressure and volume (F/L^2)
p_h	total horizontal load on pile group (F)
p_k	a specific resistance on p-y curves for sand (F/L)
p_ℓ	limit pressure of typical curve from Menard pressuremeter (F/L^2)
p_m	soil resistance at node m (F/L)
p_m	soil reaction measured from Menard pressuremeter (F/L)
p_s	ultimate soil resistance for pile in sand (F/L)
p_{sd}	ultimate soil resistance at depth for pile in sand (F/L)
P_v	total vertical load on pile group (F)
P_x	axial load at pile head (F)
P_{st}	ultimate soil resistance near ground surface for pile in sand (F/L)
P_t	lateral force at pile top (F)
P_u	ultimate soil resistance or ultimate soil reaction (F/L)
$(P_u)_{ca}$	ultimate soil resistance near ground surface for pile in clay (F/L)
$(P_u)_{cb}$	ultimate soil resistance at depth for pile in clay (F/L)
$(P_u)_{sa}$	ultimate soil resistance near ground surface for pile in sand (F/L)
$(P_u)_{sb}$	ultimate soil resistance at depth for pile in sand (F/L)
P_x	axial load at pile top (F)
P_{ult}	ultimate lateral load on a pile (F)

P_y	the distribution of the yield pressure defined by Poulos (F/L^2)
P_z	soil resistance per unit length at a depth Z below the ground surface (F/L)
PI	plasticity index for clay
$\Delta P/\Delta V$	slope of curve between V_o and V_f
q	foundation pressure (F/L^2)
q_f	failure stress for foundation (F/L^2)
q_u	unconfined compressive strength of clay (F/L^2)
q_{yc}	limiting pile-soil interaction stress (yield pressure) after cyclic loading (F/L^2)
q_{ys}	yield pressure for static loading (in Poulos method) (F/L^2)
Qn	normal shear stress (F/L^2)
Q_v	vertical shear stress (F/L^2)
Q_1, Q_2, Q_3, Q_4	terms used in difference equation solution
$r_0, r_1, r_2, \ldots$	constants in polynomial soil modulus functions
R	relative stiffness factor
R_t	$= E_t I_t$, flexural rigidity at pile top ($F\text{-}L^2$)
s_t	sensitivity of clay
S_m	slope of pile at node m
S	slope
S_t	rotation at groundline
S_1, S_2, S_3	coefficients for simplified equations for p-y curves for sand
t	degradation parameter
t	pile top node
T	$= \sqrt[5]{\frac{EI}{k}}$ relative stiffness factor (1/L)

v	shear (F)
V	volume of cavity (L^3)
Δv	vertical translation in global coordinate (L)
V_c	initial volume of the measuring cell (L^3)
V_m	midpoint volume (L^3)
V_m	shear at node m (F)
V_o	volume at start of the straight-line portion of the curve and equal to the initial volume of the cavity (L^3)
V_v	shearing force parallel to y-axis (F)
W_L	liquid limit for clay
x	coordinate along pile, beam (L)
x_r	transition depth at intersection of equations for computing ultimate soil resistance against a pile in clay (L)
x_t	transition depth at intersection of equations for computing ultimate soil resistance against a pile in sand (L)
x_t	vertical displacement at pile head (L)
y	pile deflection and for y-coordinate (L)
y_c	deflection coordinate for p-y curves for stiff clay above water surface, cyclic loading (L)
y_F	pile deflection with pile head fixed against rotation (L)
y_g	deflection at intersection of the initial linear portion and the curved portion of the p-y curve, unified criteria for clay (L)
y_k	a specific deflection on p-y curves for sand (L)
y_m	pile deflection at node m (L)
y_m	a specific deflection on p-y curves for sand (L)

y_p	a specific deflection on p-y curves for stiff clay below water surface, cyclic loading (L)
y_s	deflection coordinate for p-y curves for stiff clay above water table, static loading (L)
y_t	pile top deflection (L)
y_u	a specific deflection on p-y curves for sand (L)
Y_A, S_A, M_A, V_A, P_A	components of pile response due to an applied force P_t, namely, deflection, slope, moment, shear and soil reaction, respectively
Y_B, S_B, M_B, V_B, P_B	components of pile response due to an applied moment M_t, namely deflection, slope, moment, shear and soil reaction, respectively
Y_G	horizontal deflection of pile group (L)
z	depth (L)
z_c	critical depth for pressuremeter method suggested by Menard (L)
Z	$= \frac{X}{T}$, depth coefficient in elastic-pile theory
Z_{max}	$= \frac{L}{T}$, maximum value of elastic-pile theory coefficient
α	$= E_s$, soil modulus, coefficient of subgrade reaction (F/L^2)
α	angle used in defining geometry of soil wedge
α_s	rotational angle in the global coordinate system
α_T	Terzaghi's soil modulus for stiff clay (F/L^2)
$\alpha_{\rho Fkj}$	the coefficient to get the influence of pile j on pile k
β	the angle between the line joining the pile centers and the direction of loading
β	$\sqrt[4]{\frac{\alpha}{4EI}}$, relative stiffness factor
β	angle used in defining geometry of soil wedge
γ	average unit weight of soil (F/L^3)

γ'	bouyant unit weight or average unit weight used in computing effective stress (F/L^3)
ε	axial strain of soil
ε_c	axial strain of soil
ε_{50}	axial strain of soil corresponding to one-half the maximum principal stress difference
ε_x	axial strain
θ	angle of rotation
θ_i	the inclined angle between vertical line and pile axis of the "i-th" batter pile
λ	loading rate
λ_r	reference loading rate (perhaps static loading)
λ_z	soil modulus coefficient between the ground surface and critical depth
ν and ν_s	Poisson's ratio
ρ	mean settlement of a foundation (L)
ρ	radius of curvature of elastic curve (L)
ρ_k	deflection of the "k-th" pile (L)
ρ_F	the unit reference displacement of a single pile under a unit horizontal load, computed by using elastic theory (L)
σ	normal stress (F/L^2)
σ_x	bending stress (F/L^2)
σ_Δ	deviator stress (F/L^2)
σ_v	average effective stress (F/L^2)
τ	shear stress (F/L^2)
ϕ	angle of internal friction of sand
$\phi(h)$	$= E_s/J$, nondimensional soil modulus function of rigid pile theory
$\phi(Z)$	$= E_s \cdot T^4/EI$, nondimensional soil modulus function of elastic pile theory

CHAPTER 1. INTRODUCTION

Laterally loaded piles are found in many structures, both onshore and offshore. In many instances in the past, and even today, pile foundations have been designed so that each pile takes only a nominal lateral load or batter piles are employed. When batter piles are utilized in a structure, the assumption is frequently made that any horizontal load is sustained by the horizontal component of the axial load. The assumption that batter piles do not deflect laterally is, of course, incorrect as will be shown subsequently.

With increasing cost of labor and materials and with decreasing cost of computations, situations are arising where it is cost effective to employ more engineering effort. Furthermore, designers are finding it desirable to create more complex structures and severe loadings are being encountered, such as those on offshore structures. Thus, in some cases it is necessary to consider as well as possible the various deformations of a structure and its foundation under a wide range of loading. Therefore, procedures such as those given herein are needed to allow analyses of foundations in as rational a manner as possible.

As a foundation problem, the analysis of a pile under lateral loading is complicated by the fact that the soil reaction (resistance) is dependent on the pile movement, and the pile movement, on the other hand, is dependent on the soil response. Thus, the problem is one of soil-structure interaction.

The method of solution of the problem of the laterally loaded pile described herein (the p-y method) is being used in the United States and abroad. Numerous references in the following chapters will illustrate the use of the method. To illustrate the use abroad, references are cited from Italy (Jamilkowski, 1977), France (Baguelin, et al., 1978), Britain (George and Wood, 1976), Australia (Poulos and Davis, 1980), and Norway (Det Norske Veritas, 1977). The method is included in Planning, Designing and Constructing Fixed Offshore Platforms, RP2A, American Petroleum Institute. That publication has guided the design of offshore drilling platforms in the United States and has significantly influenced their design elsewhere. The method is expected to be used increasingly in the design of onshore facilities.

However, a number of additional developments are needed. One of the most important is simply the acquisition of sufficient data to improve the quality of the recommended soil-response curves. It would be desirable if enough data were available to allow a statistical approach to the use of the soil-response curves.

1.1 SOIL-STRUCTURE INTERACTION

The term "soil-structure interaction" has been used frequently in connection with the analysis of structures that sustain seismic loads; however, the term has relevance to loads that are short-term, repeated at relatively low frequencies, or sustained. Reflection will show that every problem in foundation design, if fully solved, is one of soil-structure interaction. For example, the strip footing in Fig. 1.1 can be considered. Not only is it desirable to know at what load the footing will plunge so that an appropriate factor of safety can be employed to prevent a soil failure, it is necessary to know the way the bearing stress is distributed at the base of the footing so that the footing can be properly reinforced.

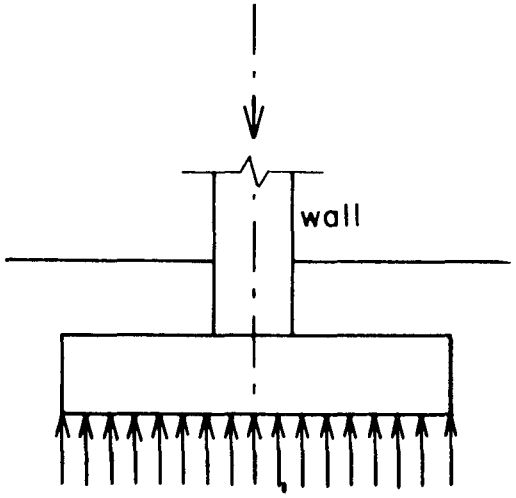

Fig. 1.1. Strip footing.

In order for a bearing stress to be mobilized the footing must move down, however slightly. It is unlikely that a uniform bearing stress will develop such as the one shown. Depending on the supporting soil, the bearing stress at the edge of the footing may either be lower or higher than the average. However, for purposes of discussion the assumption is

made that the stress is uniform as shown. The extension of the footing beyond the wall behaves as a short, cantilever beam and the downward movement of the edge of the footing is less than that at the center. Conceptually, then, the bearing stress should be different at the edge and at the center of the footing to reflect the difference in downward movement.

The pattern of the distribution of the bearing stress should change with the change in applied load because the stress-deformation characteristics of soil are nonlinear. Thus, as loading on the footing increases there will be a nonlinear increase in the bending moment in the footing at the edge of the wall. There is, of course, a complex state of stress in the soil beneath the footing and a complex pattern of deformations. The soil response at the base of the footing is more complex if the loading has a lateral component or an eccentricity.

The problem of the strip footing is frequently trivial because sufficient reinforcement can be provided for a small expense to make the footing safe against any pattern of distribution of bearing stress. The same argument cannot be made for a mat foundation, however, where the thickness of the mat and the amount of reinforcing steel will vary widely according to the distribution of bearing stress. The problem of the mat foundation is a soil-structure-interaction problem that needs additional attention.

The pile foundation is an excellent case to use in discussing soil-structure interaction. While the material in this volume is directed toward the pile under lateral loading, it is of interest to consider the general behavior of a pile under axial loading as well. Figure 1.2 shows a model of an axially loaded deep foundation. The soil has been replaced with a series of mechanisms and the pile has been replaced with a stiff spring. A study of the model will indicate the following significant points about a soil-structure-interaction problem: the pile is deformable, a movement of the pile is necessary to mobilize soil resistance, the soil response is a nonlinear function of pile movement, there is a limiting soil response, and if the model can be described numerically, computations can be made to obtain the response of the system.

The above characteristics of a pile under axial load also pertain to a pile under lateral loading, shown in Fig. 1.3. As may be seen in the figure, the soil is again replaced by a set of mechanisms that indicate a

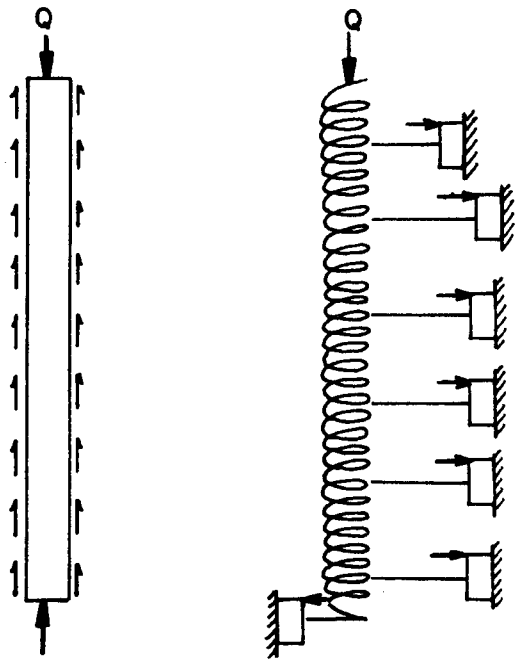

Fig. 1.2. Model of a pile under axial load.

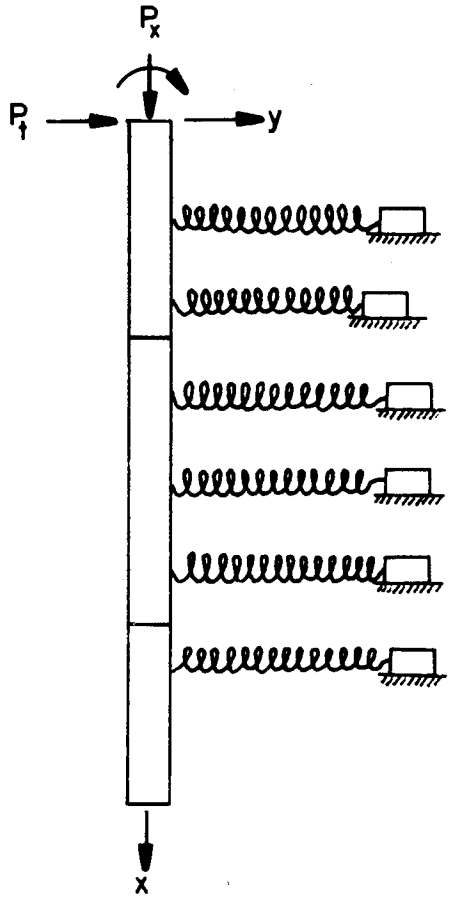

Fig. 1.3. Model of a pile under lateral load.

nonlinear response to the lateral deflection of the pile. The mechanisms indicate the soil resistance p per unit length of the pile as a function of the pile deflection y. The p-y curves will be discussed in detail in a later chapter. If such curves are available, the computations for pile deflection and bending moment can be made readily if pile dimensions and pile-head loading are known.

A feature that is common in the two models shown in Figs. 1.2 and 1.3 is that the soil is characterized by a set of discrete, independent mechanisms. This sort of modelling is not strictly correct, of course, because the soil is a continuum and a deformation at any point in the continuum will cause a deformation at all other points. The theoretical difficulty of modelling the soil as indicated in Fig. 1.3 causes little practical difficulty, as will be discussed later.

The methods that are used to analyze the behavior of a single pile under lateral load can also be extended in developing approximate methods for the analysis of a group of closely-spaced piles. This problem in soil-structure interaction is treated in a later chapter.

An important problem in the mechanics of pile behavior is the computation of the magnitude of the loads and moments that are distributed to a group of widely-spaced piles, including batter piles, that support a pile cap or structure. As demonstrated later, the solution to such a problem can be made as exactly as the behavior of the individual piles under axial and lateral load can be computed.

1.2 METHODS OF SOLUTION OF LATERALLY LOADED PILES

The principal method of solution presented herein requires the modelling of the soil by p-y curves and the computation of the pile response by digital computer. The differential equation that governs the pile behavior, even with nonlinear soil response, can be conveniently solved by use of difference equations.

In addition to the computer solution, the use of nondimensional curves has an important role in the analysis of laterally loaded piles. Nondimensional methods can be used to demonstrate with clarity the nature of the computer method and, furthermore, can be used to obtain a check of the computer results.

Two other methods of analysis are presented, the methods of Broms (1964a, 1964b, 1965) and Poulos and Davis (1980). Broms' method is ingenious and is based primarily on the use of limiting values of soil resistance. The method of Poulos and Davis is based on the theory of elasticity. Both of these methods have had considerable use in practice and the designer of a particular foundation may wish to employ one or both of them as a check or to give additional insight into a design problem.

1.3 DESIGN PROBLEMS

Some of the applications of piles under lateral loading are shown in Fig. 1.4. There are other examples, including high-rise buildings, soldier piles in a retaining structure, well-head supports, slope-stabilizing elements, and river crossings for pipelines.

The principal kind of loading in most of the cases is repeated or cyclic, and sustained loading is also present. The methods presented here-

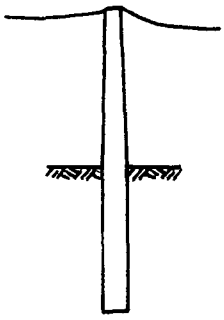

Transmission Tower

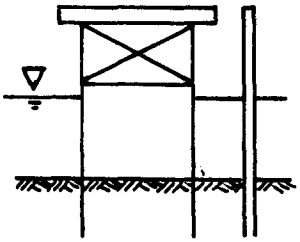

Pier & Breasting Dolphin

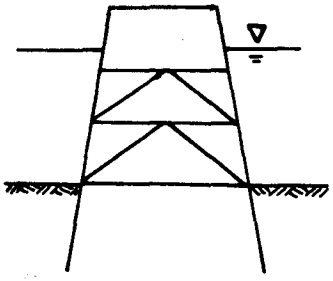

Offshore Structure

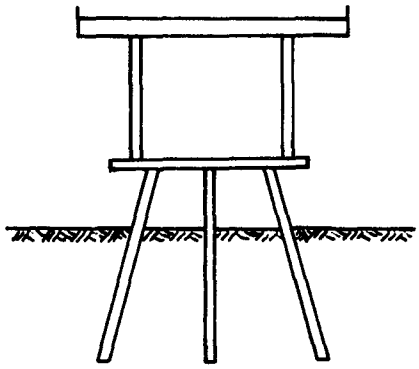

Bridge Foundation

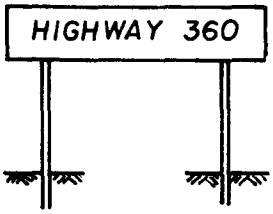

Overhead Sign

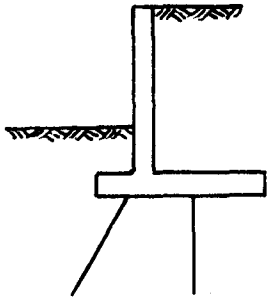

Retaining Wall; Bridge Abutment

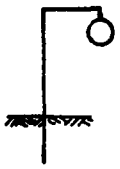

Pipe Support

Anchorage

Fig. 1.4. Examples of laterally-loaded piles.

in can be utilized to analyze directly those cases where there are repeated loadings. With regard to sustained loading, the methods yield an excellent preliminary analysis and the geotechnical engineer must use some computations and a good deal of judgement to complete a solution.

Concerning design, additional comments about the subsurface soil investigation and the inspection of construction are appropriate. In the sections giving procedures for computing p-y curves there are suggestions for the determination of significant soil properties. The importance of a soil investigation of high quality cannot be over-emphasized. In particular, because piles under lateral loading derive a significant amount of their lateral support from soils near the ground surface, the soil investigation must be especially thorough for the near-surface soils.

The inspection of the construction is important and should be done by someone familiar with the design process. A number of things could be done by the contractor inadvertently that could have a detrimental effect on the performance of a pile under lateral load.

The geotechnical engineer must give attention to factors such as expansive clay, negative friction, downslope movement, and changes in soil properties with time. These factors and many such others are not discussed herein.

1.4 DESIGN ORGANIZATION

The writer has observed that there unfortunately is sometimes a limited use of the methods presented in this work because of the separation of responsibilities. The appropriate use of the methods requires the skills of geotechnical engineers and structural engineers, along with the support of computer technicians. It is inappropriate for the geotechnical engineer to provide data on p-y curves and not be connected further with the design. It is also inappropriate for the geotechnical engineer to try to perform an analysis of a pile without careful consideration of how the pile interacts with the superstructure, the work of the structural engineer. It is inappropriate for the structural engineer to proceed with a design if there are even minor changes that affect the soil response.

Therefore, in many offices there is the need for a management decision that geotechnical engineers and structural engineers will work closely throughout the design and construction of a project involving

piles under lateral loading. Such close cooperation may already be present in many offices; it is essential in the design of laterally loaded piles.

1.5 FACTOR OF SAFETY

The ordinary procedures for establishing an appropriate factor of safety will apply to the design of a single pile and the pile group under lateral loading. Many factors are to be considered, of course, including the quality of the information on loading, the quality of the soil data and data on other materials, the adequacy of the design methods, and the possible result of a failure. In regard to a failure, the designer must consider whether loss of life might result, a large monetary loss, or a minor monetary loss.

Two aspects of a soil-structure-interaction problem differentiate that problem from others in foundation engineering: the methodology does not have much experimental validation, and the problem is nonlinear. Concerning the nonlinear aspects, the designer must put the factor of safety into the load rather than into the material properties. That is, the service load must be increased by the factor of safety and computations made with the factored load. The computations with the service load might indicate a moderate deflection and bending stress while a small increase in load could result in a failure. Such a result is possible because there could be a considerable loss in soil resistance with a small increase in deflection.

Concerning the adequacy of design methods, a study of the later section of this work will show that the methods are rational and validated to a certain extent. However, experimental data are limited. Thus, the designer should make computations not only with a range of loads but with an upper bound and with a lower bound for the soil response. These upper-bound and lower-bound values can probably best be established by taking the maximum values of soil properties that can be expected and the minimum values. Also, the effects of varying the parameters that are used in the soil-response criteria (p-y curves) can be studied. The computations will yield insight into the probable response of the pile-soil system.

There are in general two types of failure: a failure of the pile material as reflected by an excessive bending moment, and a soil failure

as reflected by excessive deflection of a pile. However, there could be some applications where the limits on pile-head deflection are small and the allowable deflection is exceeded even if the soil is still substantially in the elastic range.

There are applications of the pile under lateral loading where the pile carries little or no axial load (such as a support for an overhead sign or a breasting dolphin) and where the pile penetration is determined by lateral loading. Figure 1.5 shows how to deal with such a case. When a pile is short, the deflection of the pile at the groundline can be large because the bottom of the pile will deflect. As the pile penetration is increased, soil resistance at the bottom of the pile will increase and the groundline deflection will reach a limiting value where increased penetration will cause no decrease in groundline deflection. Thus, the designer will make computations for a series of pile penetrations and will determine a penetration that will yield an appropriate factor of safety.

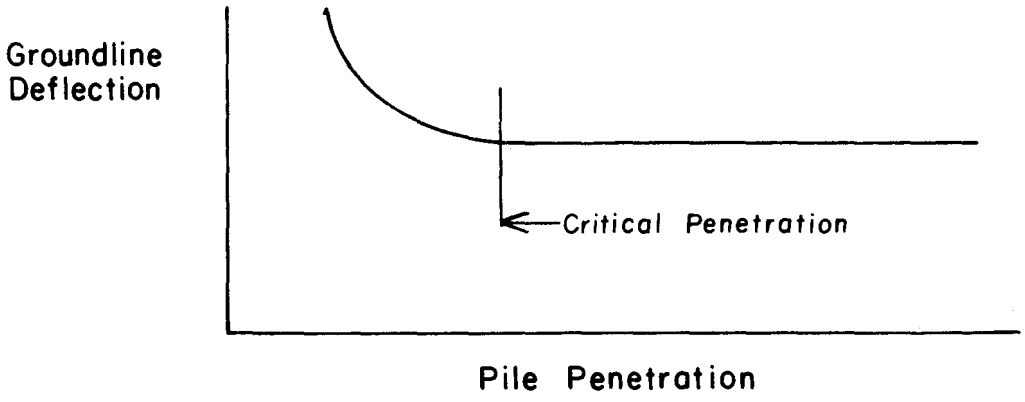

Fig. 1.5. Results of computations where pile penetration is controlled by lateral loading.

1.6 REFERENCES

American Petroleum Institute, Planning, Designing and Constructing Fixed Offshore Platforms, API RP2A, 1979.

Baguelin, F., Jézéquel, J. F., and Shields, D. H., The Pressuremeter and Foundation Engineering, Trans Tech Publications, 1978.

Broms, Bengt B., "Lateral Resistance of Piles in Cohesive Soils," Proceedings, American Society of Civil Engineers, Vol. 90, No. SM2, March 1964, pp. 27-63.

Broms, Bengt B., "Lateral Resistance of Piles in Cohesionless Soils," Proceedings, American Society of Civil Engineers, Vol. 90, No. SM3, May 1964, pp. 123-156.

Broms, Bengt B., "Design of Laterally Loaded Piles," Proceedings, American Society of Civil Engineers, Vol. 91, No. SM3, May 1965, pp. 79-99.

Det Norske Veritas, Rules for the Design, Construction, and Inspection of Offshore Structures, Det Norske Veritas, 1977.

George, P., and Wood, D., Offshore Soil Mechanics, Cambridge University Engineering Department, 1976.

Jamilkowski, M., "Design of Laterally Loaded Piles," General Lecture, International Conference on Soil Mechanics and Foundation Engineering, Tokyo, Japan, 1977.

Poulos, H. G., and Davis, E. H., Pile Foundation Analysis and Design, Wiley, New York, 1980.

CHAPTER 2. THE DIFFERENTIAL EQUATION

The problem of the laterally loaded pile is similar to the beam-on-foundation problem. The interaction between the soil and the structure (pile or beam) must be treated quantitatively in the problem solution. The two conditions that must be satisfied for a rational analysis of the problem are: (1) each element of the structure must be in equilibrium and (2) compatibility must be maintained between the superstructure, foundation, and supporting soil. If the assumption is made that compatibility between the pile and the superstructure can be maintained by selecting appropriate boundary conditions at the top of the pile, the remaining problem is to obtain a solution that insures equilibrium and compatibility of each element of the pile, taking into account the soil response along the pile. Such a solution can be made by solving the differential equation that describes the pile behavior.

A derivation of the differential equation for a beam or a pile under lateral loading is presented so that the assumptions that are made can be understood.

2.1 RELATION BETWEEN CURVATURE AND BENDING MOMENT

A segment of an initially straight beam deformed by a bending moment is shown in Fig. 2.1 (Popov, 1952). The initially straight neutral axis, A-B, becomes curved in a bent beam.

A fundamental assumption made in establishing the flexure formula is that plane sections initially perpendicular to the axis of the beam remain plane in the bent beam. The lines m-m and p-p represent two such planes. The extensions of these lines intersect at a point O which is the center for the radius of curvature ρ for the infinitesimal arc $n\text{-}n_1$.

The line $s\text{-}s_2$, at distance η away from $n\text{-}n_1$, has been stretched due to bending. The extension of the line, $s_2\text{-}s_1$, is determined by constructing line $n_1\text{-}s_1$ parallel to n-s. Triangles non_1 and $s_1n_1s_2$ are similar. Therefore:

$$\frac{\rho}{\eta-\eta_1} = \frac{\eta}{s_2-s_1} \tag{2.1}$$

$$\frac{\eta}{\rho} = \frac{s_2-s_1}{\eta-\eta_1} \ . \tag{2.2}$$

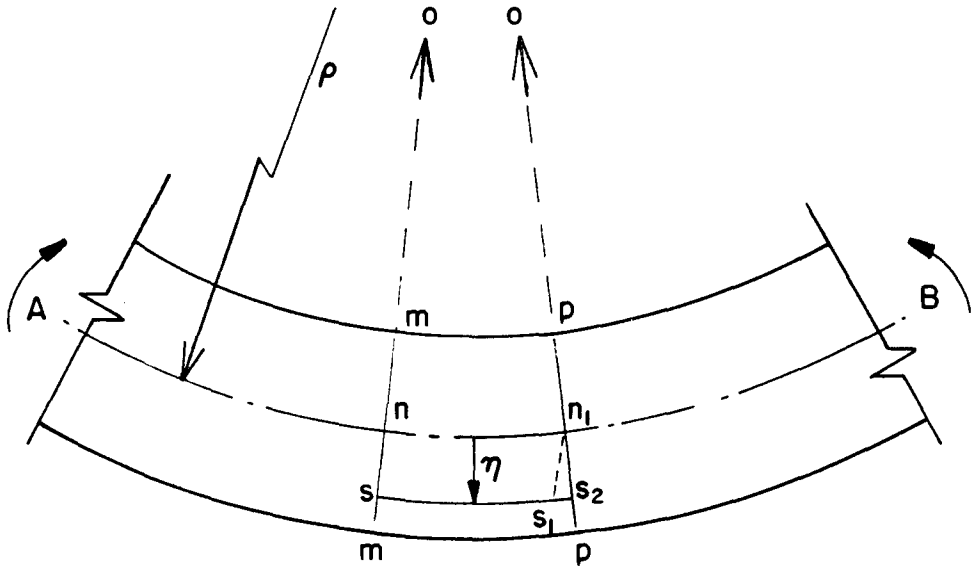

Fig. 2.1. A straight beam under bending moment (after Popov, 1952).

The strain ε is defined as the change in length of an element divided by the initial length of that element. Using this definition, the strain at any point x along the beam is equal to

$$\varepsilon_x = \frac{s_2 - s_1}{\eta - \eta_1} \quad . \tag{2.3}$$

Substituting Eq. 2.2 into Eq. 2.3

$$\varepsilon_x = \frac{\eta}{\rho} \quad . \tag{2.4}$$

Using Hooke's Law, the strain of the element $s\text{-}s_2$ is:

$$\varepsilon_x = \frac{\sigma_x}{E} \tag{2.5}$$

where

σ_x = bending stress in element $s\text{-}s_2$

E = modulus of elasticity.

Combining Eqs. 2.4 and 2.5

$$\frac{\sigma_x}{E} = \frac{\eta}{\rho} \quad \text{or} \quad \sigma_x = \frac{E\eta}{\rho} \quad . \tag{2.6}$$

The flexure formula for bending is:

$$\sigma_x = \frac{M\eta}{I} \quad . \tag{2.7}$$

Combining Eqs. 2.6 and 2.7

$$\frac{M\eta}{I} = \frac{E\eta}{\rho} \tag{2.8}$$

and

$$\frac{1}{\rho} = \frac{M}{EI} \ . \tag{2.9}$$

2.2 THE DIFFERENTIAL EQUATION OF THE ELASTIC CURVE

The next step in the derivation is to obtain an expression for ρ in terms of x and y. The curvature of a line in analytic geometry is defined by Eq. 2.10.

$$\frac{1}{\rho} = \frac{\frac{d^2y}{dx^2}}{\left[1 + \left(\frac{dy}{dx}\right)^2\right]^{3/2}} \tag{2.10}$$

In the usual cases of the bending of a beam or pile, the slope dy/dx is very small. Therefore, the square of the slope is a negligible quantity. Thus,

$$\frac{1}{\rho} = \frac{d^2y}{dx^2} \ . \tag{2.11}$$

Finally, combining Eqs. 2.9 and 2.11

$$\frac{M}{EI} = \frac{d^2y}{dx^2} \ . \tag{2.12}$$

Eq. 2.12 is the desired differential equation.

In applying Eq. 2.12, the pile is assumed to be vertical with the x-axis lying along the axis of the unloaded pile. The deflection of a point on the elastic curve of the pile is given by y, Fig. 2.2. Deflection to the right is positive. Slopes of the elastic curve at points 1 and 2 are negative while slopes at 3 and 4 are positive. However, as indicated in the figure, the moment is positive in both instances.

Other relationships which are needed, along with those already defined, are:

y = deflection of the elastic curve

$$\frac{dy}{dx} = S = \text{slope of the elastic curve} \tag{2.13}$$

$$\frac{d^2y}{dx^2} = \frac{M}{EI} \text{ , where M = moment} \tag{2.14}$$

$$\frac{d^3y}{dx^3} = \frac{V}{EI} \text{ , where } V = \text{shear} \tag{2.15}$$

$$\frac{d^4y}{dx^4} = \frac{p}{EI} \text{ , where } p = \text{soil reaction .} \tag{2.16}$$

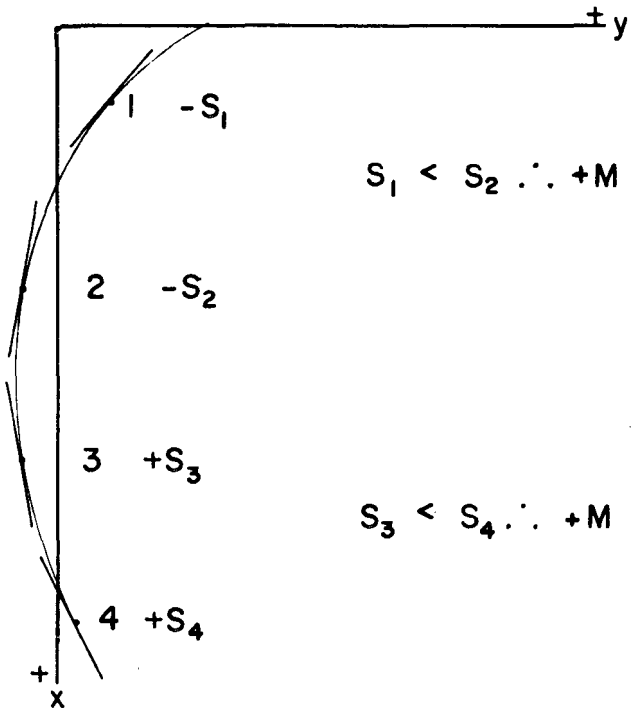

Fig. 2.2. Segment of a deflected pile.

2.3 DERIVATION OF THE DIFFERENTIAL EQUATION FOR THE BEAM-COLUMN

In most instances the axial load on a laterally loaded pile is of such magnitude that it has a small influence on bending moment. However, there are occasions when it is necessary to include a term for the effect of axial loading in the analytical process. The derivation for the differential equation has been made by Hetenyi (1946) and is shown in the following paragraphs.

Methods are presented later for the solution of the differential equation. When the solution involves consideration of the axial load, it will be necessary to employ a computer program. The program is described

later and offers the user an opportunity for doing stability analyses as well as the usual computations of pile behavior. It should be noted at this point that the interaction between behavior under lateral loading and under axial loading can normally be uncoupled because the axial load is usually almost constant over the portion of the pile where bending moment is significant.

It will now be assumed that a bar on an elastic foundation is subjected not only to the vertical loading, but also to the pair of horizontal compressive forces P_x acting in the center of gravity of the end cross-sections of the bar.

If an infinitely small unloaded element, bounded by two verticals a distance dx apart, is cut out of this bar (see Fig. 2.3), the equilibrium of moments (ignoring second-order terms) leads to the equation

$$(M + dM) - M + P_x dy - V_v dx = 0 \tag{2.17}$$

or

$$\frac{dM}{dx} + P_x \frac{dy}{dx} - V_v = 0 . \tag{2.18}$$

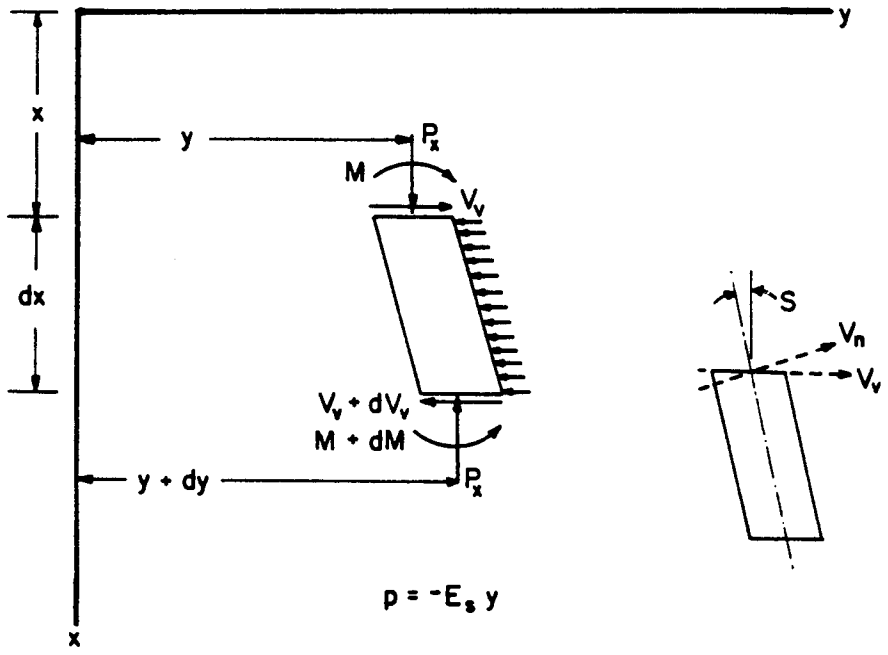

Fig. 2.3. Element from beam-column.

Differentiating Eq. 2.18 with respect to x, the following equation is obtained

$$\frac{d^2M}{dx^2} + P_x \frac{d^2y}{dx^2} - \frac{dV_v}{dx} = 0 \ . \tag{2.19}$$

The following identities are noted:

$$\frac{d^2M}{dx^2} = EI \frac{d^4y}{dx^4}$$

$$\frac{dV_v}{dx} = p$$

$$p = -E_s y \ .$$

And making the indicated substitutions, Eq. 2.19 becomes

$$EI \frac{d^4y}{dx^4} + P_x \frac{d^2y}{dx^2} + E_s y = 0 \ . \tag{2.20}$$

The direction of the shearing force V_v is shown in Fig. 2.3. The shearing force in the plane normal to the deflection line can be obtained as

$$V_n = V_v \cos S - P_x \sin S. \tag{2.21}$$

Because S is usually small, cos S = 1 and sin S = tan S = $\frac{dy}{dx}$. Thus, Eq. 2.22 is obtained.

$$V_n = V_v - P_x \frac{dy}{dx} \tag{2.22}$$

V_n will mostly be used in computations but V_v can be computed from Eq. 2.22 where dy/dx is equal to the rotation S.

2.4 SUMMARY

The assumptions that must be made in deriving the differential equations are shown below:

(1) The pile is straight and has a uniform cross section.

(2) The pile has a longitudinal plane of symmetry; loads and reactions lie in that plane.

(3) The pile material is homogeneous.

(4) The proportional limit of the pile material is not exceeded.

(5) The modulus of elasticity of the pile material is the same for tension and compression.

(6) Transverse deflections of the pile are small.

(7) The pile is not subjected to dynamic loading.

(8) Deflections due to shearing stresses are negligible.

The assumption of a uniform cross section can be eliminated by rewriting the differential equation or by solving sets of simultaneous differential equations. Also, most of the other assumptions can be eliminated if one wishes to modify the differential equation.

The sign conventions that are employed are shown in Fig. 2.4. For ease of understanding, the sign conventions are presented for a beam that is oriented like a pile. A solution of the differential equation yields a set of curves such as shown in Fig. 2.5.

Techniques for the solution of the differential equation will be discussed in a later chapter.

2.5 EXAMPLE EXERCISE

As an example of the solution of the second-order differential equation, Eq. 2.19, the problem of a simply-supported beam with uniform loading will be considered. The desired solution is an expression for y.

Cutting a free body from the beam shown in Fig. 2.6 at some point x along the beam and solving for the moment in the beam where it is cut, the following expression results:

$$M_x = \left(\frac{pL}{2}\right)x - \left(\frac{px}{2}\right)x. \tag{2.23}$$

Substituting expression for moment from Eq. 2.23 into Eq. 2.12

$$\frac{d^2y}{dx^2} = \frac{1}{EI}\left(\frac{pLx}{2} - \frac{px^2}{2}\right). \tag{2.24}$$

Integrating Eq. 2.24

$$\frac{dy}{dx} = \frac{1}{EI}\left(\frac{pLx^2}{4} - \frac{px^3}{6}\right) + C_1. \tag{2.25}$$

From symmetry, the slope is zero at the mid-point of the beam,

$$\frac{dy}{dx} = 0 \quad \text{at} \quad x = \frac{L}{2} \tag{2.26}$$

and this enables the constant of integration C_1 to be evaluated. Using expressions in Eq. 2.26 to solve Eq. 2.25

$$0 = \frac{1}{EI}\left(\frac{pL}{4} \cdot \frac{L^2}{4} - \frac{p}{6} \cdot \frac{L^3}{8}\right) + C_1. \tag{2.27}$$

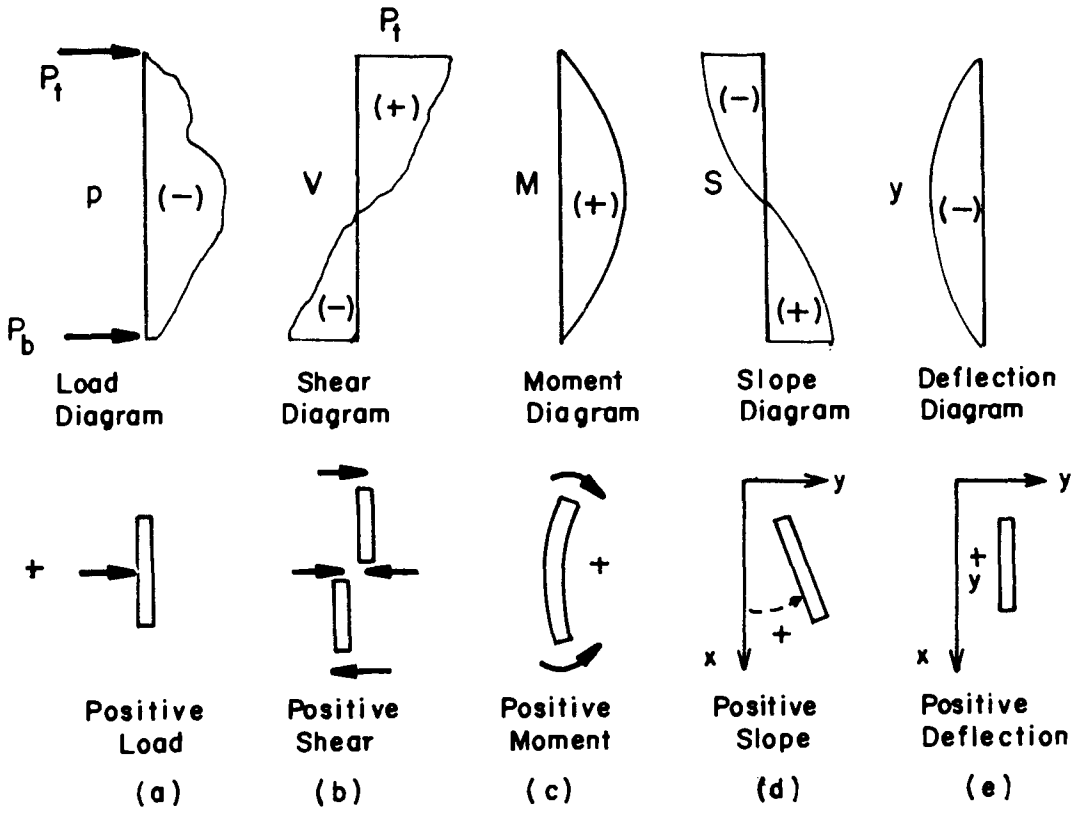

Fig. 2.4. Sign conventions.

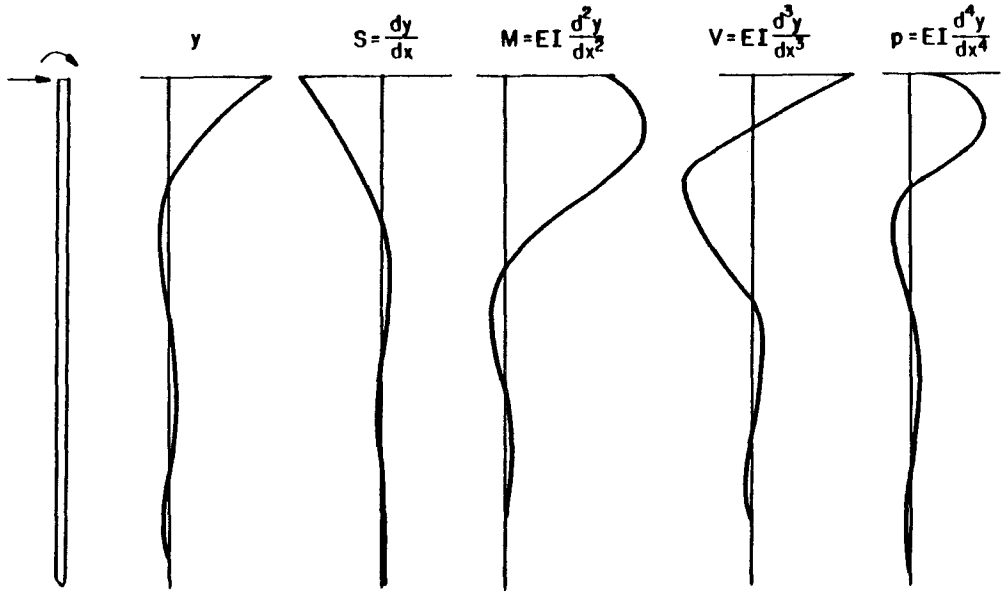

Fig. 2.5. Form of the results obtained from a complete solution.

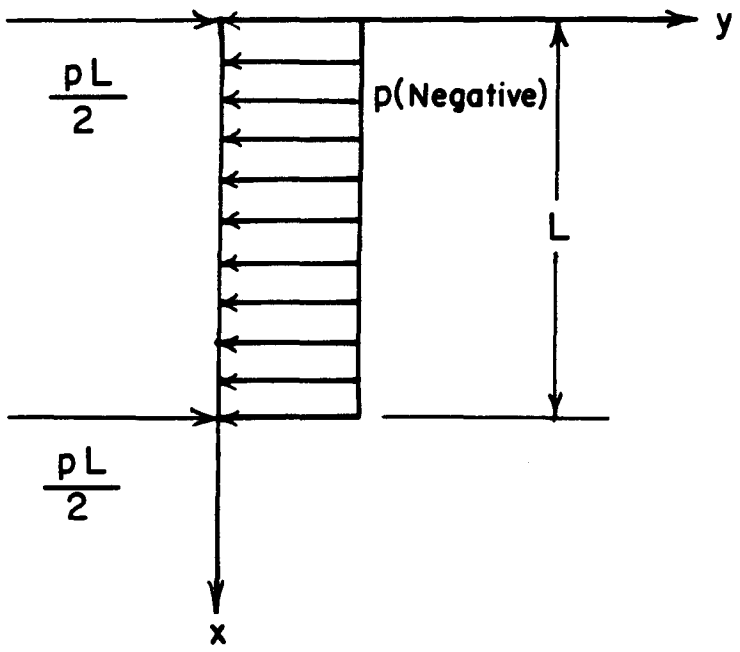

Fig. 2.6. Section of a beam (pile) with uniform load.

or

$$C_1 = \frac{-pL^3}{24EI} \cdot \tag{2.28}$$

Substituting expression for C_1 into Eq. 2.25

$$\frac{dy}{dx} = \frac{1}{EI}\left(\frac{pLx^2}{4} - \frac{px^3}{6}\right) - \frac{pL^3}{24EI} \cdot \tag{2.29}$$

Integrating Eq. 2.29

$$y = \frac{1}{EI}\left(\frac{pL}{4} \cdot \frac{x^3}{3} - \frac{px^4}{24}\right) - \frac{pL^3}{24EI} \cdot x + C_2. \tag{2.30}$$

To solve for C_2 the condition is employed that $y = 0$ at $x = 0$. Using these boundary conditions, Eq. 2.30 becomes

$$0 = \frac{1}{EI}(0 - 0) - 0 + C_2; \quad C_2 = 0. \tag{2.31}$$

Finally, Eq. 2.30 becomes

$$y = \frac{p}{24EI}(2Lx^3 - x^4 - L^3x). \tag{2.32}$$

Eq. 2.32 is the desired solution.

2.6 REFERENCES

Hetenyi, M., Beams on Elastic Foundation, The University of Michigan Press, Ann Arbor, 1946.

Popov, E. P., Mechanics of Materials, Prentice-Hall, New York, 1952, pp. 269-276.

2.7 EXERCISES

2.1 Use the method in Section 2.5 and solve each of the following problems of a cantilever beam: (a) a force at the free end, (b) a moment at the free end, (c) a rotation at the free end, and (d) a deflection at the free end.

2.2 Repeat problem 2.1 with the EI of the half of the beam at the fixed end being twice as great as the EI of the half of the beam at the free end.

CHAPTER 3. SOIL RESPONSE

As noted earlier, the soil response is characterized as a set of discrete mechanisms as suggested by Winkler (1867). The discrete mechanisms indicate that the soil response at a point is not dependent on pile deflection elsewhere; thus, a continuum is not perfectly modelled. However, the continuum could be modelled properly if information were available concerning the interaction effects from one soil slice to the next. Each discrete mechanism could then represent a family of curves, with the appropriate curve in the family at a point selected to reflect the effects from the soil above and below that point. The present state-of-the-art concerning the response of the soil to a deflected pile does not allow or justify an approach more sophisticated than that suggested by the set of discrete mechanisms. Futhermore, a small amount of unpublished experimental data suggests that the soil response at a point is unaffected by those changes in deflected shape that can be achieved by altering the rotational restraint at the pile head by any practical amount.

Proceeding with the concept that the soil response can be treated by employing a set of mechanisms, a discussion of the physical meaning of one of these mechanisms is helpful. Figure 3.1a is a view of a pile after it has been installed and before any lateral load has been applied. The behavior of the soil at the depth x_1 is to be considered. The stress distribution against the pile, before any lateral loading, is shown in Fig. 3.1b. The assumption implied by the figure is that the pile has been driven without any residual deflection and bending moment; thus, there is no lateral force against the pile at the depth x_1 or elsewhere. It is assumed that a lateral load is now applied to the pile and that it is caused to deflect an amount y_1 at the depth x_1. The stress distribution is altered, of course, and that shown in Fig. 3.1c could represent the new distribution.

The integration of the stress distribution shown in Fig. 3.1c would yield the force per unit length along the pile, p_1. The quantity p is defined as the soil reaction or soil resistance. It acts in opposition to the deflection y; hence, p and y are opposite in sign. If one were able to predict the stress distribution for a range of deflections, the successive integrations would yield p-values corresponding to y-values, allowing the

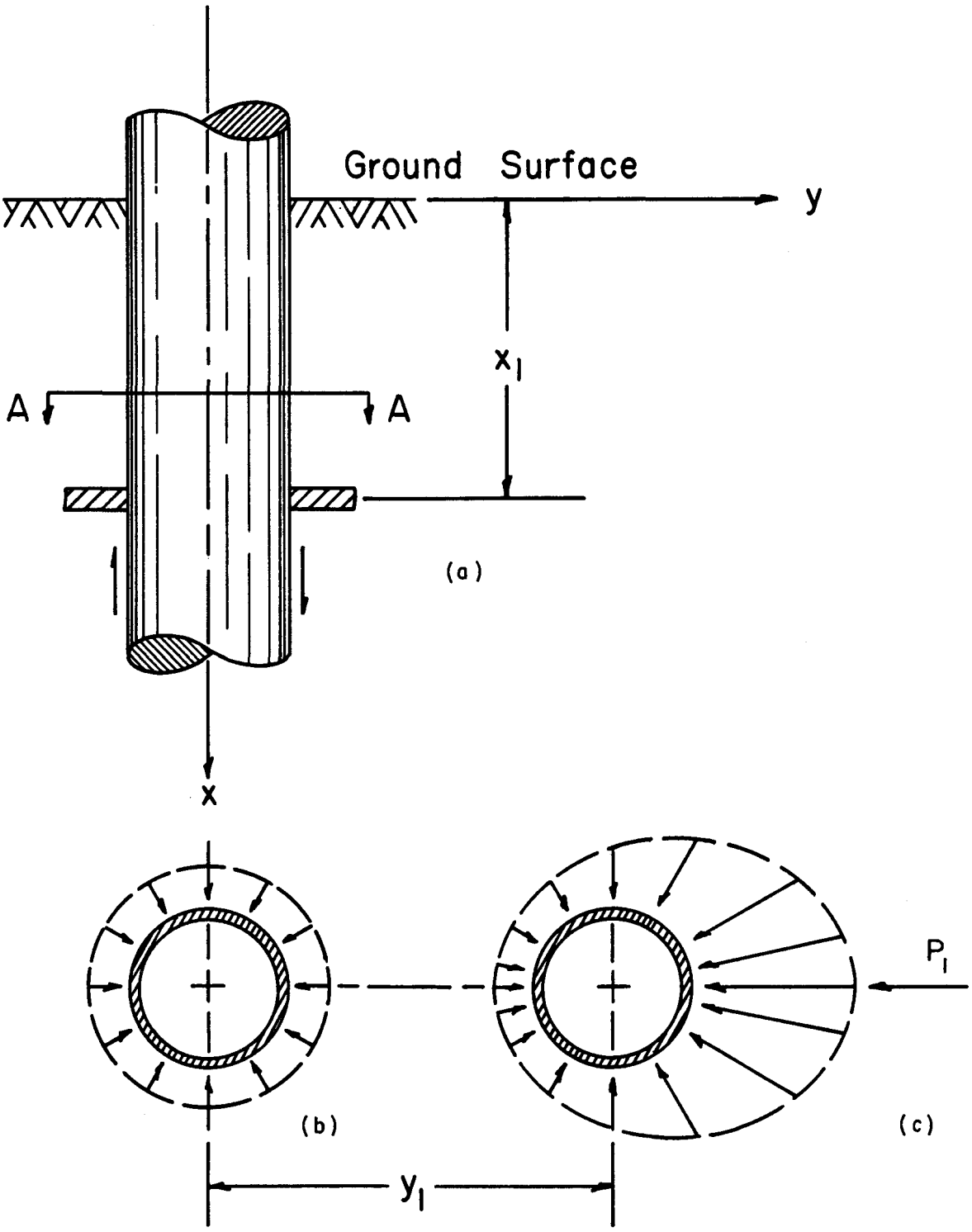

Fig. 3.1. Graphical definition of p and y
(a) view of elevation of section of pile
(b) view A-A - earth pressure distribution prior to lateral loading
(c) view A-A - earth pressure distribution after lateral loading.

p-y curve to be developed for the depth x_1. Similar exercises at other depths would yield a family of p-y curves.

With regard to p-y curves, the assumptions are made (1) that there is no shear stress at the surface of the pile parallel to its axis (the direction of the soil resistance is perpendicular to the axis of the pile) and (2) that any lateral resistance or moment at the base of the pile can be accounted for by a p-y curve at the side of the pile near the base. Any errors due to these assumptions are thought to be negligible.

3.1 REACTION OF SOIL TO LATERAL DEFLECTION OF PILE

As might be expected, from the definition of a p-y curve given in the previous section, the soil resistance p is a nonlinear function of the deflection y. A family of p-y curves, plotted in the appropriate quadrants, is shown in Fig. 3.2a. That the curves are plotted in the second and fourth quadrants is merely an indication that the soil resistance p is opposite in sign to the deflection y. While the p-y curves in Fig. 3.2a are only illustrative, they are typical of many such families of curves in that the initial stiffness and the maximum resistance increase with depth.

A typical p-y curve is shown in Fig. 3.2b; it is plotted in the first quadrant for convenience. The curve is strongly nonlinear, changing from an initial stiffness E_{si} to an ultimate resistance p_u. As is evident, the soil modulus E_s is not a constant except for a small range of deflections.

The three factors that have the most influence on a p-y curve are the soil properties, the pile geometry, and the nature of loading. The correlations that have been developed for predicting soil response are based on the best estimate of the properties of the in situ soil with no adjustment for the effects of the method of installation on soil properties. The logic supporting this approach is that the effects of pile installation on soil properties are principally confined to a zone of soil close to the pile wall, while a mass of soil of several diameters from the pile is stressed as lateral deflection occurs. There are instances, of course, where the method of pile installation must be considered; for example, if a pile is jetted into place, a considerable volume of soil could be removed with a significant effect on the soil response.

The principal dimension of a pile affecting the soil response is its diameter. All of the recommendations for developing p-y curves include a

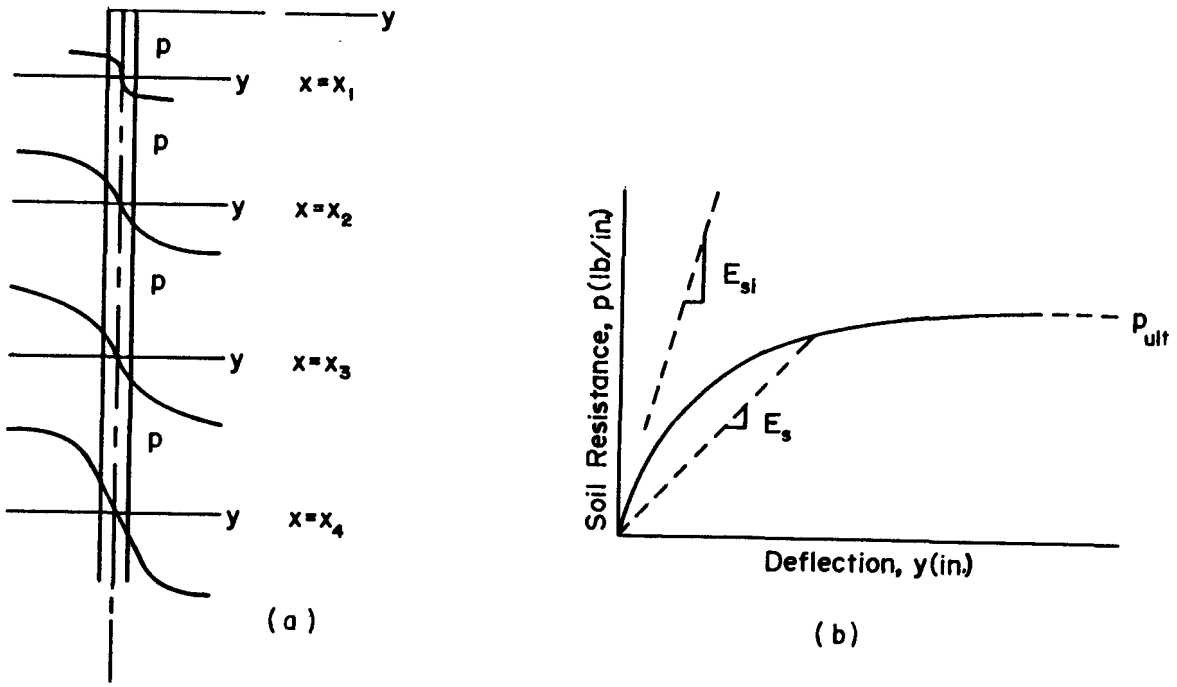

Fig. 3.2. Typical p-y curves
(a) family of curves
(b) characteristic shape of p-y curve.

term for the diameter of the pile; if the cross-section of the pile is not circular, the width of the pile perpendicular to the direction of loading is usually taken as the diameter.

The p-y curves are strongly responsive to the nature of the loading. Recommendations have been developed for predicting curves for short-term static loading and for cyclic (or repeated) loading. However, there are no current recommendations for the cases where the loading is dynamic or sustained. Recommendations for p-y curves where the inertia of the soil is considered are needed because of the desirability of developing rational methods of analyzing pile-supported structures that are subjected to earthquake loadings. With regard to sustained loadings, as from a retaining wall, it is unlikely that criteria can be developed for predicting p-y curves. The problem must be solved as a whole, taking into account the three-dimensional consolidation that will occur as well as the time-dependent changes in loading. From the standpoint of practice, the engineer can probably estimate some additional amount of deflection that will occur if he has the earth pressure distribution along a pile at the beginning of the loading period.

3.2 USE OF THEORY OF ELASTICITY TO DETERMINE SOIL BEHAVIOR

The theory of elasticity is of limited use in solving the problem of the response of soil to pile deflection because experience has shown that the soil-response curve is linear only for small deflections of the pile. In spite of this limitation, some useful contributions, based essentially on the theory of elasticity, have been made. The papers of Skempton (1951), Terzaghi (1955), and McClelland and Focht (1958) have been selected for review.

Skempton

The author states that "simple theoretical considerations" were employed to develop a prediction for load-settlement curves for footings. The theory can be employed to obtain the p-y curve for a pile if it is assumed that the depth is such that the curve is not affected by the free surface of the soil, that the state of stress is the same in the horizontal and vertical directions, and that the soil is isotropic.

The mean settlement of a foundation, ρ, of width b, on the surface of a semi-infinite solid, based on the theory of elasticity, is given by the following expression.

$$\rho = qbI_\rho \frac{1-\nu^2}{E} \tag{3.1}$$

where

q = foundation pressure,
I_ρ = influence value,
ν = Poisson's ratio of the solid, and
E = Young's modulus of the solid.

With regard to Eq. 3.1, Poisson's ratio can be assumed to be equal to 1/2 for saturated clays if there is no change in water content and I_ρ can be taken as $\pi/4$ for a rigid circular footing on the surface. Furthermore, for a rigid circular footing, the failure stress q_f may be taken as equal to 6.8c, where c is the undrained shear strength. Making the substitutions indicated, and setting ρ equal to ρ_1 for the particular case

$$\frac{\rho_1}{b} = \frac{4}{E/c} = \frac{q}{q_f} . \tag{3.2}$$

Skempton noted that the influence value I_ρ decreases with depth below the surface but the bearing capacity factor increases; therefore, as a first approximation Eq. 3.2 is valid for any depth.

In an undrained compression test the axial strain is given by the following equation.

$$\varepsilon = \frac{(\sigma_1 - \sigma_3)}{E} = \frac{\sigma_\Delta}{E} \tag{3.3}$$

where

E = Young's modulus at the stress $(\sigma_1 - \sigma_3)$.

For saturated clays with no water content change, Eq. 3.3 may be rewritten as follows.

$$\varepsilon = \frac{2}{E/c} \frac{(\sigma_1 - \sigma_3)}{(\sigma_1 - \sigma_3)_f} \tag{3.4}$$

where

$(\sigma_1 - \sigma_3)_f$ = failure stress.

It may be noted by comparing Eqs. 3.2 and 3.4 that, for the same ratio of applied stress to ultimate stress, the strain in the footing test (or pile under lateral loading) is related to the strain in the laboratory compression test by the following equation.

$$\frac{\rho_1}{b} = 2\varepsilon \tag{3.5}$$

Skempton's arguments based on the theory of elasticity and also on the actual behavior of full-scale foundations led to the following conclusion:

> Thus, to a degree of approximation (20 percent) comparable with the accuracy of the assumptions, it may be taken that Eq. 3.5 applies to a circular or any rectangular footing.

While the analytical approach employed by Skempton involves numerous approximations, the method has gained some acceptance because of the experimental evidence presented by Skempton and others (Reese, et al., 1975).

Skempton stated that the failure stress for a footing reaches a maximum value of 9c. If one takes that value of a pile in saturated clay under lateral loading, p_u becomes 9cb. A p-y curve could be obtained, then, by taking points from a laboratory stress-strain curve and using Eq. 3.5 to obtain deflection and 4.5 $\sigma_\Delta b$ to obtain soil resistance. The procedure would presumably be valid at depths beyond where the presence of the ground surface would not reduce the soil resistance. Skempton did not suggest that his ideas could be used in obtaining p-y curves and no sug-

gestions in that regard are made here. However, the concepts employed by Skempton are useful and of interest.

Terzaghi

While Skempton presented an analytical approach for the prediction of curves giving the deflection of a footing as a function of bearing stress, Terzaghi's approach is much less direct. He does call on principles of mechanics in his presentation; however, he fails to give a step-by-step procedure for his derivations and he also fails to cite any experimental evidence that would verify his recommendations. One would suppose that Terzaghi has used the theory of elasticity freely in his development of the recommended coefficients and that he had some experimental evidence at his disposal but that he chose not to cite his references for his own reasons. While the paper has some obvious shortcomings, the numerical recommendations for soil response are summarized here because of their historical importance and because the recommendations continue to have value.

A reference to an incident in Terzaghi's later years is pertinent. He was one of the principal speakers at the Eighth Texas Conference on Soil Mechanics and Foundation Engineering in the early Fall of 1956 where he read his notable paper, "Submarine Slope Failures." Professor Hudson Matlock and his colleagues were engaged in running the first field tests of a fully-instrumented, laterally loaded pile at Lake Austin. Terzaghi visited the site, expressed an interest in the testing program, but had no particular suggestions to make. His paper on subgrade reaction had just been published and Terzaghi remarked that he was not particularly proud of the paper and that he had only agreed to publish it at the urging of a number of his acquaintances.

Terzaghi's recommendations for the coefficient of subgrade reaction (p-y curves) for stiff clay were based on his notion that the deformational characteristics of stiff clay are "more or less independent of depth." Thus, he proposed, in effect, that the p-y curves should be constant with depth. He further proposed that the ratio between p and y should be constant and defined by the symbol α_T. Therefore, his family of p-y curves for stiff clay consists of a series of straight lines, all of the same slope, passing through the origin of the coordinate system.

Terzaghi recognized, of course, that the pile could not be deflected to an unlimited extent with a linear increase in soil reaction. He stated

that the linear relationship between p and y was valid for values of p that were smaller than about one-half of the ultimate bearing stress.

Table 3.1 presents Terzaghi's recommendations for stiff clay. The units have been changed to reflect current practices. The values of α_T, it should be noted, are independent of pile diameter.

TABLE 3.1. TERZAGHI'S RECOMMENDATIONS FOR SOIL MODULUS α_T FOR LATERALLY LOADED PILES IN STIFF CLAY.

Consistency of Clay	Stiff	Very Stiff	Hard
q_u, T/sq ft	1-2	2-4	> 4
α_T, lb/sq in.	460-925	925-1850	1850-up

With regard to sand, Terzaghi based his recommendations on the fact that the stiffness of the sand increases with confining stress (or with depth). However, he recommended, as with stiff clay, that the soil resistance should be a linear function of y. Again, as with clay he stipulated that his recommended values were valid only for a soil reaction that was no more than one-half of the maximum bearing stress.

Thus, the family of p-y curves recommended by Terzaghi for sand consists of a series of straight lines, with the slope of the lines being zero at the ground surface and increasing linearly with depth. Because E_s, the soil modulus is equal to p/y

$$E_s = kx \tag{3.6}$$

where

k = constant giving variation of soil modulus with depth, and

x = depth below ground surface.

Table 3.2 shows recommendations for k.

TABLE 3.2. TERZAGHI'S RECOMMENDATIONS FOR VALUES OF k FOR LATERALLY LOADED PILES IN SAND.

Relative Density of Sand	Loose	Medium	Dense
Dry or moist, k, lb/cu in.	3.5-10.4	13-40	51-102
Submerged sand, k, lb/cu in.	2.1-6.4	8-27	32-64

McClelland and Focht

The paper by these authors has considerable importance for several reasons: it is the first paper to report experimental p-y curves from a full-scale, instrumented, pile-load test, and it shows conclusively that the soil modulus is not a soil property but is a function of depth and pile deflection. While the paper is not strongly based on the theory of elasticity, it is included in this section because it closely parallels Skempton's approach and because stress-strain curves from laboratory tests are employed in obtaining p-y curves.

The paper recommends the performance of consolidated-undrained triaxial tests with the confining pressure equal to the overburden pressure. To obtain values of the soil resistance p from the stress-strain curves, the authors recommend the following equation:

$$p = 5.5\, b\sigma_{\Delta} \tag{3.7}$$

where

σ_{Δ} = deviator stress $(\sigma_1 - \sigma_3)$

b = pile diameter.

Equation 3.7 agrees well with Skempton's recommendations for the case where the depth divided by the pile diameter is about three or more. As noted earlier, Skempton proposed a factor of 4.5 instead of the 5.5 shown in Eq. 3.7.

To obtain values of pile deflection y from stress-strain curves, McClelland and Focht propose

$$y = 0.5\, b\varepsilon. \tag{3.8}$$

Skempton's corresponding equation suggests a value of 2 rather than 0.5. Part of the difference in these two numbers probably derives from the dif-

ference in the two sets of experiments. Skempton's studies were for footings that were at or near the ground surface; these footings could be expected to have more relative deflection than a segment of pile that is for the most part at some distance below the ground surface.

3.3 USE OF SOIL MODELS TO DETERMINE SOIL BEHAVIOR

The preceding section has presented solutions employing the theory of elasticity, or related approaches, to obtain the response of the soil to the lateral deflection of a pile. This section reviews the use of soil models to obtain expressions that will indicate approximately the ultimate resistance against a pile that can be developed near the ground surface and at some depth below the ground surface.

Soil Models for Saturated Clay

The assumed model for estimating the ultimate soil resistance near the ground surface is shown in Fig. 3.3 (Reese, 1958). The force F_p is

$$F_p = c_a bH [\tan \alpha_c + (1+K) \cot \alpha_c] + 1/2 \gamma bH^2 + c_a H^2 \sec \alpha_c \quad (3.9)$$

where

c_a = average undrained shear strength

K = a reduction factor to be multiplied by c_a to yield the average sliding stress between the pile and the stiff clay, and

γ = average unit weight of soil.

(the other terms are defined in the figure)

It is possible to take the partial derivative of Eq. 3.9 with respect to the angle α and set it equal to zero to find the angle at which the equation is minimized. However, as an approximation the angle α_c is taken as 45° and K is assumed equal to zero. Differentiation of the resulting expression with respect to H yields an expression for the ultimate soil resistance near the ground surface as follows:

$$(p_u)_{ca} = 2c_a b + \gamma bH + 2.83\, c_a H . \quad (3.10)$$

It can be reasoned that, at some distance below the ground surface, the soil must flow around the deflected pile. The model for such movement is shown in Fig. 3.4a. If it is assumed that blocks 1, 2, 4, and 5 fail by shear and that block 3 develops resistance by sliding, the stress conditions are represented by Fig. 3.4b. By examining a free body of a section of the pile, Fig. 3.4c, one can conclude that the ultimate soil resistance

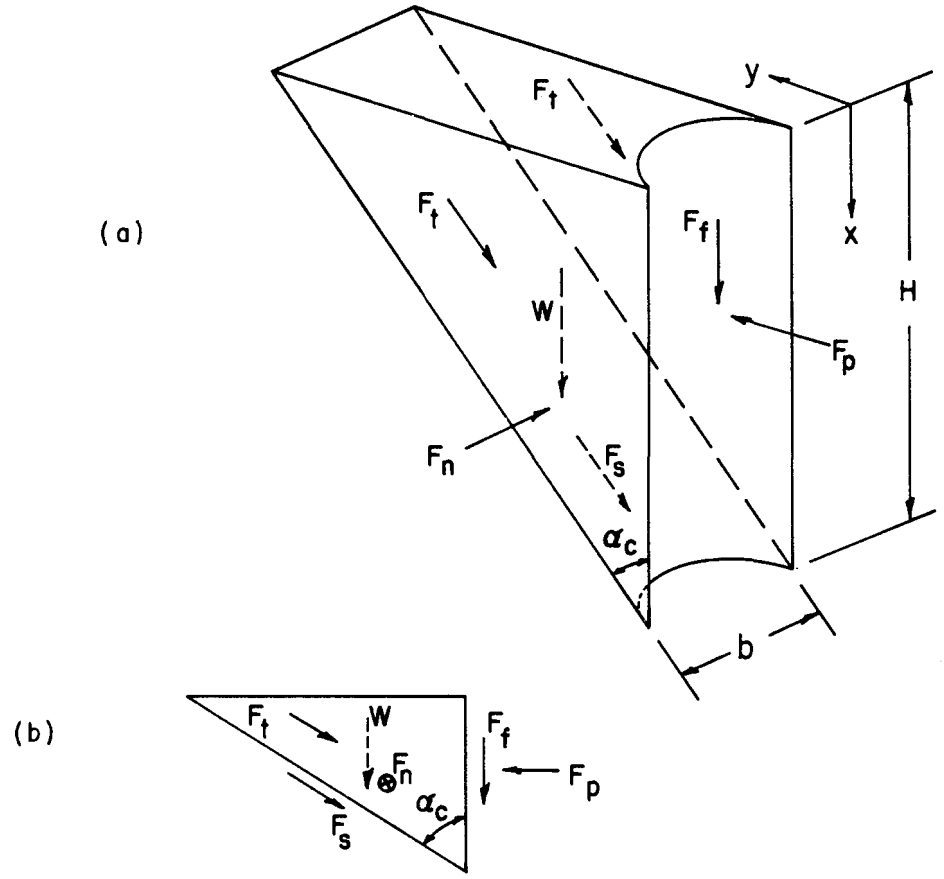

Fig. 3.3. Assumed passive wedge-type failure for clay
(a) shape of wedge
(b) forces acting on wedge.

at depth is:

$$(p_u)_{cb} = 11\ cb\ . \tag{3.11}$$

Equations 3.10 and 3.11 are, of course, approximate but they do indicate the general form of the expressions that give the ultimate soil resistance along the pile. The equations can be solved simultaneously to find the depth at which the failure would change from the wedge type to the flow-around type.

Soil Models for Sand

The soil model for computing the ultimate resistance near the ground surface for sand is shown in Fig. 3.5a (Reese, Cox, and Koop, 1974). The total lateral force F_{pt} (Fig. 3.5c) may be computed by subtracting the active force F_a, computed using Rankine theory, from the passive force F_p,

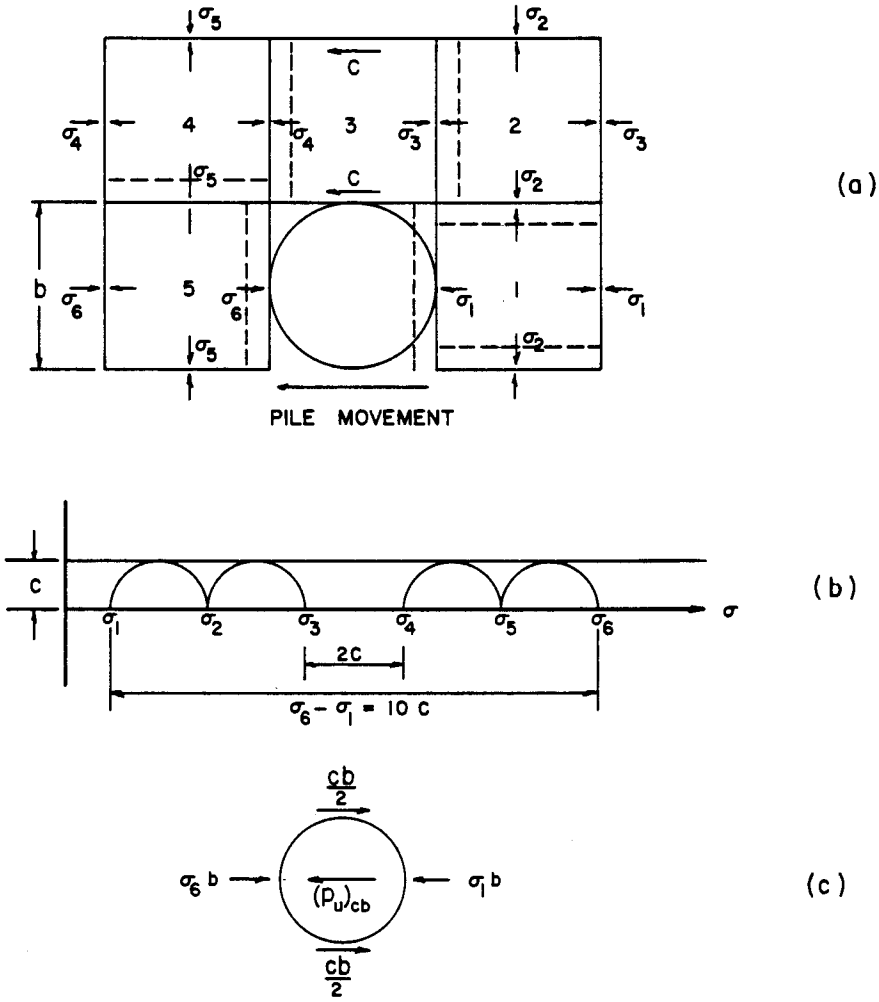

Fig. 3.4. Assumed lateral flow-around type of failure for clay (a) section through pile (b) Mohr-Coulomb diagram (c) forces acting on section of pile.

computed from the model. The force F_p is computed assuming that the Mohr-Coulomb failure condition is satisfied on planes ADE, BCF, and AEFB. The directions of the forces are shown in Fig. 3.5b. No frictional force is assumed to be acting on the face of the pile. The equation for F_{pt} is as follows.

$$F_{pt} = \gamma H^2 \left[\frac{K_o H \tan\phi \sin\beta}{3 \tan(\beta-\phi) \cos\alpha_s} + \frac{\tan\beta}{\tan(\beta-\phi)} \left(\frac{b}{2} + \frac{H}{3} \tan\beta \tan\alpha_s \right) + \frac{K_o H \tan\beta}{3} (\tan\phi \sin\beta - \tan\alpha_s) - \frac{K_a b}{2} \right] \quad (3.12)$$

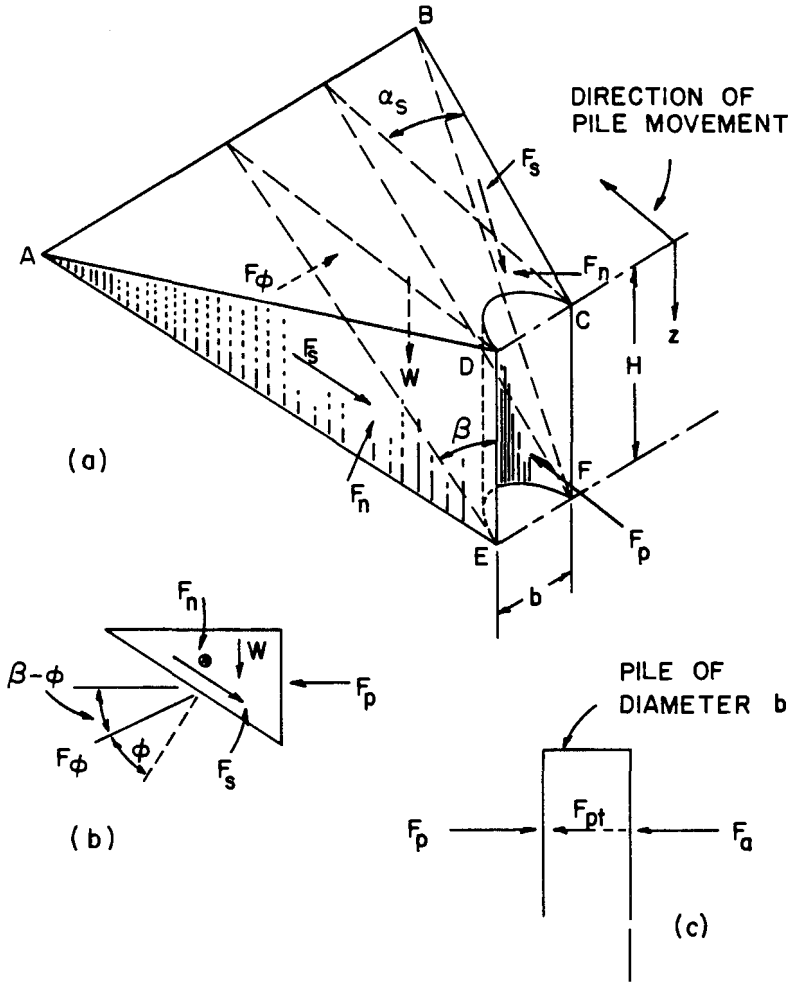

Fig. 3.5. Assumed passive wedge-type failure of pile in sand (a) general shape of wedge (b) forces on wedge (c) forces on pile.

where

K_o = coefficient of earth pressure at rest

K_a = minimum coefficient of active earth pressure.

The ultimate soil resistance near the ground surface per unit length of the pile is obtained by differentiating Eq. 3.12.

$$(p_u)_{sa} = \gamma H \left[\frac{K_o H \tan\phi \sin\beta}{\tan(\beta-\phi)\cos\alpha_s} + \frac{\tan\beta}{\tan(\beta-\phi)} (b + H \tan\beta \tan\alpha_s) \right.$$
$$\left. + K_o H \tan\beta (\tan\phi \sin\beta - \tan\alpha_s) - K_a b \right] \qquad (3.13)$$

Bowman (1958) suggested values of α_s from $\phi/3$ to $\phi/2$ for loose sand up to ϕ for dense sand. The value of β is approximated as follows.

$$\beta = 45 + \frac{\phi}{2} \tag{3.14}$$

The model for computing the ultimate soil resistance at some distance below the ground surface is shown in Fig. 3.6a. The stress σ_1, at the back of the pile must be equal to or larger than the minimum active earth pressure; if not, the soil could fail by slumping. This assumption is based on two-dimensional behavior, of course, and is subject to some uncertainty. However, the assumption should be adequate for the present purposes. Assuming the states of stress shown in Fig. 3.6b, the ultimate soil resistance for horizontal flow around the pile is

$$(p_u)_{sb} = K_a b\gamma H (\tan^8\beta - 1) + K_o b\gamma H \tan\phi \tan^4\beta. \tag{3.15}$$

As in the case for clay, Eqs. 3.14 and 3.15 are approximate but they serve a useful purpose in indicating the form, if not the magnitude, of the ultimate soil resistance. The two equations can be solved simultaneously to find the approximate depth at which the soil failure changes from the wedge type to the flow-around type.

3.4 EXPERIMENTAL METHODS FOR OBTAINING SOIL RESPONSE CURVES

The above paragraphs describe methods for obtaining soil response based primarily on theory. (An exception is the method of McClelland and Focht that was based on some experimental results.) The strategy that has been employed for obtaining design criteria is to make use of the theoretical methods, to obtain p-y curves from full-scale field experiments, and to derive such empirical factors as necessary so that there is close agreement between results from adjusted theoretical solutions and those from experiments. Thus, an important procedure is obtaining experimental p-y curves.

Soil Response from Direct Measurement

A number of attempts have been made to make direct measurement of p and y in the field. Measuring the deflection involves the conceptually simple process of sighting down a hollow pipe from a fixed position at scales that have been placed at intervals along the length of the pile. The method is cumbersome in practice and has not been very successful.

The measurement of the soil resistance directly involves the design of an instrument that will integrate the soil stresses at a point along

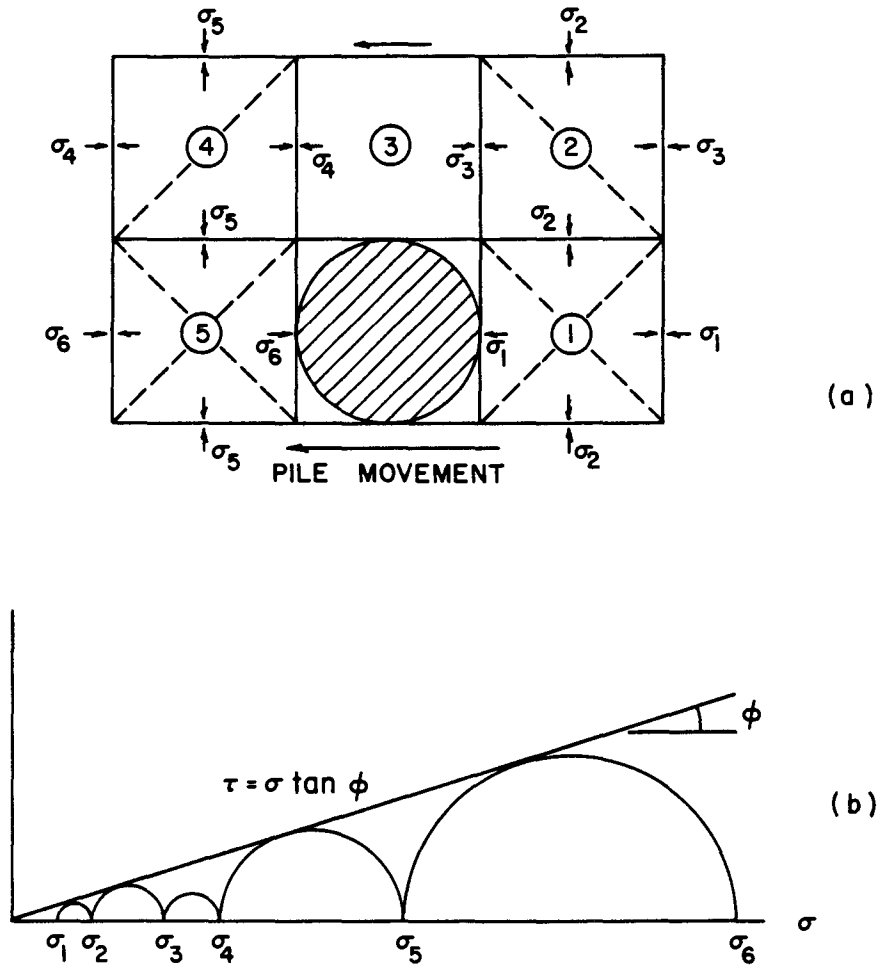

Fig. 3.6. Assumed mode of soil failure by lateral flow around a pile in sand
(a) section through the pile
(b) Mohr-Coulomb diagram representing states of stress of soil flowing around a pile.

the pile. The design of such an instrument has been proposed but none has yet been built. Some attempts have been made to measure the soil pressure at a few points around the exterior of a pile with the view that the soil pressures at other points can be estimated. This method has met with little success.

Soil Response from Experimental Moment Curves

Almost all of the successful experiments that yielded p-y curves have involved the measurement of bending moment by the use of electrical resistance strain gauges. The deflection can be obtained with considerable accuracy by two integrations of the moment curves. The deflection

and the slope at the groundline have to be measured accurately and it is helpful if the pile is long enough so that there are at least two points of zero deflection along the lower portion of the pile.

The computation of soil resistance along the length of the pile involves two differentiations of a bending moment curve. Matlock (1970) made extremely accurate measurements of bending moment and was able to do the differentiations numerically. However, most other investigators have fitted analytic curves through the points of experimental bending moment and have performed the differentiations mathematically.

With families of curves showing the distribution of deflection and soil resistance, p-y curves can be plotted. A check can be made of the accuracy of the analyses by using the experimental p-y curves to compute bending-moment curves. The computed bending moments should agree closely with those from experiment.

Nondimensional Methods for Obtaining Soil Response

Reese and Cox (1968) described a method for obtaining p-y cuves for those instances where only pile-head measurements were made during lateral loading. They noted that nondimensional curves can be obtained for many variations of soil modulus with depth. Equations for the soil modulus involving two parameters were employed, such as shown in Eqs. 3.16 and 3.17.

$$E_s = k_1 + k_2 x \tag{3.16}$$

$$E_s = k_1 x^n \tag{3.17}$$

From measurement of pile-head deflection and rotation at the groundline, the two parameters were computed for a given applied load and moment. With an expression for soil modulus for a particular load, the soil resistance and deflection along the pile were computed.

The procedure was repeated for each of the applied loadings and p-y curves were plotted from the computed families of curves of deflection and soil resistance. While the method is approximate, the p-y curves computed in this fashion do reflect the measured behavior of the pile head. Soil response derived from a sizeable number of such experiments can add significantly to the existing information.

As previously indicated, the major field experiments that have led to the development of the current criteria for p-y curves have involved the acquisition of experimental moment curves. However, nondimensional methods of analyses have assisted in the development of p-y curves in some instances.

3.5 RECOMMENDATIONS FOR p-y CURVES FOR CLAYS

Three major experimental programs were performed for piles in clays to yield the criteria which follow. In each case the piles were subjected to short-term static loads and to repeated (cyclic) loads. The experimental program is described briefly in the paragraphs that follow, a step-by-step procedure is given for computing the p-y curves, recommendations are given for obtaining the necessary data on soil properties, and example curves are presented.

The final portion of this section on clays presents a method that has been developed for predicting p-y curves in clays of any shear strength. This "unified" method is based on all of the major experiments in clay below the water table.

As noted in the following sections, repeated loading of the clay has a pronounced effect on the soil response, particularly when water covers the ground surface. The loss of resistance from repeated loading is due to two effects: the breakdown of the structure of the clay (remolding) and scour. The remolding is a result of the repeated strains that occur due to the deflection of the pile. The scour occurs when the pile deflects enough to cause a gap to remain between pile and soil when the load is removed. Water will flow into the gap and will be ejected on the next application of load. The water in most cases will move out at a high velocity and carry out particles of clay.

If the clay is above the water table, only the first of the two effects will be present. Therefore, the recommendations for p-y curves that are presented are dependent on the position of the water table.

Response of Soft Clay below the Water Table

Field Experiments. Matlock (1970) performed lateral load tests employing a steel pipe pile that was 12.75 in. in diameter and 42 ft long. It was driven into clays near Lake Austin that had a shear strength of about 800 lb/sq ft. The pile was recovered, taken to Sabine Pass, Texas, and driven into clay with a shear strength that averaged about 300 lb/sq ft in the significant upper zone.

Recommendations for Computing p-y Curves. The following procedure is for short-term static loading and is illustrated by Fig. 3.7a.

1. Obtain the best possible estimate of the variation with depth of undrained shear strength c and submerged unit weight γ'. Also obtain the values of ε_{50}, the strain corre-

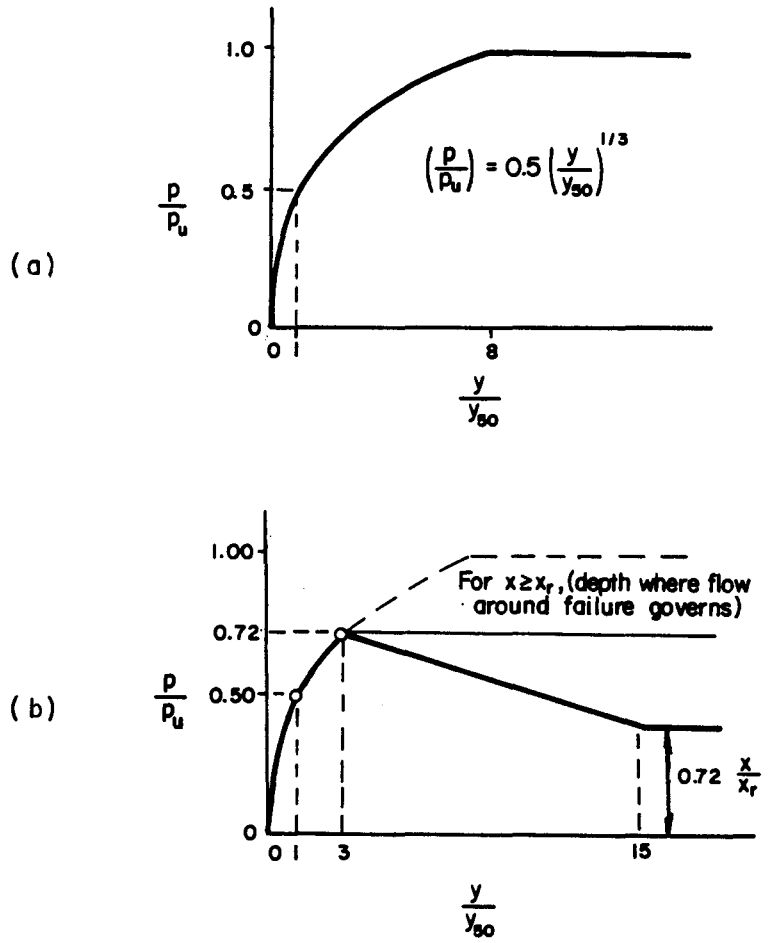

Fig. 3.7. Characteristic shapes of the p-y curves for soft clay below the water table
(a) for static loading
(b) for cyclic loading
(from Matlock, 1970).

sponding to one-half the maximum principal-stress difference. If no stress-strain curves are available, typical values of ε_{50} are given in Table 3.3.

2. Compute the ultimate soil resistance per unit length of pile, using the smaller of the values given by equations below.

$$p_u = \left[3 + \frac{\gamma'}{c} x + \frac{J}{b} x\right] cb \qquad (3.18)$$

$$p_u = 9\, cb \qquad (3.19)$$

TABLE 3.3. REPRESENTATIVE VALUES OF ε_{50}.

Consistency of Clay	ε_{50}
Soft	0.020
Medium	0.010
Stiff	0.005

(Also see Tables 3.5 and 3.6)

where

γ' = average effective unit weight from ground surface to p-y curve

x = depth from ground surface to p-y curve

c = shear strength at depth x

b = width of pile.

Matlock (1970) states that the value of J was determined experimentally to be 0.5 for a soft clay and about 0.25 for a medium clay. A value of 0.5 is frequently used for J. The value of p_u is computed at each depth where a p-y curve is desired, based on shear strength at that depth.

3. Compute the deflection, y_{50}, at one-half the ultimate soil resistance from the following equation:

$$y_{50} = 2.5\ \varepsilon_{50} b. \tag{3.20}$$

4. Points describing the p-y curve are now computed from the following relationship.

$$\frac{p}{p_u} = 0.5 \left(\frac{y}{y_{50}}\right)^{\frac{1}{3}} \tag{3.21}$$

The value of p remains constant beyond $y = 8y_{50}$.

The following procedure is for cyclic loading and is illustrated in Fig. 3.7b.

1. Construct the p-y curve in the same manner as for short-term static loading for values of p less than $0.72p_u$.

2. Solve Eqs. 3.18 and 3.19 simultaneously to find the depth, x_r, where the transition occurs. If the unit weight and shear strength are constant in the upper zone, then

$$x_r = \frac{6cb}{(\gamma' b + Jc)} . \qquad (3.22)$$

If the unit weight and shear strength vary with depth, the value of x_r should be computed with the soil properties at the depth where the p-y curve is desired.

3. If the depth to the p-y curve is greater than or equal to x_r, then p is equal to $0.72p_u$ for all values of y greater than $3y_{50}$.
4. If the depth to the p-y curve is less than x_r, then the value of p decreases from $0.72p_u$ at $y = 3y_{50}$ to the value given by the following expression at $y = 15y_{50}$.

$$p = 0.72p_u \left(\frac{x}{x_r} \right) \qquad (3.23)$$

The value of p remains constant beyond $y = 15y_{50}$.

Recommended Soil Tests. For determining the various shear strengths of the soil required in the p-y construction, Matlock (1970) recommended the following tests in order of preference:

1. in-situ vane-shear tests with parallel sampling for soil identification,
2. unconsolidated-undrained triaxial compression tests having a confining stress equal to the overburden pressure with c being defined as half the total maximum principal stress difference,
3. miniature vane tests of samples in tubes, and
4. unconfined compression tests.

Tests must also be performed to determine the unit weight of the soil.

Example Curves. An example set of p-y curves was computed for soft clay for a pile with a diameter of 48 in. The soil profile that was used is shown in Fig. 3.8. The submerged unit weight was assumed to be 20 lb/cu ft at the mudline and 40 lb/cu ft at a depth of 80 ft and to vary linearly. In the absence of a stress-strain curve for the soil, ε_{50} was taken as 0.01 for the full depth of the soil profile. The loading was assumed to be cyclic.

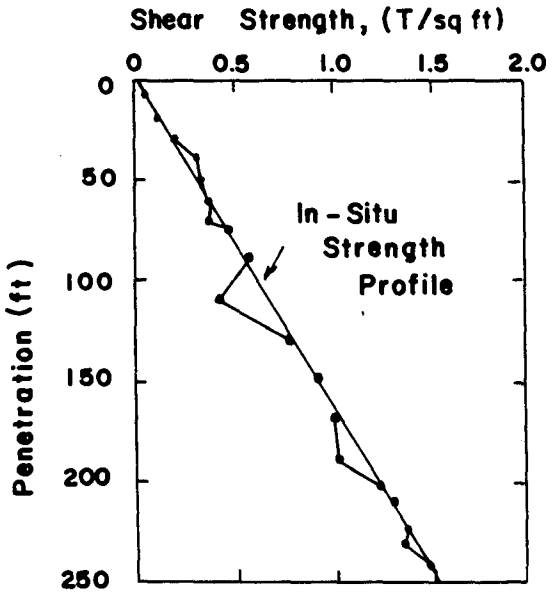

Fig. 3.8. Soil profile used for example p-y curves for soft clay.

The p-y curves were computed for the following depths below the mudline: 0, 1, 2, 4, 8, 12, 20, 40, and 60 ft. The plotted curves are shown in Fig. 3.9 (curves for 0 and 1 ft too close to axis to be shown).

Response of Stiff Clay below the Water Table

Field Experiments. Reese, Cox, and Koop (1975) performed lateral load tests employing steel-pipe piles that were 24 in. in diameter and 50 ft long. The piles were driven into stiff clay at a site near Manor, Texas. The clay had an undrained shear strength ranging from about 1 T/sq ft at the ground surface to about 3 T/sq ft at a depth of 12 ft.

Recommendations for Computing p-y Curves. The following procedure is for short-term static loading and is illustrated by Fig. 3.10.

1. Obtain values for undrained soil shear strength c, soil submerged unit weight γ', and pile diameter b.
2. Compute the average undrained soil shear strength c_a over the depth x.
3. Compute the ultimate soil resistance per unit length of pile using the smaller of the values given by the equation below:

$$P_{ct} = 2c_a b + \gamma' bx + 2.83\, c_a x\,, \tag{3.24}$$

$$P_{cd} = 11\, cb. \tag{3.25}$$

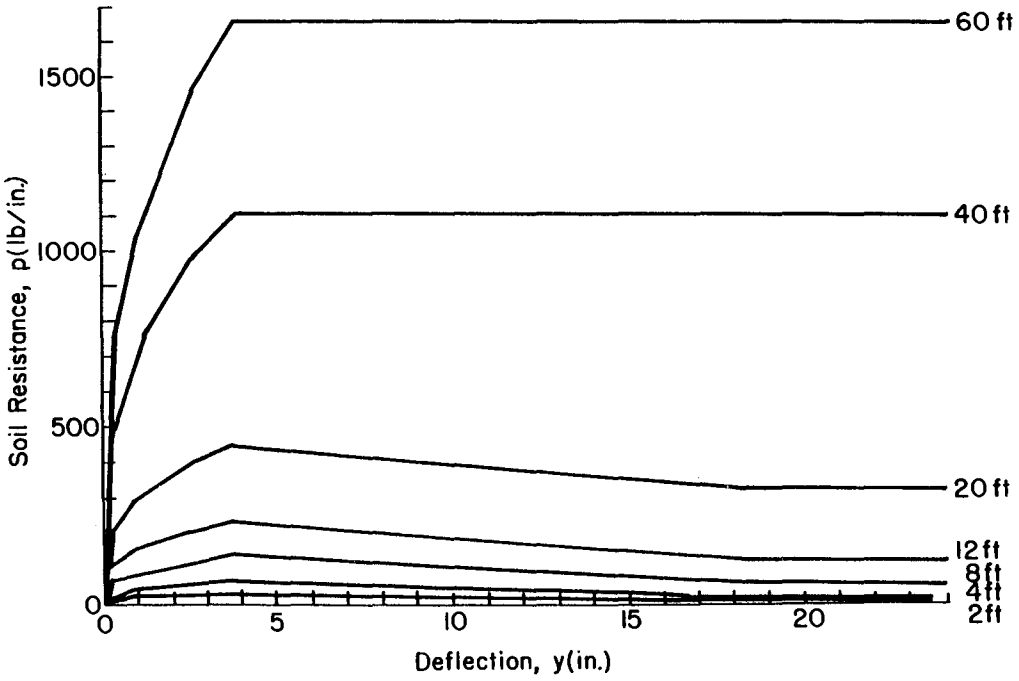

Fig. 3.9. Example p-y curves for soft clay below water table, Matlock criteria, cyclic loading.

4. Choose the appropriate value of A_s from Fig. 3.11 for the particular nondimensional depth.
5. Establish the initial straight-line portion of the p-y curve:

$$p = (kx)y. \tag{3.26}$$

Use the appropriate value of k_s or k_c from Table 3.4 for k.

6. Compute the following:

$$y_{50} = \varepsilon_{50} b. \tag{3.27}$$

Use an appropriate value of ε_{50} from results of laboratory tests or, in the absence of laboratory tests, from Table 3.5.

7. Establish the first parabolic portion of the p-y curve, using the following equation and obtaining p_c from Eqs. 3.24 or 3.25.

$$p = 0.5 p_c \left(\frac{y}{y_{50}}\right)^{0.5} \tag{3.28}$$

Equation 3.28 should define the portion of the p-y curve

TABLE 3.4. REPRESENTATIVE VALUES OF k FOR STIFF CLAYS.

	Average Undrained Shear Strength* T/sq ft		
	0.5-1	1-2	2-4
k_s (Static) lb/cu in.	500	1000	2000
k_c (Cyclic) lb/cu in.	200	400	800

* The average shear strength should be computed from the shear strength of the soil to a depth of 5 pile diameters. It should be defined as half the total maximum principal stress difference in an unconsolidated undrained triaxial test.

TABLE 3.5. REPRESENTATIVE VALUES OF ε_{50} FOR STIFF CLAYS

	Average Undrained Shear Strength T/sq ft		
	0.5-1	1-2	2-4
ε_{50} (in./in.)	0.007	0.005	0.004

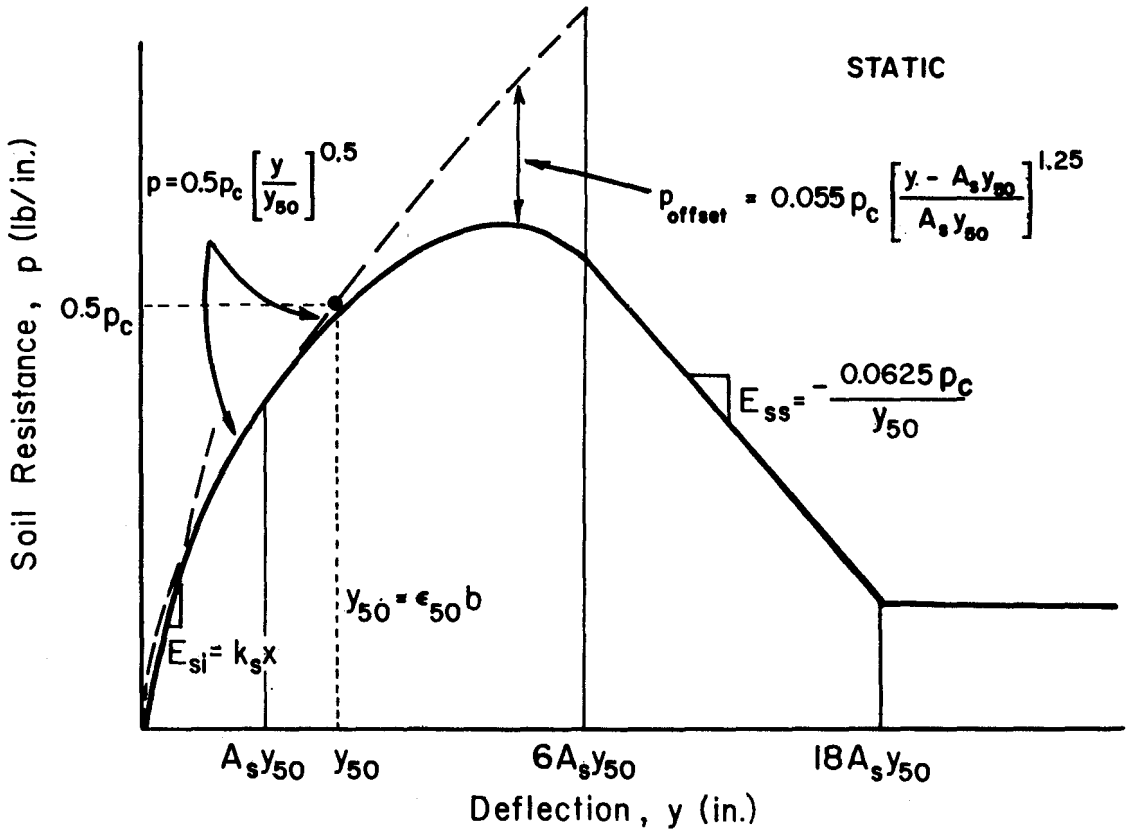

Fig. 3.10. Characteristic shape of p-y curve for static loading in stiff clay below the water table (after Reese, Cox, Koop, 1975).

from the point of the intersection with Eq. 3.26 to a point where y is equal to $A_s y_{50}$ (see note in step 10).

8. Establish the second parabolic portion of the p-y curve,

$$p = 0.5p_c \left(\frac{y}{y_{50}}\right)^{0.5} - 0.055p_c \left(\frac{y - A_s y_{50}}{A_s y_{50}}\right)^{1.25}. \quad (3.29)$$

Equation 3.29 should define the portion of the p-y curve from the point where y is equal to $A_s y_{50}$ to a point where y is equal to $6A_s y_{50}$ (see note in step 10).

9. Establish the next straight-line portion of the p-y curve,

$$p = 0.5p_c(6A_s)^{0.5} - 0.411p_c - \frac{0.0625}{y_{50}} p_c(y - 6A_s y_{50}). \quad (3.30)$$

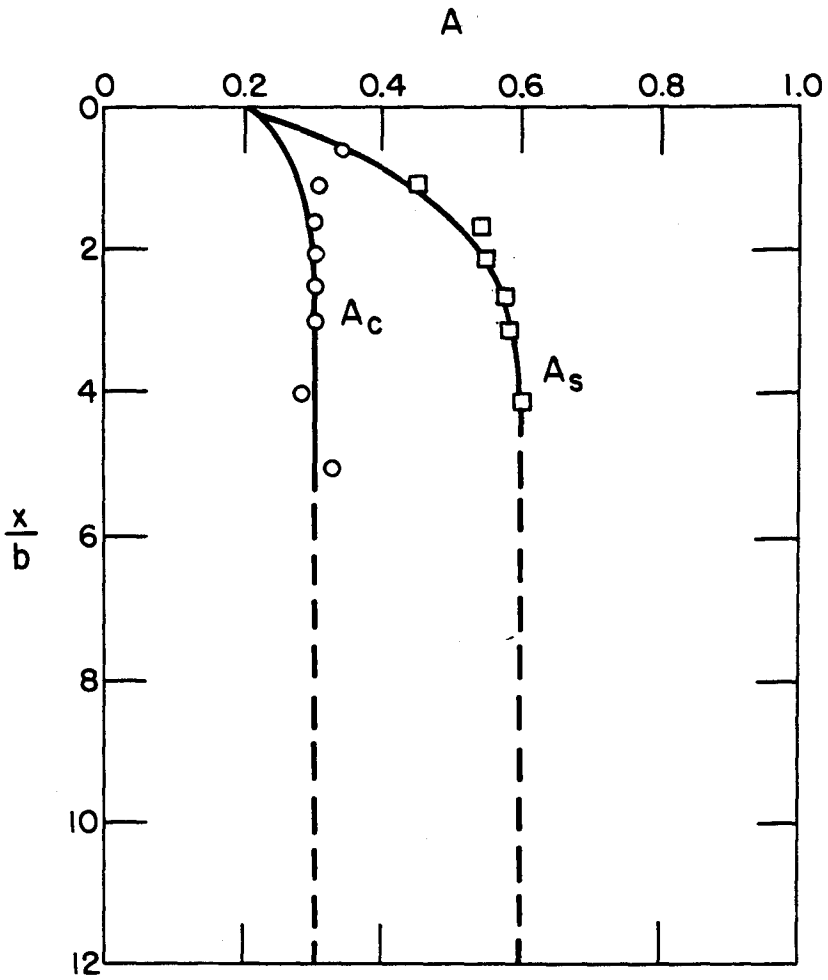

Fig. 3.11. Values of constants A_s and A_c.

Equation 3.30 should define the portion of the p-y curve from the point where y is equal to $6A_s y_{50}$ to a point where y is equal to $18A_s y_{50}$ (see note in step 10).

10. Establish the final straight-line portion of the p-y curve,

$$p = 0.5p_c(6A_s)^{0.5} - 0.411p_c - 0.75p_cA_s \qquad (3.31)$$

or

$$p = p_c(1.225\sqrt{A_s} - 0.75A_s - 0.411). \qquad (3.32)$$

Equation 3.32 should define the portion of the p-y curve from the point where y is equal to $18A_s y_{50}$ and for all larger values of y (see following note).

Note: The step-by-step procedure is outlined, and Fig. 3.10 is drawn, as if there is an intersection between Eqs.

3.26 and 3.28. However, there may be no intersection of Eq. 3.26 with any of the other equations or, if no intersection occurs, Eq. 3.26 defines the complete p-y curve.

The following procedure is for cyclic loading and is illustrated in Fig. 3.12.

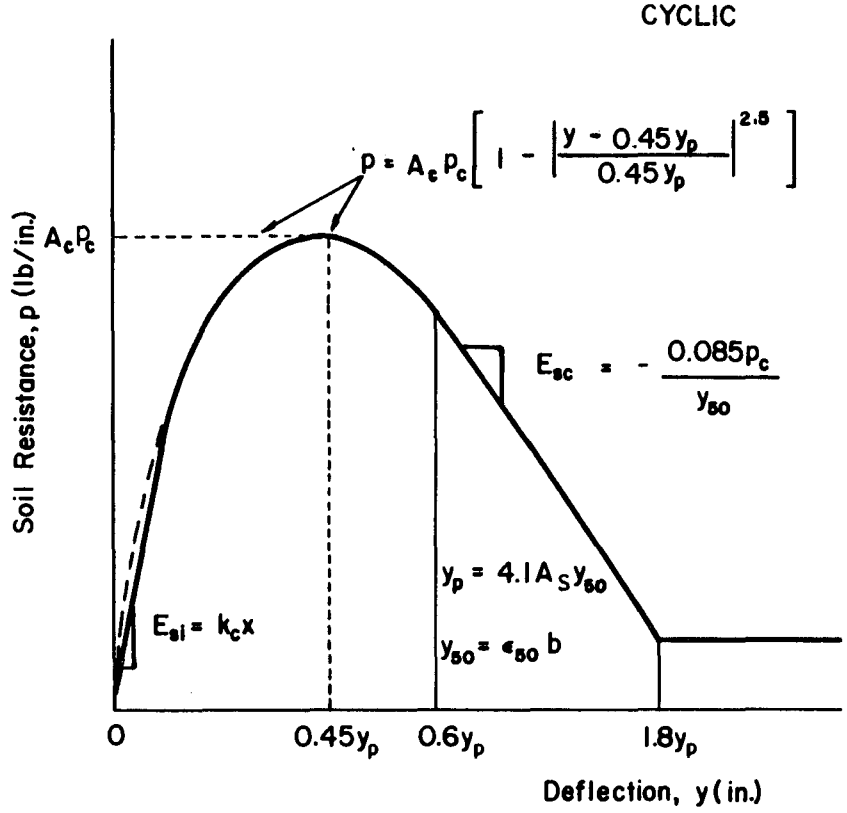

Fig. 3.12. Characteristic shape of p-y curve for cyclic loading in stiff clay below water table (after Reese, Cox, Koop, 1975).

1. Steps 1, 2, 3, 5, and 6 are the same as for the static case.
4. Choose the appropriate value of A_c from Fig. 3.11 for the particular nondimensional depth.

Compute the following:

$$y_p = 4.1\, A_s y_{50}. \tag{3.33}$$

7. Establish the parabolic portion of the p-y curve,

$$p = A_c p_c \left[1 - \left| \frac{y - 0.45\, y_p}{0.45\, y_p} \right| 2.5 \right]. \tag{3.34}$$

Equation 3.34 should define the portion of the p-y curve from the point of the intersection with Eq. 3.26 to where y is equal to $0.6y_p$ (see note in step 9).

8. Establish the next straight-line portion of the p-y curve,

$$p = 0.936\ A_c p_c - \frac{0.085}{y_{50}}\ p_c\ (y - 0.6y_p)\ . \qquad (3.35)$$

Equation 3.35 should define the portion of the p-y curve from the point where y is equal to $0.6y_p$ to the point where y is equal to $1.8y_p$ (see note in step 9).

9. Establish the final straight-line portion of the p-y curve,

$$p = 0.936\ A_c p_c - \frac{0.102}{y_{50}}\ p_c y_p\ . \qquad (3.36)$$

Equation 3.36 should define the portion of the p-y curve from the point where y is equal to $1.8y_p$ and for all larger values of y (see following note).

Note: The step-by-step procedure is outlined, and Fig. 3.12 is drawn, as if there is an intersection between Eqs. 3.26 and 3.34. However, there may be no intersection of those two equations and there may be no intersection of Eq. 3.26 with any of the other equations defining the p-y curve. If there is no intersection, the equation should be employed that gives the smallest value of p for any value of y.

Recommended Soil Tests. Triaxial compression tests of the unconsolidated-undrained type with confining pressures conforming to the in situ overburden pressures are recommended for determining the shear strength of the soil. The value of ε_{50} should be taken as the strain during the test corresponding to the stress equal to half the maximum total-principal-stress difference. The shear strength, c, should be interpreted as one-half of the maximum total-stress difference. Values obtained from the triaxial tests might be somewhat conservative but would represent more realistic strength values than other tests. The unit weight of the soil must be determined.

Example Curves. An example set of p-y curves was computed for stiff clay for a pile with a diameter of 48 in. The soil profile that was used is shown in Fig. 3.13. The submerged unit weight of the soil was assumed to be 50 lb/cu ft for the entire depth. In the absence of a stress-strain

curve, ε_{50} was taken as 0.005 for the full depth of the soil profile. The slope of the initial portion of the p-y curve was established by assuming a value of k of 463 lb/cu in. The loading was assumed to be cyclic.

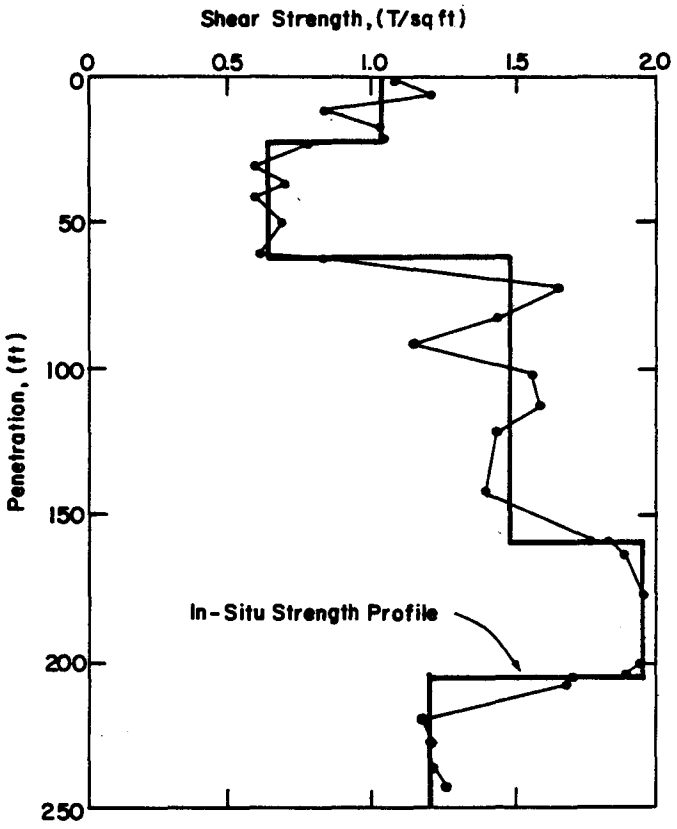

Fig. 3.13. Soil profile used for example p-y curves for stiff clay.

The p-y curves were computed for the following depths below the mudline: 0, 2, 4, 8, 12, 20, 40, and 60 ft. The plotted curves are shown in Fig. 3.14.

Response of Stiff Clay above the Water Table

Field Experiments. A lateral load test was performed at a site in Houston on a drilled shaft, 36 in. in diameter. A 10-in. diameter pipe, instrumented at intervals along its length with electrical-resistance-strain gauges, was positioned along the axis of the shaft before concrete was placed. The embedded length of the shaft was 42 ft. The average undrained shear strength of the clay in the upper 20 ft

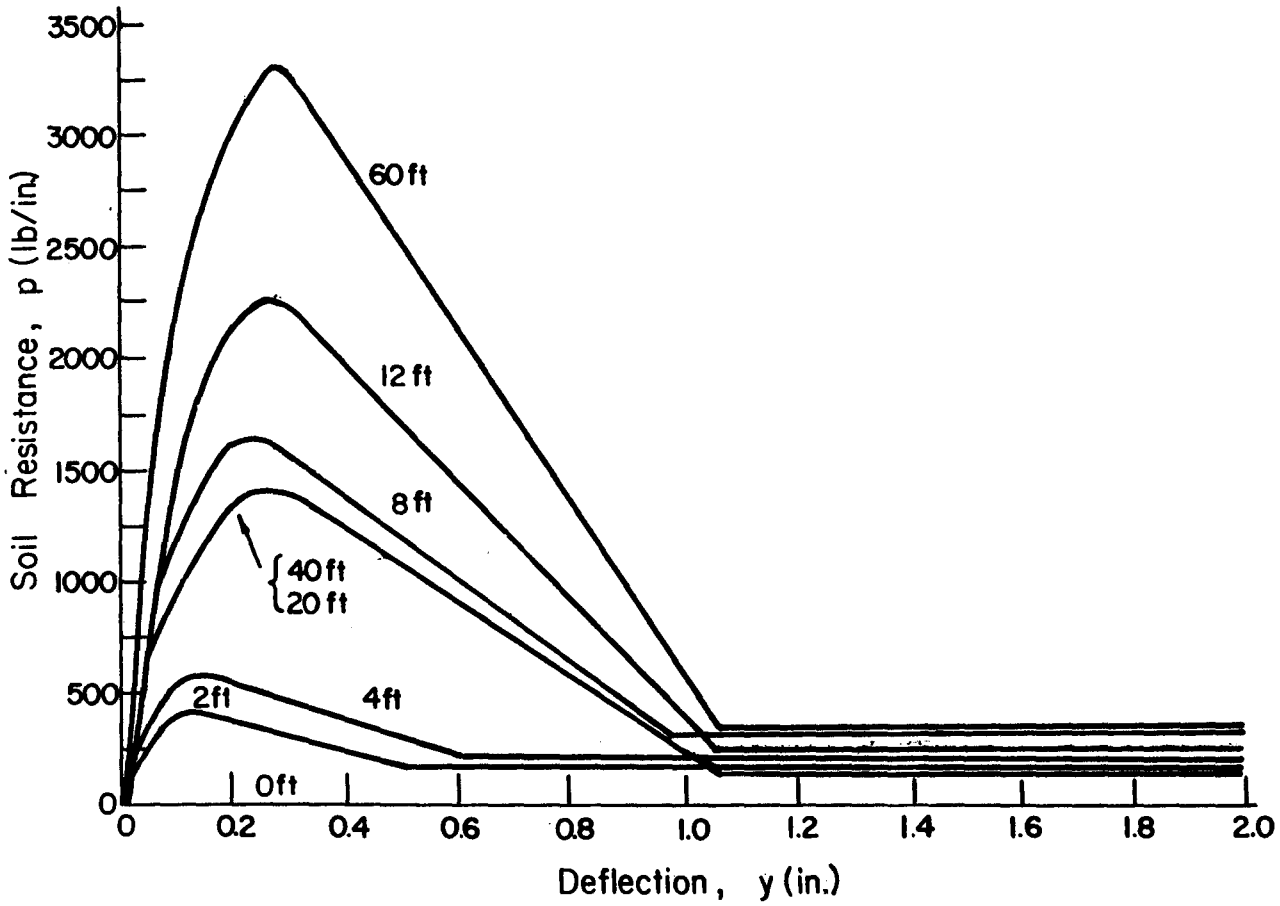

Fig. 3.14. Example p-y curves for stiff clay below the water table, Reese criteria, cyclic loading.

was approximately 2,200 lb/sq ft. The experiments and their intepretation are discussed in detail by Welch and Reese (1972) and Reese and Welch (1975).

Recommendations for Computing p-y Curves. The following procedure is for short-term static loading and is illustrated in Fig. 3.15a.

1. Obtain values for undrained shear strength c, soil unit weight γ, and pile diameter b. Also obtain the values of ε_{50} from stress-strain curves. If no stress-strain curves are available, use a value from ε_{50} of 0.010 or 0.005 as given in Table 3.3, the larger value being more conservative.

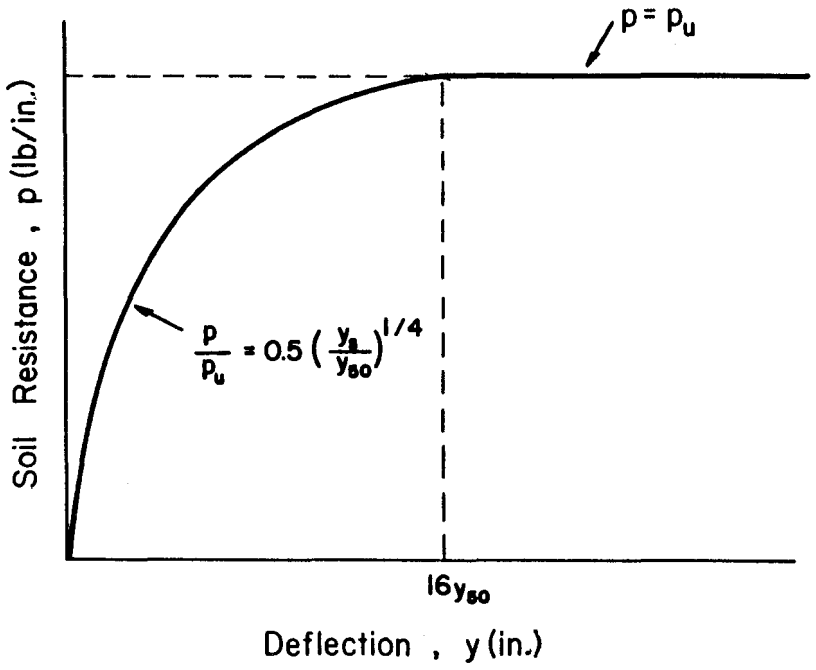

Fig. 3.15a. Characteristic shape of p-y curve for static loading in stiff clay above water table.

2. Compute the ultimate soil resistance per unit length of shaft, p_u, using the smaller of the values given by Eqs. 3.18 and 3.19. (In the use of Eq. 3.18 the shear strength is taken as the average from the ground surface to the depth being considered and J is taken as 0.5. The unit weight of the soil should reflect the position of the water table.)
3. Compute the deflection, y_{50}, at one-half the ultimate soil resistance from Eq. 3.20.
4. Points describing the p-y curve may be computed from the relationship below.

$$\frac{p}{p_u} = 0.5 \left(\frac{y}{y_{50}}\right)^{1/4} \tag{3.37}$$

5. Beyond $y = 16y_{50}$, p is equal to p_u for all values of y.

The following procedure is for cyclic loading and is illustrated in Fig. 3.15b.

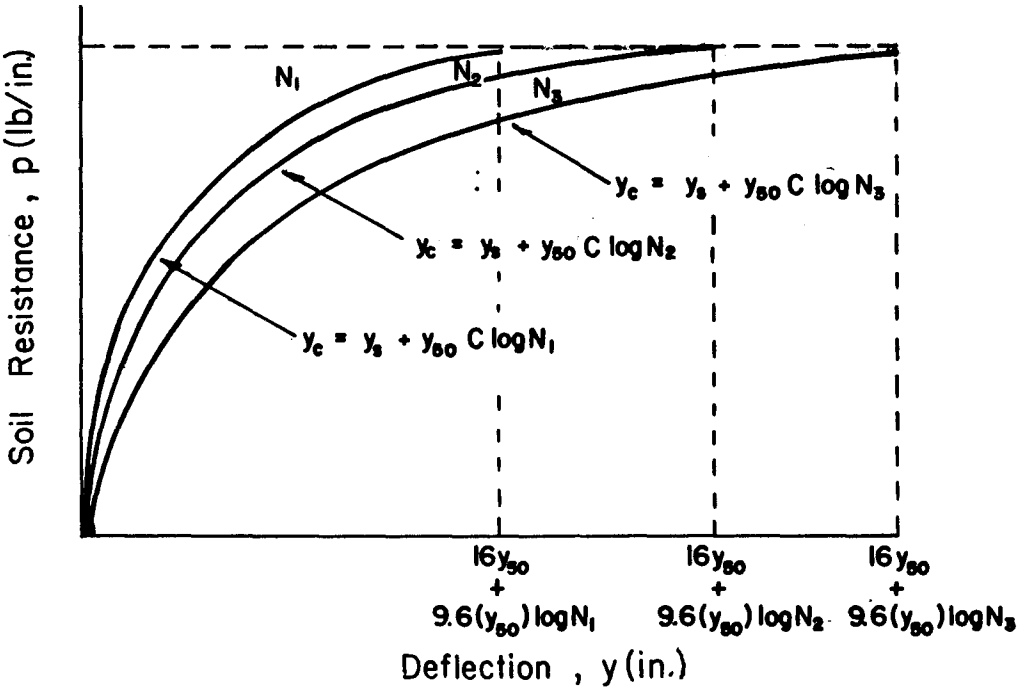

Fig. 3.15b. Characteristic shape of p-y curve for cyclic loading in stiff clay above water table.

1. Determine the p-y curve for short-term static loading by the procedure previously given.
2. Determine the number of times the design lateral load will be applied to the pile.
3. For several values of p/p_u obtain the value of C, the parameter describing the effect of repeated loading on deformation, from a relationship developed by laboratory tests, (Welch and Reese, 1972), or in the absence of tests, from the following equation.

$$C = 9.6 \left(\frac{p}{p_u} \right)^4 \tag{3.38}$$

4. At the value of p corresponding to the values of p/p_u selected in step 3, compute new values of y for cyclic loading from the following equation.

$$y_c = y_s + y_{50} \cdot C \cdot \log N \tag{3.39}$$

where

y_c = deflection under N-cycles of load,
y_s = deflection under short-term static load,
y_{50} = deflection under short-term static load at one-half the ultimate resistance, and
N = number of cycles of load application.

5. The p-y curve defines the soil response after N-cycles of load.

Recommended Soil Tests. Triaxial compression tests of the unconsolidated-undrained type with confining stresses equal to the overburden pressures at the elevations from which the samples were taken are recommended to determine the shear strength. The value of ε_{50} should be taken as the strain during the test corresponding to the stress equal to half the maximum total principal stress difference. The undrained shear strength, c, should be defined as one-half the maximum total-principal-stress difference. The unit weight of the soil must also be determined.

Example Curves. An example set of p-y curves was computed for stiff clay above the water table for a pile with a diameter of 48 in. The soil profile that was used is shown in Fig. 3.13. The unit weight of the soil was assumed to be 112 lb/cu ft for the entire depth. In the absence of a stress-strain curve, ε_{50} was taken as 0.005. Equation 3.38 was used to compute values for the parameter C and it was assumed that there is to be 100 cycles of load application.

The p-y curves were computed for the following depths below the groundline: 0, 1, 2, 4, 8, 12, 20, 40, and 60 ft. The plotted curves are shown in Fig. 3.16.

Unified Criteria for Clays below the Water Table

Introduction. As was noted in the previous section, no recommendations were made for ascertaining for what range of undrained shear strength one should employ the criteria for soft clay and for what range one should employ the criteria for stiff clay. Sullivan (1977) examined the original experiments and developed a set of recommendations that yield computed behaviors in reasonably good agreement with the experimental results from the Sabine tests reported by Matlock (1970) and with those from the Manor tests reported by Reese, Cox and Koop (1975). However, as will be seen from the following presentation, there is a need for the

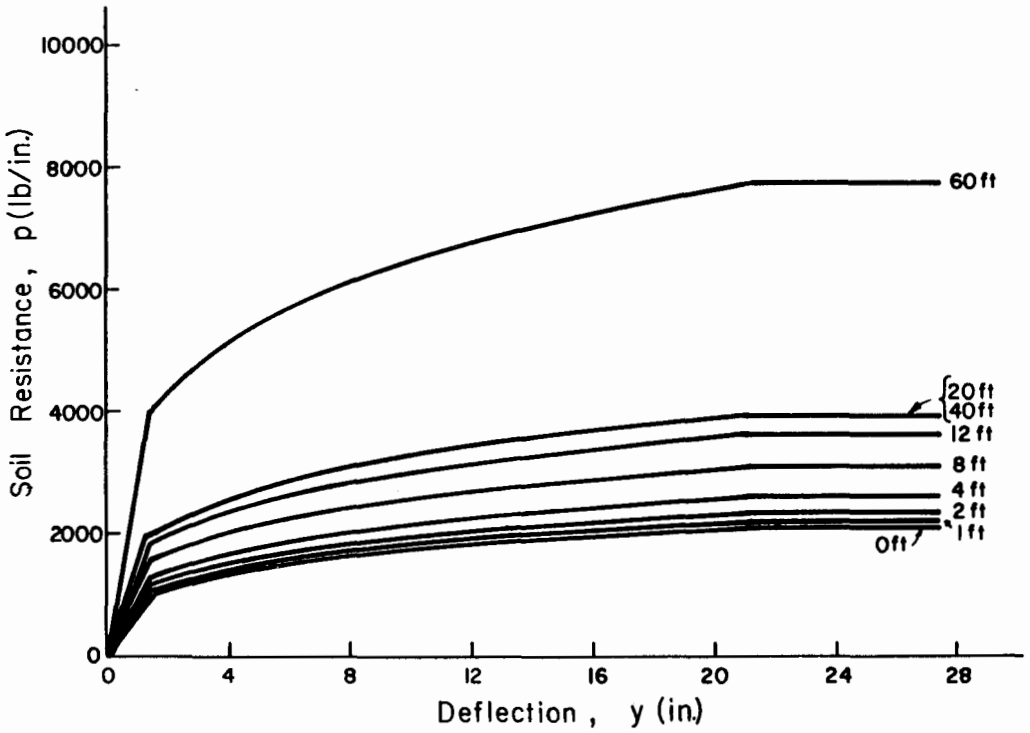

Fig. 3.16. Example p-y curves for stiff clay above water table, Welch criteria, cyclic loading.

engineer to employ some judgement in selecting appropriate parameters for use in the prediction equations.

Recommendations for Computing p-y Curves. The following procedure is for short-term static loading and is illustrated in Fig. 3.17.

1. Obtain values for the undrained shear strength c, the submerged unit weight γ', and the pile diameter b. Also obtain values of ε_{50} from stress-strain curves. If no stress-strain curves are available, the values in Table 3.6 are provided as guidelines for selection of ε_{50}.
2. Compute c_a and $\bar{\sigma}_v$, for $x < 12b$, where
   c_a = average undrained shear strength,
   $\bar{\sigma}_v$ = average effective stress, and
   x = depth.
3. Compute the variation of p_u with depth using the equations below.

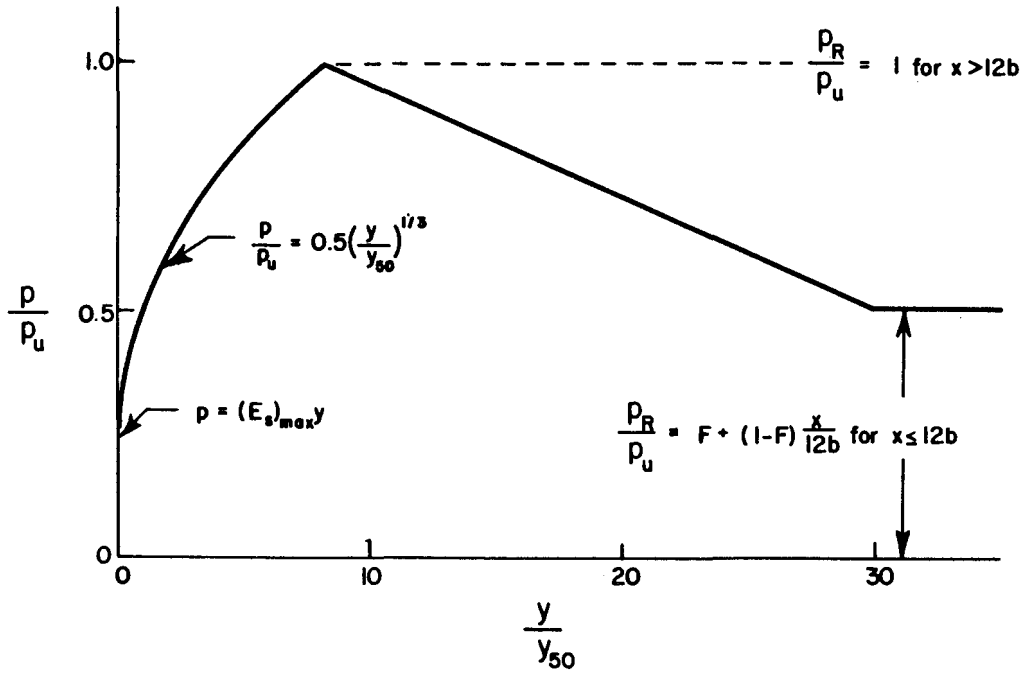

Fig. 3.17. Characteristic shape of p-y curve for unified clay criteria for static loading.

a. For $x < 12b$, p_u is the smaller of the values computed from the two equations below.

$$p_u = \left(2 + \frac{\overline{\sigma}_v}{c_a} + 0.833\,\frac{x}{b}\right) c_a b \tag{3.40}$$

$$p_u = \left(3 + 0.5\,\frac{x}{b}\right) cb \tag{3.41}$$

b. For $x > 12b$,

$$p_u = 9\,cb. \tag{3.42}$$

The steps below are for a particular depth, x.

4. Select the coefficients, A and F, as indicated below. The coefficients A and F, determined empirically for the load tests at Sabine and Manor, are given in Table 3.7. The terms used in Table 3.7, not defined previously, are defined below.

   W_L = liquid limit,

   PI = plasticity index,

TABLE 3.6. REPRESENTATIVE VALUES OF ε_{50}.

$\frac{c}{(lb/sq\ ft)}$	$\frac{\varepsilon_{50}}{\%}$
250 - 500	2
500 - 1000	1
1000 - 2000	0.7
2000 - 4000	0.5
4000 - 8000	0.4

(Also see Tables 3.3 and 3.5)

LI = liquidity index,
O_R = overconsolidation ratio, and
S_t = sensitivity.

The recommended procedure for estimating A and F for other clays is given below.

a. Determine as many of the following properties of the clay as possible, c, ε_{50}, O_R, S_t, degree of fissuring, ratio of residual to peak undrained shear strength, W_L, PI, and LI.
b. Compare the properties of the soil in question to the properties of the Sabine and Manor clays listed in Table 3.7.
c. If the properties are similar to either the Sabine or Manor clay properties, use A and F for the similar clay.
d. If the properties are not similar to either, the engineer should estimate A and F using his judgement and Table 3.7 as guides.

5. Compute:

$$y_{50} = A\varepsilon_{50}{}^{b}. \tag{3.43}$$

TABLE 3.7. CURVE PARAMETERS FOR THE UNIFIED CRITERIA.

Clay Description	A	F
Sabine River	2.5	1.0
Inorganic, Intact		
c = 300 lb/sq ft		
ε_{50} = 0.7%		
O_R ≃ 1		
S_t ≃ 2		
w_L = 92		
PI = 68		
LI = 1		
Manor	0.35	0.5
Inorganic, Very fissured		
c ≃ 2400 lb/ sq ft		
ε_{50} = 0.5%		
O_R > 10		
S_t ≃ 1		
w_L = 77		
PI = 60		
LI = 0.2		

6. Obtain $(E_s)_{max}$. When no other method is available Eq. 3.44 and Table 3.8 may be used as guidelines.

$$(E_s)_{max} = kx. \tag{3.44}$$

TABLE 3.8. REPRESENTATIVE VALUES FOR k.

c	k
(lb/sq ft)	(lb/cu in.)
250 - 500	30
500 - 1000	100
1000 - 2000	300
2000 - 4000	1000
4000 - 8000	3000

(Also see Table 3.4)

7. Compute the deflection at the intersection between the initial linear portion and curved portion, from the equation below.

$$y_g = \left|\frac{0.5p_u}{(E_s)_{max}}\right|^{\frac{3}{2}} (y_{50})^{-\frac{1}{2}} \tag{3.45}$$

(y_g can be no larger than $8y_{50}$)

8a. For $0 < y < y_g$,

$$p = (E_s)_{max} y. \tag{3.46}$$

8b. For $y_g < y < 8y_{50}$,

$$p = 0.5p_u \left(\frac{y}{y_{50}}\right)^{\frac{1}{3}}. \tag{3.47}$$

8c. For $8y_{50} < y < 30y_{50}$,

$$p = p_u + \frac{p_R - p_u}{22\ y_{50}} (y - 8y_{50}) \tag{3.48}$$

where

$$p_R = p_u \left(F + (1-F) \frac{x}{12\ b} \right). \tag{3.49}$$

(p_R will be equal to or less than p_u)

8d. For $y > 30y_{50}$,

$$p = p_R. \tag{3.50}$$

The following procedure is for cyclic loading and is illustrated in Fig. 3.18.

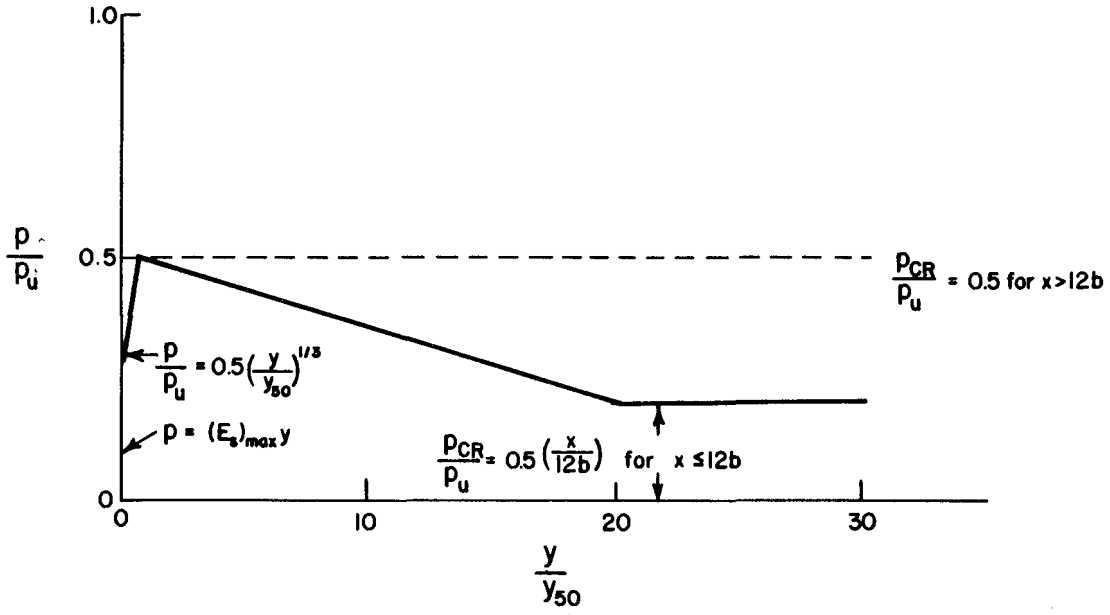

Fig. 3.18. Characteristic shape of p-y curve for unified clay criteria for cyclic loading.

1. Repeat steps 1 through 8a for static loading.
2. Compute

$$p_{CR} = 0.5\ p_u \frac{x}{12\ b} \leq 0.5\ p_u. \tag{3.51}$$

3a. For $y_g < y < y_{50}$,

$$p = 0.5\ p_u \left(\frac{y}{y_{50}} \right)^{\frac{1}{3}}. \tag{3.52}$$

3b. For $y_{50} < y < 20y_{50}$,

$$p = 0.5\ p_u + \frac{p_{CR} - 0.5\ p_u}{19\ y_{50}}\ (y - y_{50}). \qquad (3.53)$$

3c. For $y > 20y_{50}$,

$$p = p_{CR}. \qquad (3.54)$$

The procedure outlined above for both static and cyclic loading assumes an intersection of the curves defined by Eqs. 3.46 and 3.47. If that intersection does not occur, the p-y curve is defined by Eq. 3.46 until it intersects a portion of the curve defined by Eqs. 3.48 or 3.50 for static loading, and Eqs. 3.52 or 3.53 for cyclic loading.

Example Curves. Two example sets of p-y curves were computed using the unified criteria; each of the sets is for a pile of 48 in. in diameter and for cyclic loading.

Figure 3.19 shows the set of p-y curves for soft clay; the soil profile used is shown in Fig. 3.8. The value of ε_{50} was assumed to be 0.02 at the mudline and 0.01 at a depth of 80 ft. The unit weight was assumed to be 20 lb/cu ft at the groundline and 40 lb/cu ft at a depth of 80 ft. The value of A was assumed to be 2.5 and the value of F was assumed to be 1.0. The value of k for computing the maximum value of the soil modulus was assumed to be 400,000 lb/cu ft. The p-y curves were computed for the following depths: 0, 1, 2, 4, 8, 12, 20, and 40 ft (curves for 0 and 1 ft too close to axis to be shown).

Figure 3.20 shows the set of p-y curves for stiff clay; the soil profile used is shown in Fig. 3.13. The value of ε_{50} was assumed to be 0.006 and the unit weight of the soil was assumed to be 50 lb/cu ft. The value of A was assumed to be 0.35 and the value of F was assumed to be 0.5. The value of k for computing the maximum value of the soil modulus was assumed to be 800,000 lb/cu ft. The p-y curves were computed for the following depths: 0, 1, 2, 4, 8, 12, 20, and 40 ft.

3.6 RECOMMENDATIONS FOR p-y CURVES FOR SAND

As shown below, a major experimental program was conducted on the behavior of laterally loaded piles in sand below the water table. The results can be extended to sand above the water table.

Response of Sand below the Water Table

Field Experiments. An extensive series of tests were performed at a site on Mustang Island, near Corpus Christi (Cox, Reese, and Grubbs,

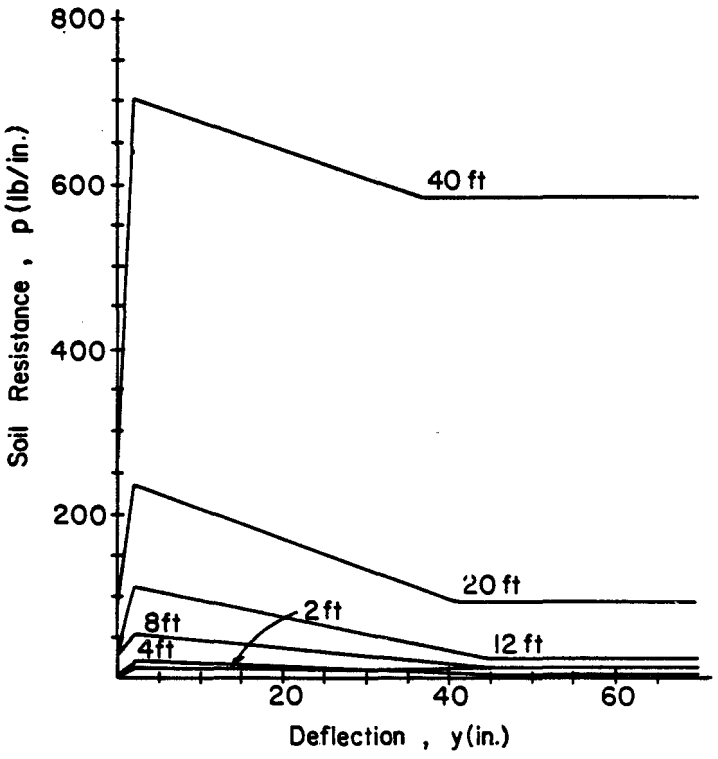

Fig. 3.19. Example p-y curves for soft clay below water table, unified criteria, cyclic loading.

1974). Two steel pipe piles, 24 in. in diameter, were driven into sand in a manner to simulate the driving of an open-ended pipe, and were subjected to lateral loading. The embedded length of the piles was 69 ft. One of the piles was subjected to short-term loading and the other to repeated loading.

The soil at the site was a uniformly graded, fine sand with an angle of internal friction of 39 degrees. The submerged unit weight was 66 lb/cu ft. The water surface was maintained a few inches above the mudline throughout the test program.

Recommendations for Computing p-y Curves. The following procedure is for short-term static loading and for cyclic loading and is illustrated in Fig. 3.21 (Reese, Cox, and Koop, 1974).

1. Obtain values for the angle of internal friction ϕ, the soil unit weight γ, and pile diameter b.
2. Make the following preliminary computations.

$$\alpha = \frac{\phi}{2} \; ; \; \beta = 45 + \frac{\phi}{2} \; ; \; K_o = 0.4; \text{ and } K_a = \tan^2(45 - \frac{\phi}{2}) \tag{3.55}$$

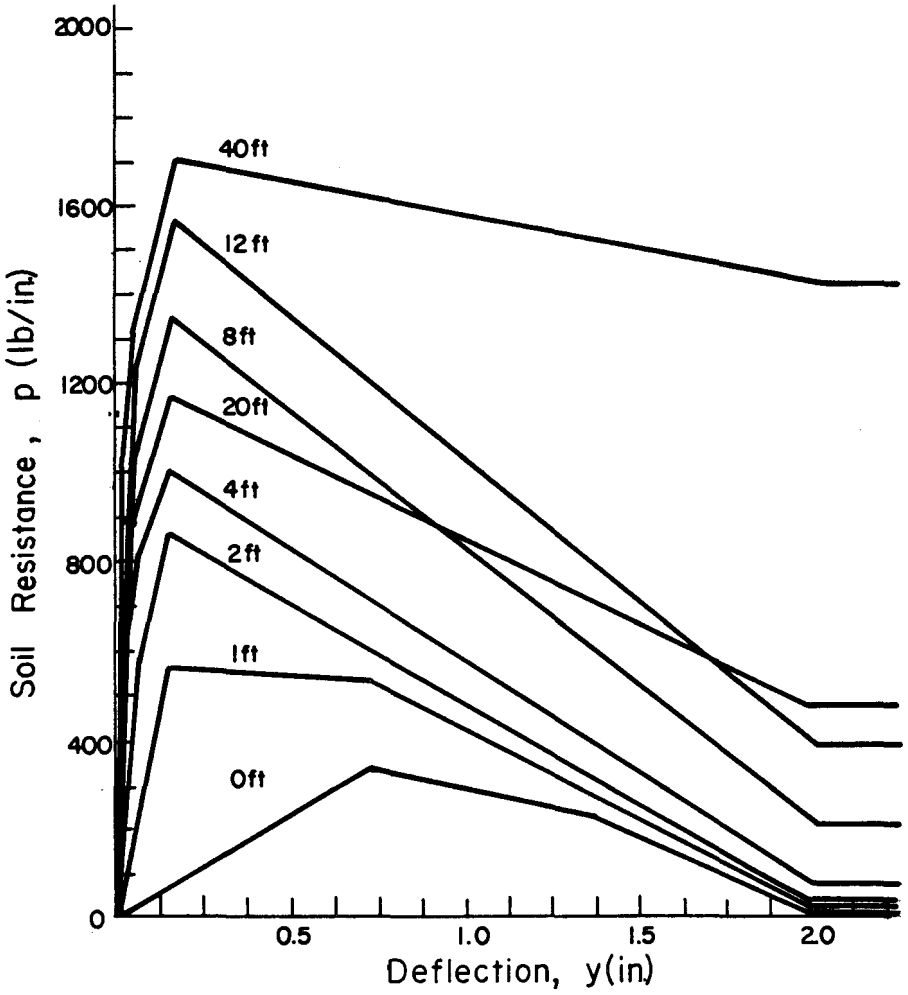

Fig. 3.20. Example p-y curves for stiff clay below water table, unified criteria, cyclic loading.

3. Compute the ultimate soil resistance per unit length of pile using the smaller of the values given by the equations below, where x is equal to the depth below the ground surface.

$$p_{st} = \gamma x \left[\frac{K_o x \tan\phi \sin\beta}{\tan(\beta-\phi)\cos\alpha} + \frac{\tan\beta}{\tan(\beta-\phi)} (b + x \tan\beta \tan\alpha) + K_o x \tan\beta (\tan\phi \sin\beta - \tan\alpha) - K_a b \right] \quad (3.56)$$

$$P_{sd} = K_a b \gamma x (\tan^8\beta - 1) + K_o b \gamma x \tan\phi \tan^4\beta \quad (3.57)$$

For sand below the water table, the submerged unit weight γ' should be used.

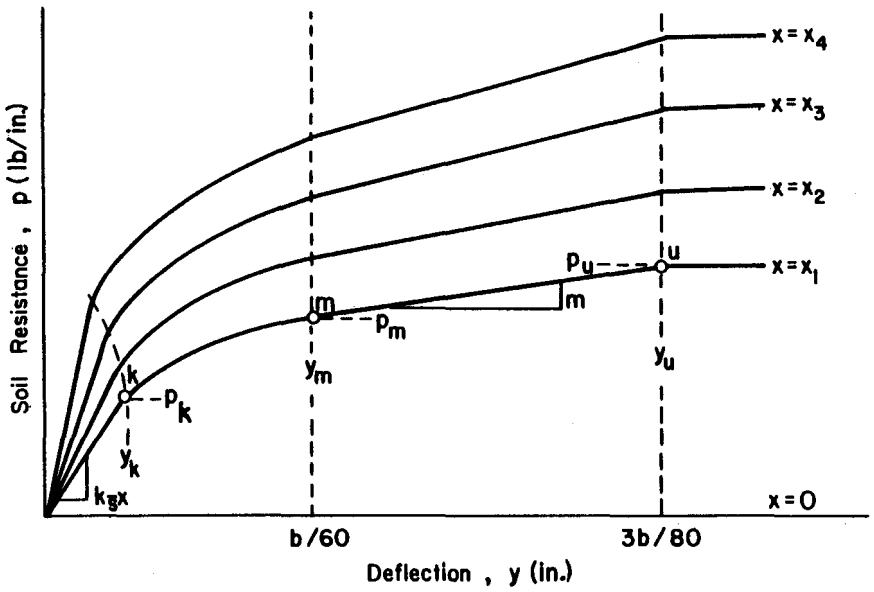

Fig. 3.21. Characteristic shape of a family of p-y curves for static and cyclic loading in sand.

4. In making the computations in Step 3, find the depth x_t at which there is an intersection at Eqs. 3.56 and 3.57. Above this depth use Eq. 3.56. Below this depth use Eq. 3.57.
5. Select a depth at which a p-y curve is desired.
6. Establish y_u as 3b/80. Compute p_u by the following equation:

$$p_u = \bar{A}_s p_s \text{ or } p_u = \bar{A}_c p_s. \tag{3.58}$$

Use the appropriate value of $\bar{A}_s$ or $\bar{A}_c$ from Fig. 3.22 for the particular nondimensional depth, and for either the static or cyclic case. Use the appropriate equation for p_s, Eq. 3.56 or Eq. 3.57 by referring to the computation in step 4.

7. Establish y_m as b/60. Compute p_m by the following equation:

$$p_m = B_s p_s \text{ or } p_m = B_c p_s. \tag{3.59}$$

Use the appropriate value of B_s or B_c from Fig. 3.23 for the particular nondimensional depth, and for either the static or cylic case. Use the appropriate equation for p_s. The two straight-line portions of the p-y curve, beyond the point where y is equal to b/60, can now be established.

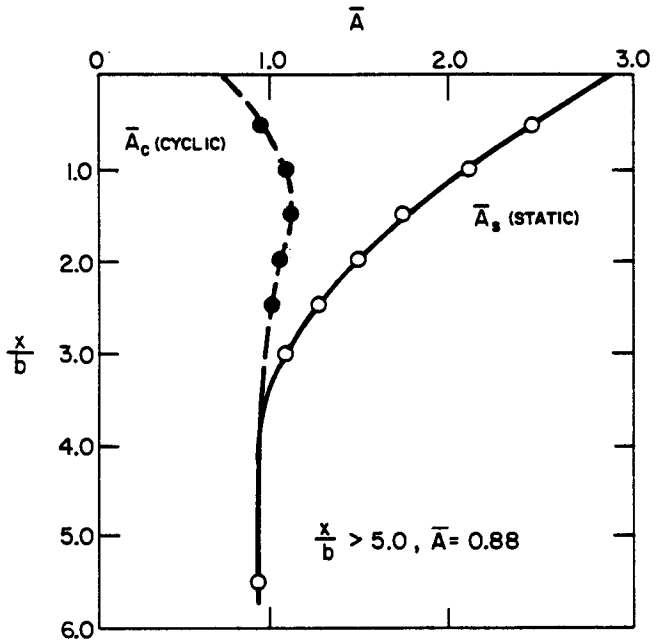

Fig. 3.22. Values of coefficients $\bar{A}_C$ and $\bar{A}_S$.

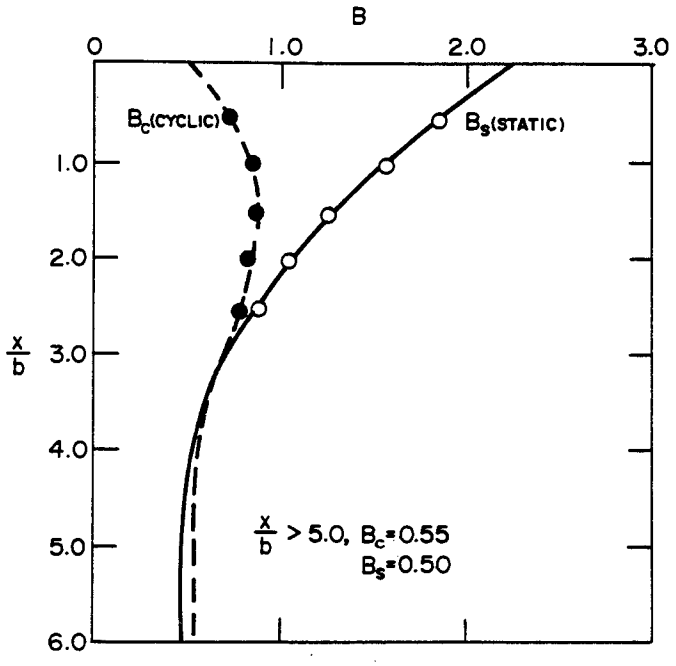

Fig. 3.23. Nondimensional coefficient B for soil resistance versus depth.

8. Establish the initial straight-line portion of the p-y curve,

$$p = (kx)y. \tag{3.60}$$

Use the appropriate value of k from Table 3.9 or 3.10.

TABLE 3.9. REPRESENTATIVE VALUES OF k FOR SUBMERGED SAND.

Relative Density	Loose	Medium	Dense
Recommended k (lb/cu in.)	20	60	125

TABLE 3.10. REPRESENTATIVE VALUES OF k FOR SAND ABOVE WATER TABLE.

Relative Density	Loose	Medium	Dense
Recommended k (lb/cu in.)	25	90	225

9. Establish the parabolic section of the p-y curve,

$$p = \overline{C}\, y^{1/n}. \tag{3.61}$$

Fit the parabola between points k and m as follows:

a. Get the slope of line between points m and u by,

$$m = \frac{p_u - p_m}{y_u - y_m}. \tag{3.62}$$

b. Obtain the power of the parabolic section by,

$$n = \frac{p_m}{m y_m} \quad . \tag{3.63}$$

c. Obtain the coefficient $\bar{C}$ as follows:

$$\bar{C} = \frac{p_m}{y_m^{1/n}} \quad . \tag{3.64}$$

d. Determine point k as,

$$y_k = \left(\frac{\bar{C}}{kx} \right)^{n/n-1} \quad . \tag{3.65}$$

e. Compute appropriate number of points on the parabola by using Eq. 3.61.

Note: The step-by-step procedure is outlined, and Fig. 3.21 is drawn, as if there is an intersection between the initial straight-line portion of the p-y curve and the parabolic portion of the curve at point k. However, in some instances there may be no intersection with the parabola. Equation 3.60 defines the p-y curve until there is an intersection with another branch of the p-y curve or if no intersection occurs, Eq. 3.60 defines the complete p-y curve. The soil response curves for other depths can be found repeating the above steps for each desired depth.

Simplified Equations

In his work on the ultimate resistance of a plate in sand, Bowman (1958) stated that the angle α ranges from $\phi/2$ for loose sand to ϕ for dense sand. Reese, et al. (1974) reported that the value of α was found from measurements of the contours of the wedge that formed at the ground surface and that α from the Mustang Island tests ranged from $\phi/3$ for static loading to $3\phi/4$ for cyclic loading. The angle β that further defines the shape of the wedge of sand at the ground surface is not easy to measure experimentally and also can be expected to vary. However, Reese, et al. (1974) selected values of α and β of $\phi/2$ and $45 + \phi/2$, respectively, in developing correlations with experimental results from Mustang Island.

Fenske (1981) points out that Eqs. 3.56 and 3.57 can be simplified if α is $\phi/2$ and β is $45 + \phi/2$. The simplified equations are:

$$p_{st} = \gamma b^2 [S_1(x/b) + S_2(x/b)^2] \tag{3.66}$$

$$p_{sd} = \gamma b^2 [S_3(x/b)] \tag{3.67}$$

where

$$S_1 = (K_p - K_a) \tag{3.68}$$

$$S_2 = (\tan \beta)(K_p \tan \alpha + K_o[\tan \phi \sin \beta(\sec \alpha + 1) - \tan \alpha]) \tag{3.69}$$

$$S_3 = K_p^2(K_p + K_o \tan \phi) - K_a. \tag{3.70}$$

The depth of transition x_t can be found by equating the expressions in Eqs. 3.66 and 3.67, as follows:

$$x_t/b = (S_3 - S_1)/S_2. \tag{3.71}$$

It can be seen that S_1, S_2, S_3, and x_t/b are functions only of ϕ; therefore, the values shown in Table 3.11 can be computed.

TABLE 3.11. NONDIMENSIONAL COEFFICIENTS FOR p-y CURVES FOR SAND (after Fenske).

ϕ, deg.	S_1	S_2	S_3	x_t/b
25.0	2.05805	1.21808	15.68459	11.18690
26.0	2.17061	1.33495	17.68745	11.62351
27.0	2.28742	1.46177	19.95332	12.08526
28.0	2.40879	1.59947	22.52060	12.57407
29.0	2.53509	1.74906	25.43390	13.09204
30.0	2.66667	1.91170	28.74513	13.64147
31.0	2.80394	2.08866	32.51489	14.22489
32.0	2.94733	2.28134	36.81400	14.84507
33.0	3.09732	2.49133	41.72552	15.50508
34.0	3.25442	2.72037	47.34702	16.20830
35.0	3.41918	2.97045	53.79347	16.95848
36.0	3.59222	3.24376	61.20067	17.75976
37.0	3.77421	3.54280	69.72952	18.61673
38.0	3.96586	3.87034	79.57113	19.53452
39.0	4.16799	4.22954	90.95327	20.51883
40.0	4.38147	4.62396	104.14818	21.57604

Recommended Soil Tests. Triaxial compression tests are recommended for obtaining the angle of internal friction of the sand. Confining pressures should be used which are close or equal to those at the depths being considered in the analysis. Tests must be performed to determine the unit weight of the sand. In many instances, however, undisturbed samples of sand cannot be obtained and the value of ϕ must be obtained from correlations with static cone penetration tests or from dynamic penetration tests.

Example Curves. An example set of p-y curves was computed for sand below the water table for a pile with a diameter of 48 in. The sand is assumed to have an angle of internal friction of 34° and a submerged unit weight of 62.4 lb/cu ft. The loading was assumed to be cyclic.

The p-y curves were computed for the following depths below the mudline: 0, 1, 2, 4, 8, 12, and 20 ft. The plotted curves are shown in Fig. 3.24.

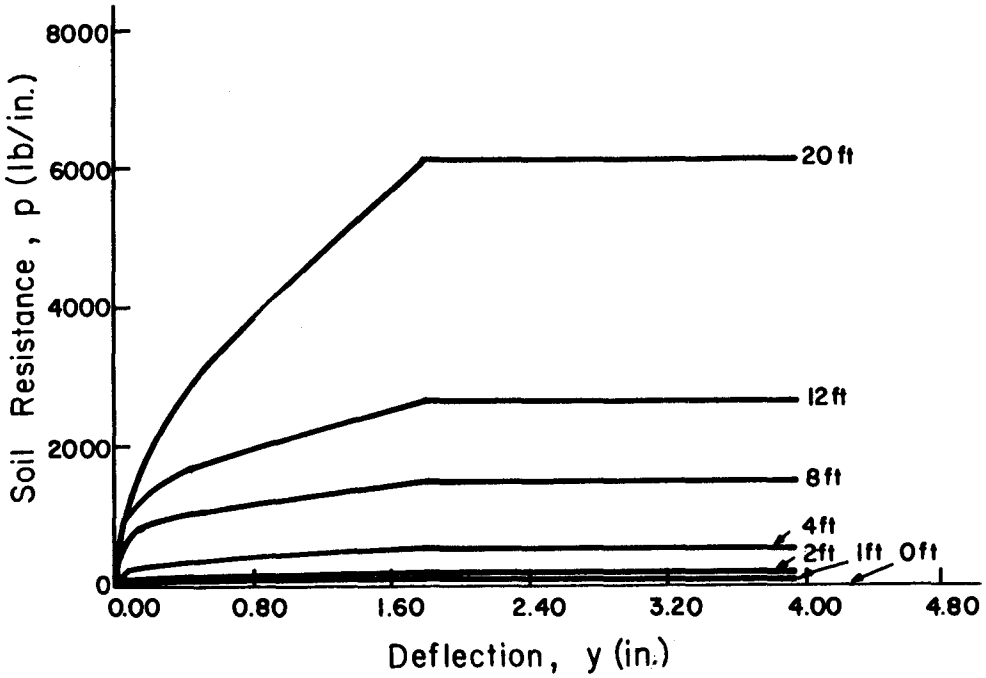

Fig. 3.24. Example p-y curves for sand below water table, Reese criteria, cyclic loading.

Response of Sand Above the Water Table

The procedure in the previous section can be used for sand above the water table if appropriate adjustments are made in the unit weight and angle of internal friction of the sand. Some small-scale experiments were performed by Parker and Reese (1971) and recommendations for p-y curves for dry sand were developed from those experiments. The results from the Parker and Reese experiments should be useful as check of solutions made using results from the test program using full-scale piles.

3.7 RECOMMENDATIONS FOR p-y CURVES FOR ROCK

It is hardly surprising that not much information is available on the behavior of piles that have been installed in rock. Some other type of foundation would normally be used. However, a study was made of the behavior of an instrumented drilled shaft that was installed in a vuggy limestone in the Florida Keys (Reese and Nyman, 1978). The test was performed for the purpose of gaining information for the design of foundations for highway bridges in the Florida Keys.

Difficulty was encountered in obtaining properties of the intact rock. Cores broke during excavation and penetrometer tests were misleading (because of the vugs) or could not be run. It was possible to test two cores from the site. The small discontinuities on the outside surface of the specimens were coated with a thin layer of gypsum cement in an effort to minimize stress concentrations. The ends of the specimens were cut with a rock saw and lapped flat and parallel. The specimens were 5.88 in. in diameter and with heights of 11.88 in. for Specimen 1 and 10.44 in. for Specimen 2. The undrained shear strength of the specimens were taken as one-half the unconfined compressive strength and were 17.4 and 13.6 T/sq ft for Specimens 1 and 2, respectively.

The rock at the site was also investigated by in-situ-grout-plug tests under the direction of Dr. John Schmertmann (1977). A 5.5 in. diameter hole was drilled into the limestone, a high strength steel bar was placed to the bottom of the hole, and a grout plug was cast over the lower end of the bar. The bar was pulled until failure occurred and the grout was examined to see that failure occurred at the interface of the grout and limestone. Tests were performed at three borings and the following results were obtained, in T/sq ft: depth into limestone from 2.5 to 5 ft, 23.8, 13.7, and 12.0; depth into limestone from 8 to 10 ft, 18.2, 21.7,

and 26.5; depth into limestone from 18 to 20 ft, 13.7 and 10.7. The average of the eight tests was 16.3 T/sq. However, the rock was stronger in the zone where the deflections of the drilled shaft were most significant and a shear strength of 18 T/sq ft was selected for correlation.

The drilled shaft was 48 in. in diameter and penetrated 43.7 ft into the limestone. The overburden of fill was 14 ft thick and was cased. The load was applied about 11.5 ft above the limestone. A maximum load of 75 tons was applied to the drilled shaft. The maximum deflection at the point of load applicaton was 0.71 in. and at the top of the rock (bottom of casing) it was 0.0213 in. While the curve of load versus deflection was nonlinear, there was no indication of failure of the rock.

A single p-y curve, shown in Fig. 3.25, was proposed for the design of piles under lateral loading in the Florida Keys. Data are insufficient to indicate a family of curves to reflect any increased resistance with depth. Cyclic loading caused no measurable decrease resistance by the rock.

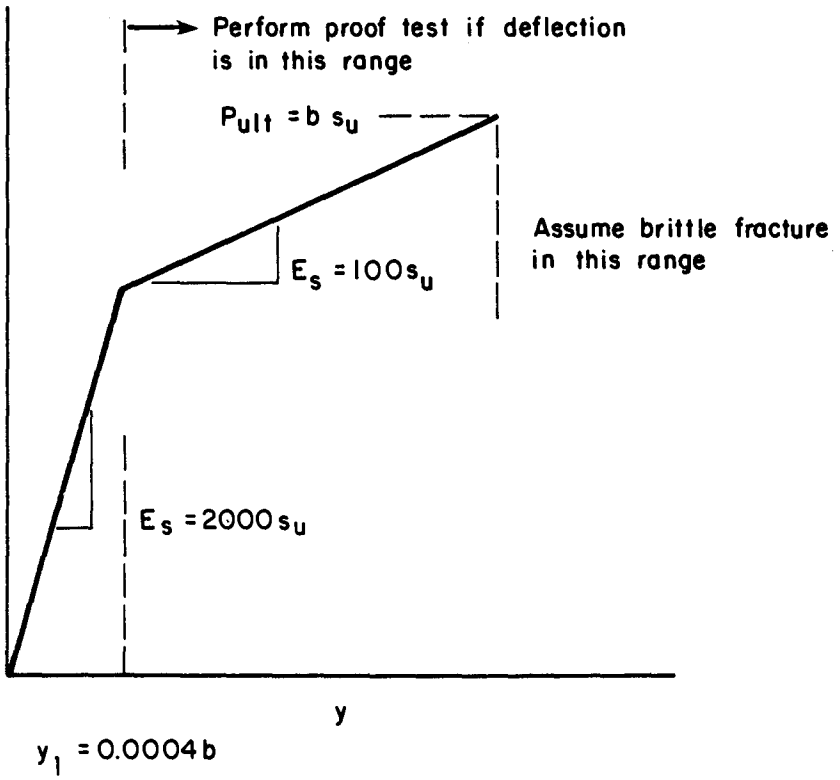

Fig. 3.25. Recommended p-y curve for design of drilled shaft in vuggy limestone.

As shown in the figure, load tests are recommended if deflections of the rock (and pile) are greater than 0.004b and brittle fracture is assumed if the lateral stress (force per unit of length) against the rock becomes greater than the diameter times the shear strength s_u of the rock.

The p-y curve shown in Fig. 3.25 should be employed with considerable caution because of the limited amount of experimental data and because of the great variability in rock. The behavior of rock at a site could very well be controlled not by the strength of intact specimens but by joints, cracks, and secondary structure of the rock.

3.8 REFERENCES

Bowman, E. R., "Investigation of the Lateral Resistance to Movement of a Plate in Cohesionless Soil," Unpublished Thesis, The University of Texas, January 1958.

Cox, W. R., Reese, L. C., and Grubbs, B. R., "Field Testing of Laterally Loaded Piles in Sand," Proceedings, Offshore Technology Conference, Paper No. 2079, Houston, Texas, May 1974.

Fenske, Carl W., personal communication, 1981.

Matlock, Hudson, "Correlations for Design of Laterally Loaded Piles in Soft Clay," Paper No. OTC 1204, Proceedings, Second Annual Offshore Technology Conference, Houston, Texas, Vol. 1, 1970, pp. 577-594.

McClelland, B. and Focht, J. A., Jr., "Soil Modulus for Laterally Loaded Piles," Transactions, American Society of Civil Engineers, Vol. 123, 1958, pp. 1049-1086.

Parker, F., Jr., and Reese, L. C., "Lateral Pile - Soil Interaction Curves for Sand," Proceedings, The International Symposium on the Engineering Properties of Sea-Floor Soils and their Geophysical Identification, The University of Washington, Seattle, Washington, July 1971.

Reese, L. C., Discussion of "Soil Modulus for Laterally Loaded Piles," by Bramlette McClelland and John A. Focht, Jr., Transactions, American Society of Civil Engineers, Vol. 123, 1958, pp. 1071.

Reese, L. C. and Cox, W. R., "Soil Behavior from Analysis of Tests of Uninstrumented Piles under Lateral Loading," ASTM Special Technical Publication 444, American Society for Testing and Materials, San Francisco, California, June 1968, pp. 161-176.

Reese, L. C., Cox, W. R., and Koop, F. D., "Analysis of Laterally Loaded Piles in Sand," Paper No. OTC 2080, Proceedings, Fifth Annual Offshore Technology Conference, Houston, Texas, 1974, Vol. II, pp. 473-485.

Reese, L. C., Cox, W. R. and Koop, F. D., "Field Testing and Analysis of Laterally Loaded Piles in Stiff Clay," Paper No. OTC 2312, Proceedings,

Seventh Offshore Technology Conference, Houston, Texas, Vol. II, 1975, pp. 672-690.

Reese, L. C., and Nyman, K. J., "Field Load Tests of Instrumented Drilled Shafts at Islamorado, Florida," a report to Girdler Foundation and Exploration Corporation, Clearwater, Florida, Bureau of Engineering Research, The University of Texas at Austin, February 28, 1978.

Reese, L. C. and Welch, R. C., "Lateral Loading of Deep Foundations in Stiff Clay," Proceedings, American Society of Civil Engineers, Vol. 101, No. GT7, February 1975, pp. 633-649.

Schmertmann, John H., "Report on Development of a Keys Limerock Shear Test for Drilled Shaft Design," a report to Girdler Foundation and Exploration Company, Clearwater, Florida, 1977.

Skempton, A. W., "The Bearing Capacity of Clays," Proceedings , Building Research Congress, Division I, London, England, 1951.

Sullivan, W. R., "Development and Evaluation of a Unified Method for the Analysis of Laterally Loaded Piles in Clay," Unpublished Thesis, The University of Texas at Austin, May 1977.

Terzaghi, Karl, "Evaluation of Coefficients of Subgrade Reaction," Geotechnique, Vol. 5, December 1955, pp. 297-326.

Winkler, E., Die Lehre von Elastizitat und Festigkeit (On Elasticity and Fixity), Prague, 1867.

Welch, R. C. and Reese, L. C., "Laterally Loaded Behavior of Drilled Shafts," Research Report No. 3-5-65-89, Center for Highway Research, University of Texas at Austin, May 1972.

3.9 EXERCISES

3.1 Given a clay with an undrained shear strength of 800 lb/sq ft a submerged unit weight of 48 lb/cu ft and an ε_{50} of 0.02, make necessary computations and plot p-y curves for both static and cyclic loading for depths of 6 ft and 12 ft. Assume the pile diameter to be 24 in. Use recommendations for p-y curves for soft clay below the water surface.

3.2 Repeat problem 1 using the Unified Criteria Method.

3.3 Repeat problem 1 for a stiff clay with undrained shear strength of 4000 lb/sq ft, ε_{50} of 0.005, and a dry unit weight of 115 lb/cu ft. Plot p-y curves for both stiff clay above water surface and stiff clay below the water surface.

3.4 Repeat problem 1 for a sand with an angle of internal friction of 38° and a submerged unit weight of 55 lb/cu ft.

CHAPTER 4. SOLUTIONS FOR LATERALLY LOADED PILES WITH SOIL MODULUS ASSUMED CONSTANT, CONSTANT PILE STIFFNESS, NO AXIAL LOADING

4.1 SOLUTION OF THE DIFFERENTIAL EQUATION

The pile is assumed to be supported along its entire length by a continuous stratum of soil which is capable of exerting a reaction to the pile in a direction opposite to the pile deflection. Fig. 4.1 shows that the soil resistance p per unit of length of the pile is related to the deflection y by the soil modulus E_s. For the case being considered the soil modulus E_s is assumed to have the same value for all points along the pile and is defined by the constant α. Furthermore, EI is constant and there is no axial loading.

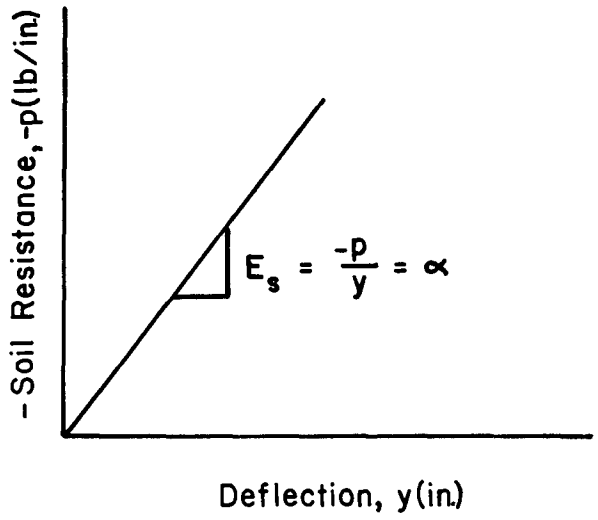

Fig. 4.1. Soil response curve.

The second-order differential equation is shown in Eq. 4.1 and the fourth-order differential equation is shown in Eq. 4.2. It should be noted that the fourth-order equation is derived by differentiation, assuming that the stiffness EI is constant.

$$\frac{d^2y}{dx^2} = \frac{M}{EI} \qquad (4.1)$$

$$\frac{d^4y}{dx^4} = \frac{p}{EI} \tag{4.2}$$

Employing the basic relationship between the soil resistance p and pile deflection y, Eq. 4.3, and employing the identity in Eq. 4.4, Eq. 4.5 is derived.

$$p = -\alpha y \tag{4.3}$$

$$\beta^4 = \frac{\alpha}{4EI} \tag{4.4}$$

$$\frac{d^4y}{dx^4} + 4\beta^4 y = 0 \tag{4.5}$$

The parameter β may be defined as the relative stiffness factor; the influence of β on the solution of Eq. 4.5 will be indicated later.

The solution of Eq. 4.5 can be easily obtained by standard techniques, as shown in Eqs. 4.6 through 4.10.

$$(D^4 + 4\beta^4)y = 0 \tag{4.6}$$

$$m^4 + 4\beta^4 = 0 \tag{4.7}$$

$$m_1 = -m_3 = \beta(1 + i) \tag{4.8}$$

$$m_2 = -m_4 = \beta(-1 + i) \tag{4.9}$$

$$y = e^{\beta x}(\bar{C}_1 \cos \beta x + \bar{C}_2 \sin \beta x) + e^{-\beta x}(\bar{C}_3 \cos \beta x + \bar{C}_4 \sin \beta x) \tag{4.10}$$

The coefficients $\bar{C}_1$, $\bar{C}_2$, $\bar{C}_3$, and $\bar{C}_4$ must be evaluated for the various boundary conditions that are desired. The evaluation of these coefficients must involve the use of the derivatives that are shown in Eqs. 4.11 through 4.14.

$$\frac{dy}{dx} = \beta e^{\beta x}(\bar{C}_1 \cos \beta x + \bar{C}_2 \sin \beta x - \bar{C}_1 \sin \beta x + \bar{C}_2 \cos \beta x) + \beta e^{-\beta x}(-\bar{C}_3 \cos \beta x - \bar{C}_4 \sin \beta x - \bar{C}_3 \sin \beta x + \bar{C}_4 \cos \beta x) \tag{4.11}$$

$$\frac{d^2y}{dx^2} = 2\beta^2 e^{\beta x}(\bar{C}_2 \cos \beta x - \bar{C}_1 \sin \beta x) + 2\beta^2 e^{-\beta x}(\bar{C}_3 \sin \beta x - \bar{C}_4 \cos \beta x) \tag{4.12}$$

$$\frac{d^3y}{dx^3} = 2\beta^3 e^{\beta x}(\bar{C}_2 \cos \beta x - \bar{C}_1 \sin \beta x - \bar{C}_2 \sin \beta x - \bar{C}_1 \cos \beta x) + 2\beta^3 e^{-\beta x}(-\bar{C}_3 \sin \beta x + \bar{C}_4 \cos \beta x + \bar{C}_3 \cos \beta x + \bar{C}_4 \sin \beta x) \tag{4.13}$$

$$\frac{d^4y}{dx^4} = 4^{\beta 4} e^{\beta x}(-\bar{C}_2 \sin \beta x - \bar{C}_1 \cos \beta x) + 4^{\beta 4} e^{-\beta x}(-\bar{C}_3 \cos \beta x - \bar{C}_4 \sin \beta x) \tag{4.14}$$

4.2 PILE OF INFINITE LENGTH

If one considers a long pile, one which can be considered to have an infinite length, a simple set of equations can be derived. Because deflections must be small for large values of x, $\bar{C}_1 = \bar{C}_2 = 0$. This conclusion is reached by examining Eq. 4.10. The term $e^{\beta x}$ increases without limit as x increases. The terms sin βx and cos βx oscillate between +1 and -1; therefore, the only way that the expression for y can have a finite value is for $\bar{C}_1$ and $\bar{C}_2$ to approach zero as x becomes large. The first case to be considered is shown in Fig. 4.2(a). The boundary conditions are given by Eqs. 4.15 and 4.16.

$$\text{at } x = 0, \quad \frac{d^2y}{dx^2} = \frac{M_t}{EI} \tag{4.15}$$

$$\frac{d^3y}{dx^3} = \frac{P_t}{EI} \tag{4.16}$$

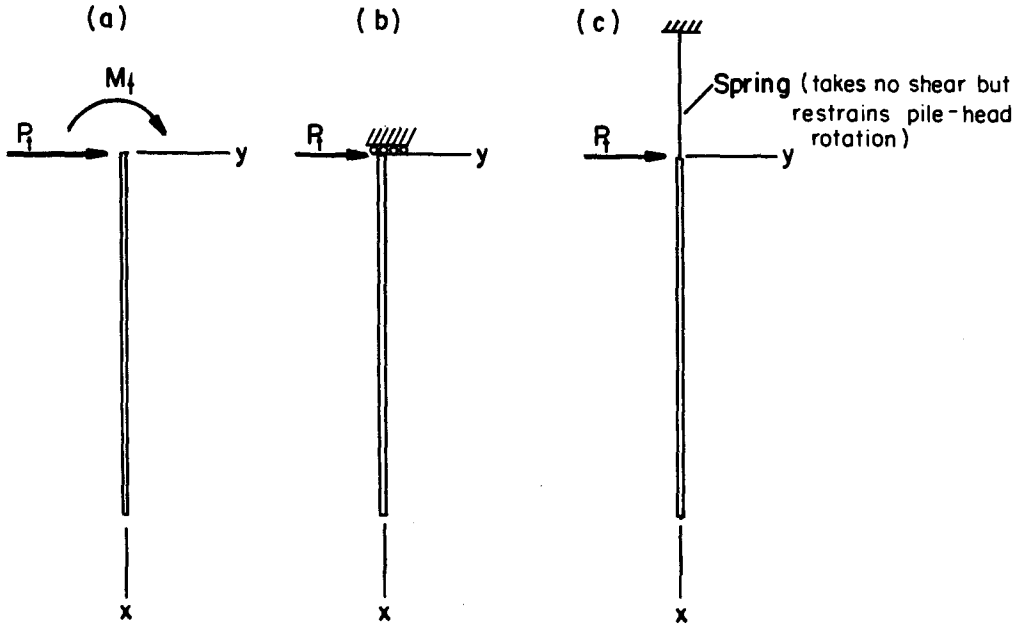

Fig. 4.2. Boundary conditions at top of pile

The use of Eq. 4.15 leads to

$$2EI\beta^2[\bar{C}_3(0) - \bar{C}_4(1)] = M_t, \text{ and}$$

$$\bar{C}_4 = \frac{-M_t}{2EI\beta^2}. \tag{4.17}$$

The use of Eq. 4.16 leads to

$$2EI\beta^3[-\overline{C}_3(0) + \overline{C}_4(1) + \overline{C}_3(1) + \overline{C}_4(0)] = P_t, \text{ and}$$

$$\overline{C}_3 + \overline{C}_4 = \frac{P_t}{2EI\beta^3} . \tag{4.18}$$

With the determination of the coefficients, substitutions can be made and relevant equations derived as shown below.

Timoshenko (1941) says the "long" pile solution is satisfactory where $\beta L \geq 4$. Solutions will be shown later for the case where the nondimensional length of the pile is less than 4.

Making use of Eqs. 4.17 and 4.18, expressions for y, S, M, V, and p can be written and are shown in Eqs. 4.19 through 4.23.

$$y = \frac{e^{-\beta x}}{2EI\beta^2}\left[\frac{P_t}{\beta}\cos\beta x + M_t(\cos\beta x - \sin\beta x)\right] \tag{4.19}$$

$$S = -e^{-\beta x}\left[\frac{2P_t\beta^2}{E_s}(\sin\beta x + \cos\beta x) + \frac{M_t}{EI\beta}\cos\beta x\right] \tag{4.20}$$

$$M = e^{-\beta x}\left[\frac{P_t}{\beta}\sin\beta x + M_t(\sin\beta x + \cos\beta x)\right] \tag{4.21}$$

$$V = e^{-\beta x}[P_t(\cos\beta x - \sin\beta x) - 2M_t\beta\sin\beta x] \tag{4.22}$$

$$p = 2\beta e^{-\beta x}[-P_t\cos\beta x - M_t\beta(\cos\beta x - \sin\beta x)] \tag{4.23}$$

It is convenient to define some functions which make it easier to write the above equations. These are:

$$A_1 = e^{-\beta x}(\cos\beta x + \sin\beta x) \tag{4.24}$$

$$B_1 = e^{-\beta x}(\cos\beta x - \sin\beta x) \tag{4.25}$$

$$C_1 = e^{-\beta x}\cos\beta x \tag{4.26}$$

$$D_1 = e^{-\beta x}\sin\beta x. \tag{4.27}$$

Using these functions, Eqs. 4.19 through 4.23 become:

$$y = \frac{2P_t\beta}{\alpha}C_1 + \frac{M_t}{2EI\beta^2}B_1 \tag{4.28}$$

$$S = \frac{-2P_t\beta^2}{\alpha}A_1 - \frac{M_t}{EI\beta}C_1 \tag{4.29}$$

$$M = \frac{P_t}{\beta}D_1 + M_tA_1 \tag{4.30}$$

$$V = P_tB_1 - 2M_t\beta D_1 \tag{4.31}$$

$$p = -2P_t\beta C_1 - 2M_t\beta^2B_1 . \tag{4.32}$$

Values for A_1, B_1, C_1, and D_1 are shown in Table 4.1.

TABLE 4.1. TABLE OF FUNCTIONS FOR PILE OF INFINITE LENGTH.

βx	A_1	B_1	C_1	D_1	βx	A_1	B_1	C_1	D_1
0	1.0000	1.0000	1.0000	0.0000	2.4	-0.0056	-0.1282	-0.0669	0.0613
0.1	0.9907	0.8100	0.9003	0.0903	2.6	-0.0254	-0.1019	-0.0636	0.0383
0.2	0.9651	0.6398	0.8024	0.1627	2.8	-0.0369	-0.0777	-0.0573	0.0204
0.3	0.9267	0.4888	0.7077	0.2189	3.2	-0.0431	-0.0383	-0.0407	-0.0024
0.4	0.8784	0.3564	0.6174	0.2610	3.6	-0.0366	-0.0124	-0.0245	-0.0121
0.5	0.8231	0.2415	0.5323	0.2908	4.0	-0.0258	0.0019	-0.0120	-0.0139
0.6	0.7628	0.1431	0.4530	0.3099	4.4	-0.0155	0.0079	-0.0038	-0.0117
0.7	0.6997	0.0599	0.3798	0.3199	4.8	-0.0075	0.0089	0.0007	-0.0082
0.8	0.6354	-0.0093	0.3131	0.3223	5.2	-0.0023	0.0075	0.0026	-0.0049
0.9	0.5712	-0.0657	0.2527	0.3185	5.6	0.0005	0.0052	0.0029	-0.0023
1.0	0.5083	-0.1108	0.1988	0.3096	6.0	0.0017	0.0031	0.0024	-0.0007
1.1	0.4476	-0.1457	0.1510	0.2967	6.4	0.0018	0.0015	0.0017	0.0003
1.2	0.3899	-0.1716	0.1091	0.2807	6.8	0.0015	0.0004	0.0010	0.0006
1.3	0.3355	-0.1897	0.0729	0.2626	7.2	0.0011	-0.00014	0.00045	0.00060
1.4	0.2849	-0.2011	0.0419	0.2430	7.6	0.00061	-0.00036	0.00012	0.00049
1.5	0.2384	-0.2068	0.0158	0.2226	8.0	0.00028	-0.00038	-0.0005	0.00033
1.6	0.1959	-0.2077	-0.0059	0.2018	8.4	0.00007	-0.00031	-0.00012	0.00019
1.7	0.1576	-0.2047	-0.0235	0.1812	8.8	-0.00003	-0.00021	-0.00012	0.00009
1.8	0.1234	-0.1985	-0.0376	0.1610	9.2	-0.00008	-0.00012	-0.00010	0.00002
1.9	0.0932	-0.1899	-0.0484	0.1415	9.6	-0.00008	-0.00005	-0.00007	-0.00001
2.0	0.0667	-0.1794	-0.0563	0.1230	10.0	-0.00006	-0.00001	-0.00004	-0.00002
2.2	0.0244	-0.1548	-0.0652	0.0895					

For a pile whose head is fixed against rotation, as shown in Fig. 4.2(b), the solution may be obtained by employing the boundary conditions as given in Eqs. 4.33 and 4.34.

$$\text{at } x = 0, \quad \frac{dy}{dx} = 0 \tag{4.33}$$

$$\frac{d^3y}{dx^3} = \frac{P_t}{EI} \tag{4.34}$$

Using procedures as shown above, it was found that $\bar{C}_3 = \bar{C}_4 = P_t/4EI\beta^3$. The solution for long piles is given in Eqs. 4.35 through 4.39.

$$y = \frac{P_t\beta}{\alpha} A_1 \tag{4.35}$$

$$S = -\frac{P_t}{2EI\beta^2} D_1 \tag{4.36}$$

$$M = -\frac{P_t}{2\beta} B_1 \tag{4.37}$$

$$V = P_t C_1 \tag{4.38}$$

$$p = -P_t \beta A_1 \tag{4.39}$$

It is convenient frequently to have a solution for a third set of boundary conditions, as shown in Fig. 4.2(c). The boundary conditions are given in Eqs. 4.40 and 4.41.

$$\text{at } x = 0, \quad \frac{EI\,\frac{d^2y}{dx^2}}{\frac{dy}{dx}} = \frac{M_t}{S_t} \tag{4.40}$$

$$\frac{d^3y}{dx^3} = \frac{P_t}{EI} \tag{4.41}$$

Employing these boundary conditions, the coefficients $\bar{C}_3$ and $\bar{C}_4$ were evaluated as shown in Eqs. 4.42 and 4.43. For convenience in writing, the rotational restraint M_t/S_t is given the symbol k_θ.

$$\bar{C}_3 = \frac{P_t(2EI\beta + k_\theta)}{EI(\alpha + 4\beta^3 k_\theta)} \tag{4.42}$$

$$\bar{C}_4 = \frac{KP_t}{EI(\alpha + 4\beta^3 k_\theta)} \tag{4.43}$$

Equations 4.42 and 4.43 may be substituted into Eqs. 4.10 through 4.14 to obtain the expressions for the pile response.

4.3 PILE OF FINITE LENGTH

A solution for the case of the pile of finite length is useful. The following derivation is for one set of boundary conditions, as shown.

$$\text{at } x = 0 \qquad M = M_t \text{ or } \frac{d^2y}{dx^2} = \frac{M_t}{EI} \tag{4.44}$$

$$V = P_t \text{ or } \frac{d^3y}{dx^3} = \frac{P_t}{EI} \tag{4.45}$$

$$\text{at } x = L \qquad M = 0 \text{ or } \frac{d^2y}{dx^2} = 0 \tag{4.46}$$

$$V = 0 \text{ or } \frac{d^3y}{dx^3} = 0 \tag{4.47}$$

Employing Eqs. 4.44 and 4.12, Eq. 4.48 results.

$$\frac{M_t}{EI} = 2\beta^2(\bar{C}_2 - \bar{C}_4) \tag{4.48}$$

Employing Eqs. 4.45 and 4.13, Eq. 4.49 is obtained.

$$\frac{P_t}{EI} = 2\beta^3(-\bar{C}_1 + \bar{C}_2 + \bar{C}_3 + \bar{C}_4) \tag{4.49}$$

Employing Eqs. 4.46 and 4.12, Eq. 4.50 is obtained.

$$0 = 2\beta^2 e^{\beta L}(\bar{C}_2 \cos \beta L - \bar{C}_1 \sin \beta L) + 2\beta^2 e^{-\beta L}(\bar{C}_3 \sin \beta L - \bar{C}_4 \cos \beta L) \tag{4.50}$$

Employing Eqs. 4.47 and 4.13, Eq. 4.51 is obtained.

$$0 = 2\beta^3 e^{\beta L}(\bar{C}_2 \cos \beta L - \bar{C}_1 \sin \beta L - \bar{C}_2 \sin \beta L - \bar{C}_1 \cos \beta L) + 2\beta^3 e^{-\beta L}(-\bar{C}_3 \sin \beta L + \bar{C}_4 \cos \beta L + \bar{C}_3 \cos \beta L + \bar{C}_4 \sin \beta L) \tag{4.51}$$

Equations 4.48 through 4.51 can be solved in any convenient way for the coefficients $\bar{C}_1$ through $\bar{C}_4$. A step-by-step procedure that is straightforward is shown in the Appendix.

4.4 REFERENCES

Timoshenko, S. P., Strength of Materials, Part II, Advanced Theory and Problems, 2nd Edition - Tenth Printing. D. Van Nostrand Company, Inc., 1941, p. 20.

4.5 EXERCISES

4.1 Assume a fixed-head steel pipe pile with a 36-in. outside diameter and a wall thickness of 1.0 in. a length of 70 ft, and a lateral load of 40 kips at the mudline. Assume no axial load and that EI is constant with depth. Assume E_s = 2000 lb/sq in. and constant with depth. Compute deflection and bending moment as a function of depth.

4.2 Assume the pile in problem 1 is free to rotate at the mudline, find the maximum bending moment, and depth to point of maximum bending moment for increments of load of 10 kips until a plastic hinge develops in the steel.

4.3 Derive expressions for pile response with pile head restrained against rotation as shown in Fig. 4.2(c) for a "long" pile. Then repeat problem 1 assuming $k_\theta = M_t/S_t = 6 \times 10^8$ in.-lb.

CHAPTER 5. THE DIFFERENCE EQUATION METHOD FOR SOLVING THE DIFFERENTIAL EQUATION FOR A LATERALLY LOADED PILE

5.1 INTRODUCTION

If the relationship between soil reaction p and deflection y is linear and defined by the soil modulus E_s as shown in Fig. 3.2(b), the soil resistance per unit length of pile is equal to the modulus multiplied by the deflection. If the soil modulus is constant with depth and if the pile can be considered to be of infinite length, the differential equation can be solved rather easily. The solution is

$$y = e^{\beta x}(\bar{C}_1 \cos \beta x + \bar{C}_2 \sin \beta x) + e^{-\beta x}(\bar{C}_3 \cos \beta x + \bar{C}_4 \sin \beta x)$$

as shown in Chapter 4. As was shown, the coefficients $\bar{C}_1$, $\bar{C}_2$, $\bar{C}_3$, and $\bar{C}_4$ can be evaluated by using the boundary conditions.

If the soil modulus has a random variation with depth, the soil resistance is equal to some function of x multiplied by the deflection. The solution of the differential equation can be made by writing the differential equation in difference form. This method was suggested by Palmer and Thompson (1948). A convenient way of solving the difference equation has been suggested by Gleser (1953). Contributions to the general method have been made by Focht and McClelland (1955) and Howe (1955).

The differential equation is

$$\frac{d^4y}{dx^4} + \frac{E_s}{EI} y = 0 . \tag{5.1}$$

5.2 RELATIONSHIPS IN DIFFERENCE FORM

Figure 5.1 shows a portion of the elastic curve of a pile. Relationships in difference form are as follows:

$$\left(\frac{dy}{dx}\right)_{x=m} \cong \frac{y_{m-1} - y_{m+1}}{2h} \tag{5.2}$$

$$\left(\frac{d^2y}{dx^2}\right)_{x=m} \cong \frac{\frac{y_{m-1} - y_m}{h} - \frac{y_m - y_{m+1}}{h}}{h} \cong \frac{y_{m-1} - 2y_m + y_{m+1}}{h^2} . \tag{5.3}$$

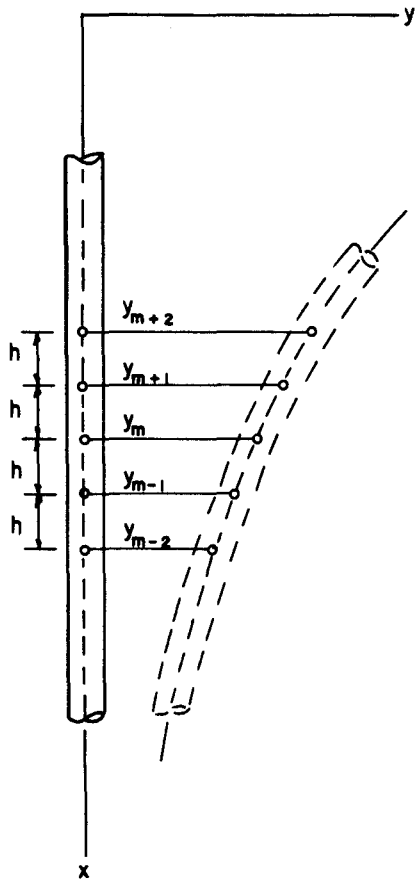

Fig. 5.1. Representation of deflected pile.

In a similar manner

$$\left(\frac{d^3y}{dx^3}\right)_{x=m} \cong \frac{y_{m-2} - 2y_{m-1} + 2y_{m+1} - y_{m+2}}{2h^3} \tag{5.4}$$

$$\left(\frac{d^4y}{dx^4}\right)_{x=m} \cong \frac{y_{m-2} - 4y_{m-1} + 6y_m - 4y_{m+1} + y_{m+2}}{h^4} \ . \tag{5.5}$$

Equation 5.5 is substituted into Eq. 5.1

$$y_{m-2} - 4y_{m-1} + 6y_m - 4y_{m+1} + y_{m+2} = \frac{-E_{sm}h^4}{EI} y_m \ . \tag{5.6}$$

Figure 5.2 shows the manner in which the pile is subdivided. Two imaginary points are shown below the tip of the pile and two above the top of the pile. Since E_s is presumably known for all points along the pile, it is possible to write t + 1 algebraic equations, similar to Eq. 5.6, for points 0 through t. Two boundary conditions at the tip of the pile and two

at the top of the pile yield four additional equations, giving a total of t + 5 simultaneous equations. When solved, these equations give the deflection of the pile from point -2 through point t + 2. A solution can be obtained for any number of subdivisions of the pile.

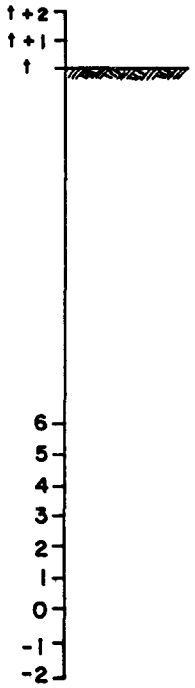

Fig. 5.2. Method of subdividing pile.

5.3 THE GLESER METHOD OF SOLUTION

Appendix 2 presents a detailed derivation of the method proposed by Gleser (1953) for the solution of the simultaneous algebraic equations.

The detailed derivations that are presented are intended to provide the reader with sufficient information on the difference-equation method to allow for the evaluation of the method. In addition, the derivations that are presented provide guidance in developing equations for additional sets of boundary conditions. For further guidance, a step-by-step computation procedure is presented.

1. Compute the A-values, using Eq. A2.7.
2. Compute B_0, B_1, and B_2 using Eqs. A2.14, A2.15, and A2.23.
3. Compute other B-values, using Eqs. A2.35 and A2.36 through B_{2t+1}.

4. Compute C_1^*, C_2^*, and C_3^* using Eqs. A2.47, A2.56, and A2.57. These steps are applicable to all cases.

(Steps 5 through 11 pertain to Cases 1 and 2)

5. Compute b_1 using Eq. A2.41 and b_5 using Eq. A2.63.
6. Compute y_t, y_{t+1}, and y_{t+2} using Eqs. A2.42, A2.73, and A2.74.
7. Compute y_{t-1}, y_{t-2}, and other y-values using Eq. A2.34 and appropriate B-values.
8. Compute slope using

$$S_m = \frac{y_{m-1} - y_{m+1}}{2h} . \tag{5.7}$$

9. Compute moment using

$$M_m = \frac{EI}{h^2} (y_{m-1} - 2y_m + y_{m+1}). \tag{5.8}$$

10. Compute shear using

$$V_m = \frac{EI}{2h^3} (y_{m-2} - 2y_{m-1} + y_{m+1} - y_{m+2}). \tag{5.9}$$

11. Compute soil reaction using

$$p_m = -E_{s_m} y_m. \tag{5.10}$$

(Steps 12 through 14 pertain to Case 3)

12. Compute b_1 using Eq. A2.41.
13. Compute y_t, y_{t+1}, and y_{t+2} using Eqs. A2.89, A2.82, and A2.80.
14. Other computations proceed as from Step 7, above.

5.4 EXAMPLE COMPUTATION

An example computation is presented to illustrate the step-by-step procedure.

Pile: 24 in. in diameter by 1 in. wall thickness;

$I = 4787$ in.^{4} ; length = 1200 in.

Loading: fixed-head case, $P_t = 60{,}000$ lb

Soil modulus: $E_s = kx$, $k = 5$ lb/cu in.

Number of increments: 5, $h = 240$ in.

Find: y_t and M_t

Computation of A-values:

$$A_m = \frac{k \times h^4}{EI} = 0.1155\ x$$

Point	x, in.	A_m
0	1,200	138.60
1	960	110.88
2	720	83.16
3	480	55.44
4	240	27.72
5	0	0

Computation of B-values:

$$B_0 = \frac{2}{A_0 + 2} = \frac{2}{138.60 + 2} = 0.014225$$

$$B_1 = 2B_0 = 0.028450$$

$$B_2 = \frac{1}{5 + A_1 - 2B_1} = \frac{1}{5 + 110.88 - (0.028450)2} = 0.008634$$

$$B_3 = B_2(4-B_1) = 0.008634(4-0.028450) = 0.034290$$

$$B_4 = \frac{1}{6 + A_2 - B_0 - B_3\,(4-B_1)}$$

$$= \frac{1}{6 + 83.16 - 0.014225 - 0.034290(4-0.028450)} = 0.011235$$

$$B_5 = B_4(4-B_3) = 0.011235(4-0.034290) = 0.044555$$

$$B_6 = \frac{1}{6 + A_3-B_2-B_5(4-B_3)}$$

$$= \frac{1}{6 + 55.44 - 0.008634 - 0.044555(4-0.034290)} = 0.016327$$

$$B_7 = B_6(4-B_5) = 0.016327(4-0.044555) = 0.064581$$

$$B_8 = \frac{1}{6 + A_4-B_4-B_7(4-B_5)} = \frac{1}{6 + 27.72 - 0.011235 - 0.064581(4-0.044555)}$$

$$= 0.029895$$

$$B_9 = B_8(4-B_7) = 0.029895(4-0.064581) = 0.117649$$

$$B_{10} = \frac{1}{6 + A_5 - B_6 - B_9(4-B_7)}$$

$$= \frac{1}{6 + 0 - 0.016327 - 0.117649(4-0.064581)} = 0.181127$$

$$B_{11} = B_{10}(4-B_9) = 0.181127(4-0.117649) = 0.703199 .$$

Computation of C*-values:

$$C_1^* = \frac{1}{B_{2t}} = \frac{1}{B_{10}} = \frac{1}{0.181127} = 5.520988$$

$$C_2^* = C_1^* B_{2t+1} - 2 - B_{2t-2}(2 - B_{2t-3}) = C_1^* B_{11} - 2 - B_8(2-B_7)$$

$$= 5.520988(0.703199) - 2 - 0.029895(2-0.064581) = 1.824494$$

$$C_3^* = C_1^* - B_{2t-4} - B_{2t-1}(2-B_{2t-3}) = C_1^* - B_6 - B_9(2 - B_7)$$

$$= 5.520988 - 0.016327 - 0.117649(2-0.064581) = 5.276961 .$$

Computation of y-values:

$$b_1 = \frac{2P_t h^3}{EI} = \frac{2(60{,}000)}{(30 \times 10^6)(4787)} \left(\frac{1200}{5}\right)^3 = 11.55128$$

$$y_5 = y_t = \frac{b_1(1 + B_{2t-2})}{C_3^*(1 + B_{2t-2}) - C^*_2 B_{2t-1}}$$

$$= \frac{11.55128(1 + 0.29895)}{5.276961(1+0.029895) - 1.824494(0.117649)} = 2.2719015 \text{ in.}$$

$$y_6 = y_{t+1} = \frac{B_{2t-1}(y_t)}{1 + B_{2t-2}} = \frac{0.117649(2.2719015)}{1 + 0.029895} = 0.260341 \text{ in.}$$

$$y_7 = y_{t+2} = C_1^*(B_{2t+1})(y_{t+1}) - C_1^* y_t = C_1^* B_{11} y_6 - C_1^* y_5$$

$$= 5.520988(0.703199)(0.260341) - 5.520988(2.2719015) = -11.571676 \text{ in.}$$

$$y_m = -B_{2m} y_{m+2} + B_{2m+1} y_{m+1}$$

$$y_4 = -B_8 y_6 + B_9 y_5 = - (0.029895 \times 0.260341) + (0.117649 \times 2.2719015) = 0.259504 \text{ in.}$$

$$y_3 = -B_6 y_5 + B_7 y_4 = - (0.016327 \times 2.2719015) + (0.064581 \times 0.259504) = - 0.0203344 \text{ in.}$$

$$y_2 = -B_4y_4 + B_5y_3 = - (0.011235 \times 0.259504) + (0.044555 \times$$
$$- 0.0203344) = - 0.0038215 \text{ in.}$$
$$y_1 = -B_2y_3 + B_3y_2 = - (0.008634 \times -0.0203344) + (0.034290 \times$$
$$- 0.0038215) = 0.0000442 \text{ in.}$$
$$y_0 = -B_0y_2 + B_1y_1 = - (0.014225 \times -0.0038215) + (0.028450 \times$$
$$0.0000442) = 0.0000556 \text{ in.}$$

Computation of shear and moment at mudline:

$$V_5 = \frac{EI}{2h^3} (y_3 - 2y_4 + 2y_6 - y_7)$$

$$V_5 = \frac{30 \times 10^6(4787)}{2(240)^3} [-0.0203344 - 2(0.259504) + 2(0.260341) - (-11.532405)]$$

$V_5 = 59{,}800$ lbs. Checks load at mudline.

$$M_5 = \frac{EI}{h^2} (y_4 - 2y_5 + y_6)$$

$$M_5 = \frac{30 \times 10^6(4787)}{(240)^2} [0.259504 - 2(2.2719015) + 0.260341]$$

$= -10{,}060{,}000$ in.-lbs

Dividing the pile into only 5 increments leads to serious errors because of failure to represent properly the elastic curve. Using 50 increments, the values of moment and deflection at the top of the pile were calculated to be

$$M_t = - 6{,}870{,}000 \text{ in.-lb},$$
$$y_t = 0.730 \text{ in.}$$

As may be understood, care should be used in deciding the mesh size and the number of significant figures to employ in solving the difference equations.

5.5 DIFFERENCE EQUATIONS FOR CASE OF AXIAL LOADING AND FOR CHANGES IN BENDING STIFFNESS

The solution procedure as presented by Gleser serves to illustrate the difference-equation method and the equations, for the case of a coarse

mesh, can be readily solved by hand. But for many practical problems it is necessary to address the effects of axial loading and changes in bending stiffness. Thus, the following derivation is presented but not in detail as was done in Appendix 2.

The governing differential equation was presented in Chapter 2; renumbered here for convenience.

$$EI \frac{d^4y}{dx^4} + P_x \frac{d^2y}{dx^2} + E_s y = 0 \tag{5.11}$$

Rewriting the first term of the equation with respect to moment and setting E_s to κ for ease in writing, we have

$$\frac{d^2M}{dx^2} + P_x \frac{d^2y}{dx^2} + \kappa y = 0. \tag{5.12}$$

The finite difference expressions for the first two terms of Eq. 5.12 at point m are

$$\left(\frac{d^2M}{dx^2}\right)_m = \Big[y_{m-2} R_{m-1} + y_{m-1} \left(-2R_m - 2R_{m-1}\right) + y_m(4R_m + R_{m-1} + R_{m+1}) + y_{m+1} \left(-2R_m - 2R_{m+1}\right) + y_{m+2} R_{m+1} \Big] \frac{1}{h^4} \tag{5.13}$$

and

$$P_x\left(\frac{d^2y}{dx^2}\right)_m = P_x \frac{\left(y_{m-1} - 2y_m + y_{m+1}\right)}{h^2}, \tag{5.14}$$

where

R_m = flexural rigidity at point (m), that is,
$R_m = E_m I_M$.

Substituting expressions from Eqs. 5.13 and 5.14 into 5.12 results in the differential equation in finite difference form.

$$y_{m-2}R_{m-1} + y_{m-1}\left(-2R_{m-1} - 2R_m + P_x h^2\right) + y_m\left(R_{m-1} + 4R_m + R_{m+1} - 2P_x h^2 + \kappa_m h^4\right) + y_{m+1}\left(-2R_m - 2R_{m+1} + P_x h^2\right) + y_{m+2} R_{m+1} = 0 \tag{5.15}$$

It is noted that the axial force P_x which produces compression is assumed to be positive. It is also noted that P_x acts through the axis of the pile; thus, P_x causes no moment at the top of the pile.

Applying the boundary conditions to the top and bottom of the pile, the solution to Eq. 5.15 can proceed (Gleser, 1953).

Using the previous notation, the two boundary conditions at the bottom of the pile (point 0) are zero bending moment,

$$\left(\frac{d^2y}{dx^2}\right)_0 = 0, \tag{5.16}$$

and zero shear,

$$R_0\left(\frac{d^3y}{dx^3}\right)_0 + P_x\left(\frac{dy}{dx}\right)_0 = 0. \tag{5.17}$$

For simplicity it is assumed that

$$R_{-1} = R_0 = R_1.$$

These boundary conditions are, in finite difference form,

$$y_{-1} - 2y_0 + y_1 = 0, \tag{5.18}$$

$$y_{-2} = y_{-1}\left(2 - \frac{P_x h^2}{R_0}\right) - y_1\left(2 - \frac{P_x h^2}{R_0}\right) + y_2, \tag{5.19}$$

respectively. Using these boundary conditions in finite difference form with Eq. 5.15 where m is equal to zero, and rearranging terms, results in the following equations.

$$y_0 = a_0 y_1 - b_0 y_2, \tag{5.20}$$

$$a_0 = \frac{2R_0 + 2R_1 - 2P_x h^2}{R_0 + R_1 + \kappa_0 h^4 - P_x h^2}, \tag{5.21}$$

$$b_0 = \frac{R_0 + R_1}{R_0 + R_1 + \kappa_0 h^4 - 2P_x h^2} \tag{5.22}$$

Equation 5.15 can be expressed for all values of m other than 0 and the top of the pile by the following relationships:

$$y_m = a_m y_{m+1} - b_m y_{m+2}, \tag{5.23}$$

$$a_m = \frac{-2b_{m-1}R_{m-1} + a_{m-2}b_{m-1}R_{m-1} + 2R_m - 2b_{m-1}R_m + 2R_{m+1} - P_x h^2(1-b_{m-1})}{c_m} \tag{5.24}$$

$$b_m = \frac{R_{m+1}}{c_m} \text{ , and} \tag{5.25}$$

$$c_m = R_{m-1} - 2a_{m-1}R_{m-1} - b_{m-2}R_{m-1} + a_{m-2}a_{m-1}R_{m-1} + 4R_m$$

$$- 2a_{m-1}R_m + R_{m+1} + \kappa_m h^4 - P_x h^2 \left(2-a_{m-1}\right). \tag{5.26}$$

Three sets of boundary conditions are considered at the top of the pile where m = t.

1. The lateral load (P_t) and the moment (M_t) are known.
2. The lateral load (P_t) and the slope of the elastic curve (S_t) are known.
3. The lateral load (P_t) and the rotational-restraint constant (M_t/S_t) are known.

For convenience in establishing expressions for these boundary conditions, the following constants are defined:

$$J_1 = 2hS_t \text{ ,} \tag{5.27}$$

$$J_2 = \frac{M_t h^2}{R_t} \text{ ,} \tag{5.28}$$

$$J_3 = \frac{2P_t h^3}{R_t} \text{ ,} \tag{5.29}$$

$$J_4 = \frac{h}{2R_t} \frac{M_t}{S_t} \text{ , and} \tag{5.30}$$

$$E = \frac{P_x h^2}{R_t} \text{ .} \tag{5.31}$$

The difference equations expressing the first of the boundary conditions for the top of the pile are:

$$\frac{R_t}{2h^3}\left(y_{t-2} - 2y_{t-1} + 2y_{t+1} - y_{t+2}\right)$$

$$+ \frac{P_x}{2h}\left(y_{t-1} - y_{t+1}\right) = P_t \text{ ,} \tag{5.32}$$

$$\frac{R_t}{h^2}\left(y_{t-1} - 2y_t + y_{t+1}\right) = M_t \text{ .} \tag{5.33}$$

After some substitutions the difference equations for the deflection at the top of the pile and at the two imaginary points above the top of the pile are:

$$y_t = \frac{Q_2}{Q_1} , \tag{5.34}$$

$$y_{t+1} = \frac{J_2 + G_1 y_t}{G_2} , \text{ and} \tag{5.35}$$

$$y_{t+2} = \left(\frac{a_t y_{t+1} - y_t)}{b_t} \right) , \tag{5.36}$$

where

$$Q_1 = H_1 + \frac{G_1 H_2}{G_2} + \left(1 - a_t \frac{G_1}{G_2} \right) \frac{1}{b_t} , \tag{5.37}$$

$$Q_2 = J_3 + \frac{a_t J_2}{b_t G_2} - \frac{J_2 H_2}{G_2} , \tag{5.38}$$

$$G_1 = 2 - a_{t-1} , \tag{5.39}$$

$$G_2 = 1 - b_{t-1} , \tag{5.40}$$

$$H_1 = -2a_{t-1} - Ea_{t-1} - b_{t-2} + a_{t-1}a_{t-2} , \text{ and} \tag{5.41}$$

$$H_2 = -a_{t-2}b_{t-1} + 2b_{t-1} + 2 + E(1 + b_{t-1}) . \tag{5.42}$$

The difference equations for the second set of boundary conditions are Eqs. 5.32 and 5.43:

$$y_{t-1} - y_{t+1} = J_1 . \tag{5.43}$$

The resulting difference equations for the deflections at the three points at the top of the pile are:

$$y_t = \frac{Q_4}{Q_3} , \tag{5.44}$$

$$y_{t+1} = \frac{a_{t-1} y_t - J_1}{G_4} , \text{ and} \tag{5.45}$$

$$y_{t+2} = \frac{a_t y_{t+1} - y_t}{b_t} , \tag{5.46}$$

where

$$Q_3 = H_1 + \frac{H_2 a_{t-1}}{G_4} - \frac{a_t a_{t-1}}{b_t G_4} + \frac{1}{b_t} , \tag{5.47}$$

$$Q_4 = J_3 + \frac{J_1 H_2}{G_4} - \frac{J_1 a_t}{b_t G_4}, \text{ and} \tag{5.48}$$

$$G_4 = 1 + b_{t-1}, \tag{5.49}$$

and the other constants are as previously defined.

The difference equations for the third set of boundary conditions are Eqs. 5.32 and 5.50:

$$\frac{y_{t-1} - 2y_t + y_{t+1}}{y_{t-1} - y_{t+1}} = J_4. \tag{5.50}$$

The resulting diference equations for the deflections at the three points at the top of the pile are:

$$y_t = \frac{J_3}{H_1 + H_2 H_3 - \frac{a_t}{b_t} H_3 + \frac{1}{b_t}} \tag{5.51}$$

$$y_{t+1} = \frac{y_t (G_1 + J_4 a_{t-1})}{G_2 + J_4 G_4} = H_3 y_t, \text{ and} \tag{5.52}$$

$$y_{t+2} = \frac{1}{b_t} \left(a_t y_{t+1} - y_t \right), \tag{5.53}$$

where

$$H_3 = \frac{G_1 + J_4 a_{t-1}}{G_2 + J_4 G_4}. \tag{5.54}$$

The other constants have been previously defined.

The differential equation can be revised and difference equations can be written to deal with distributed loads, applied shear and moment at any point along the pile, and inertial effects. A wide variety of problems can be addressed with the resulting nonlinear beam-column problem. Matlock (1956, 1957, 1958, 1962, 1964) has given attention to problem solutions using an approach similar to that presented herein.

5.6 COMPUTER PROGRAM COM622

A computer program, COM622, has been written for the beam-column equations presented in Eqs. 5.12 through 5.54. A listing of the program, input forms, sample input, and sample output are in Appendix 3.

Some comments pertaining to the use of the program are presented in comment cards in the listing. The following comments may also be useful. Limitations of the program:

- The pile is assumed to remain elastic;
- The ability to analyze group effects is not included;
- Information on response of complex soil profiles, e.g., layered soils, is extremely limited at present;
- Time effects, such as those associated with sustained or cyclic loading, are not directly included but can be taken into account indirectly by adjusting p-y curves in some appropriate manner.

The prudent engineer should treat results of this program as an aid in the overall process of engineering analysis and design, not as the sole basis for design nor as the final word on how a laterally loaded deep foundation will perform.

Computer program COM622 requires that p-y curves be computed according to the procedures presented in Chapter 3; the tables of p versus y then are used as input to COM622. Computer Program COM624 has been written in which the criteria for generating p-y curves are subroutines of the program and the engineer only has to specify soil properties, pile geometry, and the kind of loading (static or cyclic). COM624 is being distributed only to a user's group in order that the program can be maintained. An individual or firm who wishes information on the program and user's group can obtain it by writing to: The Geotechnical Engineering Center, The University of Texas at Austin, College of Engineering, Cockrell Hall 6.2, Austin, Texas 78712.

5.7 REFERENCES

Focht, John A.,Jr., and McClelland, Bramlette, "Analysis of Laterally Loaded Piles by Difference Equation Solution," presented at Spring meeting of the Texas Section of American Society of Civil Engineers, Corpus Christi, Texas, April 1955. Published later in three parts in The Texas Engineer publication of the Texas Section of American Society of Engineers, 1955.

Gleser, Sol M., "Lateral Load Tests on Vertical Fixed-Head and Free-Head Piles," Symposium on Lateral Load Tests on Piles, American Society Testing Materials Special Training Publication No. 154, pp. 75-101, 1953.

Howe, R. J., "A Numerical Method for Predicting the Behavior of Laterally Loaded Piling," TS Memorandum 9, Shell Oil Company, Houston, Texas, 1955.

Matlock, Hudson, "Correlations for Design of Laterally Loaded Piles in Soft Clay," a report to Shell Development Company, Houston, Texas, September 15, 1962, 71 pp.

Matlock, Hudson, and Haliburton, T. Allan, "A Program for Finite-Element Solution of Beam-Columns on Nonlinear Supports," a report to the California Company, Shell Development Company, June, 1964, 171 pp.

Matlock, Hudson, and Ripperger, E. A., "Measurement of Soil Pressure on a Laterally Loaded Pile," Proceedings, American Society for Testing Materials, Vol. 58, pp. 1245-1259, Boston, Massachusetts, 1958.

Matlock, Hudson, Ripperger, E. A., and Fitzgibbon, Don P., "Static and Cyclic Lateral Loading of an Instrumented Pile," a report to Shell Oil Company, Austin, Texas, 1956.

Matlock, Hudson, Ripperger, E. A., and Reese, L. C., "Recommendations Pertaining to the Design of Laterally Loaded Piles," a report to Shell Oil Company, Austin, Texas, 1957.

Palmer, A. L., and Thompson, James B., "Horizontal Pressures on Pile Foundations," Proceedings, Third International Conference on Soil Mechanics and Foundation Engineering, Rotterdam, Vol. 5, pp. 156-161, 1948.

5.8 EXERCISES

5.1 Derive equations for the case where the boundary conditions at the pile head are P_t and M_t/S_t.

5.2 Derive equations for the case where the boundary conditions at the pile head are P_t and S_t.

5.3 Solve the following example by hand computations using the difference equations and compare y_t and M_{max} with similar values for the "long" pile case, using equations in Chapter 4.

Pile: 24 in. in diameter by 1 in. wall thickness, length = 1200 in.

Loading: free-head case, P_t = 40,000 lb

Soil: Stiff clay, constant modulus E_s = 800 lb/sq in.

Number of increments = 6

(Note: the solutions should be identical except for the effect of length and the effect of inaccuracy due to the crude mesh size.)

5.4 Repeat Problem 3 using COM622 and compare results.

5.5 Repeat problems 4.1 and 4.2 in Chapter 4 using COM622. Check and compare results. Vary increment lengths and study errors.

CHAPTER 6. NONDIMENSIONAL METHOD FOR THE ANALYSIS OF LATERALLY LOADED PILES

A nondimensional method for the analysis of laterally loaded piles was presented in Chapter 4 for the case where the soil modulus is constant. That solution has limited usefulness because almost never would the value of soil modulus be constant over the pile length. There is some value, however, in having nondimensional solutions for other variations of soil modulus with depth. Some such solutions are developed in this section.

While nondimensional solutions can be developed for problems where a number of parameters are involved, a limited approach has been selected. Pile stiffness is assumed to be constant and the effect of axial loading is ignored. But nondimensional curves are developed, as shown below, for a number of variations of soil modulus with depth and for piles of various lengths (Matlock and Reese, 1962).*

Considering the nonlinearity of p-y relations at various depths, E_s is a function of both x and y. Therefore, the form of the E_s-versus-depth relationship also will change if the loading is changed. However, it may be assumed temporarily (subject to adjustment of E_s values by successive trial) that the soil modulus is some function of x only, or that

$$E_s = E_s(x). \tag{6.1}$$

For solution of the problem, the elastic curve y(x) of the pile must be determined, together with various derivatives that are of interest. The derivatives yield values of slope, moment, shear, and soil reaction as functions of depth.

6.1 DIMENSIONAL ANALYSIS FOR ELASTIC PILES

The principles of dimensional analysis may be used to establish the form of nondimensional relations for the laterally loaded pile. With the use of model theory the necessary relations will be determined between a "prototype" having any given set of dimensions, and a similar "model" for which solutions may be available.

---

*Note: The derivations that are presented follow closely the referenced paper.

For very long piles, the length L loses significance because the deflection may be nearly zero for much of the length of the pile. It is convenient to introduce some characteristic length as a substitute. A linear dimension T is therefore included in the quantities to be considered. The specific definition of T will vary with the form of the function for soil modulus versus depth. However, it will be seen later that, for each definition used, T expresses a relation between the stiffness of the soil and the flexural stiffness of the pile and is called the "relative stiffness factor."

For the case of an applied shear P_t and moment M_t the solution for deflections of the elastic curve will include the relative stiffness factor and be expressed as

$$y = y(x, T, L, E_s, EI, P_t, M_t). \tag{6.2}$$

Other boundary values can be substituted for P_t and M_t.

If the assumption of elastic behavior is introduced for the pile, and if deflections remain small relative to the pile dimensions, the principle of superposition may be employed. Thus, the effects of an imposed lateral load P_t and imposed moment M_t may be considered separately. If y_A represents the deflection due to the lateral load P_t and if y_B is the deflection caused by the moment M_t, the total deflection is

$$y = y_A + y_B. \tag{6.3}$$

It is the ratios of y_A to P_t and of y_B to M_t which are sought in reaching generalized solutions for the elastic pile. The solutions may be expressed for Case A as

$$\frac{y_A}{P_t} = f_A(x, T, L, E_s, EI), \tag{6.4}$$

and for Case B as

$$\frac{y_B}{M_t} = f_B(x, T, L, E_s, EI), \tag{6.5}$$

where f_A and f_B represent two different functions of the same terms. In each case there are six terms and two dimensions (force and length). There are therefore four independent nondimensional groups which can be formed. The arrangements chosen are, for Case A,

$$\frac{y_A EI}{P_t T^3}, \quad \frac{x}{T}, \quad \frac{L}{T}, \quad \frac{E_s T^4}{EI} \tag{6.6}$$

and for Case B,

$$\frac{y_B EI}{M_t T^2}, \quad \frac{x}{T}, \quad \frac{L}{T}, \quad \frac{E_s T^4}{EI} \quad . \tag{6.7}$$

To satisfy conditions of similarity, each of these groups must be equal for both model and prototype, as shown below.

$$\frac{x_p}{T_p} = \frac{x_m}{T_m} \tag{6.8}$$

$$\frac{L_p}{T_p} = \frac{L_m}{T_m} \tag{6.9}$$

$$\frac{E_{s_p} T_p^4}{EI_p} = \frac{E_{s_m} T_m^4}{EI_m} \tag{6.10}$$

$$\frac{y_{A_p} EI_p}{P_{t_p} T_p^3} = \frac{y_{A_m} EI_m}{P_{t_m} T_m^3} \tag{6.11}$$

$$\frac{y_{B_p} EI_p}{M_{t_p} T_p^2} = \frac{y_{B_m} EI_m}{M_{t_m} T_m^2} \tag{6.12}$$

A group of nondimensional parameters may be defined which will have the same numerical value for any model and its prototype. These are shown below.

Depth Coefficient, $$Z = \frac{x}{T} \tag{6.13}$$

Maximum Depth Coefficient, $$Z_{max} = \frac{L}{T} \tag{6.14}$$

Soil Modulus Function, $$\phi(Z) = \frac{E_s T^4}{EI} \tag{6.15}$$

Case A Deflection Coefficient, $$A_y = \frac{y_A EI}{P_t T^3} \tag{6.16}$$

Case B Deflection Coefficient, $$B_y = \frac{y_B EI}{M_t T^2} \tag{6.17}$$

Thus, from definitions 6.13 through 6.17, for (1) similar soil-pile stiffnesses, (2) similar positions along the piles, and (3) similar pile lengths (unless lengths are very great and need not be considered), the solution of the problem can be expressed from Eq. 6.3 and from Eqs. 6.16 and 6.17, as

$$y = \left[\frac{P_t T^3}{EI}\right] A_y + \left[\frac{M_t T^2}{EI}\right] B_y. \tag{6.18}$$

By the same type of reasoning other forms of the solution can be expressed as shown below.

$$\text{Slope,} \qquad S = S_A + S_B = \left[\frac{P_t T^2}{EI}\right] A_s + \left[\frac{M_t T}{EI}\right] B_s \tag{6.19}$$

$$\text{Moment,} \qquad M = M_A + M_B = \left[P_t T\right] A_m + \left[M_t\right] B_m \tag{6.20}$$

$$\text{Shear,} \qquad V = V_A + V_B = \left[P_t\right] A_v + \left[\frac{M_t}{T}\right] B_v \tag{6.21}$$

$$\text{Soil Reaction,} \quad p = p_A + p_B = \left[\frac{P_t}{T}\right] A_p + \left[\frac{M_t}{T^2}\right] B_p \tag{6.22}$$

A particular set of A and B coefficients must be obtained as functions of the depth parameter, Z, by a solution of a particular model. However, the above expressions are independent of the characteristics of the model except that elastic behavior and small deflections are assumed. The parameter T is still an undefined characteristic length and the variation of E_s with depth, or the corresponding form of $\phi(Z)$, has not been specified.

While the relations derived above are applicable to step-tapered piles which are frequently used in construction, it is necessary that structural similarity be maintained between the mathematical model and the prototype.

From beam theory, as presented earlier, the basic equation for an elastic beam is

$$EI \frac{d^4y}{dx^4} = p. \tag{6.23}$$

Introducing the definition of $p = -E_s y$, the equation for a beam on an elastic foundation, or for a laterally loaded pile, is

$$\frac{d^4y}{dx^4} + \frac{E_s}{EI} y = 0. \tag{6.24}$$

Where an applied lateral load P_t and an applied moment M_t are considered separately according to principle of superposition, the equation becomes, for Case A,

$$\frac{d^4y_A}{dx^4} + \frac{E_s}{EI} y_A = 0, \tag{6.25}$$

and for Case B,

$$\frac{d^4y_B}{dx^4} + \frac{E_s}{EI} y_B = 0. \tag{6.26}$$

Substituting the definitions of nondimensional parameters contained in Eqs. 6.13 through 6.17, a nondimensional differential equation can be written for Case A as

$$\frac{d^4A_y}{dZ^4} + \phi(Z)A_y = 0, \tag{6.27}$$

and for Case B as

$$\frac{d^4B_y}{dZ^4} + \phi(Z)B_y = 0. \tag{6.28}$$

To produce a particular set of nondimensional A and B coefficients, it is necessary (1) to specify $\phi(Z)$, including a convenient definition of of the relative stiffness factor T, and (2) to solve the differential equations (6.27 and 6.28). The resulting A and B coefficients may then be used, with Eqs. 6.18 through 6.22, to compute deflection, slope, moment, shear, and soil reaction for any pile problem which is similar to the case for which nondimensional solutions have been obtained.

Based on the boundary conditions P_t and M_t and the resulting A and B coefficients, relations have been derived so that problems may be solved for cases in which other boundary conditions are known. As shown later, nondimensional relationships have been derived so that almost any conceivable structure-soil-pile problem can be solved.

To obtain the A and B coefficients that are needed to make solutions with the nondimensional method, Eqs. 6.27 and 6.28 can be solved by use of

difference equations. Coefficients for other types of boundary conditions can be obtained in a similar manner.

6.2 DIMENSIONAL ANALYSIS FOR RIGID PILES

Piles or posts having relatively shallow embedment are frequently encountered in practice. Such piles behave essentially as rigid members, and the difference-equation method used in the elastic-theory solutions may become inaccurate because of the small successive differences which are involved. For such cases, a simpler theory is applicable, in which the pile is considered to be a rigid member (Matlock and Reese, 1962).

Although computations are simpler for the rigid pile than for the elastic pile, it is still convenient to use generalized solutions and to consider separately the effects of applied lateral load and applied moment.

In the derivation of the equations for the rigid pile it is convenient to include an additional term J that is later given particular definitions. The definitions of J depend on the form of the variation of the soil modulus with depth. For the present, J is simply a constant having the same dimensions (force x length^{-2}) as the soil modulus E_s.

For either Case A ($M_t = 0$) or Case B ($P_t = 0$) there are a total of six factors to be considered. For Case A,

$$y_A = y_A\,(x, L, E_s, J, P_t), \tag{6.29}$$

and for Case B,

$$y_B = y_B\,(x, L, E_s, J, M_t). \tag{6.30}$$

In each trial computation in an actual design problem, the soil is considered to be elastic. Thus, for either Case A or Case B, it is the ratio of deflection to loading which is sought in reaching generalized solutions. This reduces the number of nondimensional groups to three. For Case A these are

$$\frac{y_A JL}{P_t}, \frac{x}{L}, \frac{E_s}{J}, \tag{6.31}$$

and for Case B,

$$\frac{y_B JL^2}{M_t}, \frac{x}{L}, \frac{E_s}{J}. \tag{6.32}$$

For similarity between a prototype and a computed model, each nondimensional group may be defined as a dimensionless parameter. These are as shown below.

Depth Coefficient, $$h = \frac{x}{L} \tag{6.33}$$

Soil Modulus Function, $$\phi(h) = \frac{E_s}{J} \tag{6.34}$$

Case A Deflection Coefficient, $$a_y = \frac{y_A JL}{P_t} \tag{6.35}$$

Case B Deflection Coefficient, $$b_y = \frac{y_B JL^2}{M_t} \tag{6.36}$$

By superposition, the total deflection is

$$y = y_A + y_B \tag{6.37}$$

$$y = \left[\frac{P_t}{JL}\right] a_y + \left[\frac{M_t}{JL^2}\right] b_y \ . \tag{6.38}$$

From reasoning similar to the above, other forms of the solution can be expressed as shown below.

Slope, $$S = S_A + S_B = \left[\frac{P_t}{JL^2}\right] a_s + \left[\frac{M_t}{JL^3}\right] b_s \tag{6.39}$$

Moment, $$M = M_A + M_B = \left[P_t L\right] a_m + \left[M_t\right] b_m \tag{6.40}$$

Shear, $$V = V_A + V_B = \left[P_t\right] a_v + \left[\frac{M_t}{L}\right] b_v \tag{6.41}$$

Soil Reaction, $$p = P_A + P_B = \left[\frac{P_t}{L}\right] a_p + \left[\frac{M_t}{L^2}\right] b_p \tag{6.42}$$

For any given problem the slope ($S = dy/dx$) is a constant and all higher derivatives of y are zero. The last three expressions are related to the first two through the relation between soil reaction and pile deflection,

$$E_s = \frac{-p}{y} \tag{6.43}$$

or, in terms of the nondimensional coefficients,

$$\phi(h) = \frac{-a_p}{a_y} = \frac{-b_p}{b_y} \ . \tag{6.44}$$

The above dimensional analysis will apply to any form of the soil modulus functions E_s or $\phi(h)$. The soil modulus constant J is to be defined subsequently.

The nondimensional soil modulus function $\phi(h)$ is equivalent to the corresponding function $\phi(Z)$ used with the elastic-pile theory except that $\phi(h)$ is related to the length of the pile rather than to a relative stiffness between the pile and the soil.

For any given $\phi(h)$, there exists a single set of nondimensional-coefficient curves (for deflection, slope, moment, shear, and soil reaction). Design problems may be solved by essentially the same procedures as for the elastic-pile case. The choice of which theory to use is aided by comparing the results of nondimensional solutions obtained by the two methods.

The equation for deflection y of a rigid pile is

$$y = y_t + S\,x \tag{6.45}$$

where y_t is the deflection at $x = 0$ and S is the constant slope of the pile. The soil reaction is

$$p = -E_s y_t - E_s\,S\,x. \tag{6.46}$$

By statics, the equation for shear is

$$V = P_t + \int_o^x p\,dx. \tag{6.47}$$

Substituting the expression for p in Eq. 6.46 into Eq. 6.47 yields

$$V = P_t - y_t \int_o^x E_s\,dx - S \int_o^x x E_s\,dx. \tag{6.48}$$

The equation for moment is

$$M = M_t + Vx - \int_o^x x p\,dx, \tag{6.49}$$

or,

$$M = M_t + Vx + y_t \int_o^x x E_s + S \int_o^x x^2 E_s\,dx. \tag{6.50}$$

The shear and moment are zero at the bottom of the pile. Thus, the following equations may be written from Eqs. 6.48 and 6.50 so that y_t and S may be evaluated by simultaneous solution.

$$P_t = y_t \int_o^L E_s\,dx + S \int_o^L x E_s\,dx \tag{6.51}$$

$$M_t = -y_t \int_o^L x E_s\,dx - S \int_o^L x^2 E_s\,dx \tag{6.52}$$

The values obtained for y_t and S are then substituted into Eqs. 6.48 and 6.50 to complete the solution.

As in the procedure used in the elastic-pile theory, unit values may be introduced into the solution to obtain numerically correct values of the nondimensional coefficients defined in Eqs. 6.33 through 6.36. This amounts to determining the nondimensional coefficients from the results

of a numerically convenient model having unit values of L, P_t, and M_t. Coefficients in $E_s(x)$ are chosen to agree with those in the soil modulus function $\phi(h)$, and J is thus made equal to unity.

6.3 FORMS OF VARIATION OF SOIL MODULUS WITH DEPTH

In solving problems of laterally loaded piles by using nondimensional methods, the constants in the expressions describing the variation of soil modulus E_s with depth x are adjusted by trial until reasonable compatibility is obtained. The selected form of the soil modulus with depth should be kept as simple as possible so that a minimum number of constants needs to be adjusted.

Two general forms are a power form,

$$E_s = kx^n \tag{6.53}$$

and a polynomial form,

$$E_s = k_o + k_1 x + k_2 x^2. \tag{6.54}$$

The form $E_s = kx$ is seen to be a special case of either of these. A form similar to Eq. 6.53 has been suggested previously (Palmer and Brown, 1954).

The relative stiffness factor T of the elastic-pile theory and the soil modulus constant J of the rigid-pile theory must be defined for each form of the soil modulus-depth relation. While T and J may be defined in any way, it is convenient to select definitions that will simplify the corresponding nondimensional functions.

From the elastic-pile theory, Eq. 6.15 defining the nondimensional function for soil modulus is

$$\phi(Z) = \frac{E_s T^4}{EI}.$$

If the form $E_s = k\,x^n$ is substituted in Eq. 6.15, the result is

$$\phi(Z) = \frac{k}{EI}\, x^n T^4. \tag{6.55}$$

For the elastic-pile case, it is convenient to define the relative stiffness factor T by the following expression.

$$T^{n+4} = \frac{EI}{k} \tag{6.56}$$

Substituting this definition into Eq. 6.55 gives

$$\phi(Z) = \frac{x^n T^4}{T^{n+4}} = \left[\frac{x}{T}\right]^n. \tag{6.57}$$

Because $x / T = Z$, the general nondimensional function for soil modulus is

$$\phi(Z) = Z^n. \tag{6.58}$$

The above expression contains only one arbitrary constant, the power n. Therefore, for each value of n which may be selected, one complete set of independent, nondimensional solutions may be obtained from solution of Eqs. 6.27 and 6.28. For relatively short, elastic piles, separate computations must be made for each Z_{max} considered.

Appendix 4 contains a number of tables for making solutions using nondimensional methods. Tables A4.1 through A4.6 are for elastic piles and for the case where $E_s = kx^n$. One of the tables is for the case where $n = 0$, or E_s is a constant, and another table is for the case where $n = 1$, or $E_s = kx$. All of the tables are for the case where the nondimensional length of the pile is 10, that is, the pile acts as a "long" pile. A cover page is placed with the tables to provide a summary of the important equations and to show the general shape of the functions. Five additional sets of nondimensional coefficients are referenced subsequently; the same general format was employed in presenting each set of tables.

From the rigid-pile theory the function for soil modulus has been defined by Eq. 6.34 as $\phi(h) = E_s/J$. If the soil modulus constant J is now defined as

$$J = kL^n, \tag{6.59}$$

the corresponding general nondimensional function for soil modulus is

$$\phi(h) = \frac{kx^n}{kL^n}; \tag{6.60}$$

or, since $h = x / L$,

$$\phi(h) = h^n. \tag{6.61}$$

Only one set of nondimensional curves will be needed for each selected value of n, regardless of the length L.

Nondimensional coefficients for rigid piles for the case where $E_s = kx^n$ are presented in Tables A4.7 through A4.12 in Appendix 4.

When a polynomial is used to express the form of the soil modulus variation with depth, the relative stiffness factor T, or the soil modulus constant J, may be defined to simplify only one of the terms in the polynomial.

For the elastic-pile case, introducing the polynomial form into Eq. 6.15 gives

$$\phi(Z) = \frac{k_o T^4}{EI} + \frac{k_1 T^5}{EI} \frac{x}{T} + \frac{k_2 T^6}{EI} \left(\frac{x}{T}\right)^2 \ldots . \qquad (6.62)$$

To simplify the second term, as an example, T may be defined by the following expression.

$$T^5 = \frac{EI}{k_1} \qquad (6.63)$$

The resulting soil modulus function is

$$\phi(Z) = r_o + Z + r_2 Z^2 \ldots \qquad (6.64)$$

where

$$r_o = \frac{k_o}{k_1} \frac{1}{T} \text{ , and} \qquad (6.65)$$

$$r_2 = \frac{k_2}{k_1} [T] . \qquad (6.66)$$

For the rigid pile theory, from Eq. 6.34,

$$\phi(h) = \frac{k_o}{J} + \frac{k_1 x}{J} + \frac{k_2 x^2}{J} \ldots . \qquad (6.67)$$

Again to simplify the second term, J is defined by

$$J = k_1 L \qquad (6.68)$$

and

$$\phi(h) = \frac{k_o}{k_1 L} + \frac{k_1 x}{k_1 L} + \frac{k_2 x^2}{k_1 L} \ldots \qquad (6.69)$$

or

$$\phi(h) = r_o + h + r_2 h^2 \ldots \qquad (6.70)$$

where $h = x / L$ and

$$r_o = \frac{k_o}{k_1 L} \text{ , and} \qquad (6.71)$$

$$r_2 = \frac{k_2 L}{k_1} . \qquad (6.72)$$

A separate set of nondimensional curves would be needed for each desired combination of r-constants. Because of the complexity which otherwise would result, it does not appear reasonable to vary more than one constant and such forms as those following appear to be about as complicated as should be considered.

$$\phi(Z) = r_o + Z \qquad (6.73)$$

$$\phi(Z) = r_o + Z^2 \qquad (6.74)$$

While it would be permissable for some of the r-constants to have negative values, care must be taken that ϕ does not become negative.

Nondimensional coefficients for elastic piles for the case where $E_s = k_o + k_1 x$ are presented in Tables A4.13 through A4.18. Nondimensional coefficients for rigid piles for the case where $E_s = k_o + k_1 x$ are presented in Tables A4.19 through A4.24.

Because of the utility of employing the relatively simple variation of E_s with depth, $E_s = kx$, tables are included in Appendix 4 for that form of variation of E_s. The coefficients are presented in Tables A4.25 through A4.40. The next section gives some details on solutions with $E_s = kx$; in that section the nondimensional coefficients for $E_s = kx$ are shown as curves.

6.4 SOLUTION PROCEDURES

Reese and Matlock (1956) presented several arguments for the use of $E_s = kx$ as a viable variation in the soil modulus with depth. McClelland and Focht (1958) made use of $E_s = kx$ in analyzing the results of a field test, and as noted in Chapter 3, $E_s = kx$ is recommended in some instances as defining the early part of p-y curves. Further, an examination of the recommended families of p-y curves reveals that the ultimate resistance is always lower at the ground surface for soils with constant shear strength with depth. That fact, coupled with the fact that computed deflections are larger near the ground surface leads to the idea of an increasing soil modulus with depth (but does not necessarily suggest a zero modulus at the ground surface for clays).

A number of authors have suggested the use of $E_s = kx$ and the nondimensional curves presented herein in solving the problem of the pile under lateral loading (Department of Navy, 1971; George and Wood, 1976; Poulos and Davis, 1980).

As was shown earlier, solutions are available for more complicated variations in E_s with depth than $E_s = kx$; however, the use of $E_s = kx$ is a favorable choice at least for the initial computations.

Prior to initiating the solution procedures, it is desirable to reiterate the limitations of the nondimensional method: the effect of axial load on bending cannot be investigated, and the pile stiffness must be assumed to be constant. Of course, all of the limitations imposed during the derivation of the differential equation, e.g., no shear distortion and small deflections, are also present. The solution procedure is described below for three sets of boundary conditions at the top of the pile:

1) pile head free to rotate, 2) pile head fixed against rotation, and 3) pile head restrained against rotation (Reese and Matlock, 1956).

Case I - Pile Head Free to Rotate

1. Construct p-y curves at various depths by procedures recommended in Chapter 3, with the spacing between p-y curves being closer near the ground surface than near the bottom of the pile.
2. Assume a value of T, the relative stiffness factor. The relative stiffness factor is given as:

$$T = \sqrt[5]{EI/k} \tag{6.75}$$

where

EI = flexural rigidity of pile, and

k = constant relating the secant modulus of soil reaction to depth ($E_s = kx$).

3. Compute the depth coefficient z_{max}, as follows:

$$z_{max} = \frac{x_{max}}{T} . \tag{6.76}$$

4. Compute the deflection y at each depth along the pile where a p-y curve is available by using the following equation:

$$y = A_y \frac{P_t T^3}{EI} + B_y \frac{M_t T^2}{EI} , \tag{6.77}$$

where

A_y = deflection coefficient, found in Fig. 6.1,

P_t = shear at top of pile,

T = relative stiffness factor,

B_y = deflection coefficient, found in Fig. 6.2,

M_t = moment at top of pile, and

EI = flexural rigidity of pile.

The particular curves to be employed in getting the A_y and B_y coefficients depend on the value of z_{max} computed in Step 3.

5. From a p-y curve, select the value of soil resistance p that corresponds to the pile deflction value y at the depth of the p-y curve. Repeat this procedure for every p-y curve that is available.

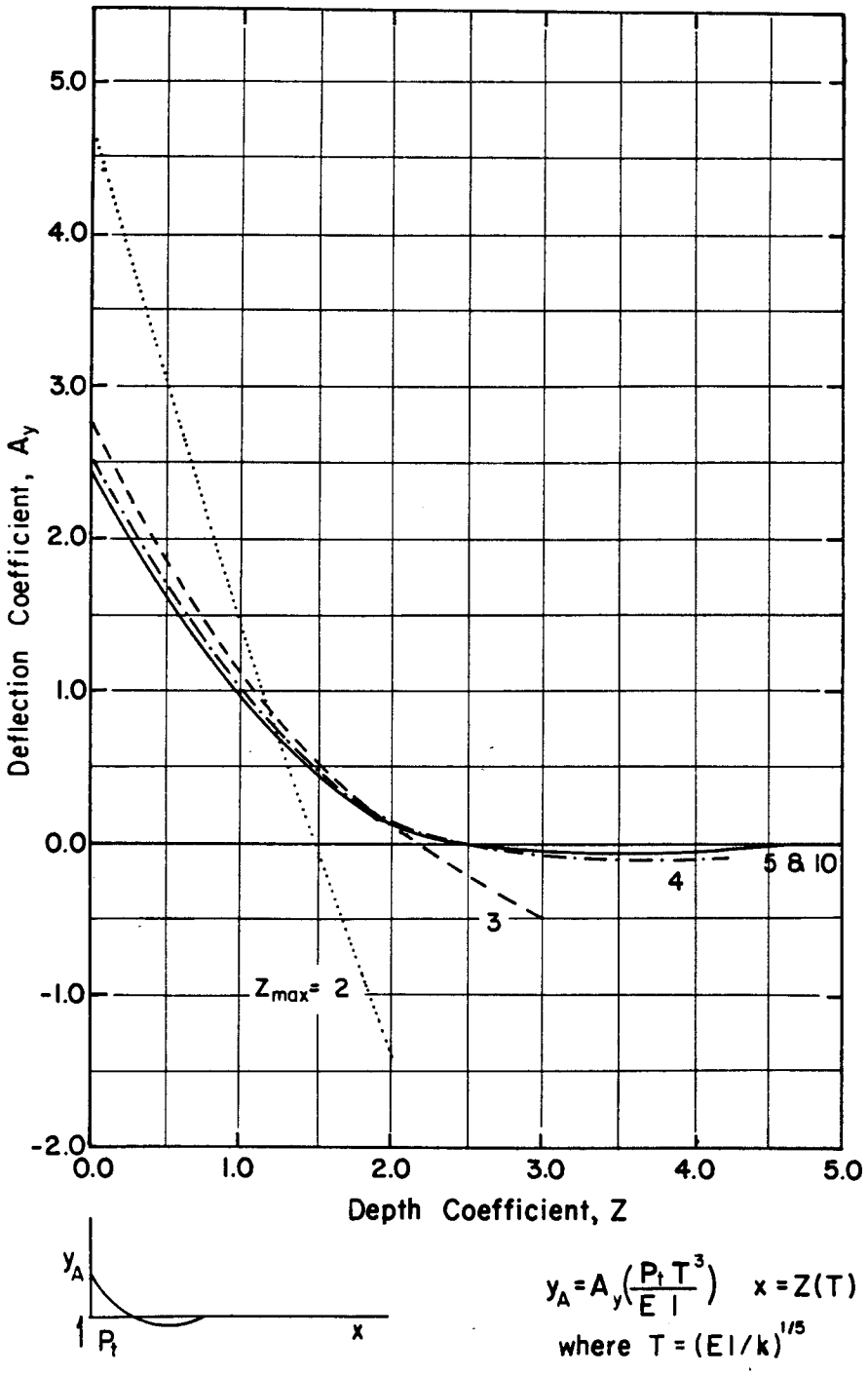

Fig. 6.1. Pile deflection produced by lateral load at groundline (Reese and Matlock, 1956).

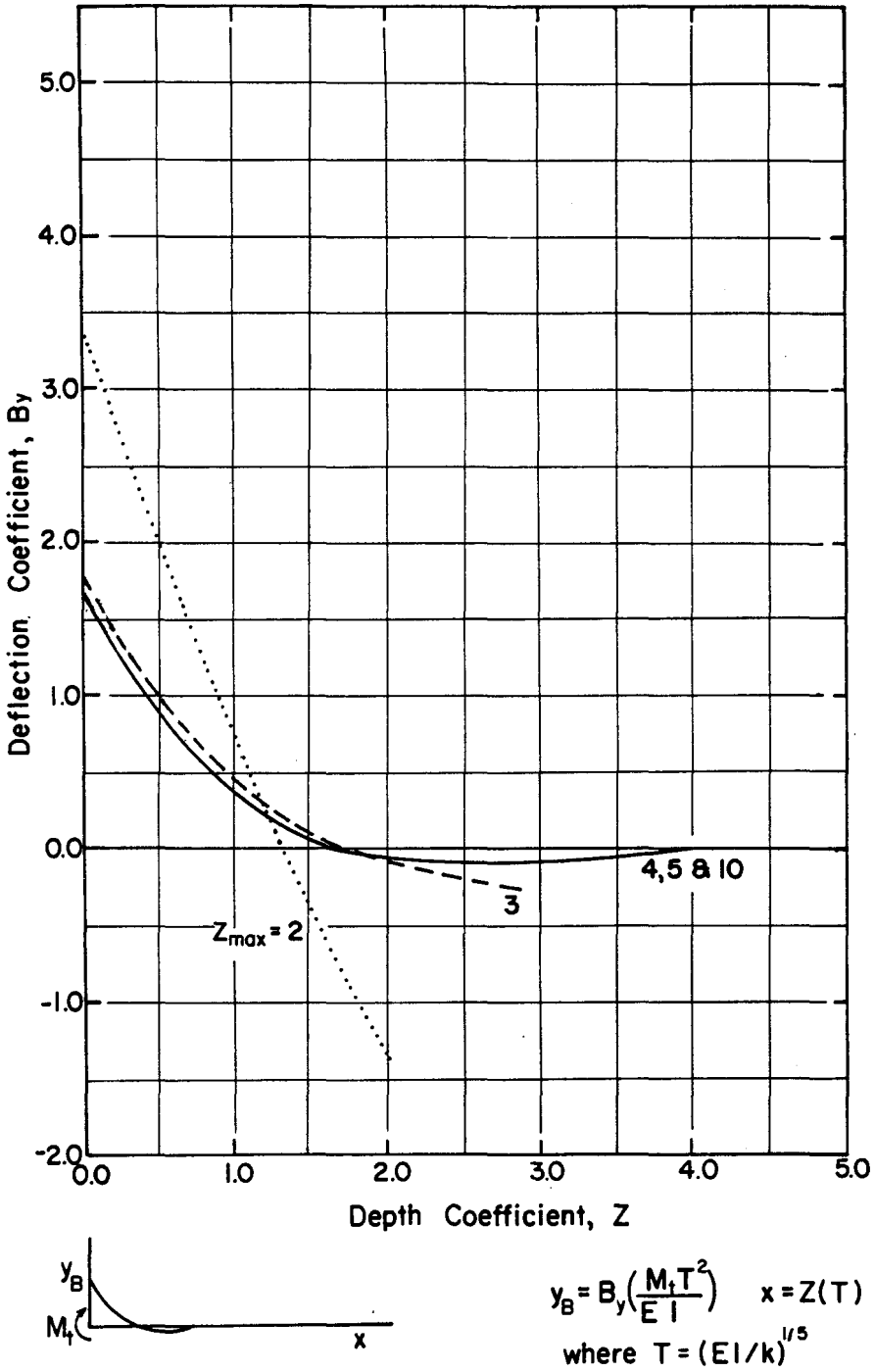

Fig. 6.2. Pile deflection produced by moment applied at groundline (Reese and Matlock, 1956).

6. Compute a secant modulus of soil reaction E_s using $E_s = -p/y$. Plot the E_s values versus depth.
7. From the E_s vs. depth plot in Step 6, compute the constant k which relates E_s to depth ($k = E_s/x$). Give more weight to the E_s values near the ground surface.
8. Compute a value of the relative stiffness factor T from the value of k found in Step 7. Compare this value of T to the value of T assumed in Step 2. Repeat Steps 2 through 8 using the new value of T each time until the assumed value of T equals the calculated value of T.
9. When the iterative procedure has been completed, the values of deflection along the pile are known from Step 4 of the final iteration. Values of soil reaction may be computed from the basic expression: $p = -E_s y$. Values of slope, moment, and shear along the pile can be found by using the following equations:

$$S = A_s \frac{P_t T^2}{EI} + B_s \frac{M_t T}{EI} \quad , \tag{6.78}$$

$$M = A_m P_t T + B_m M_t \quad ,$$

and

$$V = A_v P_t + B_v \frac{M_t}{T} \quad . \tag{6.79}$$

The appropriate coefficients to be used in the above equations may be obtained from Figs. 6.3 through 6.8.

Case II - Pile Head Fixed Against Rotation. Case II may be used to obtain a solution for the case where the superstructure translates under load but does not rotate and where the superstructure is very, very stiff in relation to the pile.

1. Perform Steps 1, 2, and 3 of the solution procedure as for free-head piles, Case I.
2. Compute the deflection y at each depth along the pile where a p-y curve is available by using the following equation:

$$y_F = F_y \frac{P_t T^3}{EI} \quad . \tag{6.80}$$

The deflection coefficients F_y may be found by entering Fig. 6.9 with the appropriate value of z_{max}.

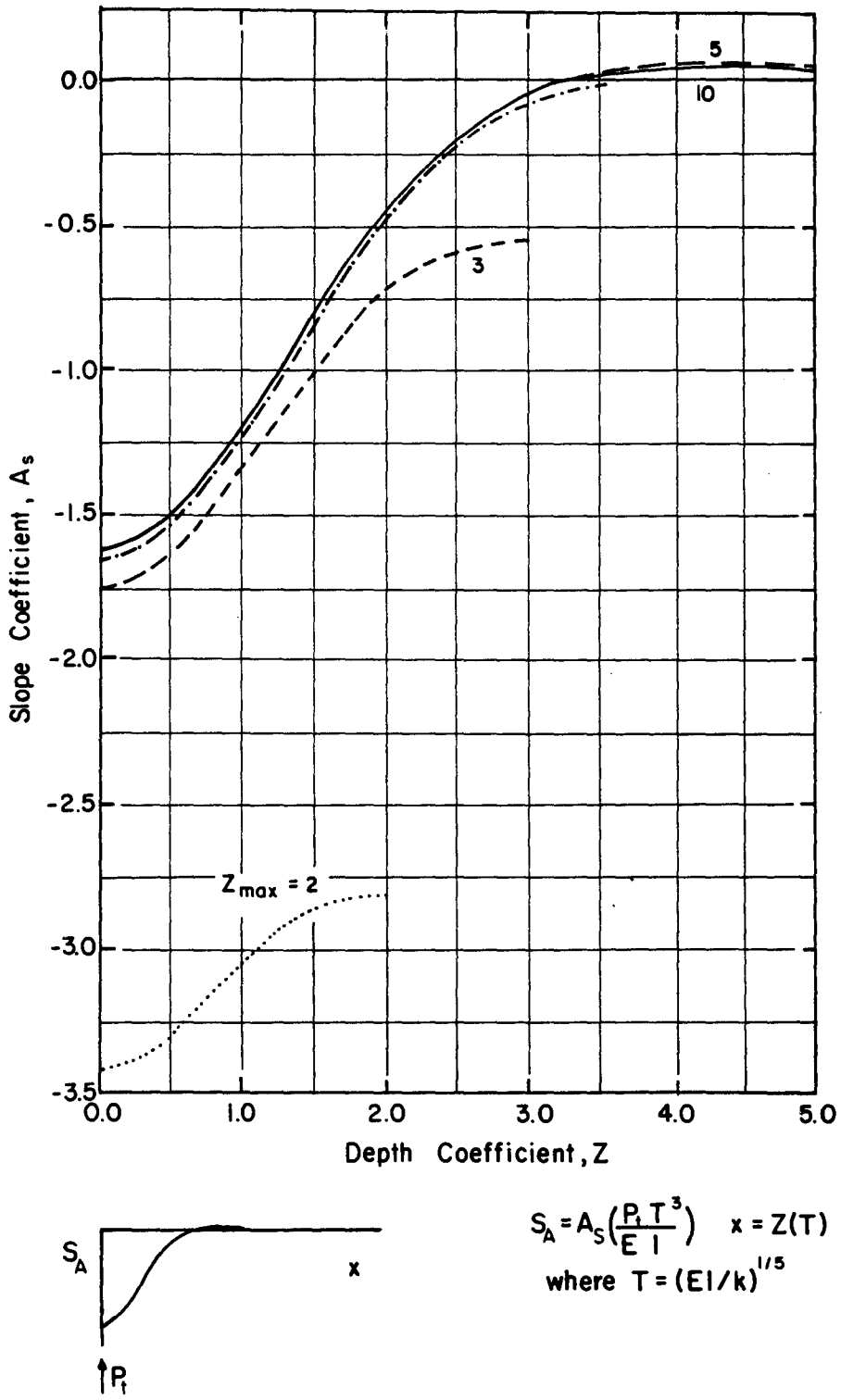

Fig. 6.3. Slope of pile caused by lateral load at groundline (Reese and Matlock, 1956).

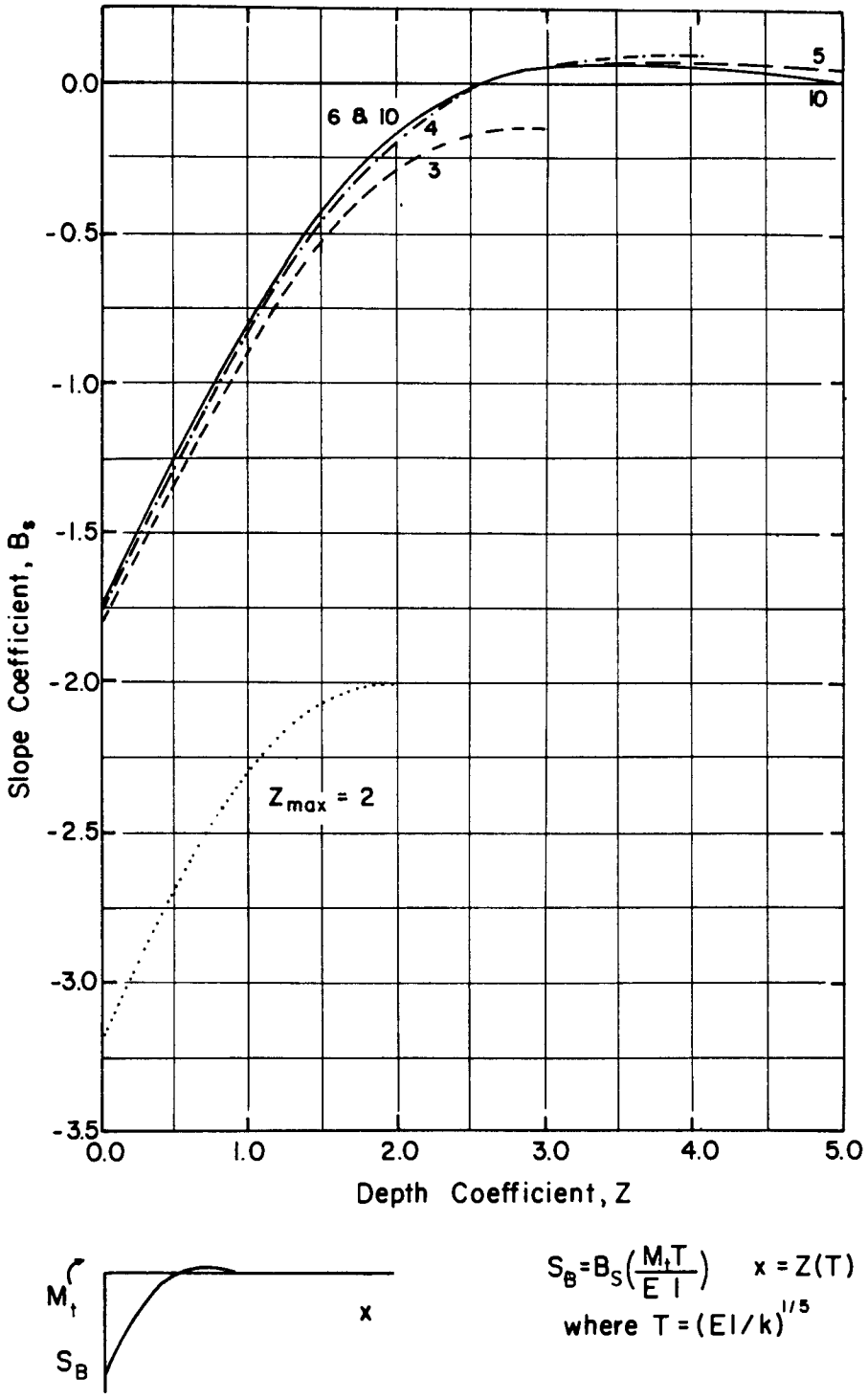

Fig. 6.4. Slope of pile caused by moment applied at groundline (Reese and Matlock, 1956).

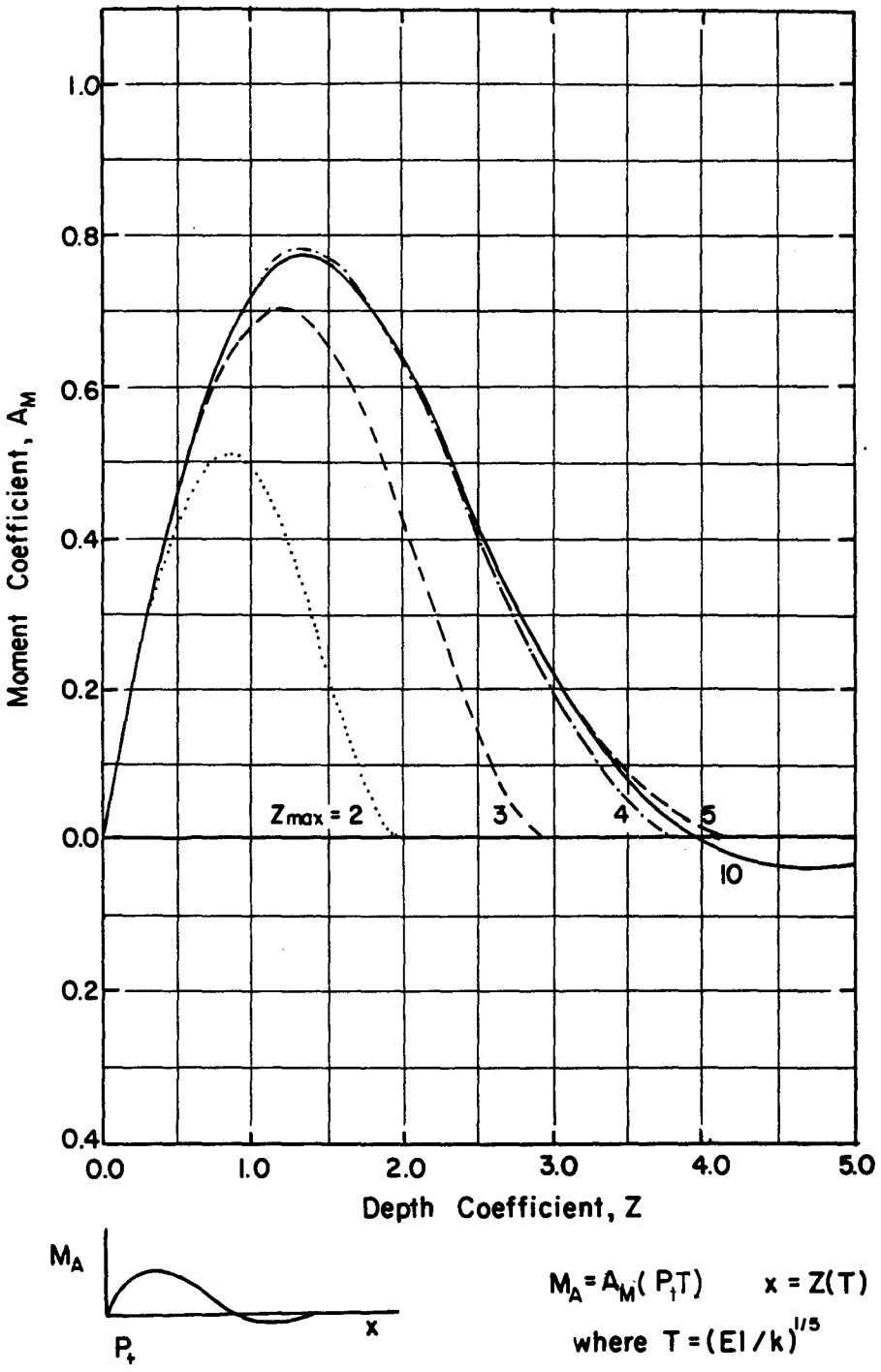

Fig. 6.5. Bending moment produced by lateral load at groundline (Reese and Matlock, 1956).

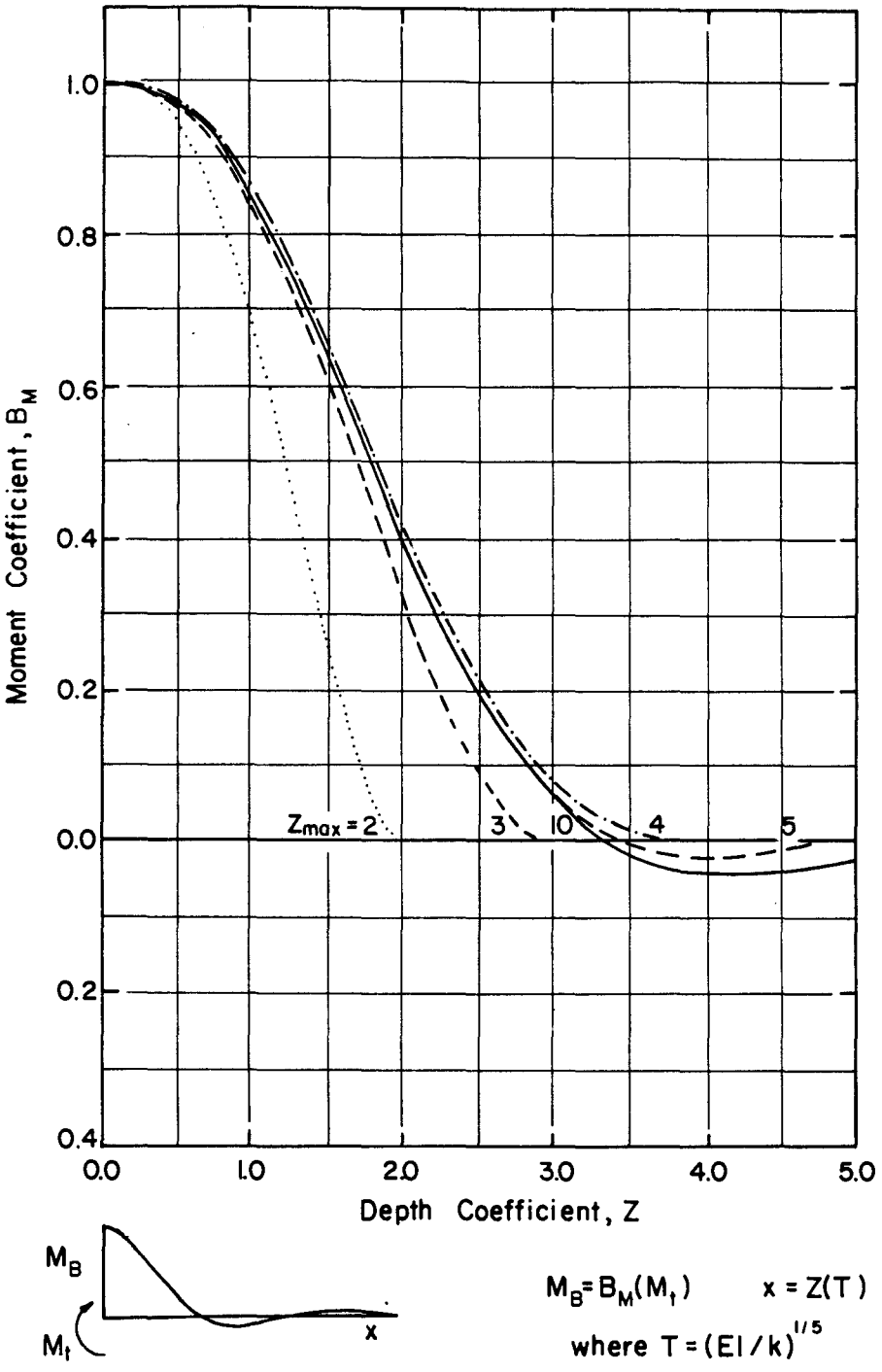

Fig. 6.6. Bending moment produced by moment applied at groundline (Reese and Matlock, 1956).

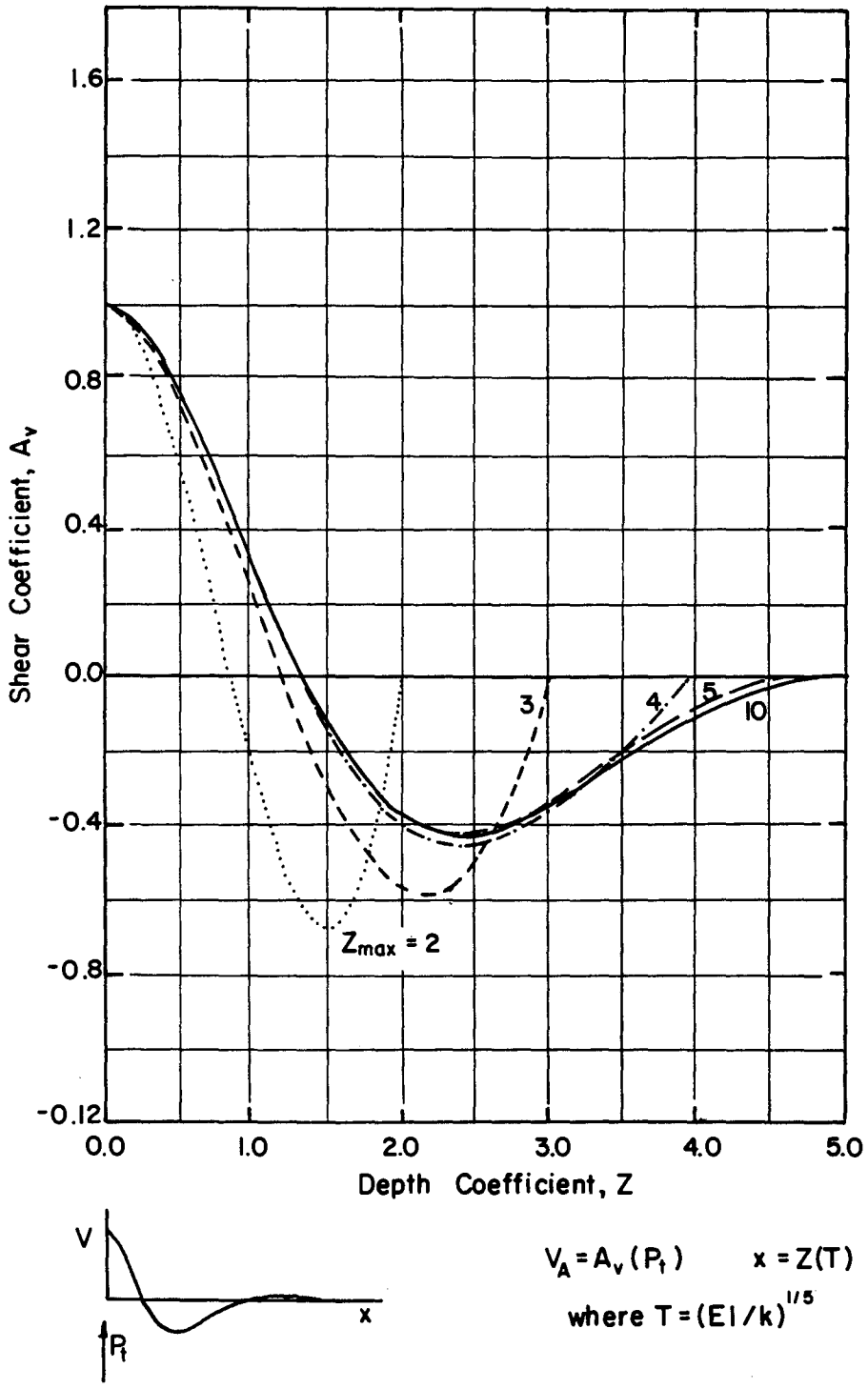

Fig. 6.7. Shear produced by lateral load at groundline (Reese and Matlock, 1956).

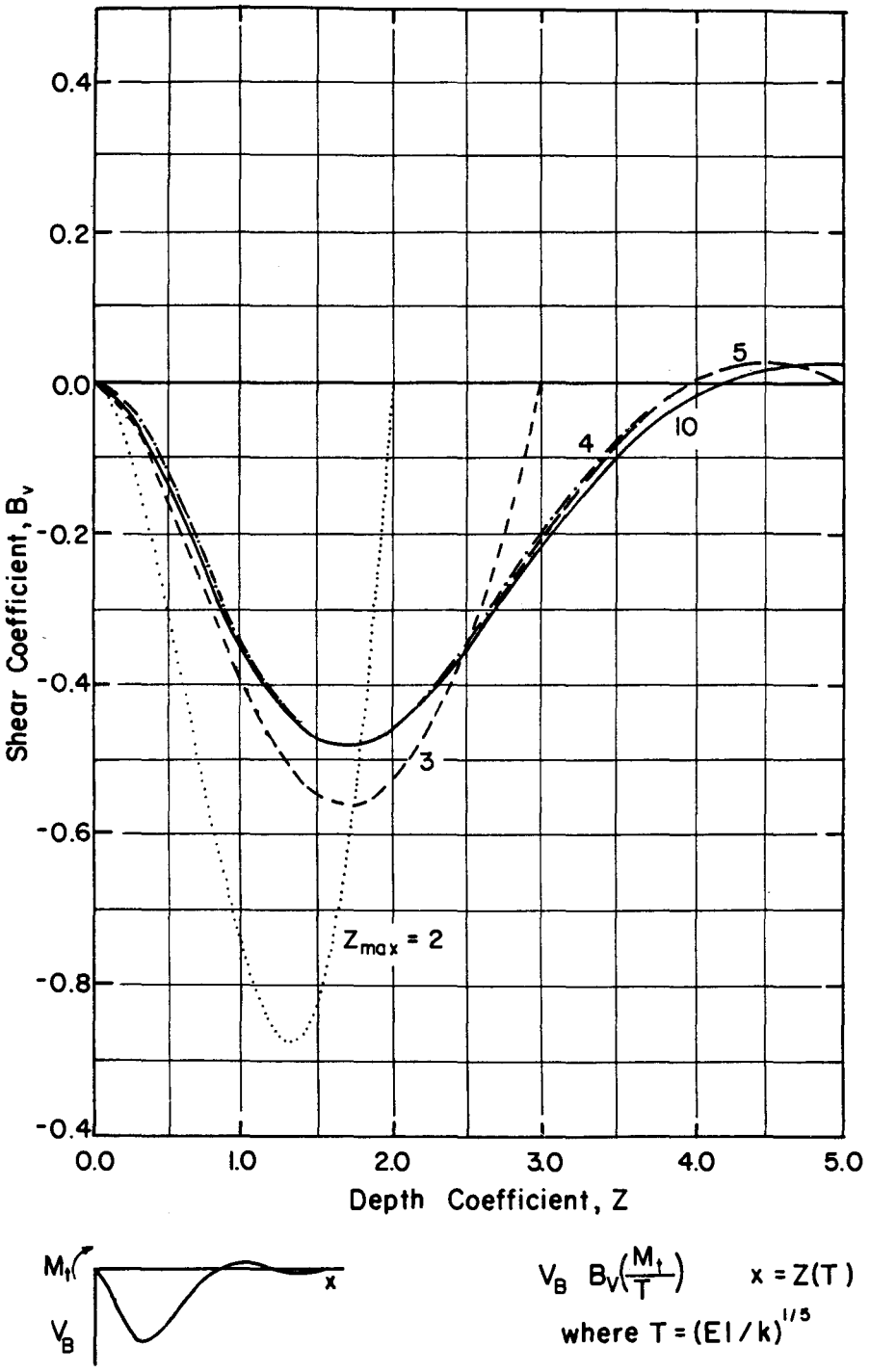

Fig. 6.8. Shear produced by moment applied at groundline (Reese and Matlock, 1956).

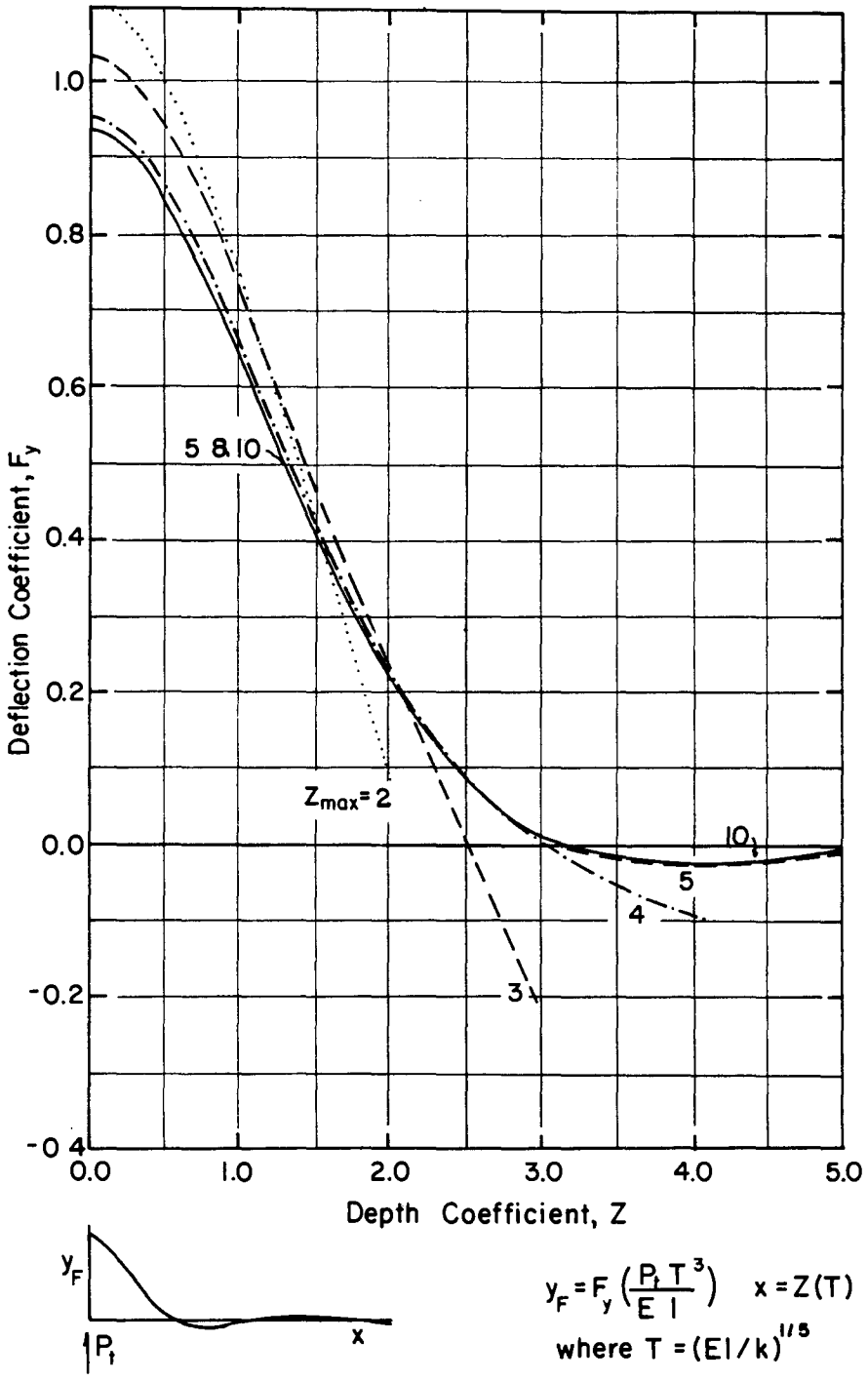

Fig. 6.9. Deflection of pile fixed against rotation at groundline (Reese and Matlock, 1956).

3. The solution proceeds in steps similar to those of Steps 5 through 8 for the free-head case.
4. Compute the moment at the top of the pile M_t from the following equation:

$$M_t = F_{mt} P_t T .$$

The value of F_{mt} may be found by entering Table 6.1 with the appropriate value of z_{max}.

TABLE 6.1. MOMENT COEFFICIENTS AT TOP OF PILE FOR FIXED-HEAD CASE.

z_{max}	F_{mt}
2	-1.06
3	-0.97
4	-0.93
5 and above	-0.93

5. Compute values of slope, moment, shear, and soil reaction along the pile by following the procedure in Step 9 for the free-head pile.

Case III - Pile Head Restrained Against Rotation. Case III may be used to obtain a solution for the case where the superstructure translates under load and where pile-head rotation is restrained.

1. Perform Steps 1, 2, and 3 of the solution procedure for free-head piles, Case I.
2. Obtain the value of the spring stiffness k_θ of the pile superstructure system. The spring stiffness is defined as follows:

$$k_\theta = \frac{M_t}{S_t} , \qquad (6.83)$$

where

M_t = moment at top of pile, and
S_t = slope at top of pile.

3. Compute the slope at the top of the pile S_t as follows:

$$S_t = A_{st} \frac{P_t T^2}{EI} + B_{st} \frac{M_t T}{EI}, \qquad (6.84)$$

where

A_{st} = slope coefficient, found in Fig. 6.3, and
B_{st} = slope coefficient, found in Fig. 6.4.

4. Solve Eqs. 6.83 and 6.84 for the moment at the top of the pile M_t.
5. Perform Steps 4 through 9 of the solution procedure for free-head piles, Case I.

This completes the solution of the laterally loaded pile problem for three sets of boundary conditions. The solution gives values of deflection, slope, moment, shear, and soil reaction as a function of depth. To illustrate the solution procedures, an example is presented.

6.5 SOLUTION OF EXAMPLE PROBLEM, ASSUMING $E_s = kx$

Find the deflection, moment and shear as a function of depth along a pile that is free to rotate and is subjected to a horizontal force and a moment. The p-y curves are to be constructed at 0, 2, 4, 8, 12, 16, and 24 ft. The soil is a stiff clay above the water table. Other data for the problem are shown below.

$P_t = 35{,}000$ lbs
$M_t = 3.02 \times 10^7$ in.-lbs
$L = 60$ ft
$b = 2$ ft
$EI = 7.39 \times 10^{10}$ lb-sq in.
$c = 1{,}000$ lb/sq ft
$\gamma = 110$ lb/cu ft
$N = 1{,}000$ cycles

The solution will proceed in the step-by-step manner as described for Case I.

1. Construct p-y curves.
   - Assume $\varepsilon_{50} = 0.01$ in the absence of stress-strain curves.
   - Compute p_u as the smaller of the values from Eqs. 3.18 and 3.19 for depths of 0, 24, 48, 96, 144, 192, and 288 in.
   - Compute y_{50} from Eq. 3.20 and compute points on the p-y curves for short-term static loading using Eq. 3.37.

- Compute y values for cyclic loading by use of Eq. 3.39 The results of the computations are shown in Table 6.2 and in Fig. 6.10.

TABLE 6.2. COMPUTED p-y CURVES*.

Depth, in.		0	24	48	96	144	192	288
y_{static}	y_{cyclic}	p, lb/in.						
0.000	0.000	0	0	0	0	0	0	0
0.001	0.003	51	63	75	99	123	147	152
0.015	0.04	100	123	147	195	243	291	299
0.24	0.67	199	247	294	390	485	580	596
0.60	1.68	250	310	370	490	610	730	750
1.24	3.48	300	372	444	588	731	875	899
2.50	7.00	357	443	529	700	872	1043	1072
5.00	14.00	425	527	629	833	1036	1240	1274
9.60	26.88	500	620	740	980	1220	1460	1500

*p-y cyclic curves are plotted in Fig. 6.10

2. Assume T: T = 125 in. The corresponding k is 2.42 cu in.
3. Compute z_{max}: $z_{max} = \frac{x_{max}}{T} = \frac{60(12)}{125} = 5.76$
4. Compute the deflection y at depths of 0, 2, 4, 8, 12, 16, and 24 ft using Eq. 6.77. (Use Figs. 6.1 and 6.2; the computations are tabulated in Table 6.3.)
5. From the set of p-y curves (Fig. 6.10 and Table 6.2), the values of p are selected corresponding to the y-values computed in Step 4. (See tabulation in Step 6.)
6. Compute the E_s value at each depth (see Table 6.4).

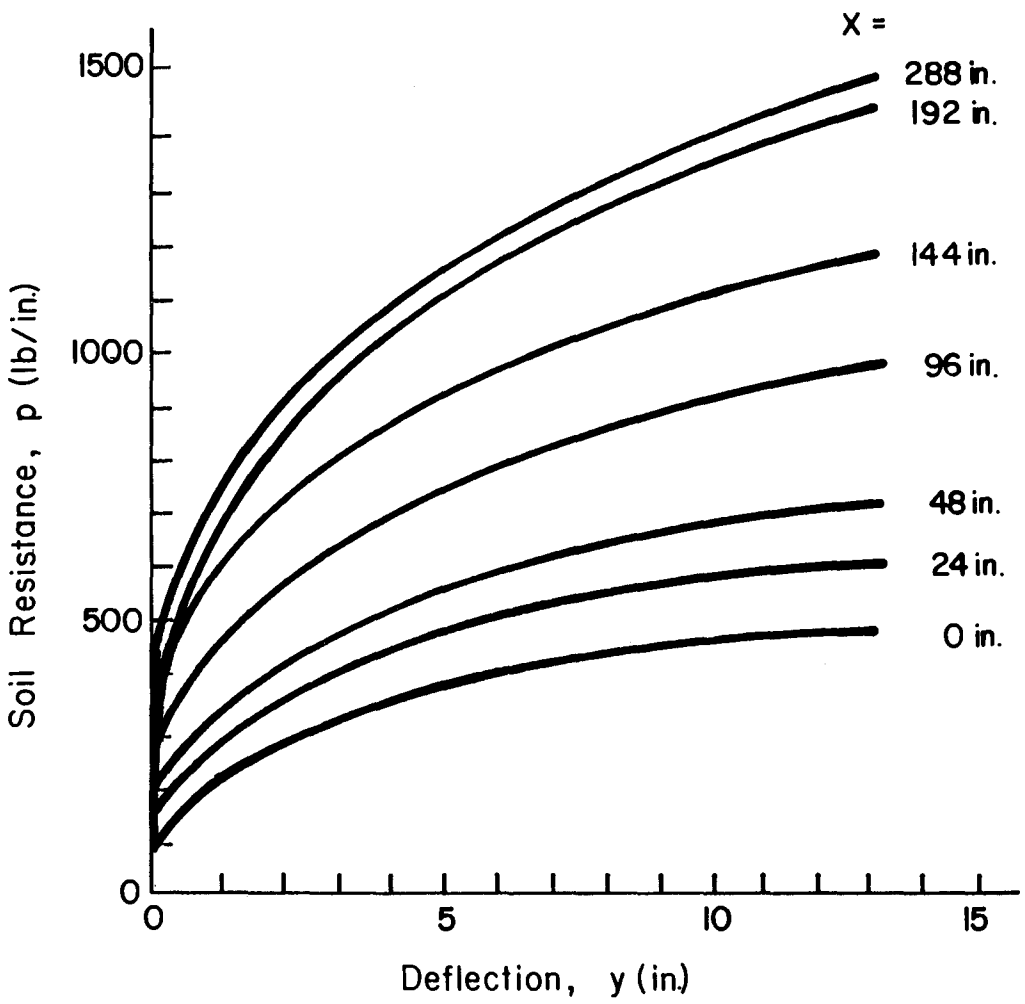

Fig. 6.10. Plot of p-y curves for example problem, stiff clay above water table, cyclic loading.

7. A plot of E_s vs. depth is shown in Fig. 6.11. The k value is:

$$k = E_s/x = \frac{500}{303} = 1.65 \text{ lb/cu in.}$$

8. Compute T:

$$T = \sqrt[5]{EI/k} = \sqrt[5]{\frac{7.39 \times 10^{10}}{1.65}} = 136 \text{ in.} \neq 126 \text{ in.}$$

TABLE 6.3. COMPUTED DEFLECTIONS.

x, in.	z	A_y	y_A, in.	B_y	y_B, in.	y, in.*
0	0	2.40	2.22	1.62	10.34	12.56
24	0.19	2.07	1.91	1.29	8.24	10.15
48	0.38	1.78	1.65	1.02	6.51	8.16
96	0.77	1.23	1.14	0.58	3.70	4.84
144	1.15	0.76	0.70	0.25	1.60	2.30
192	1.54	0.38	0.35	0.05	0.32	0.67
288	2.30	----	----	----	----	----

$$*y = A_y \frac{P_t T^3}{EI} + B_y \frac{M_t T^2}{EI} \quad (6.77)$$

TABLE 6.4. COMPUTED VALUES OF SOIL MODULUS.

x, in.	y, in.	p, lb/in.	E_s, lb/sq in.
0	12.56	411	33
24	10.15	481	47
48	8.16	546	67
96	4.84	631	130
144	2.30	652	283
192	0.67	580	866
288	----	---	---

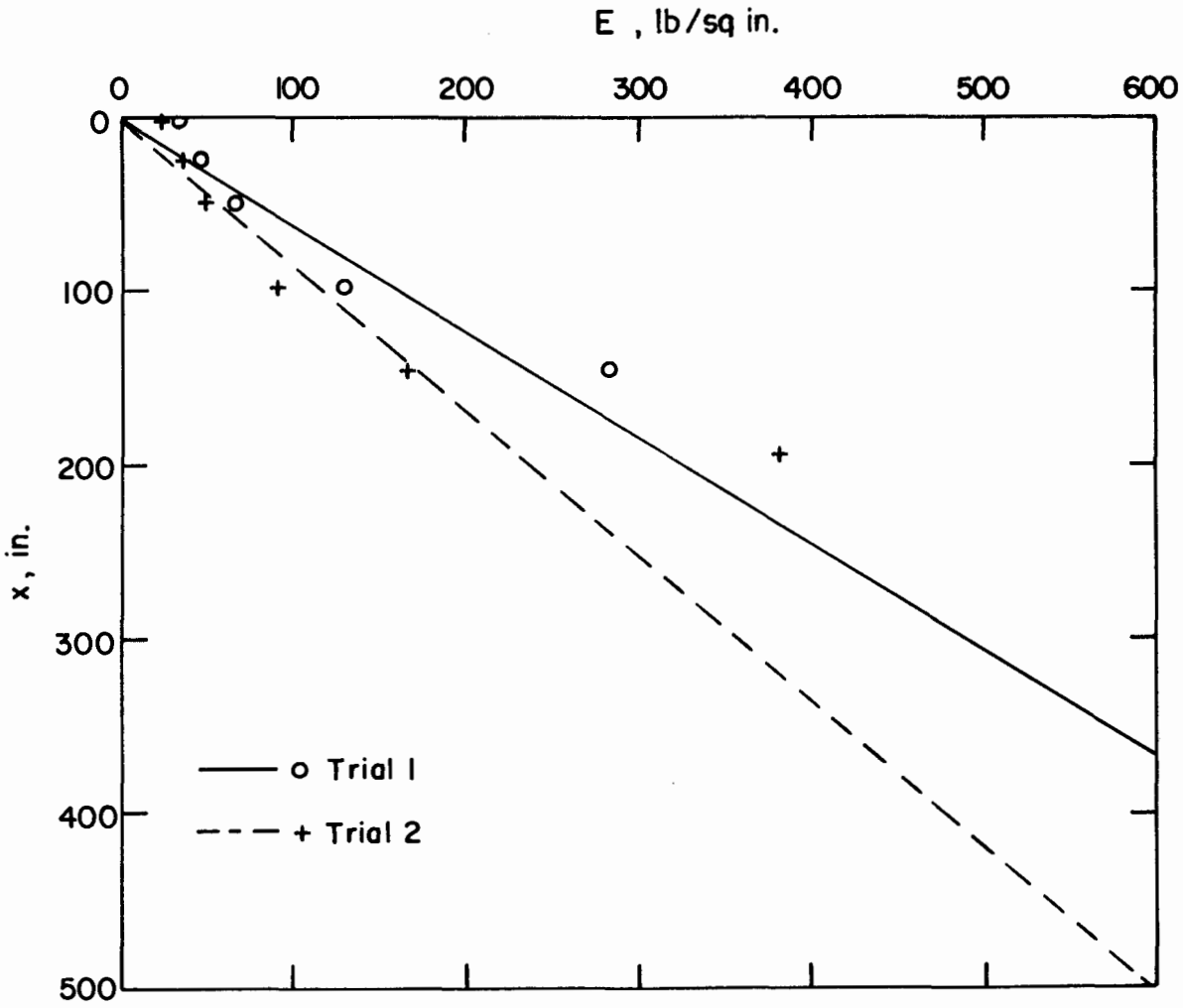

Fig. 6.11. Trial plots of soil modulus values (The first trial corresponds to computations in Table 6.4.).

This completes the first iteration of the solution procedure. Before proceeding to the next iteration, the results thus far will be examined for guidance with regard to further computations.

It is evident from Fig. 6.11 that $E_s = kx$ is not a good representation of the variation of the soil modulus with depth. A straight line passing through the origin does not fit the plotted points. At this point it could be desirable to use the nondimensional solutions based on a power or polynominal function (these solutions are presented later in this chapter). However, the solution will proceed by use of the nondimensional

curves based on E_s = kx in order to gain an approximate idea of the final design.

The solution has not been found because the k that was tried is not equal to the k that was obtained. Rather than making the next trial with a T of 136 in. (the value obtained in the first trial); it is preferable to select a larger value in order to speed the convergence; so a value of 145 in. is selected for the next trial. The selected value of T for the second trial corresponds to a k of 1.15 lb/cu in.

The computation of values of soil modulus for the second trial are not shown but proceed as shown in Tables 6.3 and 6.4. The plot of the values of soil modulus for Trial 2 is shown in Fig. 6.11. The value of k was found to be 1.20 lb/cu in., leading to a value of T of 144 in. The values of T that were tried and those obtained for each of the trials are shown in Fig. 6.12. As may be seen in the figure, convergence was achieved with a value of T of 143 in.

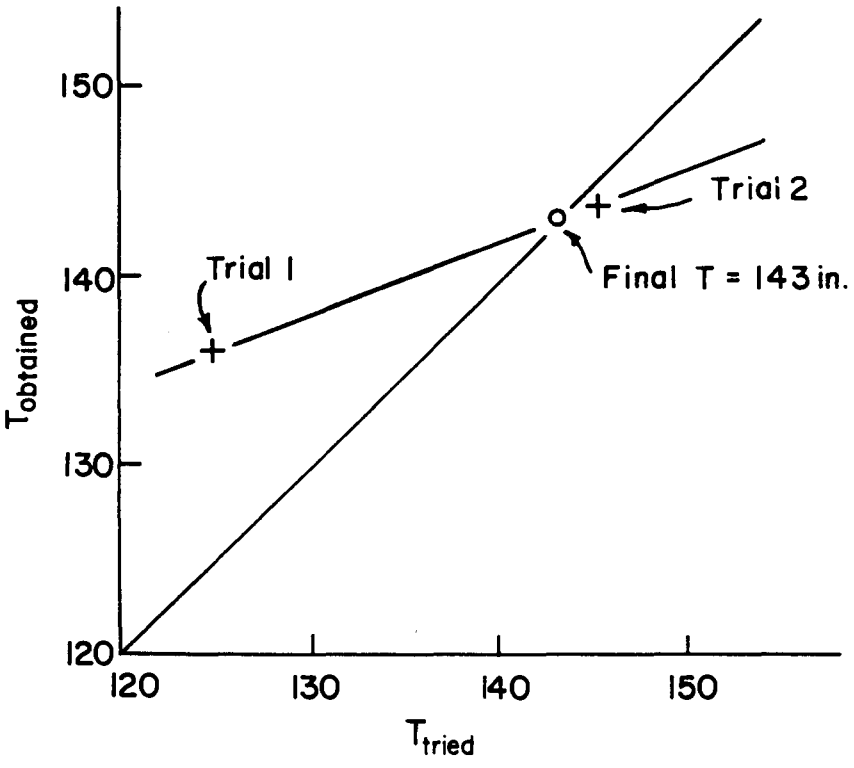

Fig. 6.12. Interpolation for final value of relative stiffness factor T.

9. Compute the values of moment and shear using Eqs. 6.79 and 6.80 (see Fig. 6.13). Also shown in Fig. 6.13 are plots of the moment and shear diagrams from a computer solution of the example problem.

As may be seen, excellent agreement is found between the computer solutions and the nondimensional solutions. This good agreement may be fortuitous; however, it is not unusual to get reasonably good agreement between solutions by computer and those by the nondimensional procedure.

The example is presented to illustrate the computational procedure and not as an exercise in design. As noted earlier, computations should be performed for a number of loads in making a design and parametric studies are desirable.

6.6 SOLUTION OF EXAMPLE PROBLEM, $E_s = kx^n$ AND $E_s = k_0 + k_1x$

As shown in Fig. 6.11, the computed values of E_s vs. x failed to pass through the origin but, except for that, seemed possibly to follow a parabolic curve. Therefore, it was decided to try the use of $E_s = kx^n$ and to see if a better fit to the computer solution could be obtained.

The first step was to use T of 143 in. and to compute the E_s values at points where p-y curves were available. These points are plotted in Fig. 6.14. The next step was to find the best fit of a parabola through those points (shown as circles in Fig. 6.14). The analytical fitting of a parabola proved unproductive because, in spite of appearances, the points from the $E_s = kx$ solution do not follow the parabolic equation.

The next step was to make some trial fits with selected values of k and n. This latter procedure is perhaps preferable to analytical fitting because the engineer can insure a better fit near the groundline where soil resistance has more influence on pile behavior. Two trials were made with different values of k and n and the results are shown in Fig. 6.14. The values in Trial 2 were thought to be preferable.

Tables A4.1 through A4.6 were then consulted and it was found that a table was not available for a value of n of 1.2. Tables were available for $n = 1$ ($E_s = kx$) and $n = 2$. It was decided to use $n = 2$ and to find values of k that would yield the best fit to E_s from p-y curves. An alternate procedure would have been to use double interpolation; that is, interpolating with z as an argument using tables with $n = 1$ and $n = 2$, and then interpolating again with n as the argument. This latter procedure did not

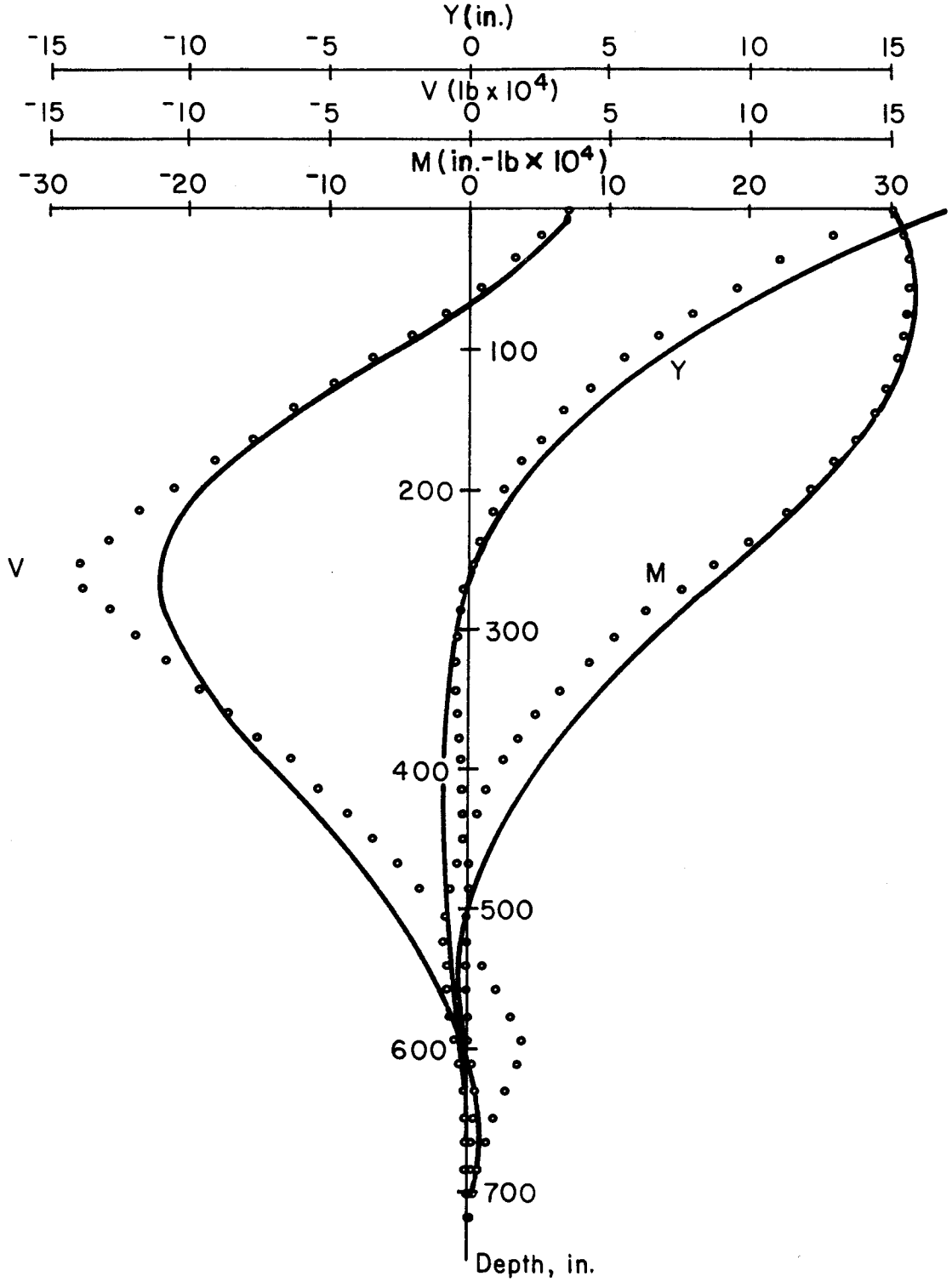

Fig. 6.13. Deflection and moment diagrams for example problem.

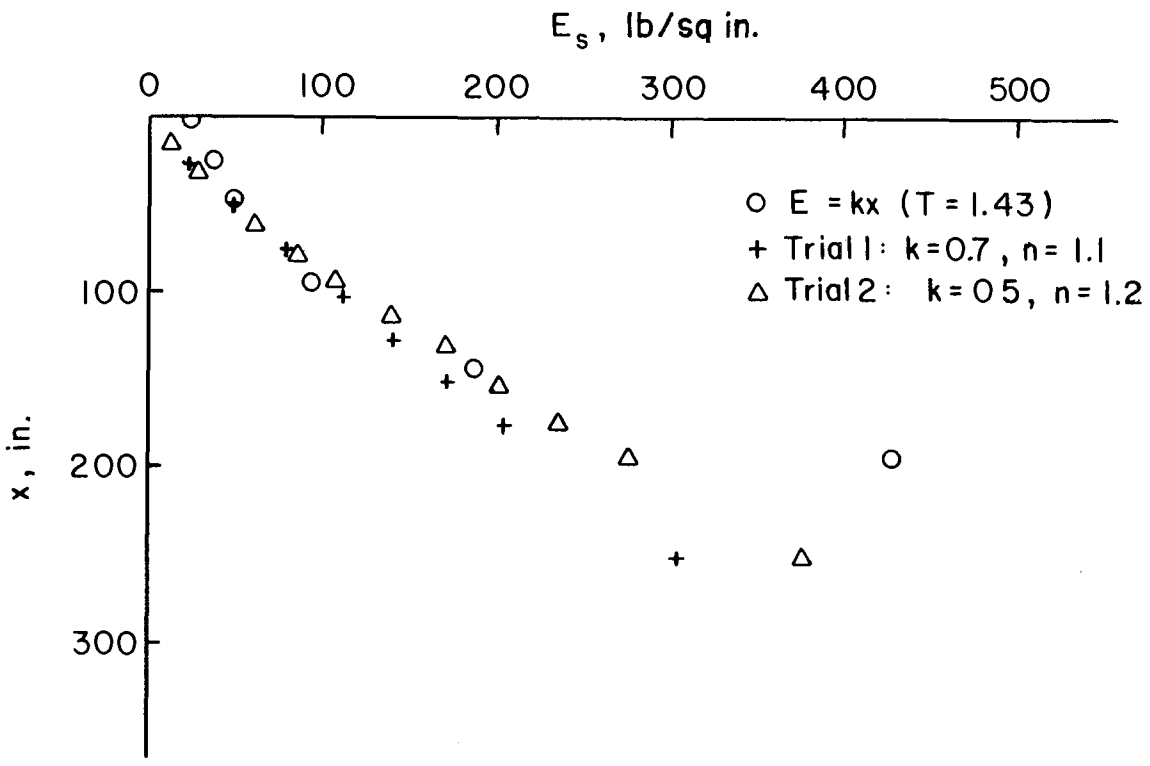

Fig. 6.14. Trial fitting of $E_s = kx^n$ for solution of example problem.

seem attractive. Of course, the computer program could be used to develop additional nondimensional coefficients; however, it seems undesirable to have large numbers of curves or tables.

Several trials were made with the table for n = 2 and it soon became apparent that the use of $E_s = kx^2$ was not yielding a good fit at all to the early part of the points for E_s versus x from the p-y curves. The computed curves for n = 2 are relatively quite steep near the origin; thus, the value of E_s at x = 0 (which is almost constant) could not be fitted and the fitting was deviating further and further from other values near the groundline. Therefore, the use of $E_s = kx^n$ was abandoned for the example problem.

The procedure continues with the use of $E_s = k_0 + k_1 x$. A trial was made by fitting a straight line, not passing through the origin, through points shown for $E_s = kx$ in Fig. 6.14. The value selected for k_0 was 20 lb/sq in. and for k_1 was 0.93 lb/cu in. With these values the following

computations were made:

$$T = \left(\frac{EI}{k_1}\right)^{1/5} = 151.37 \text{ in.}$$

$$\frac{k_0}{k_1 T} = 0.142$$

$$Z_{max} = 4.75.$$

The "long" pile solution could be used and values were taken from Tables A4.13 and A4.14. The double interpolation for values of A_y and B_y is shown in Table 6.5. The values of E_s shown in Table 6.5 agree well with the values computed using $E_s = kx$ with a T of 143 in. Therefore, it was decided to make no further trials.

Tables A4.13 and A4.14 were used to interpolate values of the coefficients for shear and moment. Computations were made and curves of computed deflection, moment, and shear are shown in Fig. 6.15. Also shown in the figure are similar curves obtained from the computer program.

An examination of the figure shows that the more complicated form of soil modulus with depth gave little or no improvement. The curves for deflection, moment, and shear as computed by $E_s = k_0 + k_1 x$ are very close to those computed with $E_s = kx$.

6.7 ALTERNATE SOLUTION TO RESTRAINED-HEAD CASE

Earlier in this chapter a procedure was presented for dealing with the problem where the pile head is attached elastically to the superstructure. Thre is an alternate solution to the restrained-head problem, as will be shown in this section. The solution is presented in connection with an example (Matlock and Reese, 1961). The solution is developed for the case where $E_s = kx$. Solutions for other variations of E_s with x are possible but the desirability for these other solutions is questionable.

A typical offshore structure is shown in Fig. 6.16. While an offshore structure is used as an exmple, the method applies equally well to a bridge bent. The specific problem considered is that of solving for the bending moments in the portion of the structural system which lies beneath the soil surface. In erecting such a structure, a prefabricated welded-pipe framework or "jacket" is set in place on the ocean bottom and pipe piles are driven through the vertical members of the jacket.

TABLE 6.5. COMPUTED VALUES OF SOIL MODULUS, $E_s = k_0 + k_1 x$.

$\frac{k_0}{k_1 T}$		0.1		0.2		0.142						
x in.	Z	A_y	B_y	A_y	B_y	A_y	B_y	y_A in.	y_B in.	y in.	p lb/in.	E_s lb/in.
0	0.000	2.151	1.468	1.930	1.348	2.058	1.418	3.38	13.28	16.66	440	26
24	0.159	1.918	1.218	1.717	1.109	1.834	1.082	3.01	10.13	13.14	517	39
48	0.317	1.690	0.993	1.508	0.895	1.656	0.952	2.72	8.91	11.63	595	51
96	0.634	1.258	0.616	1.114	0.540	1.198	0.584	1.97	5.47	7.44	708	95
144	0.951	0.880	0.333	0.771	0.277	0.834	0.309	1.37	2.89	4.26	762	179
192	1.268	0.569	0.135	0.491	0.097	0.536	0.119	0.88	1.11	1.99	755	379

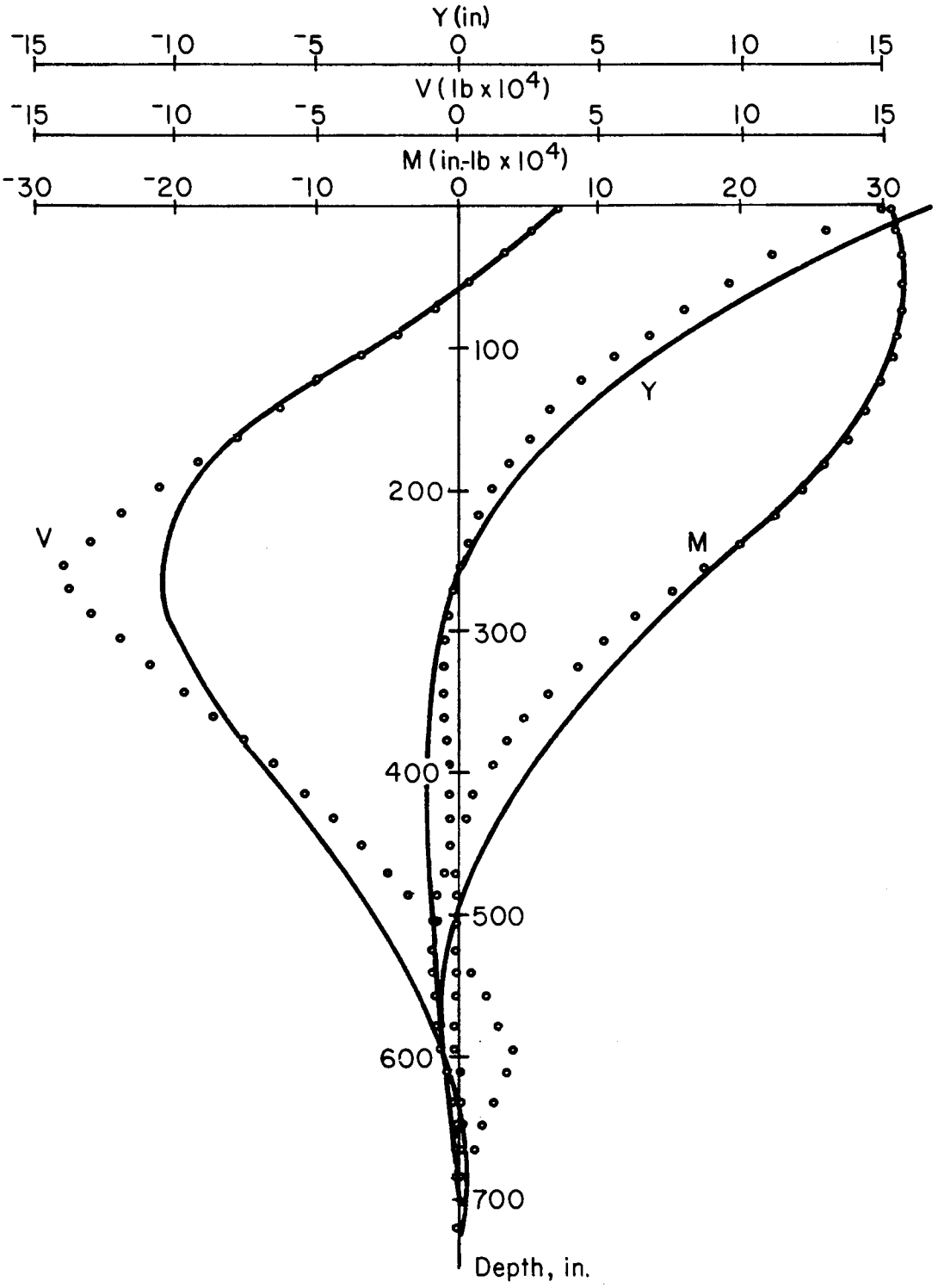

Fig. 6.15. Deflection, moment, and shear diagrams for example problem, $E_s = k_0 + k_1 x$.

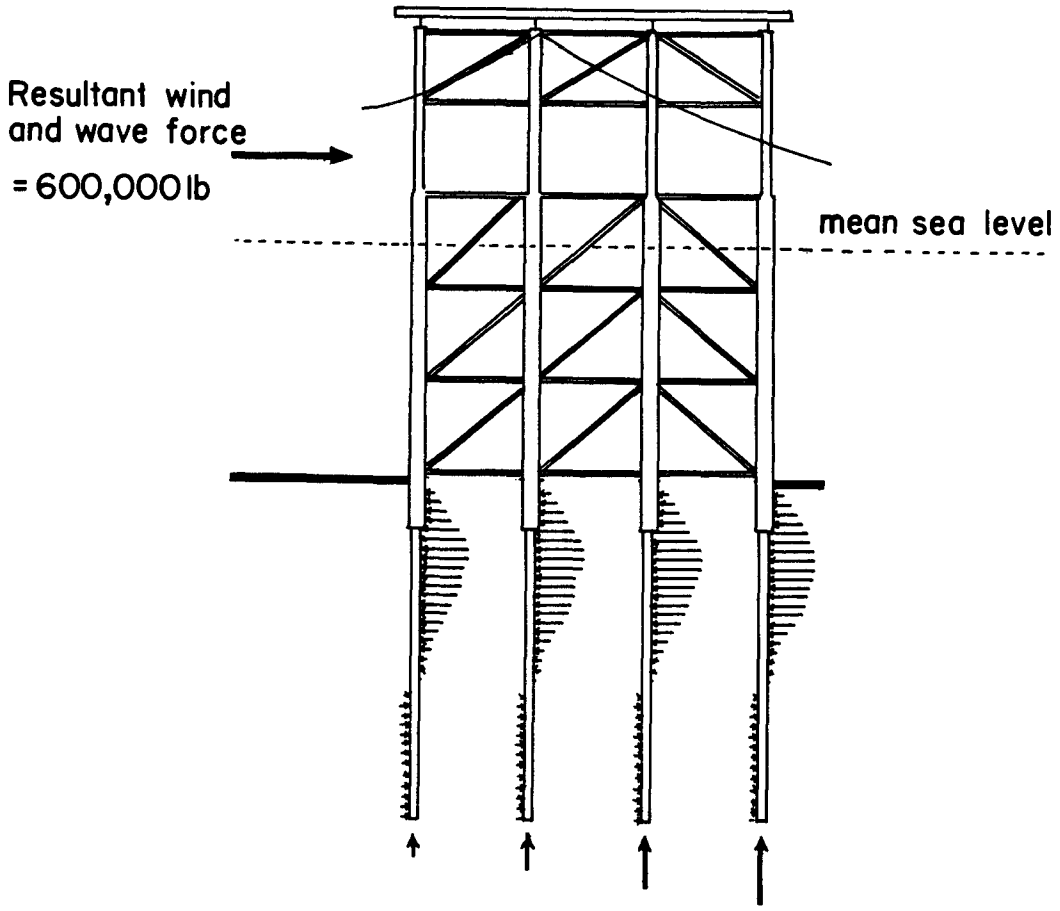

Fig. 6.16. Lateral forces applied to an offshore structure, Example Problem 2 (Matlock and Reese, 1961).

The elastic elements of the problem are described in Fig. 6.17. The annular space between the pile and the jacket column is assumed to be grouted so that the two members will bend as a composite section. This is frequently, but not always, done in actual practice.

The elastic angular restraint provided by the portion of the structure above the soil may be analyzed by determining the moment required to produce a unit value of rotation at the connection. This value, and the imposed lateral load, constitute the boundary conditions for this particular problem. For the example problem, for each pile the elastic angular restraint M_t/S_t is equal to 6.176×10^9 in.-lb/radian and the lateral load P_t is equal to 150,000 lb.

The force-deformation characteristics of the soil are described by a set of predicted p-y curves, as shown in Fig. 6.18.

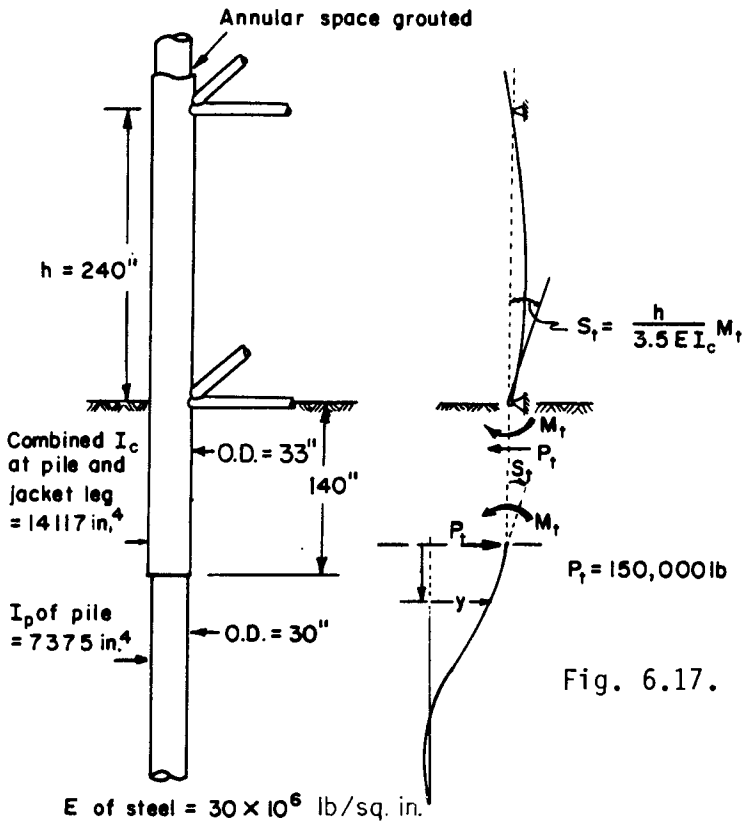

Fig. 6.17. The superstructure and the pile, considered as elastic elements of the problem (Matlock and Reese, 1961).

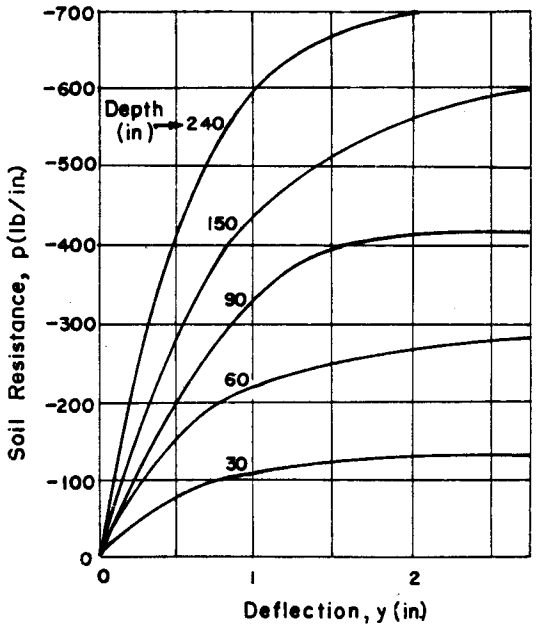

Fig. 6.18. Typical resistance-deflection curves predicted for the soil at various depths (Matlock and Reese, 1961).

As shown earlier in this chapter, the deflection y for the case where $E_s = kx$ is

$$y = A_y \frac{P_t T^3}{EI} + B_y \frac{M_t T^2}{EI} , \tag{6.77}$$

where EI is the flexural rigidity of the pile and where T is the relative stiffness factor, defined by

$$T^5 = \frac{EI}{k} . \tag{6.75}$$

It is convenient to define an additional set of nondimensional deflection coefficients by rearranging Eq. 6.77 as follows:

$$y = C_y \frac{P_t T^3}{EI} , \tag{6.85}$$

where, at any depth coefficient Z,

$$C_y = A_y + \frac{M_t}{P_t T} B_y . \tag{6.86}$$

Depending on the angular restraint provided by the structure, values of M_t/P_tT will range from zero for the pinned-end case to -0.93 for the case where the structure prevents any rotation of the pile ahead. Values of C_y are given by the curves in Fig. 6.19. Tables for C_y are also included in Appendix 4 and are Tables A4.33 through A4.40.

To begin the solution of the example problem it is necessary to assume, temporarily at least, that the form of soil modulus variation $E_s = kx$ will be a satisfactory approximation of the actual final E_s variation. Also, available nondimensional solutions are limited to a pile of constant bending stiffness. For the example hand solution, the pile stiffness will be assumed equal to that of the combined pile and jacket leg.

The slope at the top of the pile is

$$S_t = A_{S_t} \frac{P_t T^2}{EI_c} + B_{S_t} \frac{M_t T}{EI_c} , \tag{6.87}$$

where the subscript t indicates values at Z = 0. The relation between M_t and S_t from Fig. 6.17 is

$$S_t = \frac{h}{3.5\ EI_c} M_t . \tag{6.88}$$

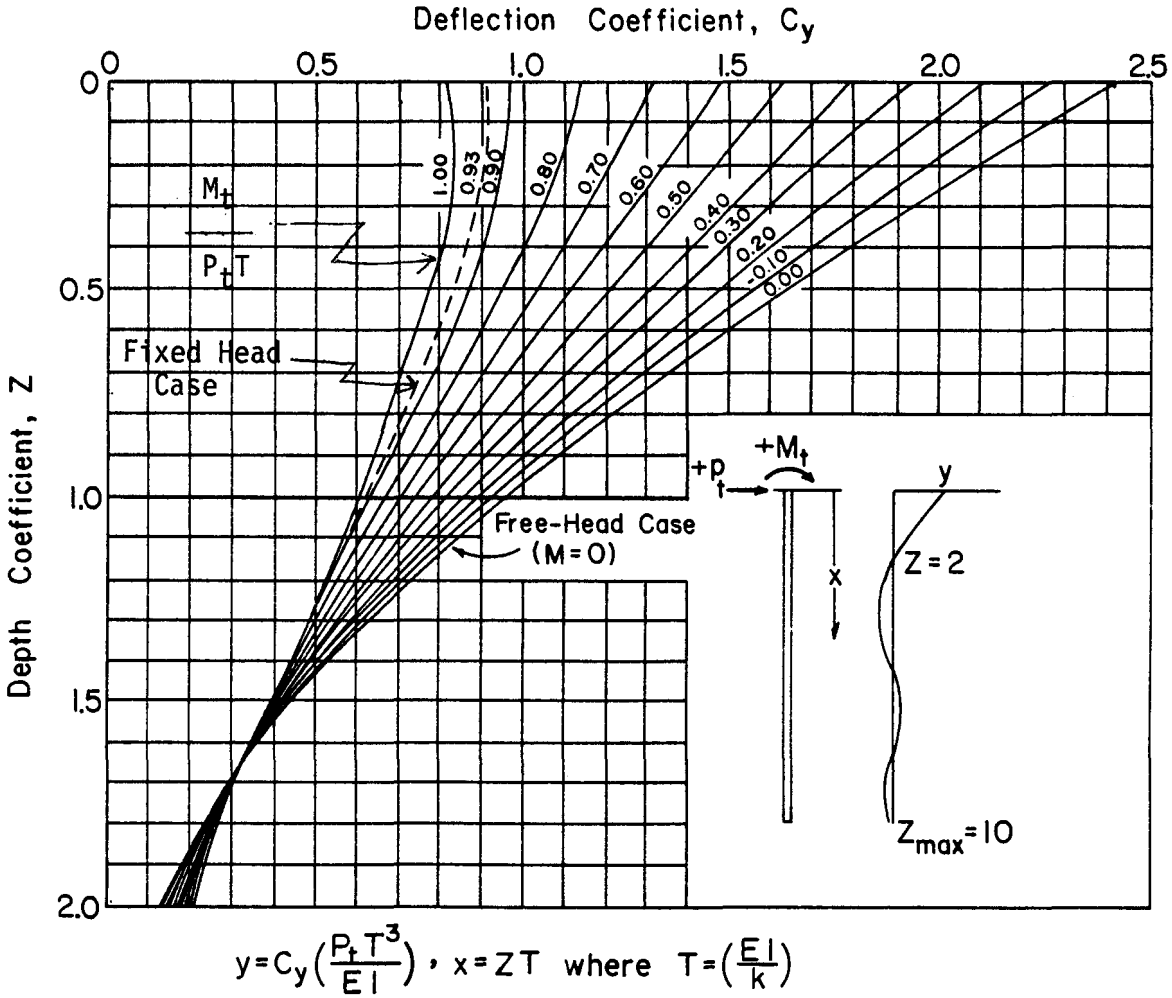

Fig. 6.19. Nondimensional coefficients for lateral deflection of a pile, assuming soil modulus proportional to depth, or $E_s = kx$, long pile case Z_{max} 5 to 10.

Combining Equations 6.87 and 6.88, and rearranging,

$$\frac{M_t}{P_tT} = \frac{A_{s_t}T}{\frac{h}{3.5} - B_{s_t}T} = \frac{-1.623T}{\frac{240}{3.5} + 1.750T} = \frac{-T}{42.25 + 1.078\,T} . \qquad (6.89)$$

Because the relative stiffness factor T depends on the coefficient of soil modulus variation k and this quantity in turn depends on nonlinear soil resistance characteristics, as noted earlier the solution must proceed by a process of repeated trial and adjustment of values of T (or k) until the deflection and resistance patterns of the piles are made to agree as closely as possible with the resistance-deflection (p-y) relations previ-

ously estimated for the soil and shown in Fig. 6.18. Also, as noted earlier, even though the final set of soil moduli ($E_s = -p/y$) may not vary in a perfectly linear fashion with depth, proper fitting of $E_s = kx$ will usually produce satisfactory solutions.

For the first trial, T will be assumed equal to 200 in. From Eq. 6.89 the corresponding value of M_t/P_tT is -0.776. For this value of M_t/P_tT, values of C_y are interpolated from Fig. 6.19 and are given in Table 6.6 at depths corresponding to the positions of the several p-y curves of Fig. 6.18. Values of deflection y are then computed at each depth. By reference to Fig. 6.18, values of soil resistance p are obtained, and soil modulus values E_s are computed.

TABLE 6.6. SAMPLE COMPUTATIONS FOR FIRST TRIAL.

Depth x	Depth Coefficient Z	Deflection Coefficient C_y	Deflection y	Soil Resistance p	Soil Modulus E_s
	$= \frac{x}{T}$	from Fig. 6.16	$= C_y \frac{P_t T^3}{EI_c}$	from Fig. 6.15	$= \frac{-p}{y}$
in.	---	---	in.	lb/in.	lb/sq in.
30	0.15	1.13	3.20	-132	41
60	0.30	1.06	3.00	-285	95
90	0.45	0.99	2.81	-420	149
150	0.75	0.82	2.32	-578	249
240	1.20	0.57	1.62	-675	416

Values of soil modulus from the first trial are plotted versus depth as shown in Fig. 6.20. A straight line through the origin is fitted to the points, with more weight being given to points at depths less than $x \simeq 0.5T$ than at greater depths. For this straight line, the coefficient of soil modulus variation resulting from the first trial is computed as

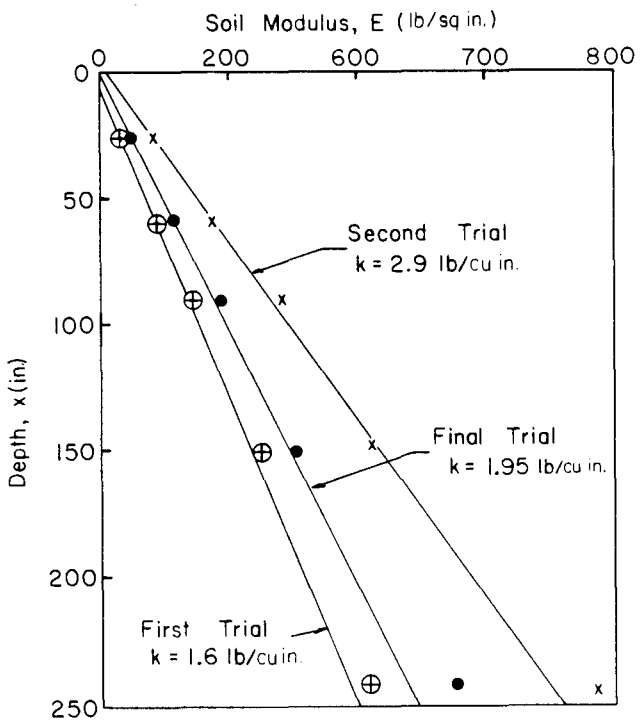

Fig. 6.20. Trial plots of soil modulus values. The first trial corresponds to computations in Table 6.5.

$$k = \frac{E_s}{x} = 1.6 \text{ lb/cu in.} \tag{6.90}$$

The correspondng value of the relative stiffness factor is

$$T_{(obtained)} = \sqrt[5]{\frac{EI_c}{k}} = 194 \text{ in.} \tag{6.91}$$

If the value of $T_{(obtained)}$ were equal to the value of $T_{(tried)}$, the process would have been completed. To facilitate additional estimating and to reach closure with a minimum of trials, a plot of T-values is used, as shown in Fig. 6.21. Two trials will usually allow interpolation for the final value of T. A final set of computations for E_s values is then made as a check.

6.8 CONCLUDING COMMENT

While the nondimensional methods described above are satisfactory for many problems, most laterally-loaded piles can be analyzed efficiently by means of a computer program such as COM622.

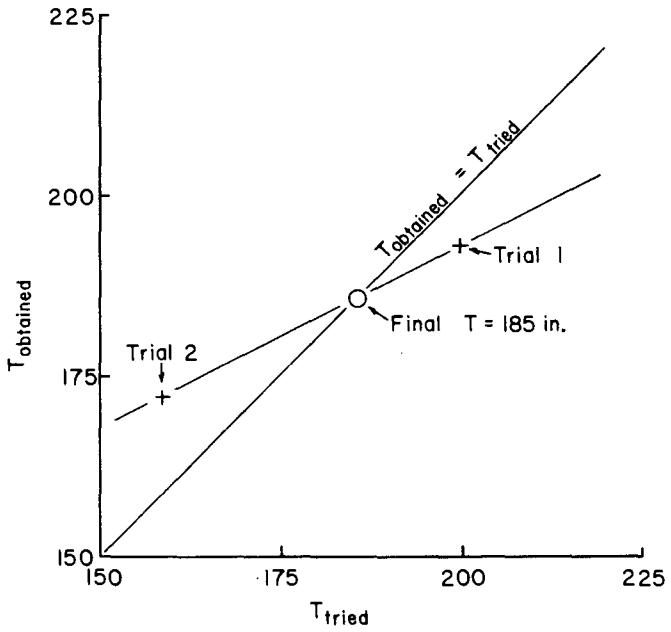

Fig. 6.21. Interpolation for final value of relative stiffness factor T.

As stated previously, the program uses successive difference-equation computations based on repeated reference to the p-y curves to determine at increments along the pile the values of soil modulus. The procedure insures both compatibility and equilibrium for the soil, the pile, and the superstructure. Some of the advantages of using the computer program are given below.

1. Step changes in the flexural stiffness of the pile may be introduced at any depth.
2. The pile length may be changed as desired.
3. The boundary conditions at the top of the pile may be specified as the lateral load and a) the moment, b) slope, and c) the rotational spring constant moment/slope). In addition, an axial load may be specified.

However, the nondimensional method should be employed on almost every occasion as a check of the computer solution or to give preliminary design information.

6.9 REFERENCES

George, P. and Wood, D., Offshore Soil Mechanics, Cambridge University Engineering Department, 1976.

Matlock, Hudson, and Reese, L. C., "Foundation Analysis of Offshore Pile-Supported Structure," Proceedings, Fifth International Conference, International Society of Soil Mechanics and Foundation Engineering, Paris, Vol. 2, 1961, p. 91.

Matlock, Hudson, and Reese, L. C. "Generalized Solutions for Laterally Loaded Piles," Transactions, American Society of Civil Engineers, Vol. 127, Part 1, 1962, p. 1220-1251.

McClelland, Bramlette, and Focht, John A., Jr., "Soil Modulus for Laterally Loaded Piles," Transactions, American Society of Civil Engineers, Vol. 123, p. 1049, New York, 1958.

Palmer, L. A., and Brown, P. P., "Piles Subjected to Lateral Thrust Part II - Analysis of Pressure, Deflection, Moment, and Shear by the Method of Difference Equations," Supplement of Symposium on Lateral Load Tests on Piles, ASTM Special Technical Publication, No. 154-A, pp. 22-44, 1954.

Poulos, H. G., and Davis, E. H., Pile Foundation Analysis and Design, John Wiley and Sons, 1980.

Reese, Lymon C., and Matlock, Hudson, "Nondimensional Solutions for Laterally Loaded Piles with Soil Modulus Assumed Proportional to Depth," Proceedings, Eighth Texas Conference on Soil Modulus and Foundation Engineering, Special Publication No. 29, Bureau of Engineering Research, The University of Texas, Austin, September 1956.

U. S. Department of the Navy, Design Manual, Soil Mechanics, Foundations, and Earth Structures, NAVFAC DM-7, 1971.

6.10 EXERCISES

1. The pile shown below is subjected to cyclic loading. The pile head is restrained against rotation. Analyze the pile response by:

(a) Computer program, and

(b) Hand calculation using nondimensional C_y curves.

Soil conditions:

Soft saturated clay deposit with the following properties:

c_u = 500 lb/sq ft

γ' = 45 lb/cu ft

ε_{50} = 0.01

$E_s = kx$

k = 300 lb/cu in.

(c) Repeat the problem with pile head

(i) free to rotate

(ii) fixed against rotation

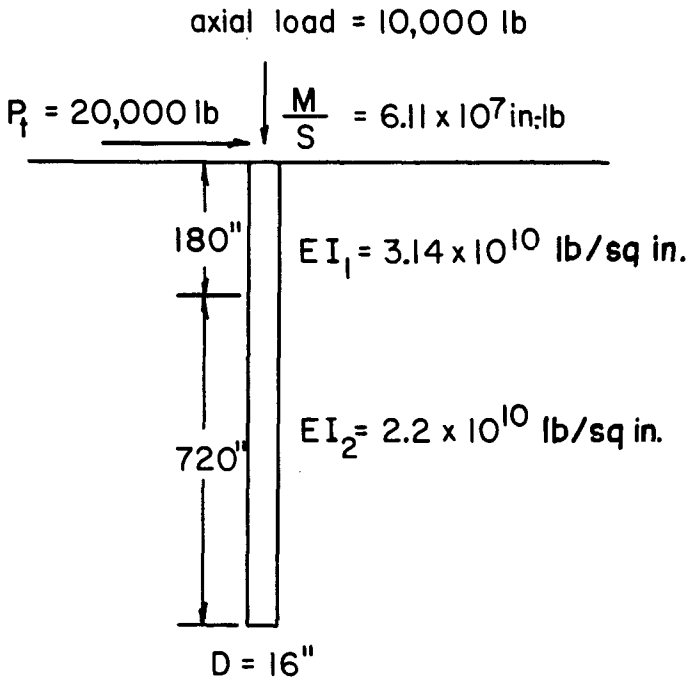

2. Rework the problem given in the example in 6.5 with the applied moment equal to zero.

3. Rework the problem given in the example in 6.5 with the load and moment decreased to 15, 45, and 75 percent of the values used in the example.

4. Develop p-y curves for a sand below water, $\phi = 36°$, $\gamma' = 50$ lb/cu ft, and cyclic loading. Find the groundline load versus deflection up to the point where the maximum steel stress is 30 ksi, keeping the applied lateral load and moment at the same ratio as given in the example.

5. Rework the problem given in 6.7 assuming no jacket-leg extension (use EI of pile alone) and compare results with computer solution.

6. Use the computer and develop nondimensional curves for $E_s = kx^n$ where n is equal to 1.2, 1.4, 1.6, and 1.8.

CHAPTER 7. OTHER METHODS OF DESIGN

Three methods for the design of piles under lateral loading are reviewed that differ from the p-y method previously presented. However, there are common features in all of the methods.

7.1 BROMS METHOD

The method was presented in three papers published in 1964 and 1965 (Broms, 1964a, 1964b, 1965). As shown in the following paragraphs, a pile can be designed to sustain a lateral load by solving some simple equations or by referring to charts and graphs.

Ultimate Lateral Load for Piles in Cohesive Soil.

Broms adopted a distribution of soil resistance, as shown in Fig. 7.1, that allows the ultimate lateral load to be computed by equations of static equilibrium. The elimination of soil resistance for the top 1.5 diameters of the pile is a result of lower resistance in that zone because a wedge of soil can move up and out when the pile is deflected. The selection of nine times the undrained shear strength times the pile diameter as the ultimate soil resistance, regardless of depth, is based on calculations with the soil flowing from the front to the back of the pile.

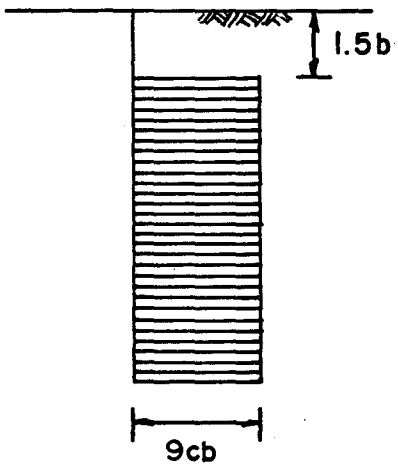

Fig. 7.1. Assumed distribution of soil resistance for cohesive soil.

Short, Free-Head Piles in Cohesive Soil. For short piles that are unrestrained against rotation, the patterns that were selected for behavior are shown in Fig. 7.2. The following equation results from the integration of the upper part of the shear diagram to the point of zero shear (the point of maximum moment)

$$M_{max}^{pos} = P(e + 1.5b + f) - 9cbf^2/2. \quad (7.1)$$

But the point where shear is zero is

$$f = P/9\,cb. \quad (7.2)$$

Therefore,

$$M_{max}^{pos} = P(e + 1.5b + 0.5f). \quad (7.3)$$

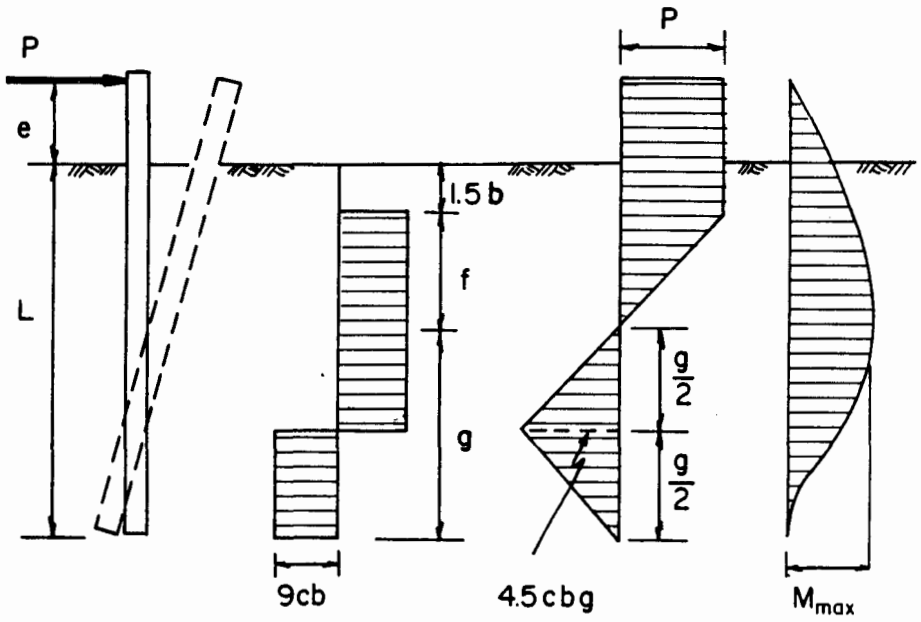

Fig. 7.2. Deflection, load, shear, and moment diagrams for a short pile in cohesive soil that is unrestrained against rotation.

Integration of the lower portion of the shear diagram yields

$$M_{max}^{pos} = 2.25cbg^2. \tag{7.4}$$

It may be seen that

$$L = (1.5b + f + g). \tag{7.5}$$

Equations 7.2 through 7.5 may be solved for the load P_{ult} that will produce a soil failure. After obtaining a value of P_{ult} the maximum moment can be computed and compared with the moment capacity of the pile. An appropriate factor of safety should be employed.

As an example of the use of the equations, assume the following:

b = 1 ft (Assume 12-in. O.D. steel pipe by 0.75 in. wall, I = 421 in.^{4}), e = 2 ft, L = 8 ft, and c = 1 kip/sq ft.

Equations 7.2 through 7.5 are solved simultaneously and the following quadratic equation is obtained.

$$P^2 + 243P - 3422 = 0$$

$$P_{ult} = 13.4 \text{ kips}$$

Substituting into Eq. 7.3 yields the maximum moment.

$$M_{max} = 13.4(2 + 1.5 + 0.744) = 57.0 \text{ ft-k}$$

Assuming no axial load, the maximum stress is

$$f_b = (57.0)(12)(6)/421 = 9.7 \text{ kips/sq in.}$$

The computed maximum stress is tolerable for a steel pipe, especially when a factor of safety is applied to P_{ult}. The computations, then, show that the short pile would fail due to a soil failure.

Broms presented a convenient set of curves for solving the problem of the short-pile (see Fig. 7.3). Entering the curves with L/b of 8 and e/b of 2, one obtains a value of P_{ult} of 13.5 kips, which agrees with the results computed above.

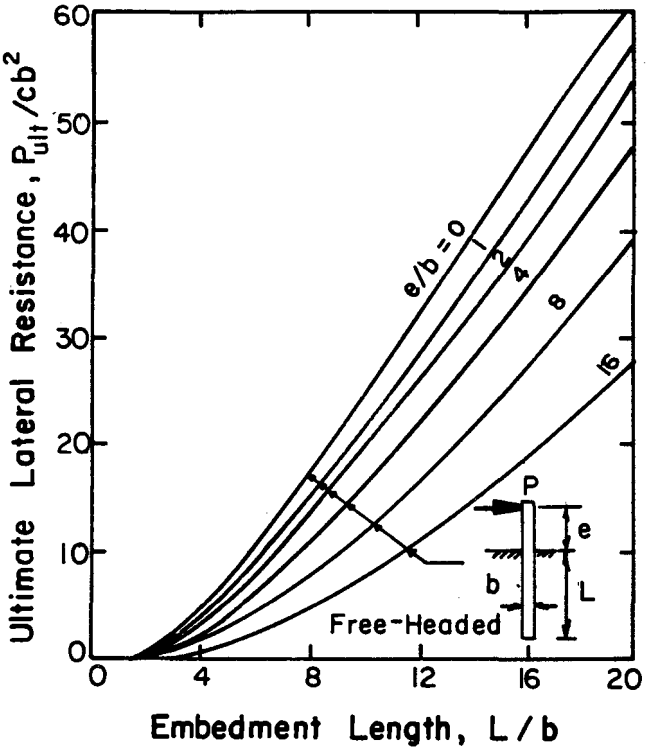

Fig. 7.3. Design curves for short piles under lateral load in cohesive soil (after Broms).

Long, Free-Head Piles in Cohesive Soil. As the pile in cohesive soil with the unrestrained head becomes longer, failure will occur with the formation of a plastic hinge at a depth of 1.50b + f. Equation 7.3 can

then be used directly to solve for the ultimate lateral load that can be applied. The shape of the pile under load will be different than that shown in Fig. 7.2 but the equations of mechanics for the upper portion of the pile remain unchanged.

A plastic hinge will develop when the yield stress of the steel is attained over the entire cross-section. For the pile that is used in the example, the yield moment is 317 ft-k if the yield strength of the steel is selected as 40,000 lb/sq in.

Substituting into Eq. 7.3

$$317 = P_{ult}(2 + 1.5 + \frac{P_{ult}}{18})$$

$$P_{ult} = 50.3 \text{ kips.}$$

Broms presented a set of curves for solving the problem of the long pile (see Fig. 7.4). Entering the curves with a value of M_y/cb^3 of 317, one obtains a value of P_{ult} of about 50 kips.

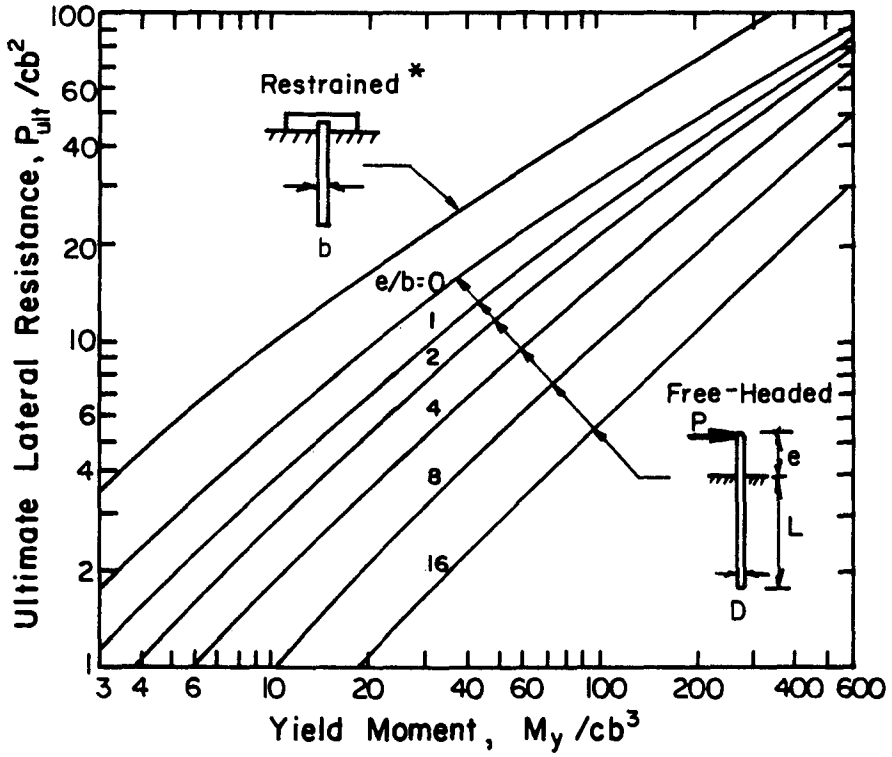

Fig. 7.4. Design curves for long piles under lateral load in cohesive soil (after Broms).

*Note: The length of the pile for which these curves are valid must be ascertained (see text).

Influence of Pile Length, Free-Head Piles in Cohesive Soil. Consideration may need to be given to the pile length at which the pile ceases to be a short pile. The value of the yield moment may be computed from the pile geometry and material properties and used with Eqs. 7.2 through 7.5 to solve for a critical length. Longer piles will fail by yielding. Or a particular solution may start with use of the short-pile equations; if the resulting moment is larger than the yield moment, the long-pile equations must be used.

For the example problem, the length at which the short-pile equations cease to be valid may be found by substituting a value of P_{ult} of 50.3 kips into Eq. 7.2 and solving for f and substituting a value of M_{max} of 317 ft-k into Eq. 7.4 and solving for g. Equation 7.5 can then be solved for L. The value of L was found to be 19.0 ft. Thus, for the example problem the value of P_{ult} increases from zero to 50.3 kips as the length of the pile increases from 1.5 ft to 19.0 ft, and above a length of 19.0 ft the value of P_{ult} remains constant at 50.3 kips.

Short, Fixed-Head Piles in Cohesive Soil. For a pile that is fixed against rotation at its top, the mode of failure depends on the length of the pile. For a short pile, failure consists of a horizontal movement of the pile through the soil with the full soil resistance developing over the length of the pile except for the top one and one-half pile diameters, where it is expressly eliminated. A simple equation can be written for this mode of failure, based on force equilibrium.

$$P_{ult} = 9cb(L - 1.5b) \tag{7.6}$$

Intermediate Length, Fixed-Head Piles in Cohesive Soil. As the pile becomes longer, an intermediate length is reached such that a plastic hinge develops at the top of the pile. Rotation at the top of the pile will occur and a point of zero deflection will exist somewhere along the length of the pile. Figure 7.5 presents the diagrams of mechanics for the case of the restrained pile of intermediate length.

The equation for moment equilibrium for the point where the shear is zero (where the positive moment is maximum) is:

$$M_{max}^{pos} = P(1.5b + f) - f(9cb)(f/2) - M_y.$$

Substituting a value for f,

$$M_{max}^{pos} = P(1.5b + 0.5f) - M_y. \tag{7.7}$$

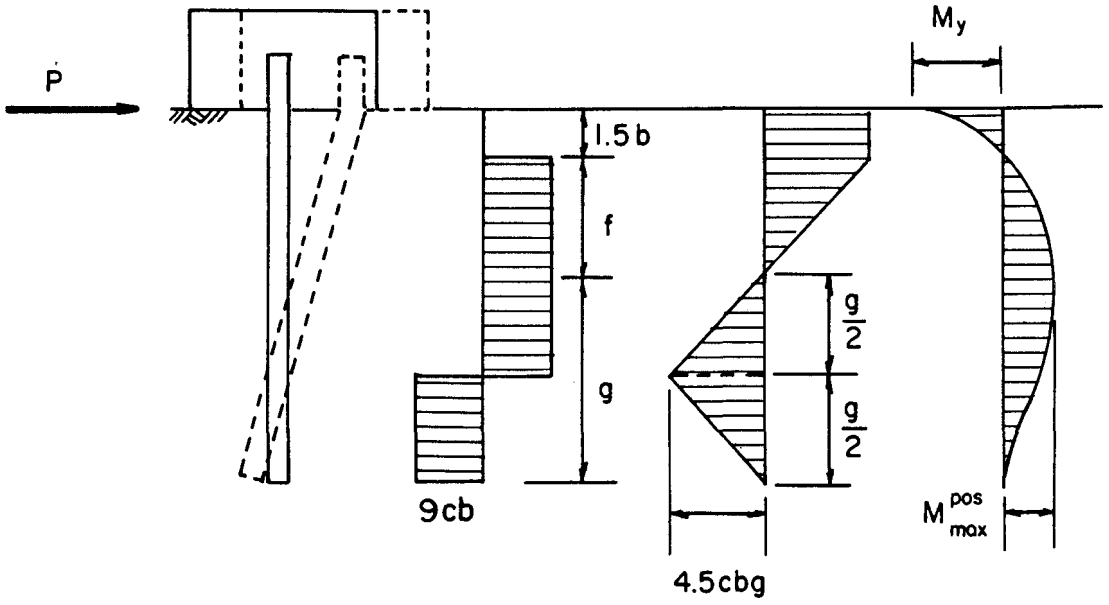

Fig. 7.5. Deflection, load, shear, and moment diagrams for an intermediate-length pile in cohesive soil that is fixed against rotation at its top.

Employing the shear diagram for the lower portion of the pile,

$$M_{max}^{pos} = 2.25cbg^2. \tag{7.8}$$

The other equations that are needed to solve for P_{ult} are:

$$L = 1.5b + f + g \tag{7.9}$$

and

$$f = P/9\ cb. \tag{7.10}$$

Equations 7.7 through 7.10 can be solved for the behavior of the restrained pile of intermediate length.

Long, Fixed-Head Piles in Cohesive Soil. The mechanics for a long pile that is restrained at its top is similar to that shown in Fig. 7.5 except that a plastic hinge develops at the point of the maximum positive moment. Thus, the M_{max}^{pos} in Eq. 7.7 becomes M_y and the following equation results:

$$P = \frac{2M_y}{(1.5b + 0.5f)}. \tag{7.11}$$

Equations 7.10 and 7.11 can be solved to obtain P_{ult} for the long pile.

Influence of Pile Length, Fixed-Head Piles in Cohesive Soil. The example problem will be solved for the pile lengths where the pile goes

from one mode of behavior to another. Starting with the short pile, an equation can be written for moment equilibrium for the case where the yield moment has developed at the top of the pile and where the moment at its bottom is zero. Referring to Fig. 7.5, but with the soil resistance only on the right-hand side of the pile, taking moments about the bottom of the pile yields the following equation.

$$PL - 9\,cb(L - 1.5b)(L - 1.5b)/2 - M_y = 0$$

Summing forces in the horizontal direction yield the next equation.

$$P - 9\,cb(L - 1.5b) = 0 \quad \text{(same as Eq. 7.6)}$$

The simultaneous solution of the two equations yields the desired expression.

$$P_{ult} = M_y/(0.5L + 0.75b) \tag{7.12}$$

Equations 7.6 and 7.12 can be solved simultaneously for P_{ult} and for L, as follows:

from Eq. 7.6, $P_{ult} = 9(L - 1.5)$

from Eq. 7.12, $P_{ult} = 317/(0.5L + 0.75)$

then L = 8.53 ft and P_{ult} = 63.2 k.

For the determination of the length where the behavior changes from that of the pile of intermediate length to that of a long pile, Eqs. 7.7 through 7.10 can be used with M_{max} set equal to M_y, as follows:

from Eq. 7.7, $P_{ult} = \dfrac{(2)(317)}{1.5 + 0.5f}$

from Eq. 7.8, $g = \left(\dfrac{317}{2.25}\right)^{0.5} = 11.87$ ft

from Eq. 7.9, $L = 1.5 + f + g$

from Eq. 7.10, $f = P_{ult}/9$

then L = 23.83 ft and P_{ult} = 94.2 k.

In summary, for the example problem the value of P_{ult} increases from zero to 63.2 kips as the length of the pile increases from 1.5 ft to 8.5 ft, increases from 63.2 kips to 94.2 kips as the length increases from 8.5 ft to 23.8 ft, and above a length of 23.8 ft the value of P_{ult} remains constant at 94.2 kips.

In his presentation, Broms showed a curve in Fig. 7.3 for the short pile that was restrained against rotation at its top. That curve is omitted here because the computation can be made so readily with Eq. 7.6. Broms' curve for the long pile that is fixed against rotation at its top is retained in Fig. 7.4 but a note is added to insure proper use of the

curve. For the example problem, a value of 93 kips was obtained for P_{ult}, which agrees well with the computed value. No curves are presented for the pile of intermediate length.

Deflection of Piles in Cohesive Soil.

Broms suggested that for cohesive soils the assumption of a coefficient of subgrade reaction that is constant with depth can be used with good results for predicting the lateral deflection at the groundline. He further suggests that the coefficient of subgrade reaction α should be taken as the average over a depth of $0.8\beta L$, where

$$\beta = \left(\frac{\alpha}{4EI}\right)^{0.25} \qquad (4.4)^*$$

where α = soil modulus (subgrade reaction)

EI = pile stiffness.

Broms presented equations and curves for computing the deflection at the groundline. His presentation follows the procedure presented in Chapter 4 and the methods in that chapter are recommended here for computing deflection.

With regard to values of the coefficient of subgrade reaction, Broms used work of himself and Vesic (1961a, 1961b) for selection of values, depending on the unconfined compressive strength of the soil. The writer believes that the values suggested by Terzaghi (1955) yield results that are compatible with other assumptions; thus, values shown in Table 3.1 are recommended.

Broms suggested that the use of a constant for the coefficient of subgrade reaction is valid only for a load of one-half to one-third of the ultimate lateral capacity of a pile.

For the example problem, the long pile in cohesive soil that is restrained against rotation at its top will be considered. A value of P_{ult} of 94.2 kips was computed. A working load of 35 kips is selected for an example computation and, using Table 3.1, a value of α is selected as 50 lb/sq in. The value of β is

$$\beta = \left(\frac{50}{(4)(30 \times 10^6)(421)}\right)^{0.25} = \frac{1}{178} \text{ in.}$$

*Broms' notation has been changed to agree with that in Chapter 4.

The value of βL must be equal to or greater than 4 for the pile to act as a long pile; therefore, the length must be at least 60 feet. The deflection at the top of the pile may be computed from Eq. 4.35, using a value from Table 4.1.

$$y_t = \frac{P_t \beta}{\alpha} A_{1t} = \frac{(35{,}000)(1.0)}{(178)(50)} = 3.9 \text{ in.} \qquad (4.35)$$

Had the pile been shorter than 60 ft, values of the deflection coefficient can be obtained from other tables in Chapter 4.

The further use of Broms' recommendation to compute the groundline deflection of piles in cohesive soils will be demonstrated in Chapter 8 where case studies are presented.

Effects of Nature of Loading on Piles in Cohesive Soil.

The values of soil modulus presented by Terzaghi are apparently for short-term loading. Terzaghi did not discuss dynamic loading or the effects of repeated loading. Also, because Terzaghi's coefficients were for overconsolidated clays only, the effects of sustained loading would probably be minimal. Because the nature of the loading is so important in regard to pile response, some of Broms' remarks are presented here.

Broms suggested that the increase in the deflection of a pile under lateral loading due to consolidation can be assumed to be the same as would take place with time for spread footings and rafts founded on the ground surface or at some distance below the ground surface. Broms suggested that test data for footings on stiff clay indicate that the coefficient of subgrade reaction to be used for long-time lateral deflections should be taken as 1/2 to 1/4 of the initial coefficient of subgrade reaction. The value of the coefficient of subgrade reaction for normally consolidated clay should be 1/4 to 1/6 of the initial value.

Broms suggested that repetitive loads cause a gradual decrease in the shear strength of the soil located in the immediate vicinity of a pile. He stated that unpublished data indicate that repetitive loading can decrease the ultimate lateral resistance of the soil to about one-half its initial value.

Ultimate Lateral Load for Piles in Cohesionless Soil.

As for the case of cohesive soil, two failure modes were considered; a soil failure and a failure of the pile by the formation of a plastic hinge. With regard to a soil failure in cohesionless soil, Broms assumed that the ultimate lateral resistance is equal to three times the Rankine

passive pressure. Thus, at a depth Z below the ground surface the soil resistance per unit of length P_z can be obtained from the following equations.

$$P_z = 3b\gamma ZK_p \tag{7.13}$$

$$K_p = \tan^2(45 + \frac{\phi}{2}) \tag{7.14}$$

γ = unit weight of soil

K_p = Rankine coefficient of passive pressure

ϕ = angle of internal friction of soil

Short, Free-Head Piles in Cohesionless Soil. For short piles that are unrestrained against rotation, a soil failure will occur. The curve showing soil reaction as a function of depth is shaped approximately as shown in Fig. 7.6. The use of M_a as an applied moment at the top of the pile follows the procedure adopted by Broms. If both P and M_a are acting, the result would be merely to increase the magnitude of e. It is unlikely in practice that M_a alone would be applied.

The patterns that were selected for behavior are shown in Fig. 7.7. Failure takes place when the pile rotates such that the ultimate soil resistance develops from the ground surface to the center of rotation. The high values of soil resistance that develop at the toe of the pile are replaced by a concentrated load as shown in Fig. 7.7.

The following equation results after taking moments about the bottom of the pile.

$$P(e + L) + M_a = (3\gamma bLK_p)(\frac{1}{2} L)(\frac{1}{3} L) \tag{7.15}$$

Solving for P when M_a is equal to zero,

$$P = \frac{\gamma bL^3K_p}{2(e + L)} \ . \tag{7.16}$$

And solving for M_a when P is equal to zero,

$$M_a = 0.5\gamma bL^3K_p \ . \tag{7.17}$$

Equations 7.15 through 7.17 can be solved for the load or moment, or a combination of the two, that will cause a soil failure. The maximum moment will then be found, at the depth f below the ground surface, and compared with the moment capacity of the pile. An appropriate factor of safety should be used. The distance f can be computed by solving for the point where the shear is equal to zero.

$$P - (3\gamma bfK_p)(\frac{f}{2}) = 0 \tag{7.18}$$

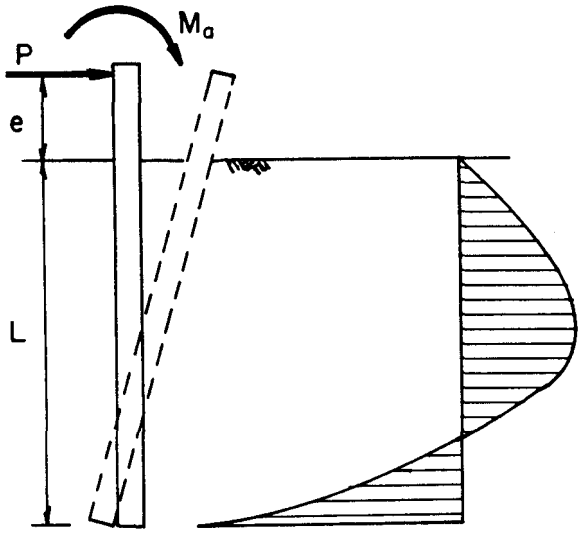

Fig. 7.6. Failure mode of a short pile in cohesionless soil that is unrestrained against rotation.

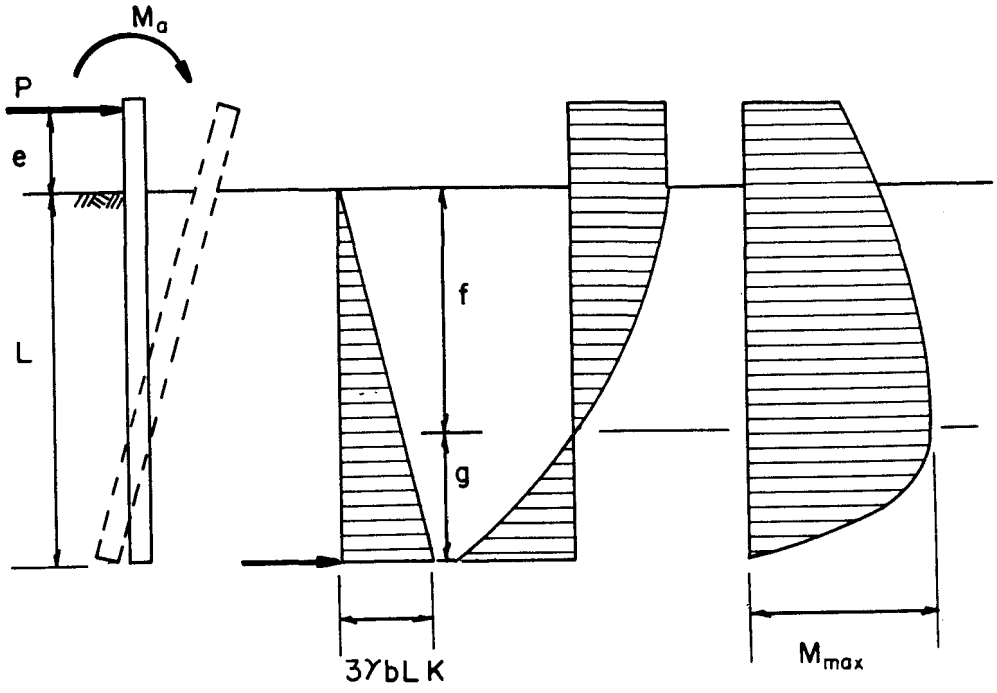

Fig. 7.7. Deflection, load, shear, and moment diagrams for a short pile in cohesionless soil that is unrestrained against rotation.

Solving Eq. 7.18 for an expression for f

$$f = 0.816(P/\gamma b K_p)^{0.5} . \qquad (7.19)$$

The maximum positive bending moment can then be computed by referring to Fig. 7.7.

$$M_{max}^{pos} = P(e + f) - \frac{K_p \gamma b f^3}{2} + M_a$$

Or, by substituting expression for Eq. 7.18 into the above equation, the following expression is obtained for maximum moment.

$$M_{max}^{pos} = P(e + f) - Pf/3 + M_a \qquad (7.20)$$

As an example of the use of the equations, the pile used previously is considered. The angle of internal friction of the sand is assumed to be 34 degrees and the unit weight is assumed to be 55 pounds per cubic foot (the water table is assumed to be above the ground surface). Assume M_a is equal to zero. Equations 7.14 and 7.16 yield the following:

$$K_p = \tan^2(45 + \frac{34}{2}) = 3.54$$

$$P_{ult} = \frac{(0.055)(1)(8)^3(3.54)}{2(2 + 8)} = 4.98 \text{ kips.}$$

The distance f can be computed by solving Eq. 7.19.

$$f = \left(\frac{4.98}{(1.5)(0.055)(1)(3.54)}\right)^{0.5} = 4.13 \text{ ft}$$

The maximum positive bending moment can be found using Eq. 7.20.

$$M_{max} = (4.98)(2 + 4.13) - (4.98)(4.13)/3 + 0 = 23.7 \text{ ft-k}$$

Assuming no axial load, the maximum bending stress f_b is

$$f_b = (23.7)(12)(6)/421 = 4.05 \text{kip/sq in.}$$

The computed maximum stress is undoubtedly tolerable, especially when a factor of safety is used to reduce P_{ult}. Broms presented curves for the solution of the case where a short, unrestrained pile undergoes a soil failure; however, Eqs. 7.15 and 7.18 are so elementary that such curves are unnecessary.

Long, Free-Head Piles in Cohesionless Soil. As the pile in cohesionless soil with the unrestrained head becomes longer, failure will occur with the formation of a plastic hinge in the pile at the depth f below the ground surface. It is assumed that the ultimate soil resistance develops from the ground surface to the point of the plastic hinge. Also, the shear is zero at the point of maximum moment. The value of f can be

obtained from Eq. 7.19 as shown above. The maximum positive moment can then be computed and Eq. 7.20 is obtained as before. Assuming that M_a is equal to zero, an expression can be developed for P_{ult} as follows:

$$P_{ult} = \frac{M_y}{e + 0.544[P_{ult}/(\gamma b K_p)]^{0.5}} . \qquad (7.21)$$

For the example problem, Eq. 7.21 can be solved, as follows:

$$P_{ult} = \frac{.317}{2 + 0.544[P_{ult}/\{(0.055)(1)(3.54)\}]^{0.5}} = 34.36 \text{ kips.}$$

Broms presented a set of curves for solving the problem of the long pile in cohesionless soils (see Fig. 7.8). Entering the curves with a value of $M_y/b^4\gamma K_p$ of 1628, one obtains a value of P_{ult} of about 35 kips. The logarithmic scales are somewhat difficult to read and it may be desirable to make a solution using Eq. 7.21. Equations 7.19 and 7.20 must be used in any case if a moment is applied at the top of the pile.

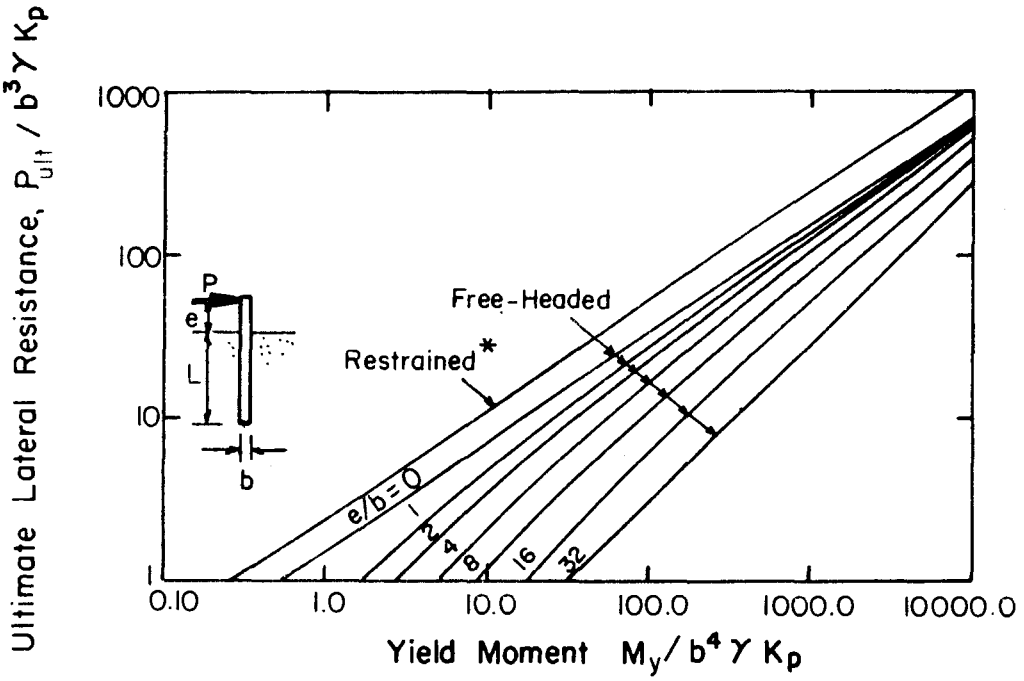

Fig. 7.8. Design curves for long piles under lateral load in cohesionless soil (after Broms).

*Note: The length of pile for which this curve is valid must be ascertained (see text).

Influence of Pile Length, Free-Head Piles in Cohesionless Soil. There may be a need to solve for the pile length where there is a change in behavior from the short-pile case to the long-pile case. As for the case of the pile in cohesive soils, the yield moment may be used with Eqs. 7.15 through 7.17 to solve for the critical length of the pile. Alternatively, the short-pile equations would then be compared with the yield moment. If the yield moment is less, the long-pile equations must be used.

For the example problem, the value of P_{ult} of 34.36 kips is substituted into Eq. 7.16 and a value of L of 19.7 ft is computed. Thus, for the pile that is unrestrained against rotation the value of P_{ult} increases from zero when L is zero to a value of 34.36 kips when L is 19.7 ft. For larger values of L, the value of P_{ult} remains constant at 34.36 kips.

Short, Fixed-Head Piles in Cohesionless Soil. For a pile that is fixed against rotation at its top, as for cohesive soils, the mode of failure for a pile in cohesionless soil depends on the length of the pile. For a short pile, the mode of failure will be a horizontal movement of the pile through the soil, with the ultimate soil resistance developing over the full length of the pile. The equation for static equilibrium in the horizontal direction leads to a simple expression.

$$P_{ult} = 1.5\gamma L^2 b K_p \tag{7.22}$$

Intermediate Length, Fixed-Head Piles in Cohesionless Soil. As the pile becomes longer, an intermediate length is reached such that a plastic hinge develops at the top of the pile. Rotation at the top of the pile will occur, and a point of zero deflection will exist somewhere along the length of the pile. The assumed soil resistance will be the same as shown in Fig. 7.7. Taking moments about the toe of the pile leads to the following equation for the ultimate load.

$$P_{ult} = M_y/L + 0.5\gamma b L^2 K_p \tag{7.23}$$

Equation 7.23 can be solved to obtain P_{ult} for the pile of intermediate length.

Long, Fixed-Head Piles in Cohesionless Soil. As the length of the pile increases more, the mode of behavior will be that of a long pile. A plastic hinge will form at the top of the pile where there is a negative bending moment and at some depth f where there is a positive bending moment. The shear at depth f is zero and the ultimate soil resistance is as shown in Fig. 7.7. The value of f may be determined from Eq. 7.19 but that equation is re-numbered and presented here for convenience.

$$f = 0.816(P/\gamma bK_p)^{0.5} \tag{7.24}$$

Taking moments at point f leads to the following equation for the ultimate lateral load on a long pile that is fixed against rotation at its top.

$$P_{ult} = \frac{M_y^+ + M_y^-}{e + 0.544[P_{ult}/\gamma bK_p)]^{0.5}} \tag{7.25}$$

Equations 7.24 and 7.25 can be solved to obtain P_{ult} for the long pile.

Influence of Pile Length, Fixed-Head Piles in Cohesionless Soil. The example problem will be solved for the pile lengths where the pile goes from one mode of behavior to another. An equation can be written for the case where the yield moment has developed at the top of the short pile. The equation is:

$$P_{ult} = M_y/L + 0.5\gamma bL^2K_p. \tag{7.26}$$

Equations 7.23 and 7.26 are, of course, identical but the repetition is for clarity. Equations 7.22 and 7.26 can be solved for P_{ult} and for L, as follows:

from Eq. 7.22, $P_{ult} = 0.292L^2$

from Eq. 7.26, $P_{ult} = 317/L + 0.09735L^2$

then L = 11.77 ft and P_{ult} = 40.4 kips.

For the determination of the length where the behavior changes from that of a pile of intermediate length to that of a long pile, the value of P_{ult} from Eq. 7.23 may be set equal to that in Eq. 7.25. It is assumed that the pile has the same yield moment over its entire length in this example.

from Eq. 7.23, $P_{ult} = 0.09735L^2 + \frac{317}{L}$

from Eq. 7.25, $P_{ult} = \frac{317}{2 + 0.544(P_{ult}/0.1947)^{0.5}}$

then L = 20.5 ft and P_{ult} = 56.4 kips

In summary, for the example problem the value of P_{ult} increases from zero to 40.4 kips as the length of the pile increases from zero to 11.77 ft, increases from 40.4 kips to 56.4 kips as the length increases from 11.77 ft to 20.5 ft, and above 20.5 ft the value of P_{ult} remains constant at 56.4 kips.

In his presentation, Broms showed curves for short piles that were unrestrained against rotation at their top. Those curves are omitted because the equations for those cases are so easy to solve. Broms' curve for the long pile that is fixed against rotation at its top is retained in

Fig. 7.8 but a note is added to ensure proper use of the curve. For the example problem, a value of 68 kips was obtained for P_{ult}, which agrees poorly with the computed value. The difficulty probably lies in the inability to read the logarithmic scales accurately. No curves are presented for the pile of intermediate length with fixed head.

Deflection of Piles in Cohesionless Soil.

Broms noted that Terzaghi (1955) has shown that the coefficient of lateral subgrade reaction for a cohesionless soil can be assumed to increase approximately linearly with depth (see discussion of Terzaghi's recommendations in Chapter 3). As noted earlier, and using the formulations of this work, Terzaghi recommends the following equation for the soil modulus.

$$E_s = kx \tag{7.27}$$

Table 3.2 presents Terzaghi's recommendations for values of k. Broms suggested that Terzaghi's values can be used only for computing deflections up to the working load and that the measured deflections are usually larger than the computed ones except for piles that are placed with the aid of jetting.

Broms presented equations and curves for use in computing the lateral deflection of a pile; however, the methods presented in Chapter 6 are considered to be appropriate.

As an example problem, the long pile in cohesionless soil that is restrained against rotation at its top is considered. The value of P_{ult} was computed to be 56.4 kips and a working load of 20 kips is selected. Using Table 3.2, a value of k of 10 lb/cu in. is selected. The groundline deflection may be computed from the following equations.

$$y_F = F_y \frac{P_t T^3}{EI} \tag{6.81}$$

$$T = (EI/k)^{0.2} \tag{6.75}$$

Obtaining a value of F_{yt} from Fig. 6.9 of 0.93 and substituting into the above equations, T is found to be equal to 66.1 in. and the deflection at the groundline is found to be 0.43 in. For the solution to be valid, the length of the pile should be at least 5T or 27.5 ft. Had the pile been shorter, other values of F_{yt} could have been obtained from Fig. 6.9.

The further use of Broms' recommendations to compute the groundline deflection of piles in cohesionless soils will be demonstrated in Chapter 8 where case studies are presented.

Effects of Nature of Loading on Piles in Cohesionless Soil.

Broms noted that piles installed in cohesionless soil will experience the majority of the lateral deflection under the initial application of the load. There will be only a small amount of creep under sustained loads.

Repetitive loading and vibration, on the other hand, can cause significant additional deflection, especially if the relative density of the cohesionless soil is low. Broms noted that work of Prakash (1962) shows that the lateral deflection of a pile group in sand increased to twice the initial deflection after 40 cycles of load. The increase in deflection corresponds to a decrease in the soil modulus to one-third its initial value.

For piles subjected to repeated loading, Broms recommended for cohesionless soils of low relative density that the soil modulus be decreased to one-fourth its initial value and that the value of the soil modulus be decreased to one-half its initial value for soils of high relative density. He suggested that these recommendations be used with caution because of the scarcity of experimental data.

7.2 POULOS METHOD

Several authors have proposed methods for the analysis of laterally loaded piles where the equations of elasticity have been used to develop interaction equations. Poulos and his co-workers at the University of Sydney have been especially active (Poulos, 1971a; Poulos, 1971b; Poulos, 1973; Poulos and Davis, 1980, Poulos, 1982) and the presentation herein is based principally on his work (1971a).

Model Employed in Elastic Analysis.

Poulos (1971a) assumed the pile to be a thin, rectangular, vertical strip of width b, length L, and constant stiffness EI. The possible horizontal shear stresses developed between the soil and the sides of the pile were not taken into account. The pile was divided into n+1 elements, as shown in Fig. 7.9, with all elements being of an equal length h, except those at the top and at the tip of the pile, which are of length h/2. Each element was acted upon by a uniform, horizontal stress q which was assumed to be constant across the width of the pile.

The soil was assumed to be an ideal, homogeneous, isotropic, linear, elastic material of semi-infinite dimensions. The soil was assumed to

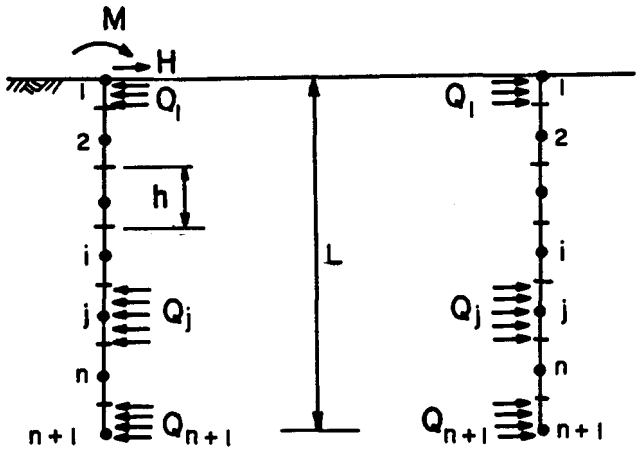

Fig. 7.9. Stresses acting on (a) pile; (b) soil adjacent to pile (after Poulos)

have a Young's modulus of E_{sP} and a Poisson's ratio of ν_s. The soil properties were assumed to be unaffected by the presence of the pile. As will be noted later, Poulos presented some discussion of cases where E_{sP} was not constant with depth.

Poulos used the Mindlin equation for horizontal displacement due to horizontal load within a semi-infinite mass to compute soil displacement. Beam theory was used to compute pile displacements. The soil and pile displacements are evaluated and equated at the element centers except that displacements are computed at the top and at the tip of the pile. Poulos sub-divided the pile into 21 elements.

Free-Head Piles, Elastic Behavior.

The behavior of a pile under lateral load was expressed by Poulos in terms of non-dimensional influence factors. For a free-head pile, one with no rotational restraint at the groundline, the equation for horizontal displacement at the groundline is* Eq. 7.28.

$$y_t = I_{yP} \frac{P_t}{E_{sP} L} + I_{yM} \frac{M_t}{E_{sP} L^2} \quad * \qquad (7.28)$$

*Some of the notation employed by Poulos has been changed to agree with notation previously used herein; however, it was necessary to retain some of the Poulos notation even though there will be more than one symbol for the same parameter. The reader should consult the section on Notation for a list of symbols and their meanings.

where

y_t = groundline deflection
P_t = shear at groundline
E_{sP} = soil modulus (values suggested by Poulos are given later)
L = pile length
I_{yP} = influence coefficient for computing pile-head deflection for applied shear at groundline
I_{yM} = influence coefficient for computing pile-head deflection for applied moment at groundline

Figures 7.10 and 7.11 give values of I_{yP} and I_{yM}, respectively, as a function of K_R, L/b, and ν_s. Poulos defined K_R as the pile flexibility factor and its value may be computed by use of Eq. 7.29.

$$K_R = \frac{EI}{E_{sP}L^4} \tag{7.29}$$

where

EI = pile stiffness

The equation for rotation of the pile head at the groundline is

$$S_t = I_{sP}\frac{P_t}{E_{sP}L^2} + I_{sM}\frac{M_t}{E_{sP}L^3} \tag{7.30}$$

where

S_t = rotation at groundline
I_{sP} = influence coefficient for computing pile-head rotation for applied shear at groundline
I_{sM} = influence coefficient for computing pile-head rotation for applied moment at groundline

Figures 7.11 and 7.12 give values of I_{sP} and I_{sM}, respectively.

The maximum moment in a free-head pile subjected to a lateral load is shown in Fig. 7.13 as a function of K_R, P_t, L, and L/b. Poulos suggested that the maximum moment typically occurs at a depth of between 0.1L and 0.4L below the groundline. The lower depths are associated with stiffer piles.

Fixed-Head Piles, Elastic Behavior.

For a pile that is fixed against rotation at the groundline, such as a pile that is built into a rigid concrete mat, the deflection at the groundline may be computed by using the following equation.

$$y_t = I_{yF}\frac{P_t}{E_{sP}L} \tag{7.31}$$

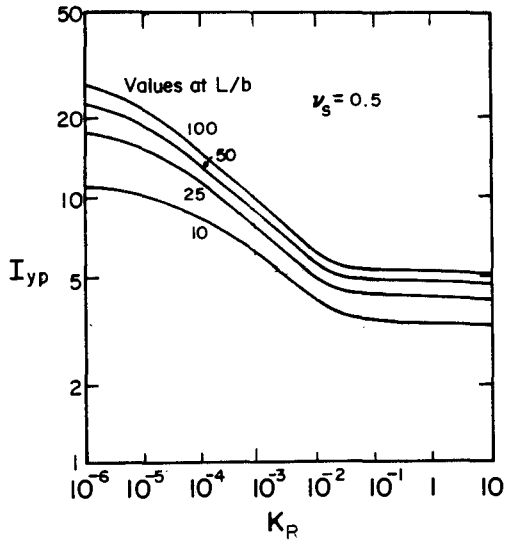

Fig. 7.10. Influence factors I_{yp} for free-head pile (after Poulos).

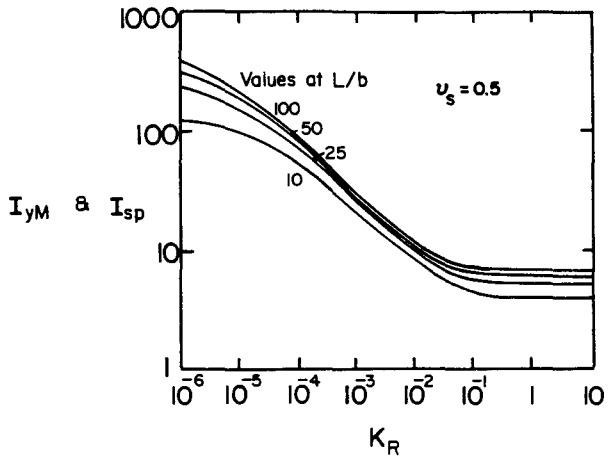

Fig. 7.11. Influence factors I_{yM} and I_{sp} for free-head pile (after Poulos).

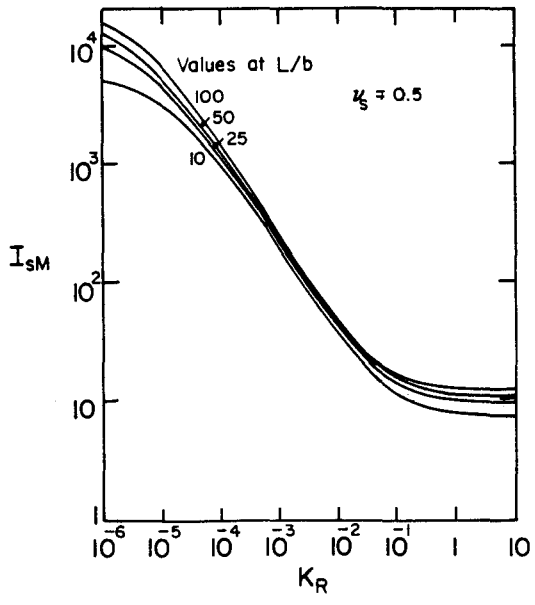

Fig. 7.12. Influence factors I_{sM} for free-head pile (after Poulos).

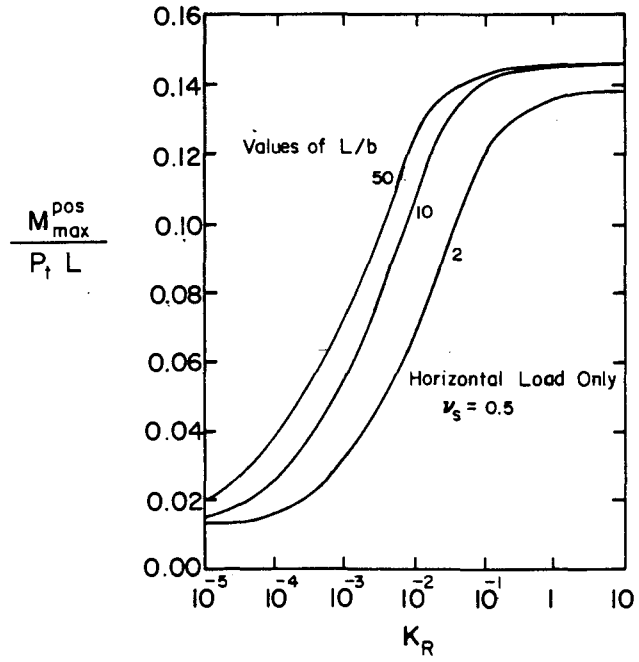

Fig. 7.13. Maximum bending moment for free-head pile (after Poulos).

where

y_t = groundline deflection

I_{yF} = influence coefficient for computing pile-head head deflection for a pile with fixed-head

Figure 7.14 gives values of I_{yF}.

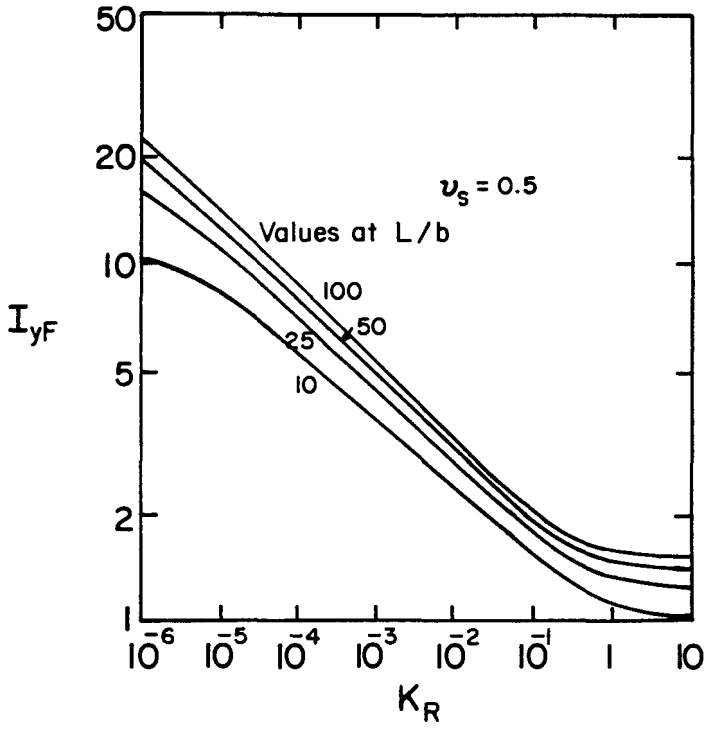

Fig. 7.14. Influence factors I_{yF} for fixed-head pile (after Poulos).

The bending moment at the top of a fixed-head pile is given by Fig. 7.15 as a function of K_R, P_t, L, and L/b.

Effect of Local Yield of Soil Along Pile.

Poulos noted that elastic analysis showed that very high values of soil pressure q developed near the top of a pile. An approximate analysis was made by modifying the elastic analysis. Yielding of soil was assumed at each element until all elements had yielded. It was assumed that the horizontal displacements of the soil at the elements where elastic conditions prevail can be computed by elastic theory using the known pressures at elements where soil has yielded.

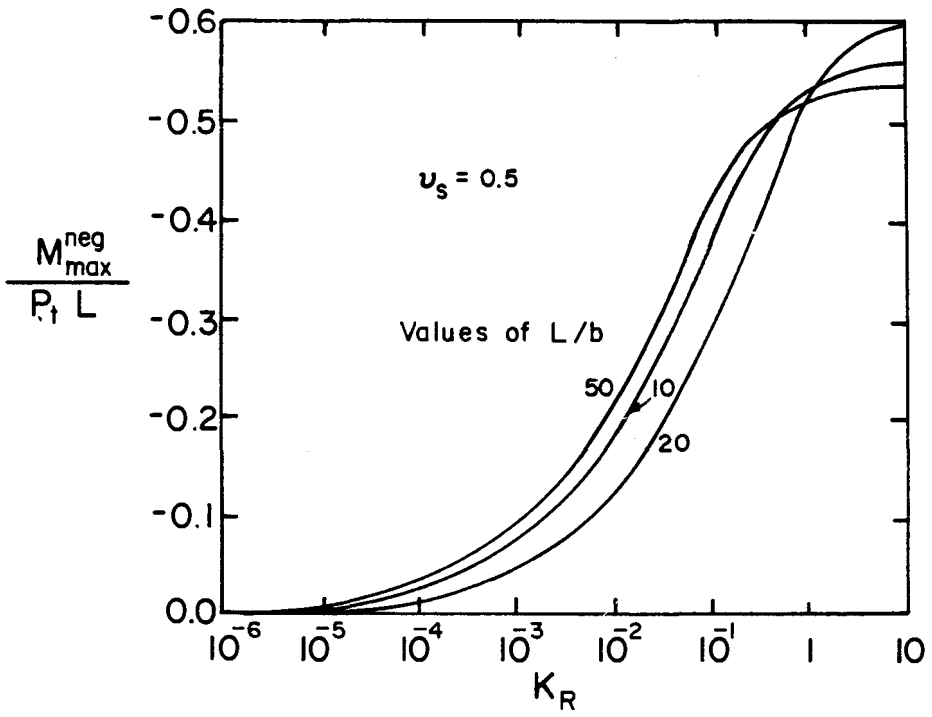

Fig. 7.15. Maximum negative bending moment for fixed-head pile (after Poulos).

Furthermore, because of the complexity of the analysis, only six elements were employed rather than the 21 elements used in the previous solutions. Poulos presented curves for the free-head case only, as shown in Fig. 7.16, that allow the groundline deflection to be computed in terms of parameters previously employed and in terms of the distribution of the yield pressure p_y. Poulos noted that the free-head case is more severe than the fixed-head case because the deflection of the free-head pile at the groundline would be more than for the fixed-head pile for the same load; hence, the computations using elastic analysis would show the soil pressures to be greater for the free-head case. He further noted that the information shown in Fig. 7.16 should be employed with caution because of the assumptions that had to be made in developing the figure.

Determination of Properties of Soil

Poulos suggested that the best method for obtaining E_{sP} is to carry out a field loading test and to compute E_{sP} from measured groundline deflections.

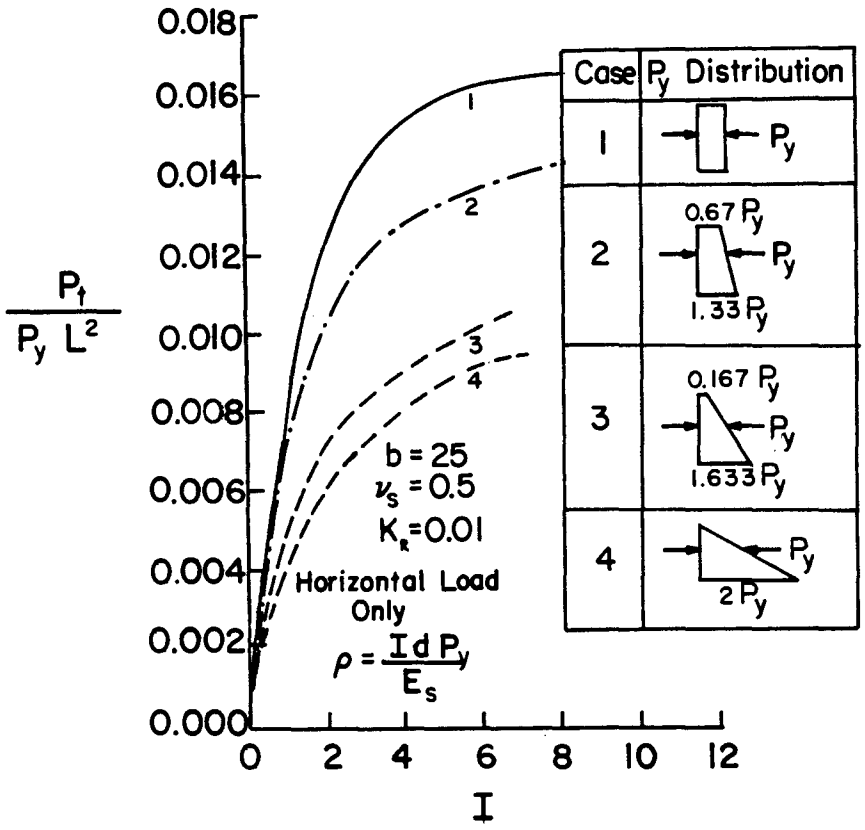

Fig. 7.16. Influence of distribution of yield pressure on load-displacement relationship, free-head case (after Poulos).

To provide a rough guide, values of E_{sP} were back-figured from data collected by Broms (March 1964; May 1964). The guidelines that were given are shown below. For cohesive soils:

$$E_{sP} = 15c \text{ to } 95c$$

where

c = undrained shear strength of clay.

For all cases considered, the average value of soil modulus was

$$E_{sP} = 40c.$$

For cohesionless soils the following table was presented. It was noted that the soil modulus for sand is not constant with depth so that the use of the values in the table below is questionable.

Soil Density	Range of E_{sP}, lb/sq in.	Average E_{sP}, lb/sq in.
Loose	130-300	250
Medium	300-600	500
Dense	600-1,400	1,000

Poulos stated that for a cohesive soil with a uniform c the value of the yield pressure p_y theoretically increases from 2c at the groundline to a value of 11.41c at a depth of about three pile diameters below the groundline. He adopted the Broms' recommendation of 9c for design purposes. With regard to cohesionless soil, Poulos suggested the use of a triangular distribution of yield pressure with the yield pressure being equal to three times the Rankine passive pressure, a suggestion made originally by Broms.

Poulos noted in the discussion of the proposed method that the creep of the soil at higher load levels can cause a discrepancy between results from analysis and those from experiment.

Poulos (1982) gave an extended discussion of the behavior of a single pile due to cycling the lateral load. He identified two effects: the structural "shakedown" of the pile-soil system in which permanent deformations accumulate with increasing load cycles with no changes in the pile-soil properties, and a decrease in strength and stiffness of the soil due to cyclic loading. His paper dealt mainly with the degradation of the soil due to cyclic loading.

Poulos defined degradation parameters for soil modulus D_E and for yield pressure D_p as shown by Eqs. 7.32 and 7.33, respectively.

$$D_E = E_{cP}/E_{sP} \tag{7.32}$$

$$D_p = q_{yc}/q_{ys} \tag{7.33}$$

where

E_{cP} = soil modulus after cyclic loading

E_{sP} = soil modulus for static loading

q_{yc} = limiting pile-soil interaction stress (yield pressure) after cyclic loading

q_{ys} = yield pressure for static loading

Poulos noted that a limited amount of data are available on degradation factors and he suggested the use of data summarized by Idriss, et al.

(1978). Poulos prepared Fig. 7.17 from the Idriss data, with ε_c redefining the cyclic strain and ε_{cr} redefining a representative value of cyclic strain. The value of ε_{cr} can be varied to influence the cyclic degradation. The parameter t is defined by Eq. 7.34.

$$D_p = D_E = N^{-t} \tag{7.34}$$

where

N = number of cycles

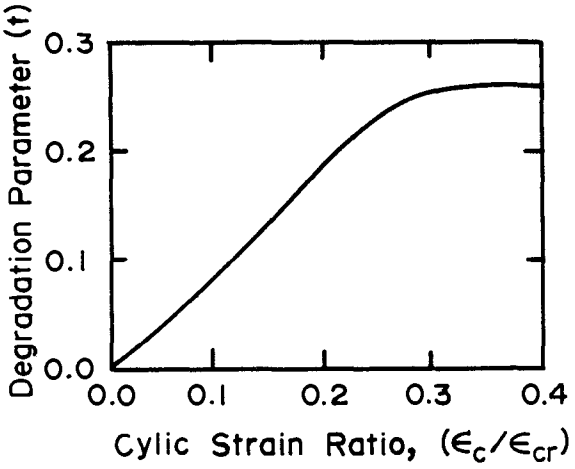

Fig. 7.17. Degradation parameter t, (from Poulos).

The effect of the rate of loading on the degradation was also considered. The degradation factors D_E and D_p were multiplied by the rate factor D_R that is defined in Eq. 7.35.

$$D_R = 1 - F_p \log \frac{\lambda r}{\lambda} \tag{7.35}$$

where

F_p = rate coefficient (limited data suggest a range of from 0.05 to 0.3)

λ_r = reference loading rate (perhaps static loading)

λ = loading rate

The computation procedure is initiated by selecting values of soil modulus and yield pressure for each element and a distribution of displacement is computed. The cyclic displacements, number of cycles, and rate of loading are used to establish degradation factors that can be used

in the next cycle. The procedure is continued until convergence is achieved. Poulos indicated that a computer program, not presented in his paper, has been written to perform the analysis.

The presentation outlined above is insufficient to allow for the computation of the behavior under cyclic loading of a given pile in a given soil profile; however, the discussion does serve to illustrate the nature of the problem.

Example Computation.

The pile and soil employed in the Broms method will be used in solving an example problem. The clay with an undrained shear strength of 1.0 kip/sq ft would have a value of E_{sP} of approximately 40 kip/sq ft. The pile length is assumed to be 40 ft; thus, the value of K_R can be computed as shown below.

$$K_R = \frac{(30 \times 10^6)(421)(144)}{(4 \times 10^4)(480)^4} = 8.57 \times 10^{-4}$$

From Fig. 7.13

$$M_{max}^{pos} = (0.06)(P_t L).$$

Assuming that the maximum moment is 317 ft-k, the P_t at failure of the pile is 132 kips. If it is assumed that a safe load of 50 kips can be applied to the pile, the groundline deflection may be computed by use of Eq. 7.28. The value of I_{yP} was obtained from Fig. 7.10.

$$y_t = I_{yP} \frac{P_t}{E_{sP} L}$$

$$= \frac{(8.5)(50)}{(40)(40)} = 0.27 \text{ ft} = 3.2 \text{ in.}$$

The computed values seem large compared to values obtained from the method of Broms. The error probably is in assuming that the elastic method can be used to compute the bending moment in the pile at the failure condition.

An alternate procedure is to assume that the maximum deflection is limited to 1.0 in. Substituting this value into Eq. 7.28 yields a lateral load as shown below.

$$P_t = \frac{y_t E_{sP} L}{I_{yP}} = \frac{(1.0/12)(40)(40)}{8.5} = 15.7 \text{ kips}$$

The bending moment corresponding to the load of 15.7 kips is found to be 37.7 ft-k which yields a bending stress of 6.45 kip/sq in.

7.3 PRESSUREMETER METHOD

The use of results from pressuremeter tests to design piles under lateral loading has been given attention in technical literature (Gambin, 1963; Baguelin and Jezequel, 1972; Baguelin, et al., 1978; Briaud, et al., 1982). The method produces p-y curves that can be used with a computer program to obtain pile response.

Introduction.

The pressuremeter as a design tool was developed by Menard (1956) and there is a considerable body of literature on the device. No attempt is made herein to present the developments that have led to the physical devices that are in use and the means of performing tests with these devices or to present the various theories that have been proposed for interpreting the pressuremeter test.

The self-boring pressuremeter has been developed (Baguelin and Jezequel, 1973) but the method outlined is based on the use of the standard Menard device. The rules for the prediction of p-y curves are empirical to a large extent but a number of field experiments have been carried out for the purpose of checking the validity of the method (Baguelin, et al., 1978, p. 312).

Pressuremeter Curve.

A typical curve from the Menard pressuremeter is shown in Fig. 7.18. The large volume change for a small increase in pressure at the early part of the curve results from the drilling of an oversized hole prior to placing the pressuremeter probe. The next portion of the curve reflects a linear relationship between pressure and volume changes. Then, the curve becomes nonlinear and a limiting pressure is indicated. The following definitions relate to the shape of the pressuremeter curve.

v_o = volume at start of the straight-line portion of the curve and equal to the initial volume of the cavity

p_f = pressure at the point where there is no longer a straight-line relationship between pressure and volume

v_c = initial volume of the measuring cell

p_ℓ = limit pressure (to be determined at point where initial volume has doubled; thus, p_ℓ is the the value of pressure at the point where the volume of fluid is equal to $2v_o + v_c$. Note that the volume of fluid in the cell when the

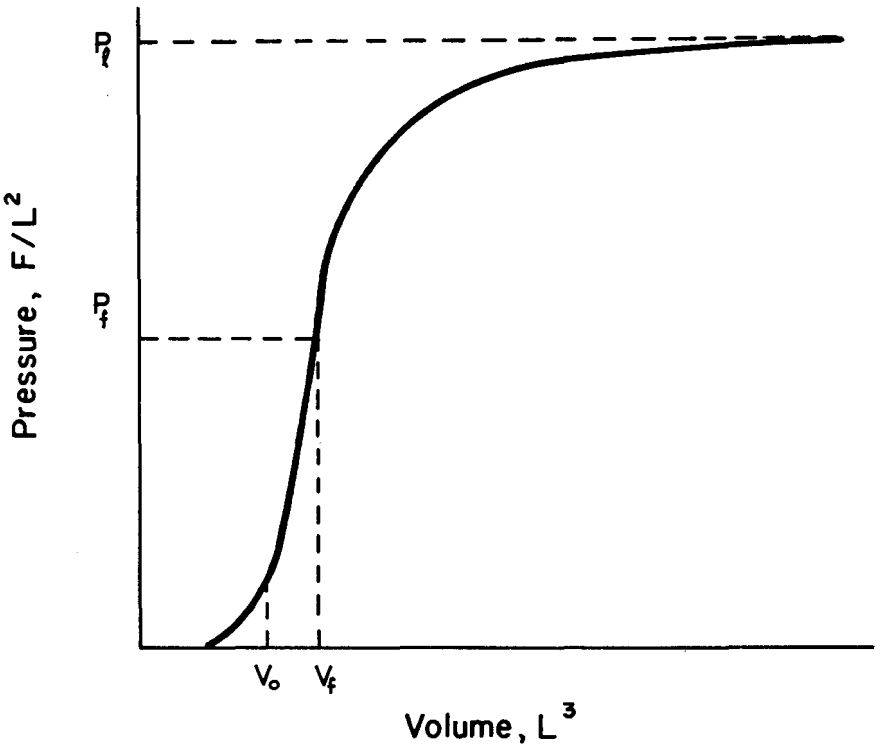

Fig. 7.18. Typical curve from Menard pressuremeter.

soil has been pushed back to its original position is v_c + v_o but the volume indicator would register only v_o.

Determining Pressuremeter Modulus

The assumption is made that the soil is elastic between v_o and v_f where the pressuremeter curve is a straight line. The following equation gives the relationship between the shear modulus and the slope of the straight-line portion of the pressuremeter curve (Baguelin, et al., 1978, p. 153).

$$G_M = v \frac{\Delta p}{\Delta v} \tag{7.36}$$

where

G_M = shear modulus from pressuremeter

v = volume of cavity

$\Delta p/\Delta v$ = slope of curve between v_o and v_f

The volume of the cavity changes between v_o and v_f and the volume v_m at the midpoint is used.

In order to obtain the Young's modulus E from the shear modulus G, the expression from mechanics is employed.

$$G = \frac{E}{2(1 + \nu)} \tag{7.37}$$

where

ν = Poisson's ratio

The value of Poisson's ratio can vary widely for a soil but Menard chose a value of 0.33 (Baguelin, et al., 1978, p. 154). Employing this value of ν, the following equation results.

$$E_M = 2.66 V_m \frac{\Delta p}{\Delta v} \tag{7.38}$$

where

E_M = the Menard modulus of deformation

v_m = midpoint volume

Development of p-y Curves

The shape of the curves giving the soil response for a pile under lateral loading is shown in Fig. 7.19. In the upper curve in Fig. 7.19, the values of p_f and p_ℓ may be taken directly from the pressuremeter curve. The curve can be drawn, then, by computing a value of k_m using one of the following two equations.

$$\frac{1}{k_M} = \frac{2}{9E_m} B_o \left(\frac{b}{B_o} 2.65 \right)^{\alpha} + \frac{\alpha}{6E_m} b; \; b > 0.6 \text{ m} \tag{7.39}$$

$$\frac{1}{k_M} = \frac{b}{E_m} \frac{4(2.65)^{\alpha} + 3\alpha}{18}; \; b < 0.6 \text{ m} \tag{7.40}$$

where

B_o = a reference width, usually 60 cm (2 ft)

k_M = slope of initial portion of Menard's soil response curve (see Fig. 7.19)

b = pile diameter

E_M = the Menard modulus of deformation

α = rheological factor (see Table 7.1)

As shown in Fig. 7.19, the ordinates for the curve where the depth Z is zero is one-half of those where the depth is equal to Z_c. The depth Z_c is defined as the critical depth and is suggested by Menard to be about 2 b for cohesive soils and about 4 b for granular soils. If there is a pile

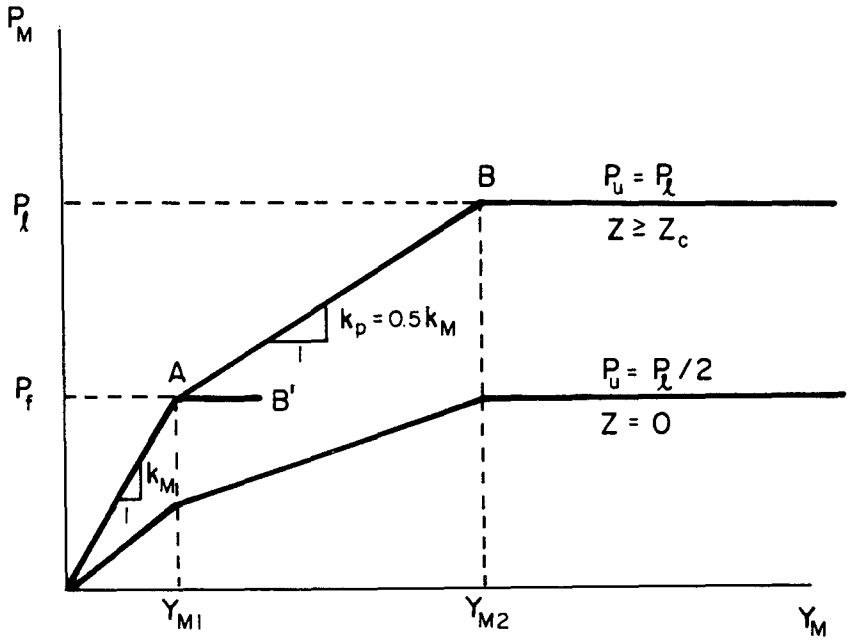

Fig. 7.19. Soil response curves proposed by Menard.

TABLE 7.1. VALUES OF RHEOLOGICAL FACTOR α (after Baguelin, et al., 1948).

Soil Type	Peat	Clay	Silt	Sand	Sand and Gravel
Over-consolidated		1	2/3	1/2	1/3
Normally Consolidated	1	2/3	1/2	1/3	1/4
Weathered and/or Remolded		1/2	1/2	1/3	1/4

cap, the critical depth is zero. Between the ground surface and the critical depth, the soil modulus should be $\lambda_Z k_M$ given by Eq. 7.41.

$$\lambda_Z = \frac{1 + (Z/Z_c)}{2} \tag{7.41}$$

The Menard curves for a pile under lateral loading can be developed from a pressuremeter curve (Fig. 7.18) and by use of Eqs. 7.38 through 7.41. The final step in the development of p-y curves as employed herein is to convert the Menard curve. As noted in the above development, the following conversions are necessary.

$$p = p_M b \tag{7.42}$$

and

$$E_{si} = k_M b \tag{7.43}$$

With Eqs. 7.42 and 7.43, a family of p-y curves can be developed from the Menard curves.

Example Computation

As an example of the use of the Menard approach to the analysis of piles under lateral loading, a report by Baguelin and Jezequel (1971) is employed. A test was performed on a stiff pile at a test site at Plancoët. A profile of the pile and soil is shown in Fig. 7.20. The following soil properties, based on information in the report, were used in analyses.

silt: total unit weight, 17.1 kN/cu m
submerged unit weight, 7.26 kN/cu m
ε_{50}, 0.020*
α (see Table 7.1), 0.5
undrained shear strength, 35 kN/sq m*

sand: submerged unit weight, 7.35 kN/cu m
α, 0.33
undrained shear strength, 29 kN/sq m*

*Note: the values of ε_{50} and shear strength are not used, of course, in getting p-y curves from pressuremeter results but are needed for use in other methods. Shear strength for sand and for silt should more properly be given in terms of an angle of internal friction; however, values of undrained shear strength were given in the report and used in making computations using methods other than the pressuremeter.

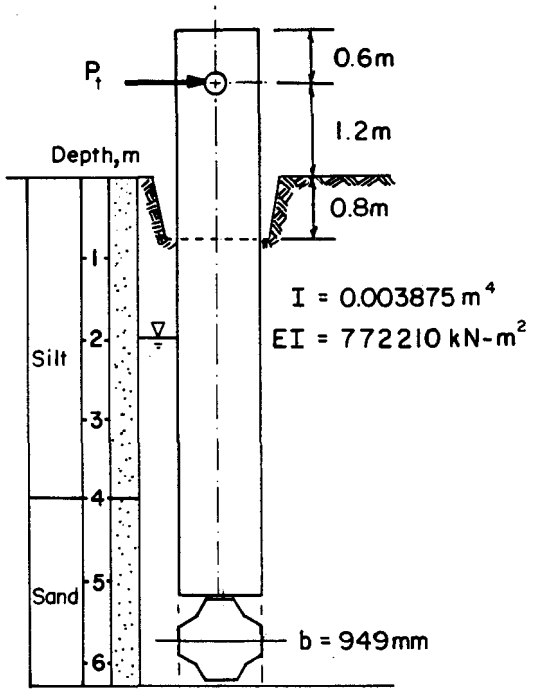

Fig. 7.20. Soil and test pile at Plancoët.

The first three columns in Table 7.2 give results from the pressuremeter tests performed at Plancoët and the other columns in the table show the development of the p-y curves. The curves were employed to compute the behavior of the pile under lateral loading. The results of the computations of deflection at the groundline are shown in Fig. 7.21, along with the measured values. Also shown in Fig. 7.21 are results from other methods of analysis. The fact that the method of analysis employing COM624 gave the best agreement between analysis and experiment could, of course, be fortuitous.

Chapter 9 presents comparisons of results from analysis with results from a number of experiments. The comparison of the results from the pressuremeter are placed here because pressuremeter tests were not performed at any of the other sites where experiments are studied.

7.4 METHOD USING CHARTS

A method of design could be used in which preliminary designs or designs for small-scale projects could be made by reference to charts or

TABLE 7.2. POINTS ON p-y CURVES DERIVED FROM DATA FROM PRESSUREMETER

Depth Z	p_f	p_ℓ	E_M	k_M	λ_Z	$\lambda_Z k_M$	$p_1=p_f b$	y_1	$p_2=p_\ell b$	y_2
m	bars	bars	bars	bars /cm		bars /cm	kN/m	m	kN/m	m
0.5	0.85	1.44	20	0.57	0.632	0.36	80.8	0.023	136.8	0.056
1.0	0.95	1.54	10.3	0.29	0.763	0.22	90.3	0.043	146.3	0.097
1.5	1.05	2.07	13	0.37	0.895	0.33	99.8	0.032	196.7	0.094
2.0	1.15	1.68	9.4	0.27	1.0	0.27	109.3	0.042	159.6	0.081
3.0	1.35	2.98	13.7	0.39	1.0	0.39	128.3	0.035	283.7	0.119
4.0	1.55	3.23	18	0.51	1.0	0.51	147.3	0.030	306.9	0.096
5.0	1.75	3.48	26.5	0.75	1.0	0.75	166.3	0.023	330.6	0.069

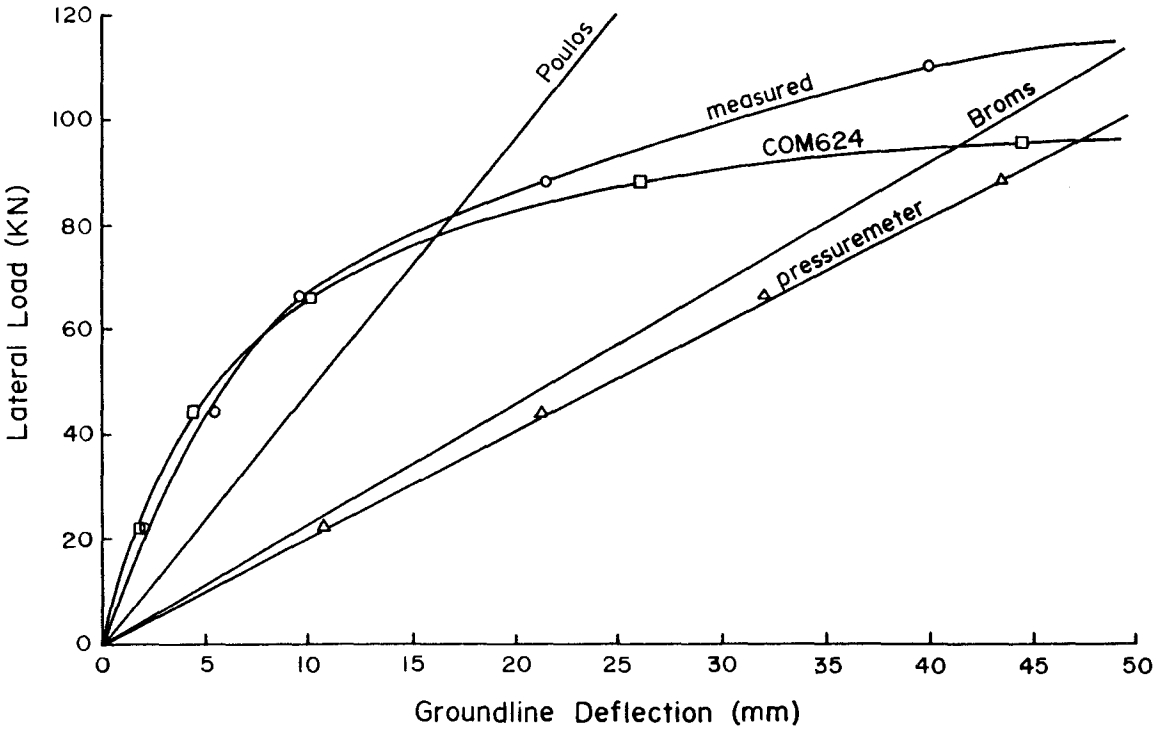

Fig. 7.21. Comparison of results from various analytical methods with results from experiment at Plancoët.

diagrams. A design office could perform a number of analyses using a computer program with assumptions being made about pile size and materials, soil properties, boundary conditions, and nature of loading. The results would then be analyzed and diagrams made for convenient use.

Examples of the kinds of charts that can be developed are shown in Figs. 7.22 and 7.23. As noted in the figures, the charts were produced for a reinforced-concrete pile with a diameter of 18 in. The soil has a constant shear strength with depth and is below the water surface. The loading is cyclic. The difference between the two charts is that Fig. 7.22 is for a soil with an undrained shear strength of 1000 lb/sq ft and Fig. 7.23 is for a strength of 2000 lb/sq ft. It is of interest to note that the limiting condition in Fig. 7.22 is deflection. The maximum deflection has arbitrarily been set at 10 percent of the diameter of the shaft or 1.8 in. On the other hand, the limiting condition in Fig. 7.23 is bending moment with the ultimate moment on the pile being reached before the limiting deflection.

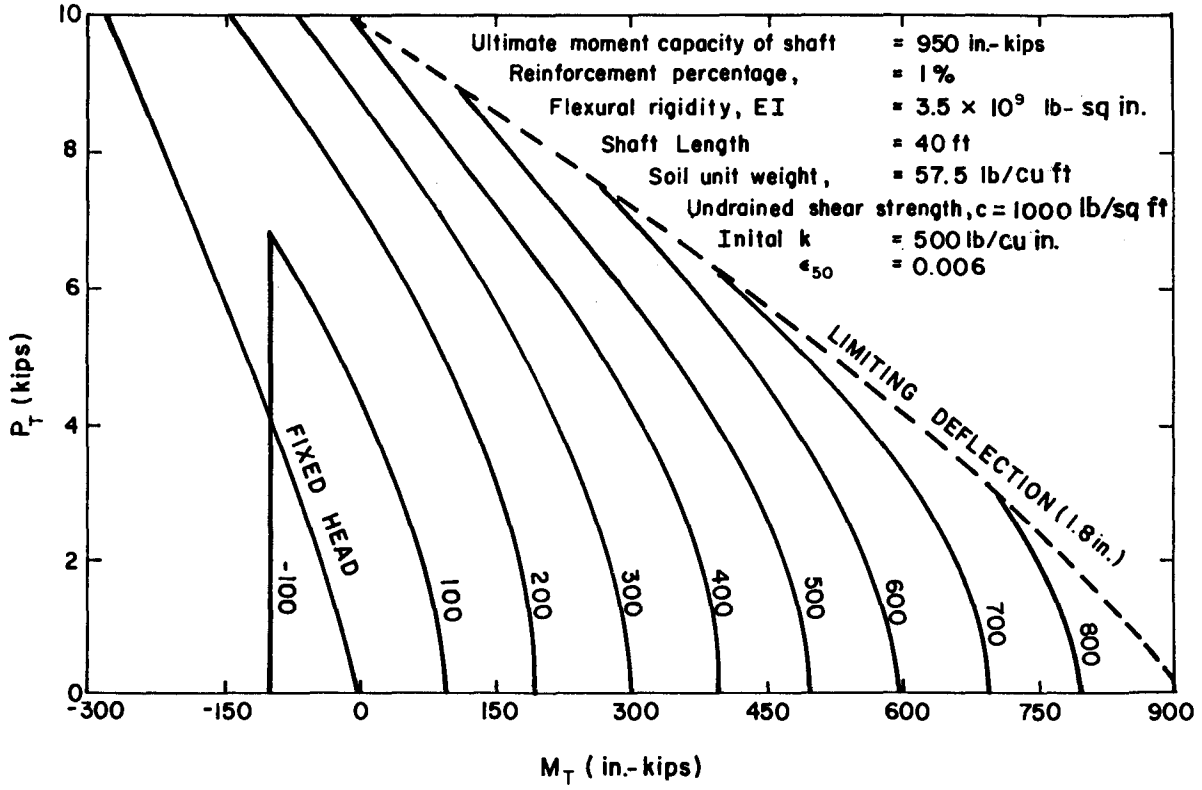

Fig. 7.22. Values of maximum bending moment in an 18-in. diameter concrete shaft in clay (after Reese and Allen).

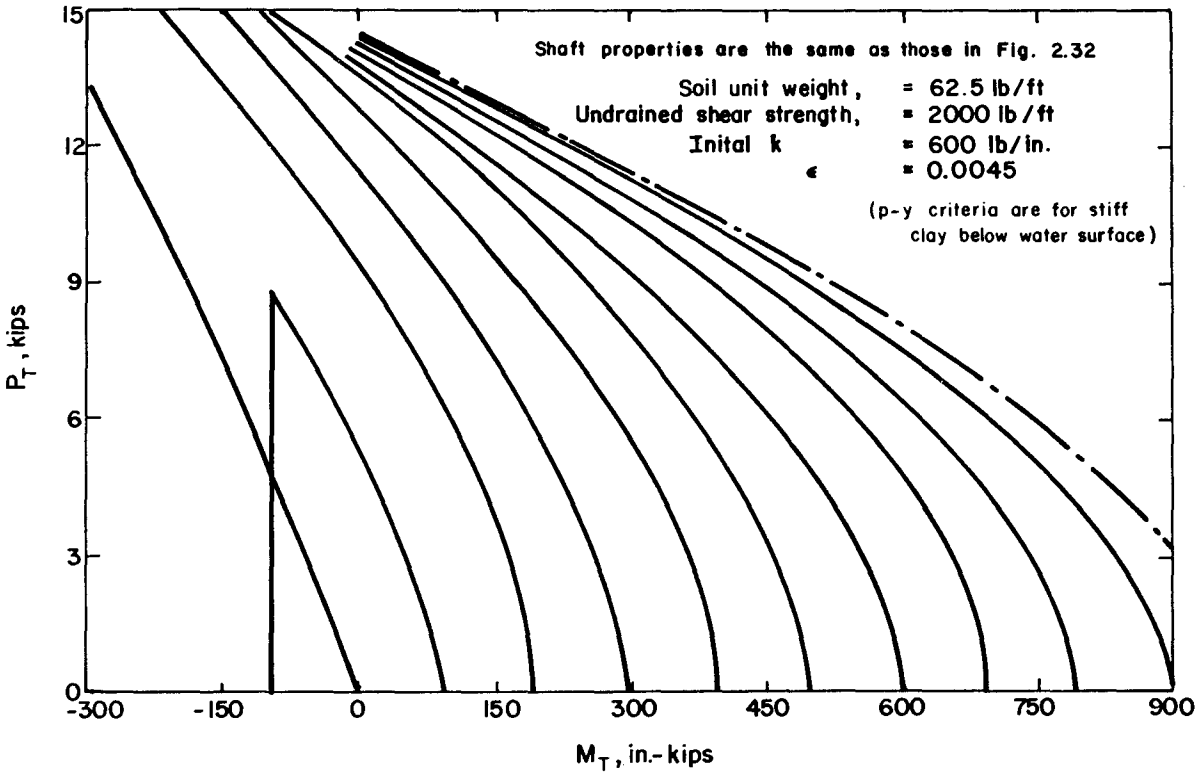

Fig. 7.23. Values of maximum bending moment in an 18-in. diameter concrete shaft in clay (after Reese and Allen).

If the moment and shear at the top of the pile (drilled shaft, drilled pier, caisson) are known, it is a simple matter to enter a curve and arrive at the maximum bending moment in the pile. The difficulty arises with the specifics: pile dimensions, shear strength and other soil properties, and nature of loading. An extremely large number of charts would be necessary if a chart is at hand for conditions that are approximately equal to those at a site.

An office could encounter designs that are similar enough in nature to each other that it would be justified to develop a series of charts. Even that approach might be questionable if the office has convenient access to a digital computer of appropriate power.

Simplified methods of design can be more useful if based on results of field load tests on piles of a certain type. Two proposals of this sort will be presented.

Manoliu (1976) examined the results from 27 different sites of 160 field tests of precast concrete piles that were installed by driving. The soils ranged from sands to gravels to soft clays. Results were plotted and empirical curves were fitted through the plotted points. There was considerable scatter but Manoliu suggested that the curves shown in Fig. 7.24 can be used for preliminary design. For a given design, a groundline deflection y_t can be selected and the value of k obtained from Fig. 7.24. Then the relative stiffness factor T can be computed from Eq. 6.75. The lateral load can then be computed depending on pile-head restraint, using methods presented in Sect. 6.4. Manoliu indicated that the piles being tested generally could be defined as "long" with a Z_{max} greater than 4.

Bhushan, et al. (1981) reported results on full-scale tests of drilled shafts that were installed in sand. The results were analyzed and Fig. 7.25 was prepared. The figure can be used for preliminary designs of

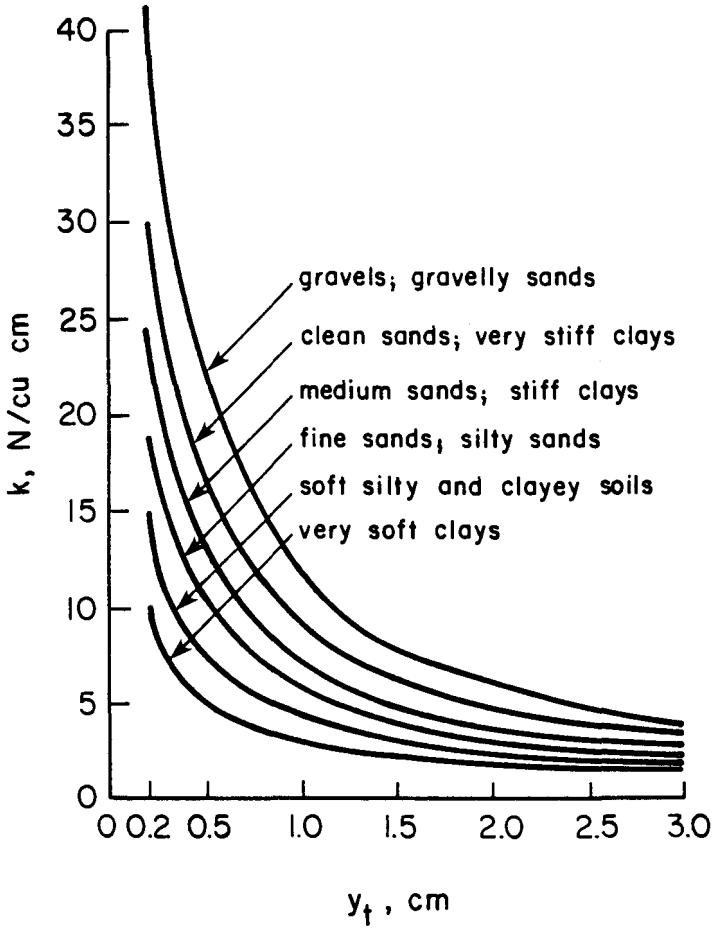

Fig. 7.24. Empirical curves showing response of driven, precast concrete piles (Manoliu, 1976).

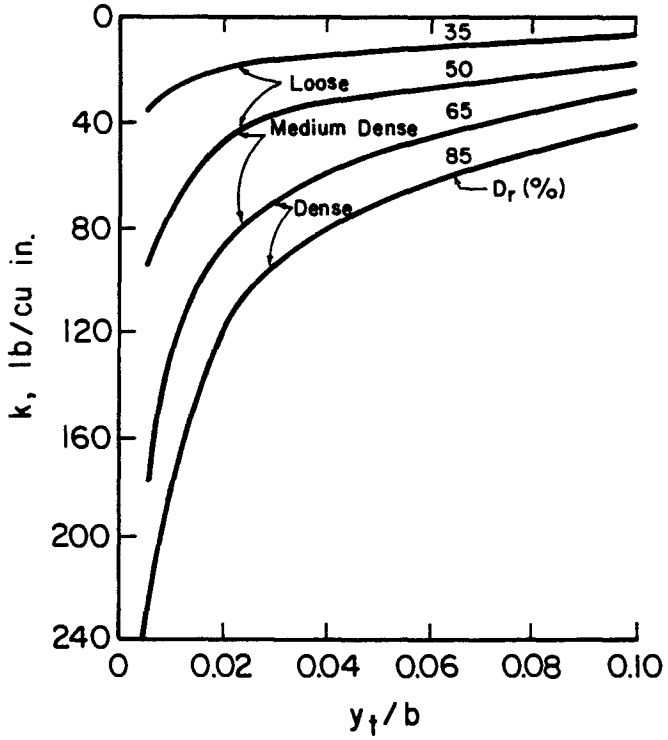

Fig. 7.25. Empirical curves showing response of drilled shafts (Bhushan, 1981)

drilled shafts in sand in a manner similar to that suggested by Manoliu. The curves in Fig. 7.25 are for sands above the water table. For sands below the water table, Bhushan suggests that the values of k from Fig. 7.25 be halved. Bhushan did not restrict his curves to long piles; if the drilled shafts are short, the appropriate values of the nondimensional deflection coefficients should be employed.

7.5 REFERENCES

Baguelin, F., and Jezequel, J. F., "Etude experimentale de foundations profonde rigides sollicitees horizontalement," Report 71-B-687, Laboratoire Central de Ponts et Chausees, Paris, May 1971.

Baguelin, F., and Jezequel, J. F., "Etude experimentale du comportement de pieux sollicites horizontalement," Annales de l'Institute Technique du Batiment et des Travaux Publics, Supplement au No. 297, Serie SF/1, September 1972, pp. 153-204.

Baguelin, F., and Jezequel, J. F., "Le pressiometre autoforeur," Annales de l'Institut Technique du Batiment et des Travaux Publics, Supplement No. 307-308, Serie Sols et Foundations, No. 97, July-August 1973, pp. 133-160.

Baguelin, F., Jezequel, J. F., and Shields, D. H., The Pressuremeter and Foundation Engineering, Trans Tech Publications, Clausthal, Germany, 1978.

Bhushan, Kul, Lee, L. J., and Grime, D. B., "Lateral Load Tests of Drilled Piers in Sand," Drilled Piers and Caissons, American Society of Civil Engineers, 1981, pp. 114-130.

Briaud, Jean-Louis, Smith, T. D., and Meyer, B., "Design of Laterally Loaded Piles Using Pressuremeter Test Results," Proceedings, Symposium on the Pressuremeter and its Marine Applications, Paris, France, April 19-20, 1982.

Broms, Bengt B., "Lateral Resistance of Piles in Cohesive Soils," Proceedings, American Society of Civil Engineers, Vol. 90, No. SM2, March 1964a, pp. 27-63.

Broms, Bengt B., "Lateral Resistance of Piles in Cohesionless Soils," Proceedings, American Society of Civil Engineers, Vol. 90, No. SM3, May 1964b, pp. 123-156.

Broms, Bengt B., "Design of Laterally Loaded Piles," Proceedings, American Society of Civil Engineers, Vol. 91, No. SM3, May 1965, pp. 79-99.

Gambin, M., "Calcul du tassement d'une foundation profonde en fonction des resultats pressiometriques, Sols-Soils, Vol. II, No. 7, December 1963, pp. 11-31.

Idriss, I. M., Dobry, R., and Singh, R. D., "Nonlinear Behavior of Soft Clays During Cyclic Loading," Proceedings, American Society of Civil Engineers, Vol. 104, No. GT12, 1978, pp. 1427-1447.

Manoliu, I., "Lateral Bearing Capacity of Precast Driven Pile," Proceedings, Sixth European Conference on Soil Mechanics and Foundation Engineering, Vienna, 1976, pp. 515-518.

Menard, L. F., "An Apparatus for Measuring the Strength of Soils in Place," M.S. Thesis, The University of Illinois, 1956.

Poulos, H. G., "Behavior of Laterally Loaded Piles: I-Single Piles," Proceedings, American Society of Civil Engineers, Vol. 97, No. SM5, May 1971a, pp. 711-731.

Poulos, H. G., "Behavior of Laterally Loaded Piles: II-Pile Groups," Proceedings, American Society of Civil Engineers, Vol. 97, No. SM5, May 1971b, pp. 733-751.

Poulos, H. G., "Load-Deflection Prediction for Laterally Loaded Piles," Austrian Geomechanics Journal, Vol. G3, No. 1, 1973, pp. 1-8.

Poulos, H. G., and Davis, E. H., Pile Foundation Analysis and Design, Wiley, New York, 1980.

Poulos, H. G., "Single Pile Response to Cyclic Lateral Load, Proceedings, American Society of Civil Engineers, Vol. 108, No. GT3, March 1982, pp. 355-375.

Prakash, S., "Behavior of Pile Groups Subjected to Lateral Loads," Unpublished Dissertation, University of Illinois, 1962.

Reese, L. C., and Allen, J. D., Drilled Shaft Manual, Vol. II, Structural Analysis and Design for Lateral Loading, I.P.77-21, U. S. Department of Transportation, Washington, D. C., July 1977.

Terzaghi, K., "Evaluation of Coefficients of Subgrade Reaction," Geotechnique, Vol. V, 1955, pp. 297-326.

Vesic, A. S., "Bending of Beams Resting on Isotropic Elastic Solid," Proceedings, American Society of Civil Engineers, Vol. 87, No. SM2, April 1961a, pp. 35-53.

Vesic, A. S., "Beams of Elastic Subgrade and the Winkler's Hypothesis," Proceedings, Fifth International Conference on Soil Mechanics and Foundation Engineering, Vol. 1, 1961b, Paris, France, pp. 845-850.

7.6 EXERCISES

7.1 Use the pile shown in the example for the Broms method and solve for the ultimate capacity of the pile as a function of depth using the soil profile. Use Broms' equations with an e of 3 ft.

7.2 Use the data in problem 1 and a long pile and select a service load at one-third the ultimate capacity of the pile. Compute the groundline deflection, using Broms and Poulos methods.

7.3 Repeat problem 1 using the soil profile in Fig. 3.13.

7.4 Repeat problem 1 using a sand with an angle of internal friction of 34° and a submerged unit weight of 62.4 lb/cu ft.

CHAPTER 8. STRUCTURAL DESIGN OF PILES AND DRILLED SHAFTS

8.1 NATURE OF LOADING

A pile or drilled shaft that supports a bridge, a bridge abutment, or a retaining wall will normally be subjected to an axial load, a lateral load, and a moment. An example is a bridge bent shown in Fig. 8.1.

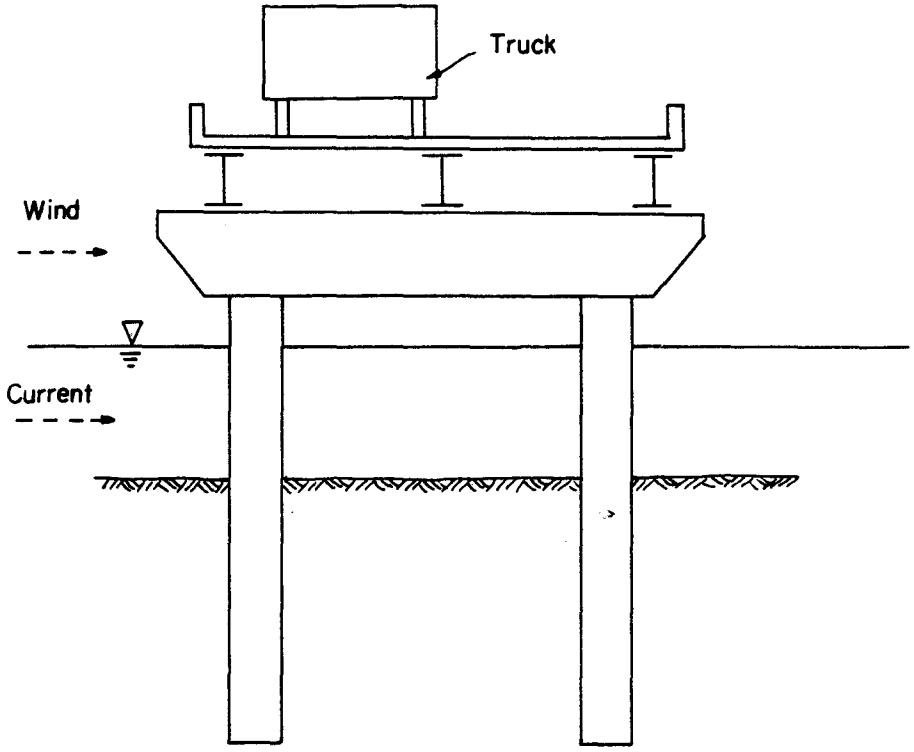

Fig. 8.1. Bridge bent.

The live loads from trucks and other vehicles as well as the dead load of the structure must be sustained by the deep foundations. In addition to the vertical loads from traffic there can be transverse loads due to wind and current. Also, the vehicles may apply longitudinal loads because of braking. In short, there can be a complicated system of forces applied to a deep foundation used in a bridge or used in other structures found in transportation facilities. Thus, a deep foundation at the groundline will be subjected to an axial load, a lateral load, and a moment. Because the pile response may be nonlinear, iterations between the piles and the

superstructure may be necessary in order to satisfy the conditions of equilibrium and continuity. That is, the loadings on a pile may have to be estimated and the pile-head movements computed. With loads and movements, the stiffness of the pile can be found; these stiffnesses can then be employed in the analysis of the superstructure and the process repeated until convergence is achieved.

It is possible that the shear and moment that act on a pile head do not lie in the same plane. However, the assumption is implicit herein that all forces on a pile head do lie in the same plane; or, if not, that the pile behavior can be found by superposition.

8.2 FAILURE MODES

The most common failure mode in a pile or drilled shaft is excessive stress. The computation of stress from an axial load is straightforward and the procedures described herein can be employed to obtain the maximum bending moment. The computation requires a knowledge of the bending stiffness of the pile and of the ultimate moment the pile can sustain. For steel piles, the stiffness and ultimate moment can be found in tables; for drilled shafts with steel reinforcement, the ultimate moment can be computed by Computer Program PMEIX (see Appendix 5). The stiffness, considering a cracked section, may also be computed by PMEIX or may be based on the gross moment of inertia of the concrete section.

Excessive deflection of a pile or drilled shaft may also constitute failure. The excessive deflection, which may be computed by procedures described herein, may be due to a soil failure where the bottom of the pile has moved laterally. Or excessive deflection may be a result of too much elastic deformation of the pile itself.

A deep foundation may also fail by buckling. Buckling is unlikely, however, if there is a pile cap at or near the ground surface. Soil that is weak can usually provide sufficient lateral restraint that buckling is not a problem.

The illustration in Fig. 8.1 shows that the deep foundation is continuous to the pile cap. There is no specific discussion of buckling included herein; however, Computer Program COM622 described earlier can be used to analyze the pile-column. The design loads (service loads times the factor of safety) are applied at the top of the unsupported pile-column, then the axial load is increased incrementally until the lat-

eral deflection becomes excessive, and at that axial load the pile is considered to have buckled. The procedure is also applicable to a pile in weak soil with little or no unsupported length.

8.3 CONCEPTS OF DESIGN

Structural Steel

Two design philosophies of steel are in current use. The working stress method has been in principal use and is still used by many designers. According to this philosophy, a structural member is designed such that stresses computed under the action of "working" or service loads do not exceed some predetermined values. These allowable stresses are given by the AISC specifications (American Institute of Steel Construction, 1978) or by the AASHTO specifications (Standard Specifications for Highway Bridges, American Association of State Highway and Transportation Officials, 1977).

The other design philosophy is generally referred to as limit states design and more recently as the load-and-resistance-factor design (LFRD). In this approach the service loads are factored and the strength at an ultimate limit state is checked to ensure that the factored loads can be achieved.

Because working-stress design is still strong in its popularity and the principal method specified by both AISC and AASHTO, it is recommended for use in the analysis of members of structural steel.

Reinforced Concrete

In general, most present-day design of reinforced concrete is being done using ultimate strength concepts. The design of a member is designed based on the ultimate strength of the member; the method is similar to the LFRD method for structural steel. In the ultimate strength approach, as in the LFRD method for steel, the service loads are factored. The computed ultimate strength of the member is reduced by a capacity-reduction factor. If the factored loads lead to a required capacity that is less than the computed value of reduced ultimate capacity of the section, the design is adequate. In general, the Building Code Requirements for Reinforced Concrete of ACI (American Concrete Institute, 1977) or AASHTO (1977) are used in design.

Timber

If a pile or drilled shaft is to be made with timber, a working-stress method is recommended as outlined in the Timber Construction Manual of the American Institute of Timber Construction (1974). Similar to structural steel, the allowable stresses prescribed in a timber specification would ensure an adequate factor of safety against failure. The stresses in the timber pile at service load levels would be compared to the allowable levels to ensure an adequate design.

8.4 DESIGN OF A STRUCTURAL STEEL MEMBER

Computation of Design Loads

For the working-stress method of structural steel design, the design loads are based on in-service conditions. The actual dead weight of the as-built structure, the calculated values of live load such as truck loading on a bridge, and the effects of other loading such as wind are used.

Step-by-Step Procedure

Frequently the design of a steel pile is controlled by the soil resistance to axial loading. The pile is then checked to see that the steel is not over-stressed. Sometimes, however, the design may be controlled by the stresses in the steel. In this latter case, the step-by-step procedure outlined below may be employed.

1. Determine the working or in-service loads acting on the member.
2. Select a member using previous experience or preliminary analysis.
3. Determine the EI value (stiffness) of the structural steel section for use in the analysis of the member.
4. Using the in-service loads and the EI of the pile, obtain the maximum shear and moment in the member. A computer program or another method may be used.
5. For the calculated maximum moment and shear, determine the stresses in the section.
6. Compare the actual stresses in the member to the allowable stresses. If the actual stresses are slightly less than the allowable stresses, the member is adequate. If the member is over-stressed or if it is grossly under-stressed, a new selection is made and the process is repeated.

The equations from the AISC specifications are listed here for convenience. To check the combined stress state for strength:

$$\frac{f_a}{0.6F_y} + \frac{f_b}{F_{bx}} \leq 1.0 \qquad (8.1)$$

where

f_a = axial stress from service loads
f_b = bending stress from service loads
F_y = yield stress of steel
F_{bx} = allowable stress in bending
(F_{bx} determined from AISC section 1.5.1.4).

Equation 8.1 has been written to indicate bending about only one axis; it is assumed that there will be no biaxial bending. To check the shear stress:

$$F_v = 0.4\ F_y \qquad (8.2)$$

where

F_v = allowable shear stress.

7. When a member of appropriate size is found, check for other failure modes such as buckling as outlined earlier.

In the example computations presented in earlier chapters, it was shown that the bending stress in a pile is maximum at or near the ground surface and decreases rapidly with depth. If a pipe pile is employed, a pipe with a thicker wall may be selected for the top several feet and a section with a thinner wall used below. If a structural shape is to be employed, it may be possible to add plates in the top few feet to withstand the bending stresses and achieve overall economy.

Example Problem

The data for an example problem are shown in Fig. 8.2. It is desired to determine if the steel pipe has adequate strength for the given conditions. Previous analyses are assumed to have shown that deflection does not control nor is buckling of concern.

Because there is bending about one axis only, AISC Eq. 1.6-1b becomes

$$\frac{f_a}{0.6F_y} + \frac{f_b}{F_{bx}} \leq 1.0.$$

The computation of the stresses to substitute into Eq. 8.1 is as follows:

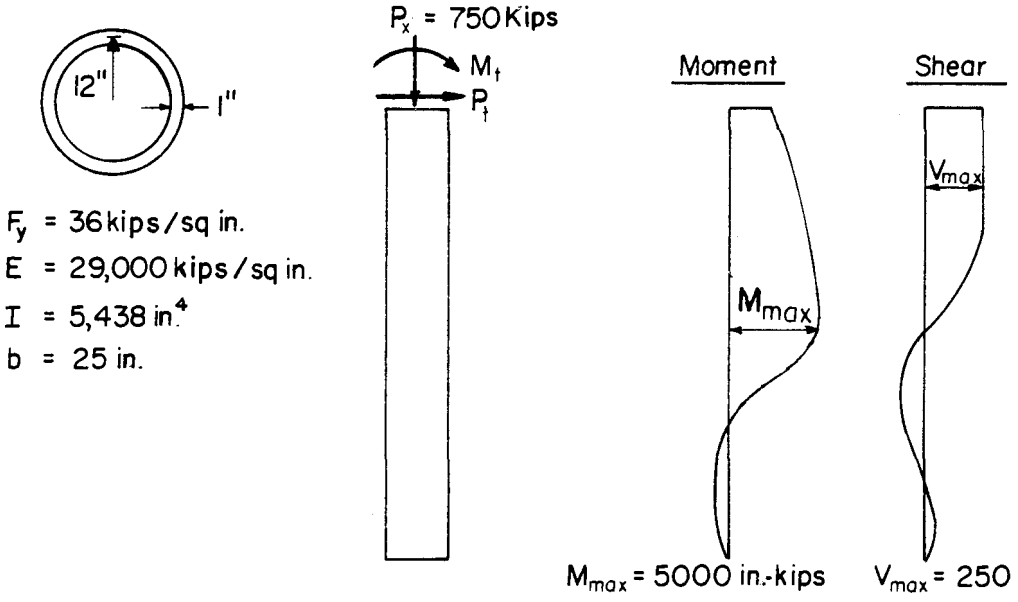

Fig. 8.2. Example to demonstrate the analysis of a steel pipe.

$$A = \pi(r_o^2 - r_i^2) = \pi[(12.5)^2 - (11.5)^2] = 75.4 \text{ sq in.}$$

$$f_a = 750/75.4 = 9.95 \text{ kips/sq in.}$$

$$f_b = \frac{Mc}{I} = \frac{(5000)(12.5)}{5438} = 11.49 \text{ kips/sq in.}$$

(see AISC Section 1.5.1.4.1, paragraph 7)

$$F_b = 0.66F_y \quad \text{if} \quad \frac{d}{t} < \frac{3300}{F_y}$$

where d = depth of section and t = thickness of wall.

$$\frac{d}{t} = \frac{25}{1} = 25$$

$$\frac{3300}{F_y} = \frac{3300}{36} = 92$$

$25 < 92$ therefore, $F_b = 0.66\ F_y$

$$F_{bx} = 0.66(36) = 23.8 \text{ kips/sq in.}$$

Substitution into Eq. 8.1 yields the following:

$$\frac{9.95}{21.6} + \frac{11.49}{23.8} = 0.461 + 0.483 = 0.943 < 1.0.$$

Therefore, the section is satisfactory for combined axial load and flexure.

To check shearing stresses, AISC Specification 1.5.1.2.1 is consulted.

$$F_v = 0.40\ F_y$$

The computation of the stresses to use in checking the adequacy of the section in resisting shear is as follows:

$F_v = 0.4\ F_y = (0.4)(36) = 14.4$ kips/sq in.

A_v = area resisting shear

$\cong (0.5)(A_{gross}) = 37.7$ sq in.

$f_a = V_{max}/A_v = 250/37.7 = 6.63$ kips/sq in.

$6.63 < 14.4$.

Therefore, the section is satisfactory with regard to shearing stresses.

8.5 DESIGN OF A REINFORCED CONCRETE MEMBER

Computation of Design Loads

Because design of reinforced concrete is currently done using ultimate strength concepts, the loads on a structure at failure are above service load levels and therefore factored loads are used. The load factors to be used depend on the type of load and the governing concrete code. The loads which need to be considered include dead load, live load, wind load, earthquake load, thermal load, creep and shrinkage effects, earth pressure; each has a specified load factor. The magnitude of the load factor for each type of load depends on which specification has been adopted. If the pile or drilled shaft is for a bridge structure, the governing code is probably AASHTO (1977). If the foundation is for a building, the ACI Specification (1977) has probably been adopted by the local building authorities. Both AASHTO and ACI require the member selected to have adequate strength for different loading combinations. The design of the member is based on the greatest required strength.

Computation of Bending Stiffness

A value of bending stiffness EI must be determined in order to compute the behavior of a pile or drilled shaft under lateral loading. Concrete has a low tensile strength and the assumption made is that the concrete cracks if there are tensile stresses. Thus, the EI of a reinforced concrete section will depend on the magnitude of the bending moment. Some investigators have suggested that the effective bending stiffness lies between that of the gross concrete section and that of the fully cracked section. Because the magnitude of bending stiffness does

not have a large effect on deflection, moment, and shear that are computed in the analysis under lateral load, some investigators prefer to use the stiffness of the gross concrete section. However, in the example that follows the stiffness of the cracked section is used.

Because the bending stiffness of a reinforced-concrete section depends on the axial load and bending moment, it follows that the EI varies along the length of a pile. If the magnitude of the EI were critical to the solution of the bending moment, a computer program for the computation of bending stiffness could be incorporated as a subroutine into the computer program for the analysis of a laterally loaded pile. In such a case, another level of iteration would be required to compute the behavior of a reinforced-concrete pile. The use of a variable stiffness in the analysis of a laterally loaded pile appears undesirable at present in view of other uncertainties of greater importance.

In any case, however, a computer program is needed in order to compute the ultimate moment that can be sustained by a reinforced concrete section. The program can also compute the bending stiffness. Computer Program PMEIX is described in Appendix 5.

Program PMEIX produces data giving moment versus curvature for a given level of axial load. The M-ϕ curve varies for different levels of axial load as is shown in the following figure. The value of the ultimate moment that can be sustained may be taken directly from such a figure as Fig. 8.3.

The EI which may be used in analyses is the slope of the M-ϕ curve after the section has cracked for the known level of axial load.

$$(EI)_{effective} = \frac{\Delta M}{\Delta \phi}$$

In using a program like PMEIX, which generates a curve for a given axial load like one of those shown in Fig. 8.3, the axial load should be the factored axial load divided by the applicable capacity reduction factor, ϕ. The reason is that the strength of the concrete section will be checked at its ultimate strength which is at the level of the factored loads.

In lieu of a more accurate analysis such as that given by Program PMEIX, ACI equations (10-9) and (10-10) can be used to detemine an EI value. However, these equations can be very conservative.

Creep of concrete under sustained loads also has an effect on stiffness. As stiffness decreases, deflections increase producing sec-

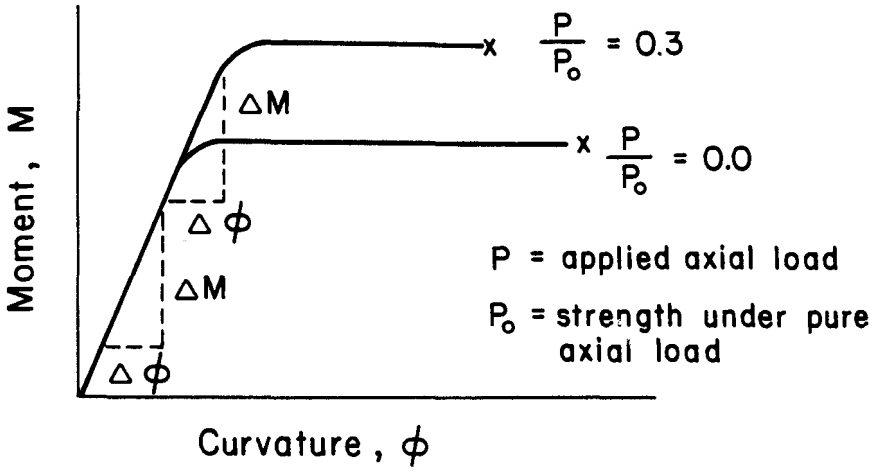

Fig. 8.3. Relationship between moment and curvature for a concrete member.

ond-order or P-delta effects. To take this into account, ACI (Sec. 10.11.5.2) recommends reducing the effective EI value by the term $(1 + \beta_d)$ where β_d is the ratio of the maximum factored dead load moment to the maximum factored total load moment.

$$(EI)_{creep} = \frac{(EI)_{effective}}{1 + \beta_d}$$

β_d is always positive and has a maximum value of 1. Because for the pile problem these moments are not known until an analysis is done, which in turn depends on the EI value used, taking a value of $\beta_d = 1$ would produce the smallest EI.

Step-by-Step Procedure

The following is a step-by-step procedure which can be used in the analysis and design of a reinforced concrete pile or drilled shaft.

1. Determine the loads acting on the structure and then use the appropriate load factors. The following load factors for gravity loads and capacity-reduction factor for a spirally reinforced shaft are specified by the American Concrete Institute.

   Load factor for dead load is 1.4,
   Load factor for live load is 1.7, and
   Capacity-reduction factor ϕ is 0.75.

2. By previous experience or preliminary analysis select a member size and reinforcement.
3. Take the factored axial load, divided by the appropriate capacity-reduction factor, and run Program PMEIX to determine a stiffness (EI) value at the level of axial load to be used in the shaft analysis program.
4. Run computer program COM622 using the factored loads which have also been divided by the appropriate capacity-reduction factor. The shaft analysis program will yield the maximum shear and moment in the member.
5. From the earlier run of PMEIX the ultimate moment capacity may be determined. Multiply this nominal ultimate moment by the appropriate capacity-reduction factor to get the allowable ultimate moment.
6. Compare the allowable ultimate moment to the maximum moment computed in the analysis of the pile under lateral loading. If the allowable ultimate moment is equal to or slightly greater than the maximum moment from the analysis, the section is adequate. If the section is under-sized or grossly over-sized, a new section is selected and the analysis is repeated. Also, check the shear capacity of the section.

In performing steps 5 and 6, the relevant equations from the code are to be employed. The equations from the ACI specifications are listed here for convenience.

$$M_u = \phi M_N \tag{8.3}$$

where

M_u = allowable ultimate moment
ϕ = capacity-reduction factor
M_N = nominal ultimate moment.

$$V_u = \phi(V_c + V_s) \tag{8.4}$$

where

V_u = shear capacity of a member
V_c = shear contribution of the concrete
V_s = shear contribution of the reinforcing steel
ϕ = capacity-reduction factor for shear (0.85).

$$V_c = 2\left(1 + \frac{N_v}{2000A_g}\right)\sqrt{f'_c}\ b_w d \tag{8.5}$$

where

N_u = factored axial load
A_g = gross area of concrete
b_w = diameter of circular section
d = distance from extreme compression fiber to centroid of tensile reinforcement.

7. The final step is to check for other failure modes such as buckling when a member of appropriate size is found. The procedure for checking for buckling was outlined earlier.

As noted in the discussion of the structural steel member, the steel reinforcement in a reinforced concrete pile may be needed only in the upper portion of the pile. The designer may be able to achieve considerable economy by matching the required reinforcement to the computed stresses.

Example Problem

The data for an example problem are shown in Fig. 8.4. It is desired to determine if the reinforced concrete section has adequate strength for the given conditions. Previous analyses are assumed to have shown that deflection does not control nor is buckling of concern. Load factors and capacity-reduction factor given earlier are used to compute loadings.

$$P_{ux} = 1.4(350) + 1.7(150) = 745 \text{ kips}$$
$$M_{ut} = 1.4(1\text{x}10^6) + 1.7(0.5\text{x}10^6) = 2.25 \text{ x } 10^6 \text{ in.-lb}$$
$$P_{ut} = 1.4(25^k) + 1.7(10^k) = 52 \text{ kips}$$

The bending stiffness EI is determined by using Computer Program PMEIX (see Appendix 5). The axial load to be used in PMEIX was found as follows:

$$P_{N_x} = \frac{P_{ux}}{\phi} = \frac{745}{0.75} = 993 \text{ kips.}$$

Using PMEIX at an axial load level of 993 kips, the moment-curvature (M-ϕ) relationship shown in Fig. 8.5 was determined. Figure 8.5 was analyzed and the following bending stiffness was obtained.

$$(EI)_{\text{effective}} = \frac{\Delta M}{\Delta \phi} \cong \frac{0.67 \text{ x } 10^7 \text{ in.-lb}}{0.80 \text{ x } 10^{-4} \text{ rad/in.}} = 8.4 \text{ x } 10^{10} \text{ lb-sq in.}$$

Taking into consideration creep yields:

$$EI = \frac{(EI)_{\text{effective}}}{1 + \beta_d} = \frac{8.4 \text{ x } 10^{10}}{1 + 1} = 4.2 \text{ x } 10^{10} \text{ lb-sq in.}$$

The factored loads divided by the capacity-reduction factor resulted in the moment and shear shown in Fig. 8.6.

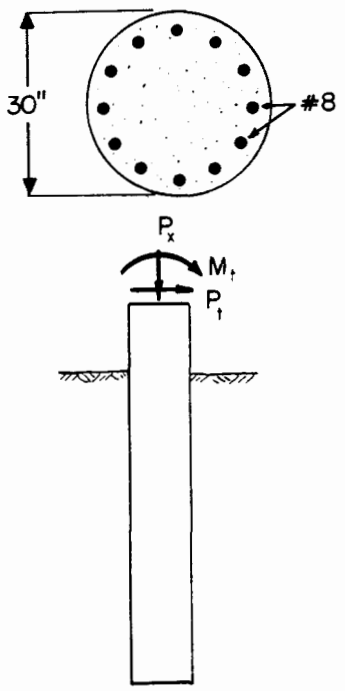

Given:

$A_{s\text{-}total}$ = 12.0 (0.79 sq in.) = 9.48 sq in.

f'_c = 4,000 lb/sq in.

f_y = 60,000 lb/sq in.

E_s = 29 × 10^6 lb/sq in.

$E_c = 57{,}000\sqrt{f'_c}$ = 3,605,000 lb/sq in.

Cover = 3" to center of bar

Spiral Column
Assume B_d = 1

Service Loads Given:

$P_x = P_{xDL} + P_{xLL}$ = 350 kips + 150 kips

$M_t = M_{tDL} + M_{tLL}$ = 1 × 10^6 in.-lb + 0.5 × 10^6 in.-lb

$P_t = P_{tDL} + P_{tLL}$ = 25 kips + 10 kips

Fig. 8.4. Example to demonstrate the analysis of a reinforced concrete pile.

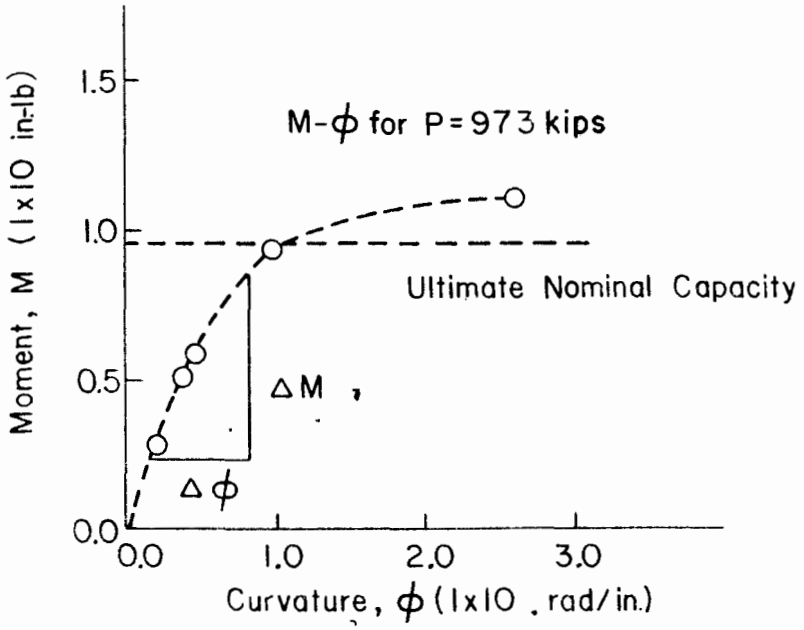

Fig. 8.5. Relationship between moment and curvature for the example problem.

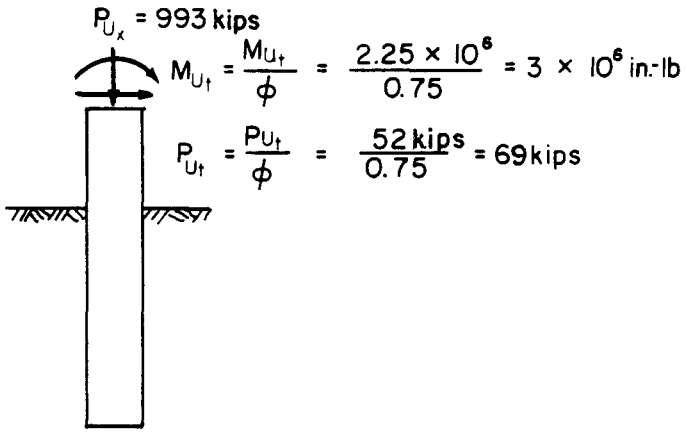

Fig. 8.6. Values of load to be employed in computer program to analyze laterally loaded drilled shaft.

The bending stiffness of 4.2×10^{10} sq in.-lb was employed, along with the loading shown in Fig. 8.6, and Computer Program COM622 was employed. The details of the computer analysis are not shown here but the significant results are presented in Fig. 8.7. The allowable ultimate values are now compared to those from analysis. From the previous M-ϕ curve, and using engineering judgement, the ultimate nominal moment capacity for the given level of axial load is 0.95×10^7 in.-lb. The reason the maximum value of about 1.1×10^7 in.-lb was not chosen is that at this value the EI value is much less, yet the shaft analysis program used an EI value in the initial range. The 0.95×10^7 in.-lb value represents the point on the M-ϕ curve where the EI value begins to be drastically reduced. The allowable ultimate moment M_u is equal to ϕM_N. Thus,

$$M_u = 0.75(0.95 \times 10^7) = 7.1 \times 10^6 \text{ in.-lb.}$$

The maximum moment was found from computer analysis (Fig. 8.7) to be 6×10^6 in.-lb; therefore $M_u > M_{max}$ and the section is satisfactory for bending.

To check the shear, Eqs. 8.5 and 8.4 are used.

$$V_c = 2\left[1 + \frac{745{,}000}{(2000)(707)}\right]\sqrt{4000}\,(30)(24) = 1.4 \times 10^5 \text{lb} = 140 \text{ kips}$$

$$V_u = 0.85\, V_c = 118 \text{ kips}$$

The maximum shear found from the computer analysis was 75 kips; therefore, the section is adequate for shear because $V_u > V_{max}$. There is no need to compute the contribution to shear of the steel reinforcement.

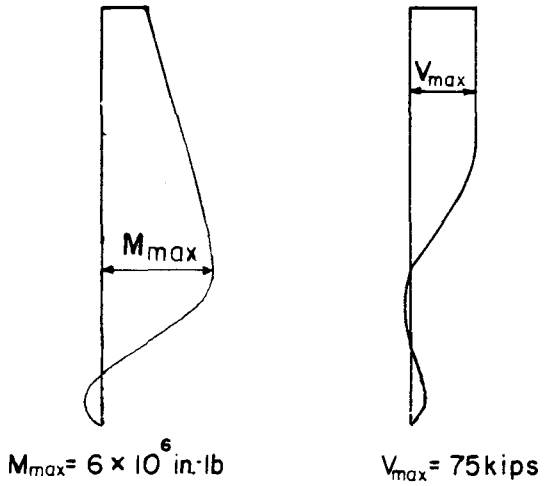

Fig. 8.7. Results from computer analysis of the drilled shaft.

The computed maximum moment at ultimate is about 15% less than the allowable maximum moment, and the capacity of the section in shear is more than adequate. Therefore, the designer might consider a reduction in the size of the section, in the amount of reinforcing steel, or in the strength of the concrete. Any change in the section would have to consider a number of factors other than the strength of the section.

8.6 REFERENCES

Manual of Steel Construction, American Institute of Steel Construction, Eighth Edition, Chicago, Illinois, 1978.

Standard Specifications for Highway Bridges, American Association of State Highway and Transportation Officials, Twelth Edition, 1977.

Building Code Requirements and Commentary for Reinforced Concrete (ACI 318-77), American Concrete Institute, Detroit, Michigan, 1977.

Timber Construction Manual, American Institute of Timber Construction, Wiley, New York, 1974.

8.7 EXERCISES

8.1 Select a steel structural shape to replace the pipe pile in the example. Assume no change in the moment and shear obtained from the computer program.

8.2 Reduce the amount of steel in the reinforced concrete section and re-work the example. Assume the moment and shear obtained from the computer program to be unchanged but re-run PMEIX to obtain the moment versus curvature relationship for the new section.

CHAPTER 9. CASE STUDIES OF SINGLE PILES UNDER LATERAL LOADING

9.1 INTRODUCTION

For single piles under lateral loading, a comparison of results from analyses with results from experiments is useful to provide an understanding concerning the quality of the analytical methods. The presumption is made that the experiments reveal the true behavior of a specific pile under lateral loading at a specific site. Emphasis in the analyses will be placed on the computer method described in detail herein; however, the Broms and Poulos methods presented in Chapter 7 will also be employed.

Separate sections in this chapter are presented for piles in sand and for piles in clay. The response of the soil is so different in these two instances that separate comparisons are desirable.

Several cases are selected for study. In order to perform the analyses it is necessary that information be available on pile dimensions and properties of the pile material, on the engineering properties of the soil, on the magnitude of load and its method of application, and on the response of the pile to loading. There are a limited number of cases in the technical literature where the above information is available.

Prior to presenting the comparisons between results from analyses and results from experiments, it is of interest to present the results of some parametric studies. Only the computer method is employed in these parametric studies.

The principal aim of the parametric studies is to investigate the influence on pile response of various parameters. Most of the parameters that were investigated involved soil properties, but some studies were aimed at investigating the influence of the bending stiffness EI of a pile. Studies were made of the four methods of predicting soil behavior for clay and of the single method of predicting the response of sand. The initial parameters selected for the soil are shown in Table 9.1 and for the pile are shown in Table 9.2. As shown in the following paragraphs, the effects of varying some of these parameters are investigated.

The general procedure employed in these studies follows that used by Meyer (1979). The parameters varied for the clay criteria are: c, ε_{50}, k, and EI; the parameters varied for the sand criteria are: ϕ, γ, k, and EI. Cyclic loading was employed in all cases because that is the condi-

TABLE 9.1. INITIAL PARAMETERS FOR SOIL.

Soil Properties	Soft Clay below W.T.	Stiff Clay below W.T.	Stiff Clay above W.T.	Unified Criteria	Sand
c(lb/sq in.)	6.0	60	15	6.0	-
ε_{50}	0.02	0.002	0.005	0.01	-
ϕ	-	-	-	-	35°
γ(lb/cu ft)	45	45	110	45	45 to 75
k(lb/cu in.)	-	500	200	100	60

TABLE 9.2. INITIAL PARAMETERS FOR PILE.

b (in.)	16
EI (lb-sq in.)	3.13×10^{10}
L (ft)	75

tion most often encountered in practice. The pile head was assumed to be free to rotate.

The percentage change of the input parameters was computed as follows:

$$\Delta\% = \frac{\text{New value - initial value}}{\text{Initial value}} 100. \qquad (9.1)$$

The change of percentage of the input parameters was based on the sensitivity of the results to the change. A change of ±50% was used in several instances.

A study was made also concerning the depth of embedment. As noted earlier, short piles fail because of soil failure and the depth of embedment is critical in such instances. Computations show that a small increase in the depth of embedment can cause a significant increase in the lateral capacity.

9.2 PARAMETRIC STUDIES OF PILES IN CLAY USING COMPUTER METHOD

Soft Clay below Water Table

The results of analyses using the Matlock (1970) criteria are shown in Figs. 9.1 through 9.3. Figure 9.1 shows the effects on maximum bending moment and deflection of varying the undrained shear strength from 432 lb/sq ft to 1296 lb/sq ft. As might have been expected, the maximum bending moment and the deflection show almost a linear variation with the undrained shear strength.

Figure 9.2 shows the effects on maximum bending moment and deflection of varying ε_{50} from 0.01 to 0.03. The changes in bending moment and deflection are relatively small.

Figure 9.3 shows the effects on maximum bending moment and on deflection of varying the EI of the 16-in.-diameter pile from 1.57×10^{10} lb-sq in. to 4.70×10^{10} lb-sq in. The effect on the bending moment is negligible to small but the effect on the deflection is significant. A tripling of the EI results in about a 50% decrease in deflection.

Stiff Clay below Water Table

The results of analyses using the Reese, Cox, Koop (1975) criteria are shown in Figs. 9.4 through 9.7. Figure 9.4 shows the effects on maximum bending moment of varying the undrained shear strength from 4,320 lb/sq ft to 12,960 lb/sq ft. At first glance it is surprising that the bending moment and deflection were not affected more by the change in shear strength; however, the loads are relatively small. As the bending moment approaches its ultimate, more differences in the curves in Fig. 9.4 would develop.

Figure 9.5 shows the effects on pile response of changing ε_{50} from 0.001 to 0.003. The changes in bending moment and deflection are relatively small except at the loads of larger magnitude.

Figure 9.6 shows the effects on pile response of changing the initial values of k (where the initial portion of a p-y curve is defined by E_s =

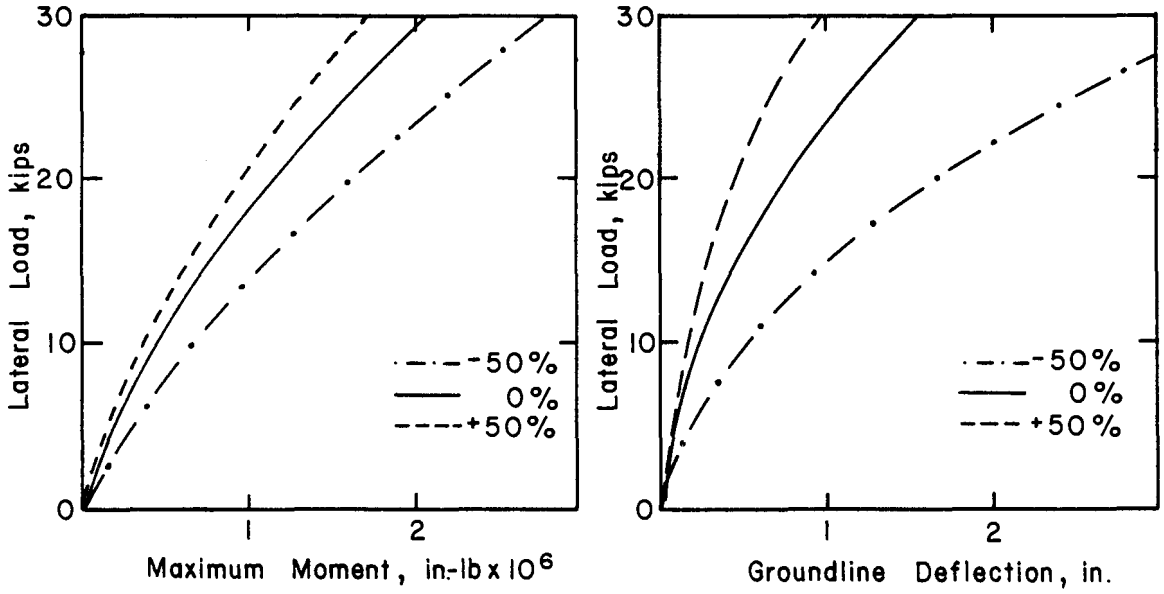

Fig. 9.1. Comparison between results for ±50 percent variation in c for soft clay below water table.

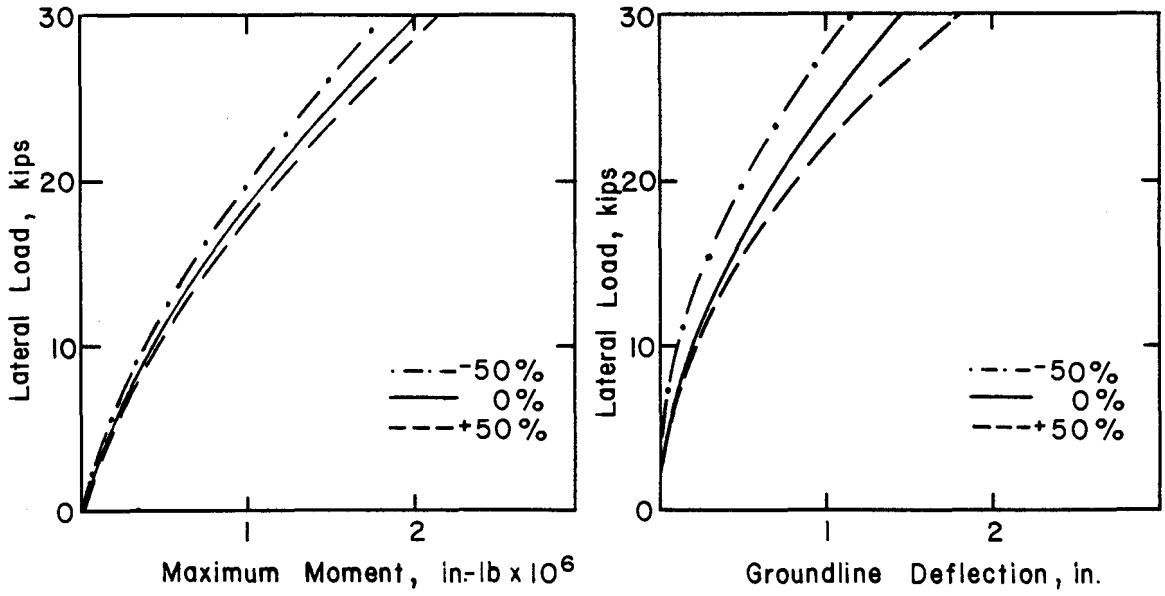

Fig. 9.2. Comparison between results for ±50 percent variation in ε_{50} for soft clay below water table.

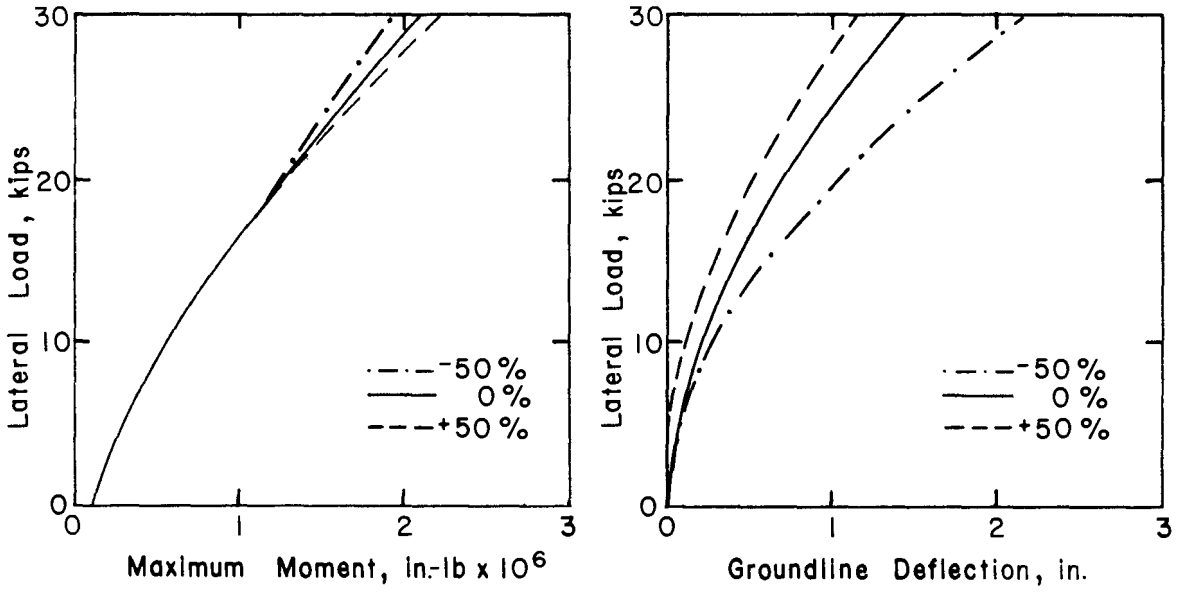

Fig. 9.3. Comparison between results for ±50 percent variation in EI for soft clay below water table.

kx). The value of k was changed from 250 lb/sq in. to 750 lb/sq in. As may be seen the lower value of k caused a significant increase in deflection and bending moment, especially at the higher loads.

Figure 9.7 shows the effects on pile response of changing the pile stiffness EI from 1.57 x 10^{10} lb-sq in. to 4.70 x 10^{10} lb-sq in. The effects on both bending moment and deflection became significant at the higher loads.

Stiff Clay above Water Table

The results of analyses using the Reese and Welch (1975) criteria are shown in Figs. 9.8 through 9.10. One hundred cycles of loading were employed in the studies. Figure 9.8 shows the effects on maximum bending moment and groundline deflection of changing the undrained shear strength from 1080 lb/sq ft to 2160 lb/sq ft. At the larger loads there are significant increases in both deflection and bending moment.

Figure 9.9 shows the effects of changing ε_{50} from 0.0025 to 0.0075. The effects are relatively small for the full range of loading.

Figure 9.10 shows the effects of changing the bending stiffness of the pile EI from 1.57 x 10^{10} lb-sq in. to 4.70 x 10^{10} lb-sq in. The effects on the maximum bending were negligible but the effects on deflection were considerable.

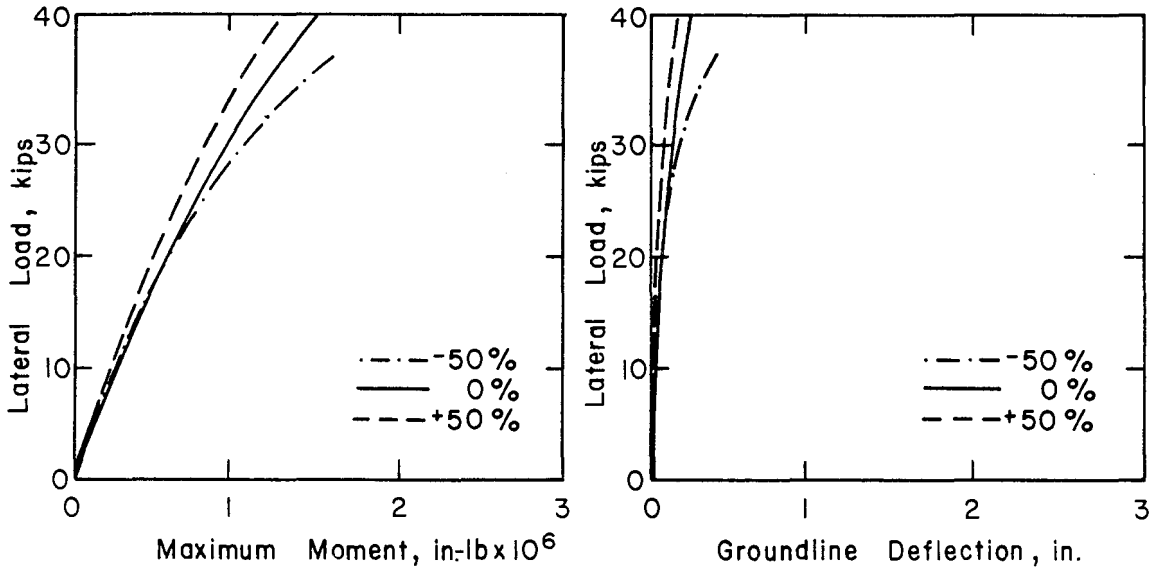

Fig. 9.4. Comparison between results for ±50 percent variation in c for submerged stiff clays.

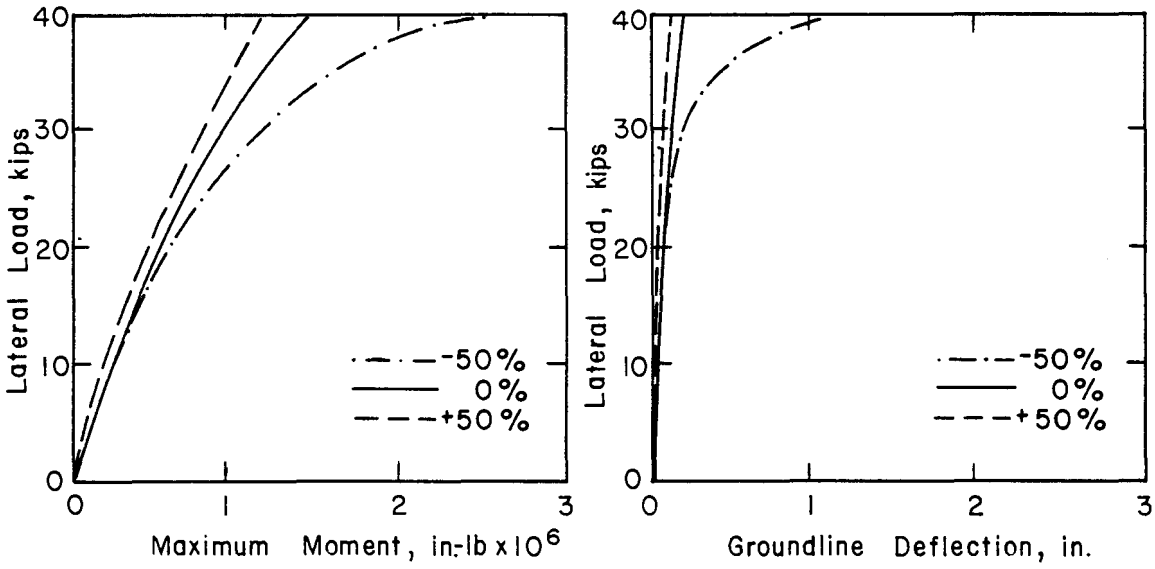

Fig. 9.5. Comparison between results for ±50 percent variation in ε_{50} for submerged stiff clays.

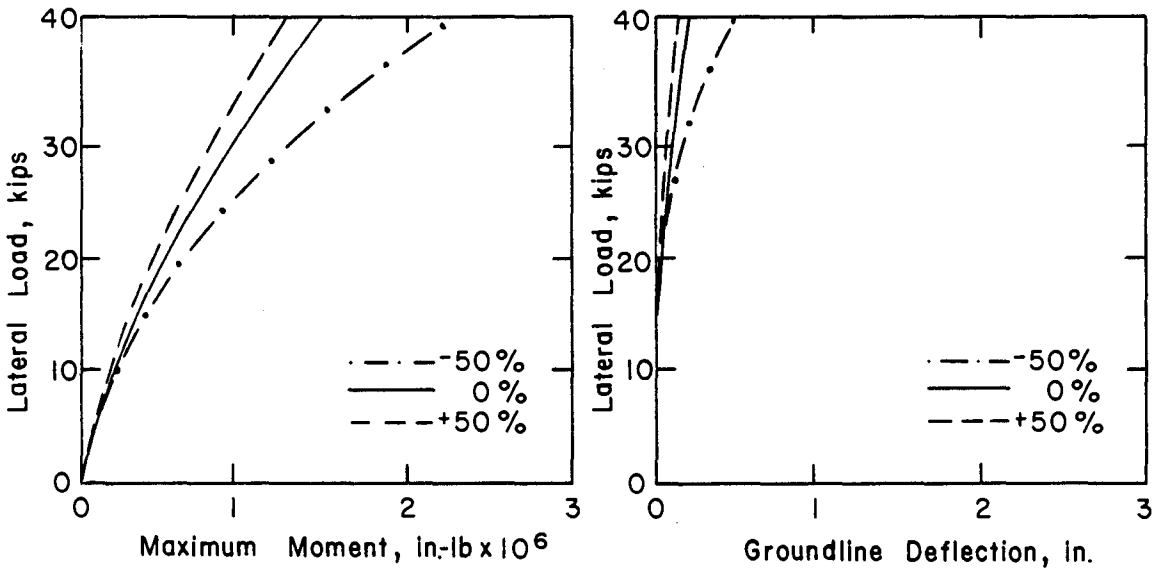

Fig. 9.6. Comparison between results for ±50 percent variation in k for submerged stiff clays.

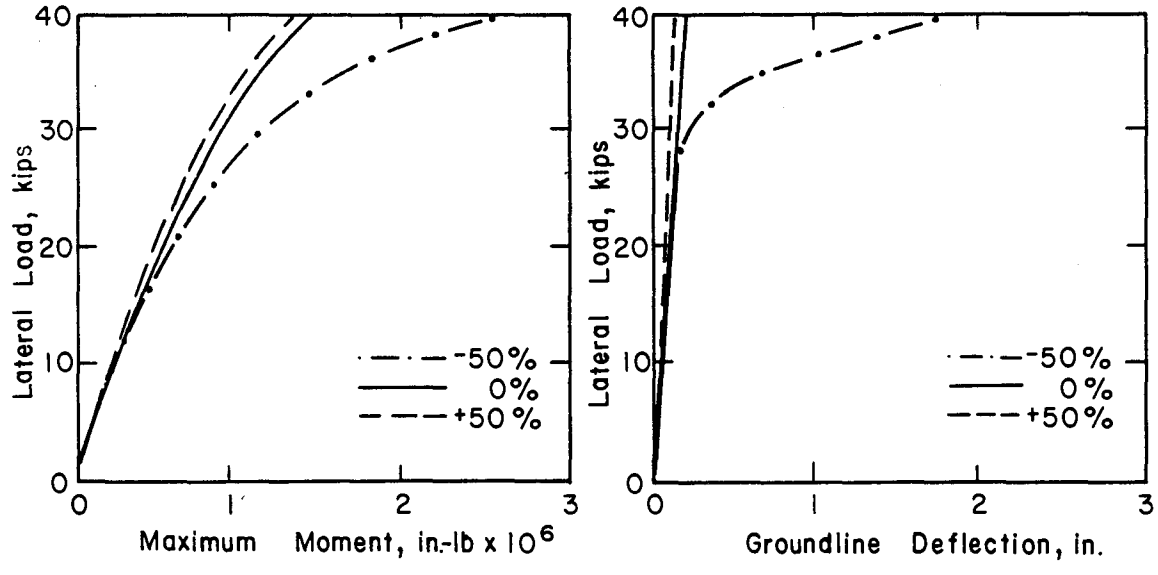

Fig. 9.7. Comparison between results for ±50 percent variation in EI for submerged stiff clays.

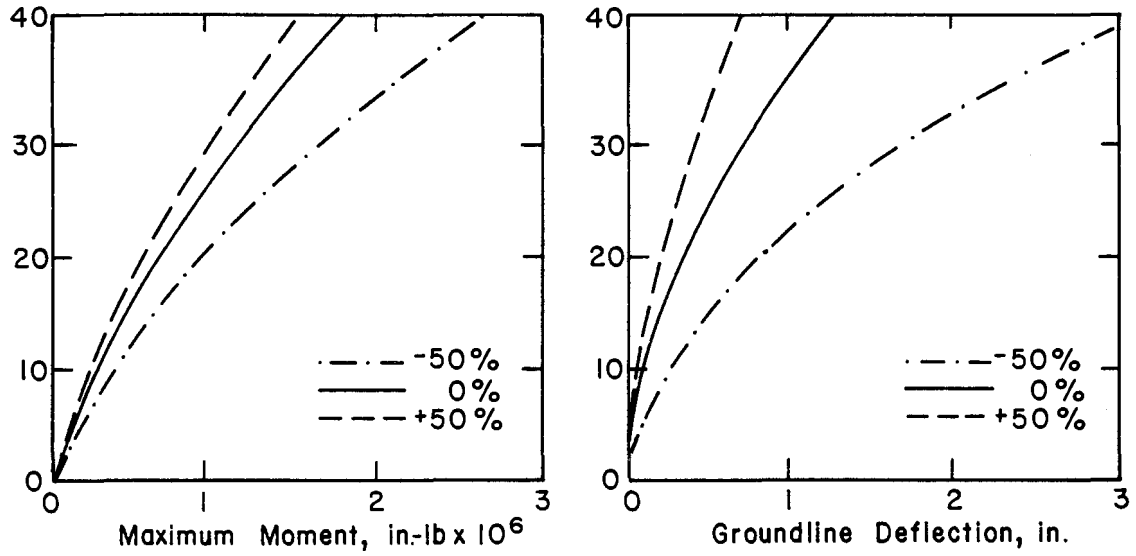

Fig. 9.8. Comparison between results for ±50 percent variation in c for stiff clay above water table.

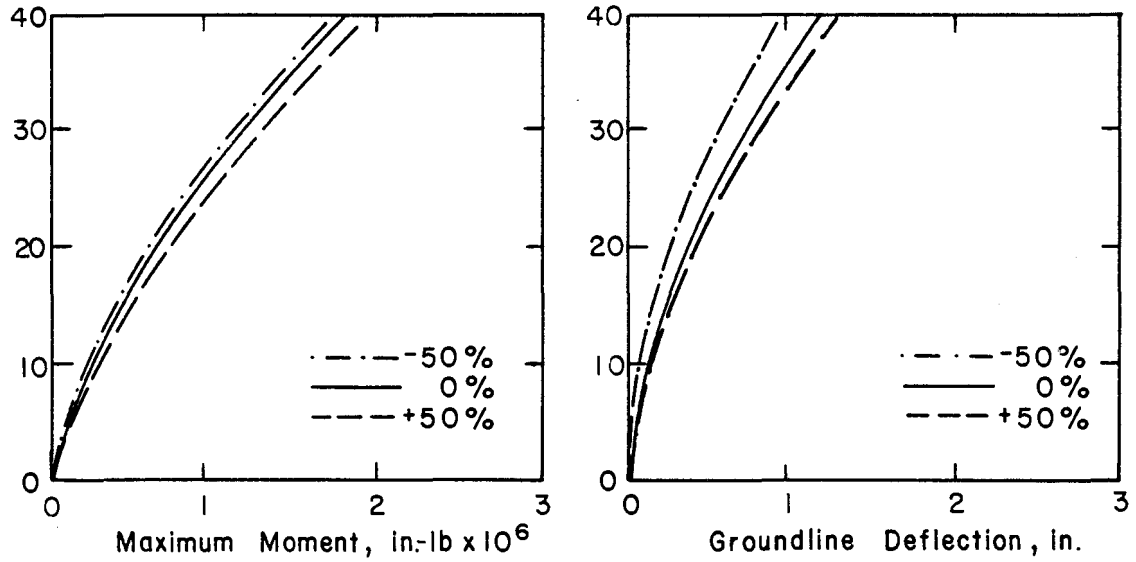

Fig. 9.9. Comparison between results for ±50 percent variation in ε_{50} for stiff clay above water table.

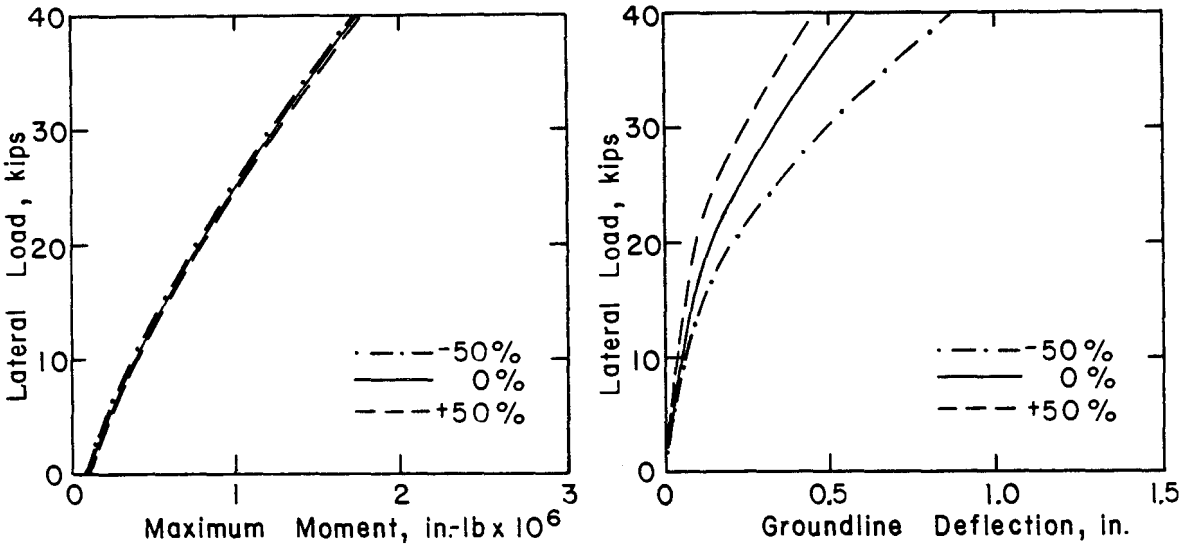

Fig. 9.10. Comparison between results for ±50 percent variation in EI for stiff clays above water table.

Unified Criteria for Stiff Clay below Water Table

The results of analyses using the Sullivan, Reese, Fenske (1980) method are shown in Figs. 9.11 through 9.14. Figure 9.11 shows the effects on bending moment of changing the undrained shear strength from 432 lb/sq ft to 1296 lb/sq ft. The effects on both maximum bending moment and deflection are severe.

Figure 9.12 shows the effects of changing ε_{50} from 0.005 to 0.015. The effects are negligible at the smaller loads but become significant as the load increases.

Figure 9.13 shows the effects of varying the value of k (the initial slope of the p-y curves is obtained from $E_s = kx$) from 100 lb/sq in. to 300 lb/sq in. The effects are negligible for the range of loading that was used.

Figure 9.14 shows the effects of changing the EI of the pile from 1.57×10^{10} lb-sq in. to 4.70×10^{10} lb-sq in. The effects are significant at the higher loads on both maximum bending moment and groundline deflection.

Sand

The results of analyses using the Reese, Cox, Koop (1974) method are shown in Figs. 9.15 through 9.18. Figure 9.15 shows the effects of chang-

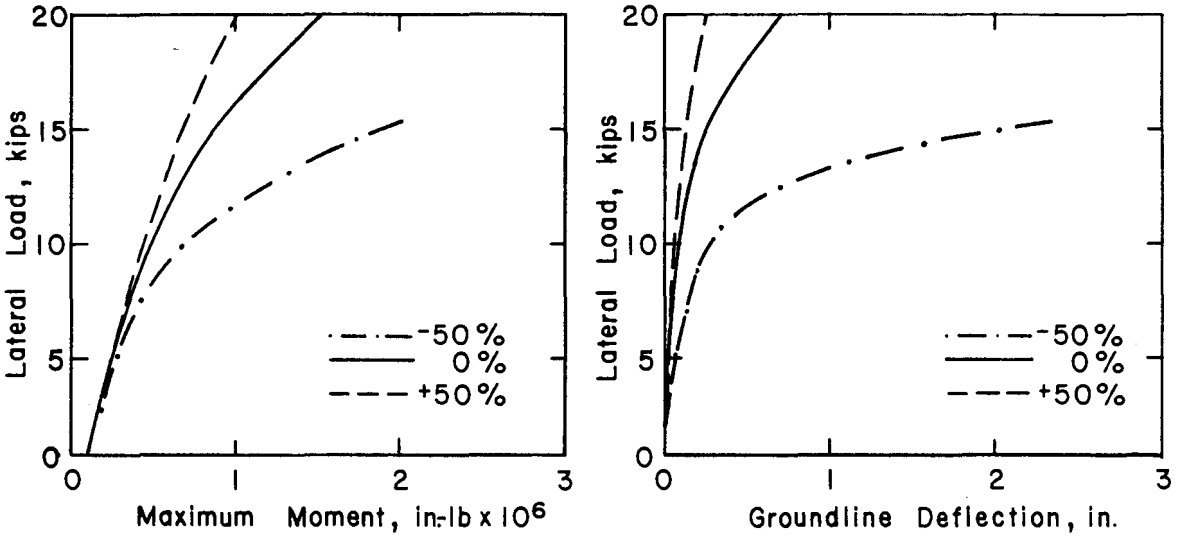

Fig. 9.11. Comparison between results for ±50 percent variation in c for unified criteria.

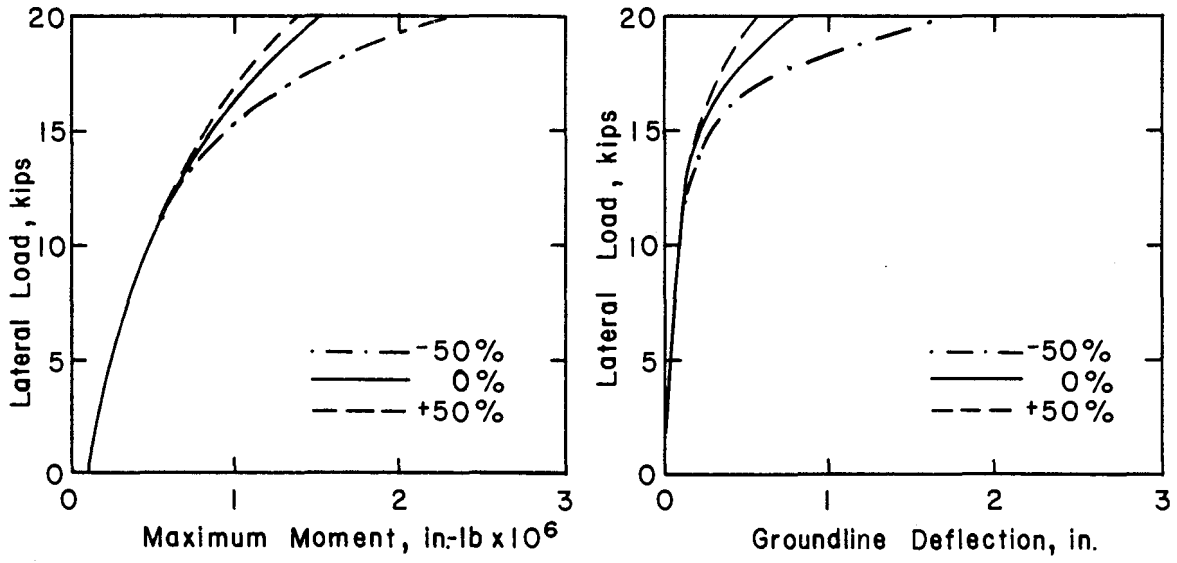

Fig. 9.12. Comparison between results for ±50 percent variation in ε_{50} for unified criteria.

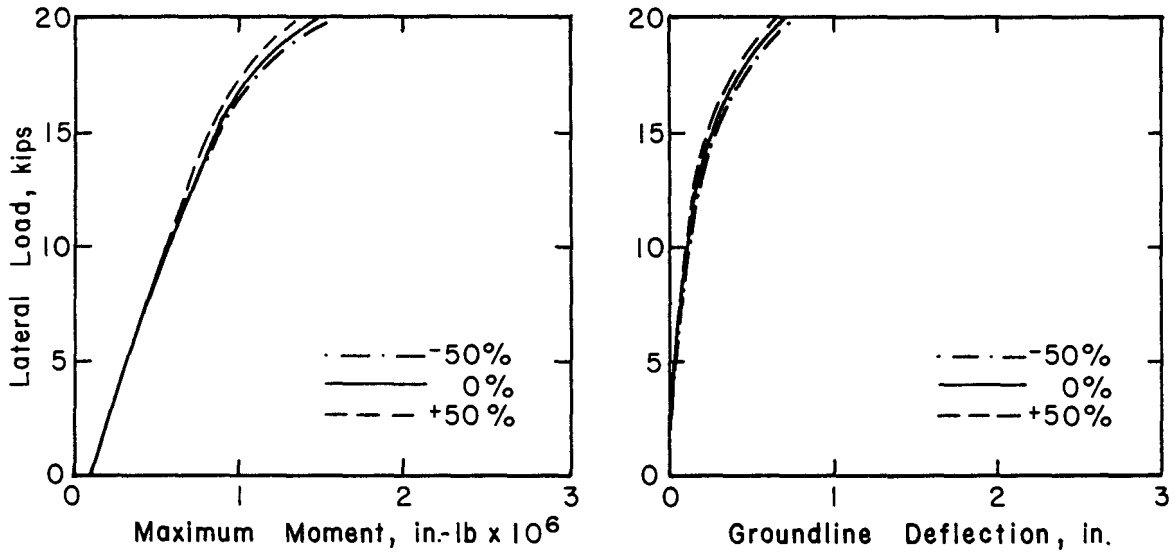

Fig. 9.13. Comparison between results for ±50 percent variation in k for unified criteria.

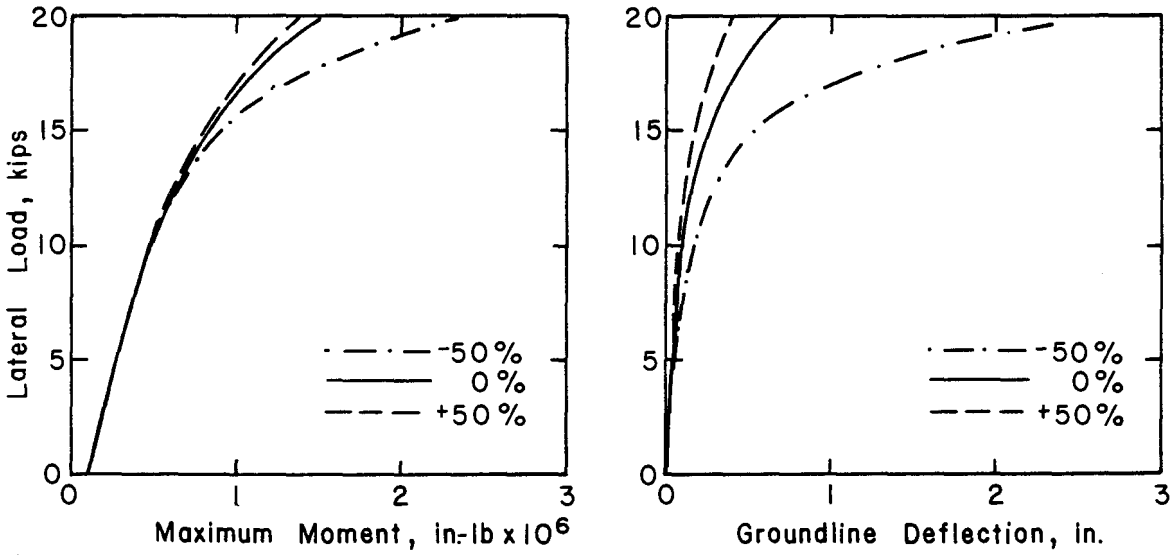

Fig. 9.14. Comparison between results for ±50 percent variation in EI for unified criteria.

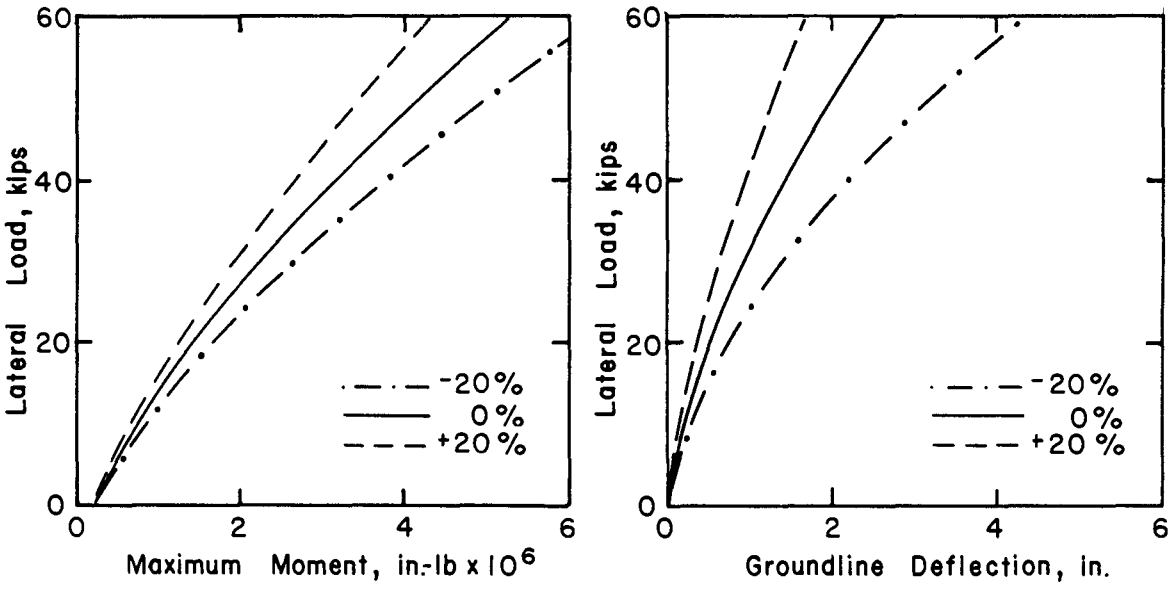

Fig. 9.15. Comparison between results for ±20 percent variation in ϕ using sand criteria for cyclic loading.

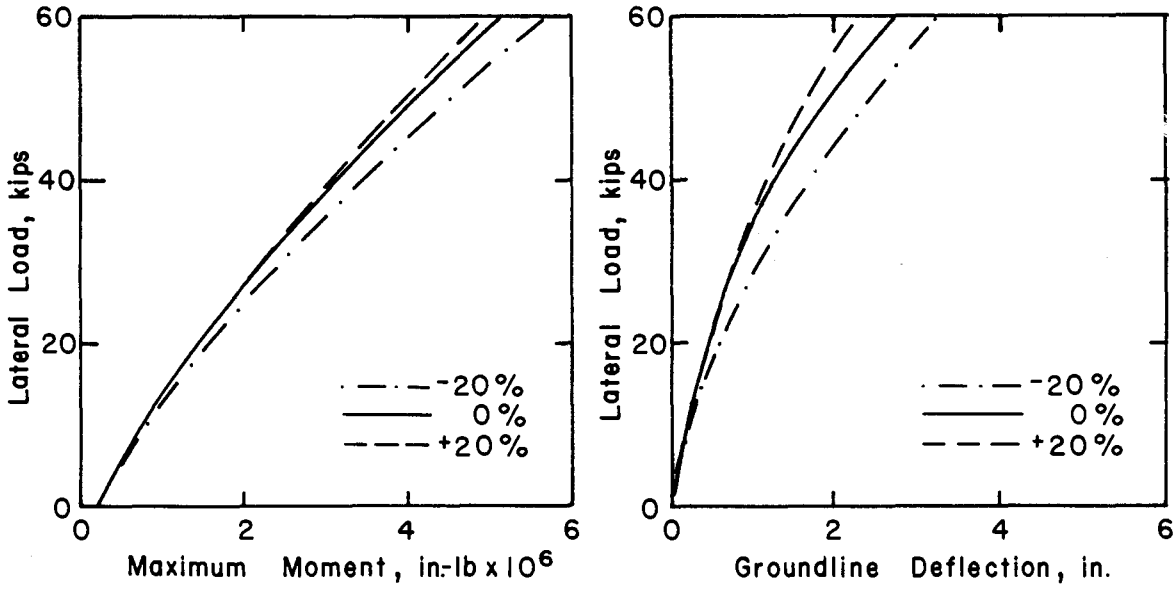

Fig. 9.16. Comparison between results for ±20 percent variation in γ using sand criteria for cyclic loading.

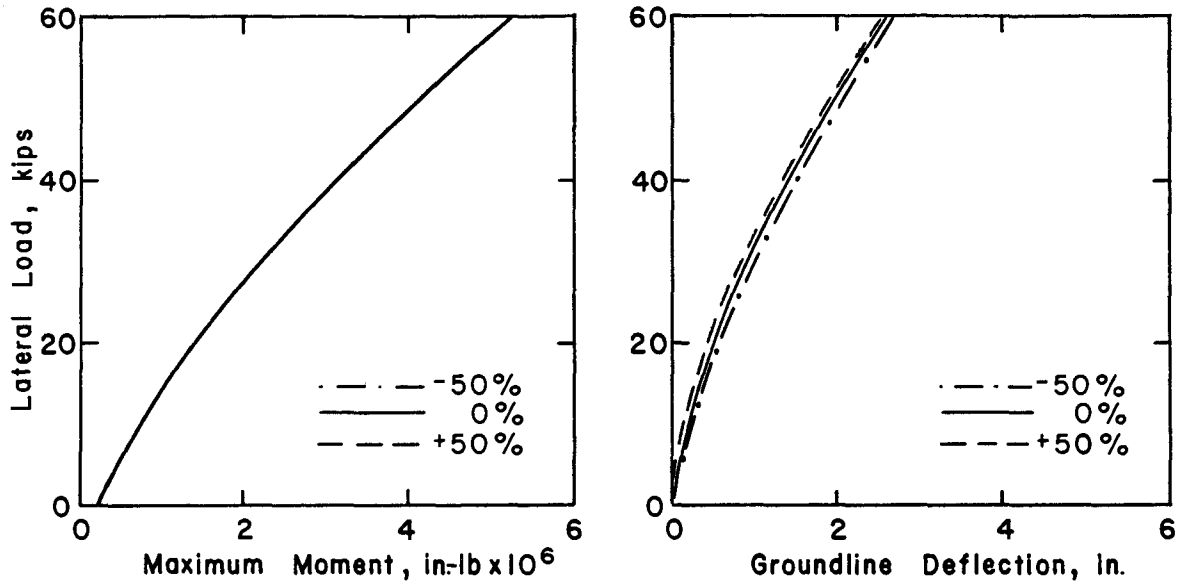

Fig. 9.17. Comparison between results for ±50 percent variation in k_s using sand criteria for cyclic loading.

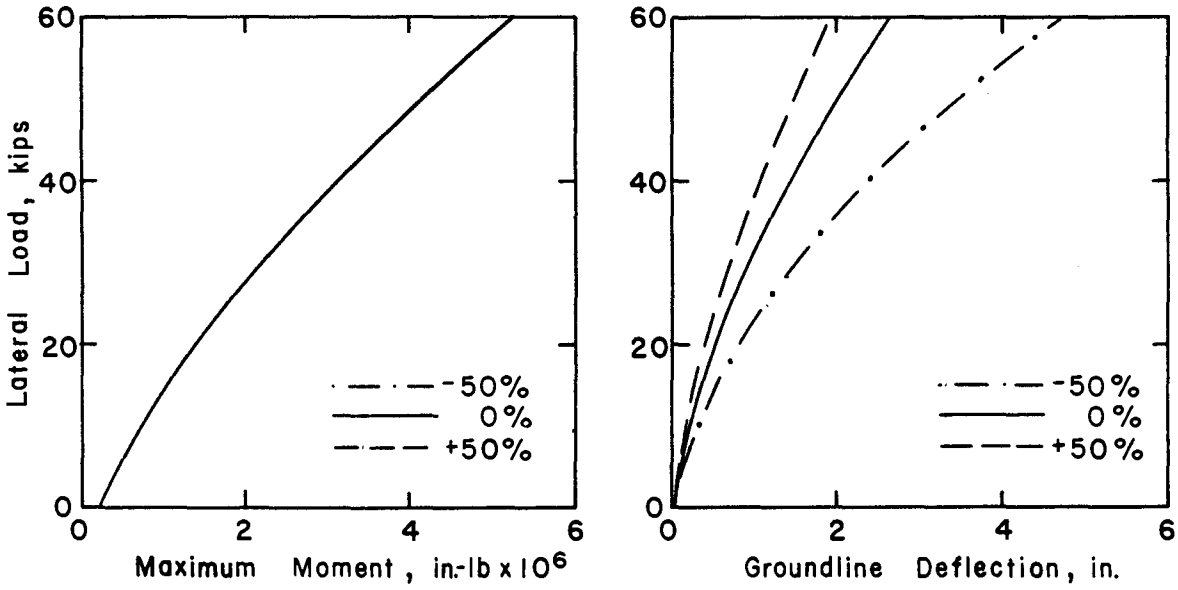

Fig. 9.18. Comparison between results for ±50 percent variation in EI using sand criteria for cyclic loading.

ing the angle of internal friction ϕ from 28 to 42 . As may be seen, the effects are significant for the full range of loading.

Figure 9.16 shows the effects of changing the submerged unit weight γ' from 48 lb/cu ft to 73 lb/cu ft (about the maximum range that could be expected in practice). The effects are relatively small for the full range of loading.

Figure 9.17 shows the effects of changing the value of k_s, that establishes the initial slope of the p-y curves, from 30 lb/sq in. to 90 lb/sq in. As may be seen, the effects are negligible on both the maximum bending moment and the groundline deflection.

Figure 9.18 shows the effects of changing the bending stiffness EI of the pile from 1.57×10^{10} lb-sq in. to 4.70×10^{10} lb-sq in. The effects are negligible on the deflection and significant on the groundline deflection.

Comments on Parametric Studies

The curves shown in Figs. 9.1 through 9.18 provide some guidance on the influence of various parameters. While there is a considerable amount of guidance to be gained by a designer from a study of the curves, the curves are specific in that the pile diameter (16 in.), method of loading (cyclic), and pile head condition (free to rotate) remained unchanged throughout the study. The designer is encouraged to perform parametric studies of a similar sort for the particular problem that is encountered.

Effect of Depth of Penetration

A further study is of interest regarding the pile selected for the parametric studies. Figure 9.19 shows the results of studies where the penetration of the pile is gradually reduced. As may be seen, the groundline deflection (and other aspects of pile response) is unaffected with increased penetration beyond a critical length. However, as the penetration becomes less than the critical length, the deflection undergoes a sharp increase, indicating a soil failure. For the free-head pile in sand, the critical depth is about 18 feet for a lateral load of 10 kips and perhaps 24 feet for a lateral load of 30 kips.

In practice, the designer should usually make certain that the penetration is below the critical depth. An increase of a few feet of pile length in some instances can ensure a much more favorable response of a pile under lateral load.

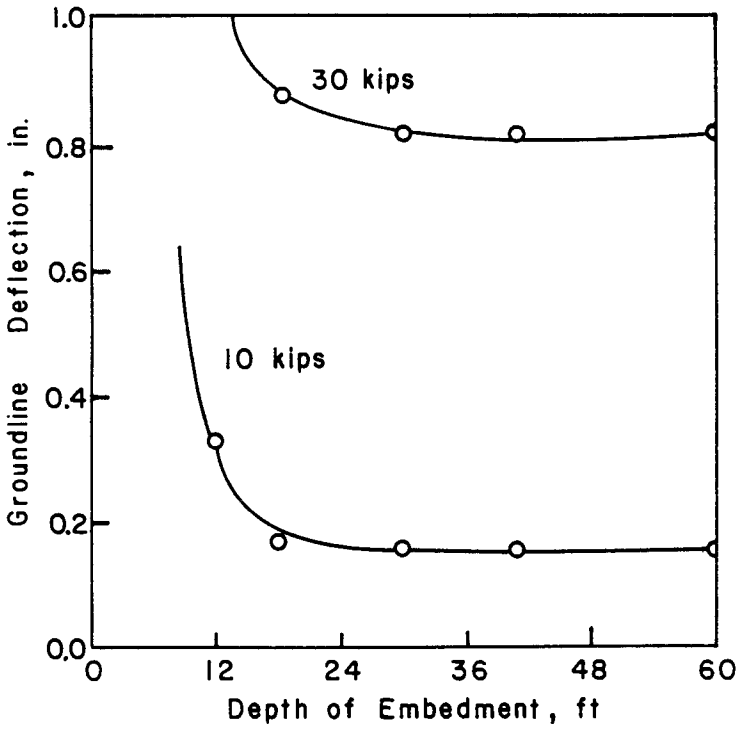

Fig. 9.19. Effect of depth of embedment on lateral deflection in sand

9.3 COMMENTS ON METHODS USED FOR CASE STUDIES

The technical literature was consulted and a number of articles or reports were found where experimental results were given on lateral load tests. The literature search was not exhaustive; however, the analyses of the tests that are presented should be useful in giving additional understanding of the methods of analysis. No attempt was made to select only those tests that appeared to correlate better with analysis; the criterion for selection was that sufficient information was available to allow a test to be analyzed. However, the tests were included from which recommendations for p-y curves were developed because those tests were well documented (Matlock, 1970; Reese, et al., 1974; Reese, et al., 1975; Reese and Welch, 1975).

No parametric studies were done to ensure the best fit of the analytical methods to the experiments with one exception. Where the pile failure came as a result of a soil failure, some computer analyses were done with piles of different penetrations. As noted earlier in this chapter, when piles are short the penetration is a critical parameter.

The computations by computer were made by using the appropriate p-y criteria. The ultimate moment of a steel member was computed by assuming that the yield stress of the steel was developed across the entire section. The ultimate moment of a reinforced concrete member was computed by using Computer Program PMEIX. The ultimate load by computer was found at the point where the computed maximum moment in the pile was equal to the ultimate moment. As noted above, there were a few cases where the piles failed by excessive deflection. Also, in some of the cases where the ultimate moment is used to control the ultimate load, the deflection could be considered to be excessive. It should be noted, however, that the ultimate lateral load must be divided by an appropriate factor of safety to obtain the service load. It is the deflection at the service load that controls the design.

The computations by the method of Broms were made as outlined in Chapter 7. An indication is given in each case as to whether or not the ultimate load was due to a soil failure or to a pile (material) failure. The computations by the method of Poulos, outlined in Chapter 7, yields only a linear relationship between load and deflection as does the Broms method for deflection. Therefore, on the figures giving comparisons between theory and experiment, the Broms and Poulos curves for deflection are stopped well below the ultimate load.

Some additional explanation beyond that presented in Chapter 7 is needed about the procedures employed in making computations with the Broms and Poulos methods. For some of the case histories considered herein, the soil deposit was not homogeneous as assumed in the analysis. Therefore, certain assumptions were used to evaluate an equivalent property representative of the non-homogeneous soil deposit.

In order to assess a single value for a soil parameter in a layered deposit, the parameters were averaged for a depth of five pile diameters. A depth of five pile diameters was used because the uppermost soils influence the pile behavior significantly. This depth was used for determining strength parameters (c, ϕ) and unit weights (γ). These parameters were used to determine the maximum lateral pile capacity according to the Broms method and horizontal deflections according to the methods of both Poulos and Broms. Lateral deflections were computed at the groundline considering the effects of both lateral load and moment.

In addition, specific relationships between parameters representing soil strength and parameters representing soil modulus had to be assumed. These relationships are discussed below.

For cohesive soils, values of the soil modulus, α, for use in the Broms method were selected based on the shear strength of the soil. Shown in Fig. 9.20 is the relationship proposed by Terzaghi (1955), and presented in Table 3.1 of this text.

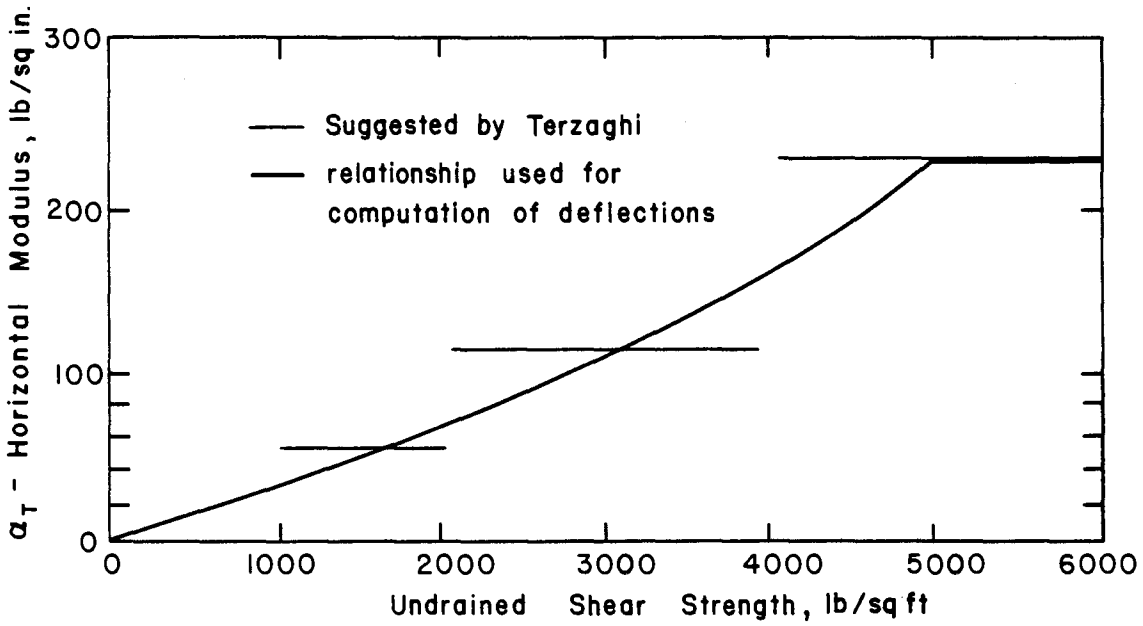

Fig. 9.20. Relationship between E_s and undrained shear strength for cohesive soil used in case studies.

For a pile in cohesive soil, the lateral deflection was calculated using a beam-on-an-elastic-foundation equation. This equation is as follows (Scott, 1981):

$$y_t = \frac{2P_t\beta}{\alpha}\,\frac{\sinh \beta L \cosh \beta L - \sin \beta L \cos \beta L}{\sinh^2 \beta L - \sin^2 \beta L} + \frac{2M_t\beta^2}{\alpha}\,\frac{\sinh^2 \beta L + \sin^2 \beta L}{\sinh^2 \beta L - \sin^2 \beta L} \qquad (9.2)$$

where

y_t = deflection at groundline
P_t = shear at groundline
M_t = moment at groundline
β = $(\alpha/4EI)^{0.25}$
EI = bending stiffness of pile
α = soil modulus
L = pile length.

For a pile in cohesionless material, a relationship between the angle of internal friction, ϕ, and the constant giving a variation in soil modulus with depth, k, was needed for the Broms computations. Terzaghi (1955) recommended values of k for different relative densities of the sand as presented in Table 3.2; however, Terzaghi's relationship is inconvenient due to inaccuracies in determining in-situ relative densities. Therefore, the correlation shown in Fig. 9.21 was used to obtain the relationship between ϕ and k.

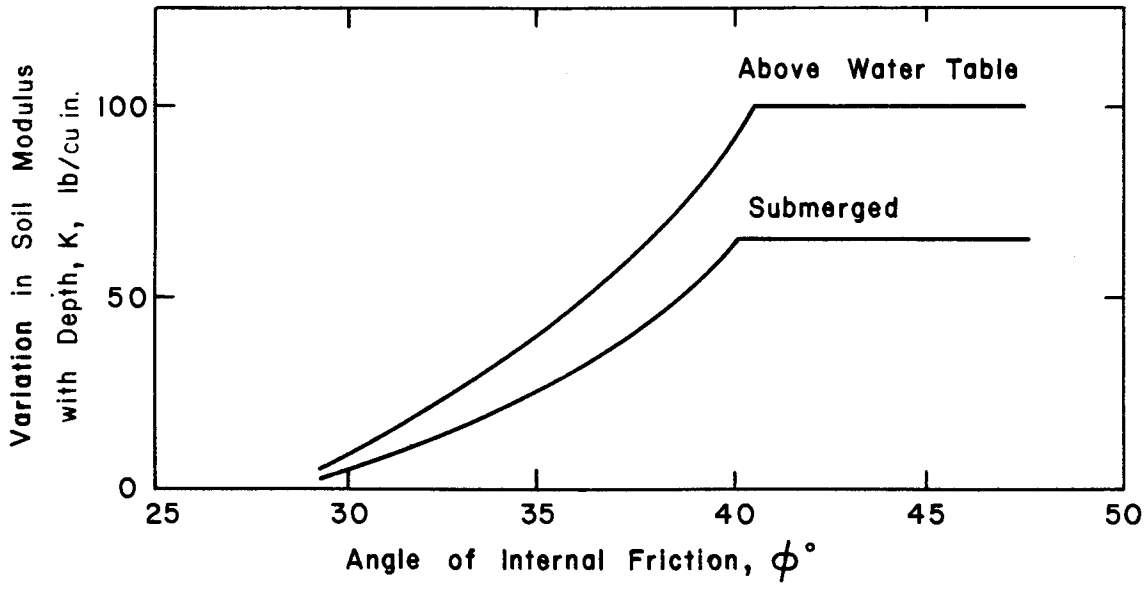

Fig. 9.21. Relationship between k and ϕ for cohesionless soil.

Using the appropriate figure to determine either α or k, the Broms deflections were computed according to the methods outlined in Chapter 7.

Values of elastic modulus, E_s, for cohesive soil for the Poulos computations were taken as equal to 40 times the undrained shear strength. Values of elastic modulus for cohesionless soils were originally presented by Poulos as functions of relative density; however, as previously done for Terzaghi's relationship, values of E_s were related to ϕ as shown in Fig. 9.22.

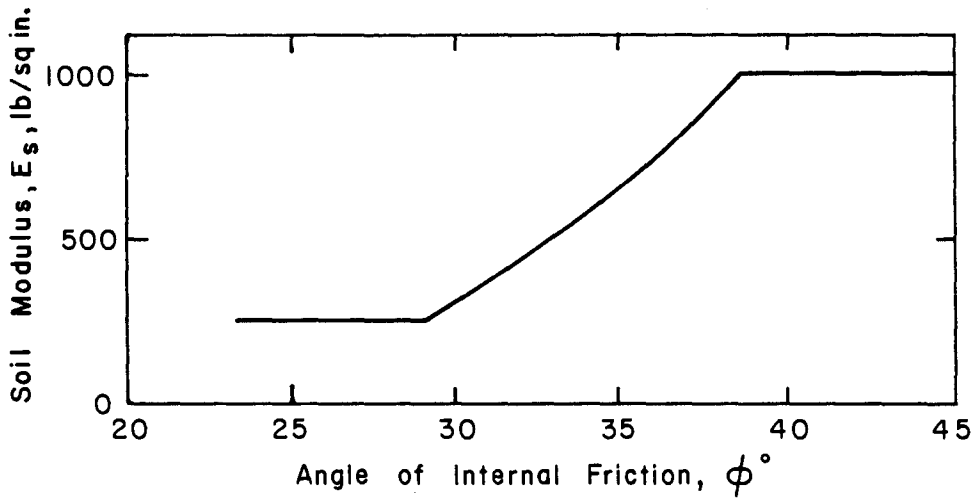

Fig. 9.22. Relationship between E_s and angle of internal friction for cohesionless soil.

9.4 CASE STUDIES OF PILES IN CLAY

Japanese Test

The results of short-term tests of free-head pipe piles under lateral load were reported by the Japanese Committee of Research for Piles Subjected to Earthquake (1965). The results of Test Pile 3 will be discussed. The test pile, shown in Fig. 9.23, was installed by jacking the closed-ended pile into place.

The soil at the site was a soft, medium to highly plastic, silty clay with a high sensitivity. The undrained shear strength for the deposit, shown in 9.23, was obtained from undrained triaxial tests. The strains at failure were generally less than 5 percent, and the specimens failed by brittle fracturing. The ε_{50} values were obtained from the reported stress-strain curves.

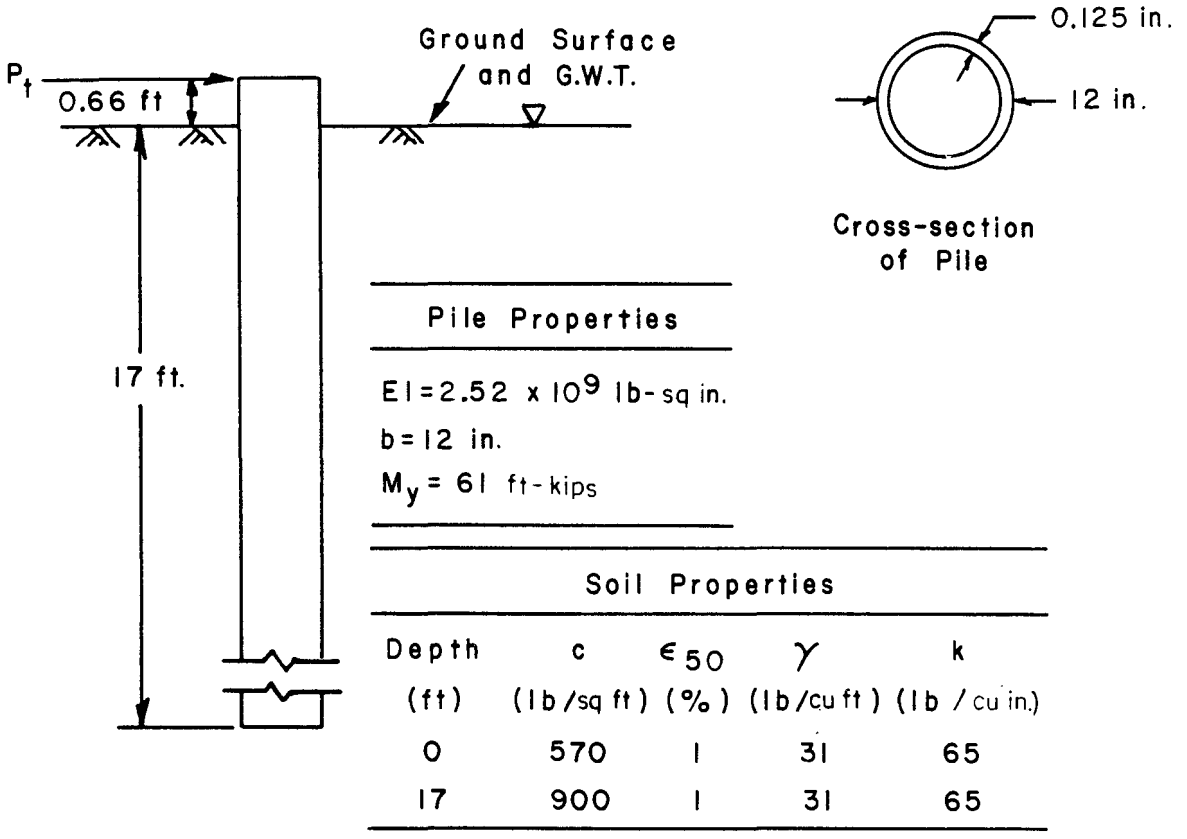

Fig. 9.23. Information for the analysis of Japanese test.

A comparison of the measured and computed results is presented in Fig. 9.24. The figure shows that the ultimate lateral load computed by the Broms method is higher than that from the computer. The load versus deflection curves from the Broms and Poulos methods are quite conservative; the computer gave a load-deflection curve that was in reasonably good agreement with the experiment. Reasonably good agreement was also obtained between computed and measured maximum moment.

St. Gabriel

A load test was performed on a free-head, 10 in., concrete-filled, pipe pile near St. Gabriel, Louisiana (Capazzoli, 1968). The loading was short-term. The test piles were driven vertically to a depth of 115 ft. The test setup and pile properties are shown in Fig. 9.25.

The soil at the site was a soft to medium, intact, silty clay. The natural moisture content of the clay varied from 35 to 46 percent in the upper 10 ft of soil. The undrained shear strengths, shown in Fig. 9.25, were obtained from triaxial tests.

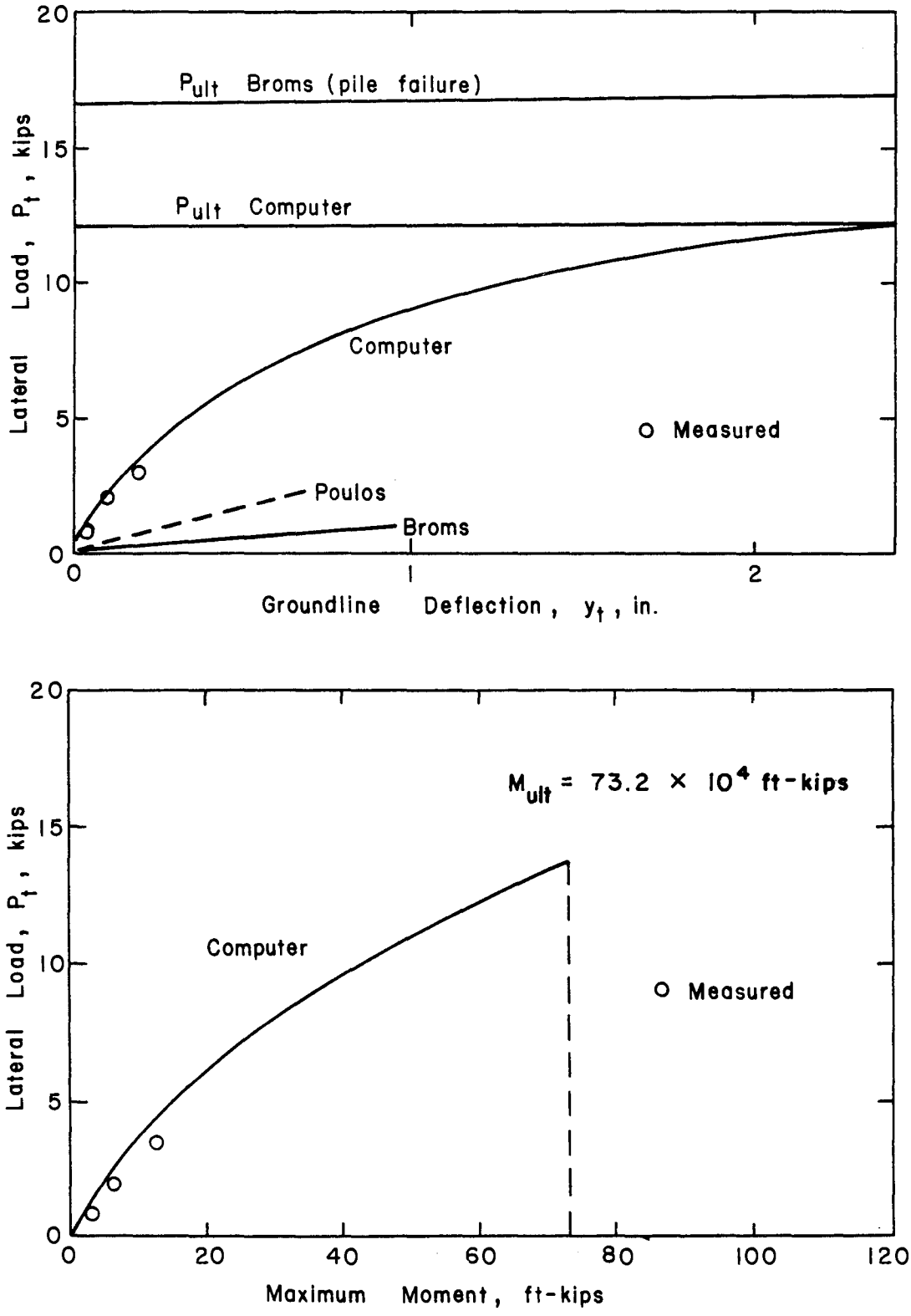

Fig. 9.24. Comparison of measured and computed results for Japanese test.

A comparison of the measured and computed results is shown in Fig. 9.26. The ultimate lateral load computed by the Broms method is higher than that from the computer. The initial slope of the load-versus-deflection curve from the computer agrees well with the experiment. The deflection curve from the computer is somewhat conservative at the higher loads. The Poulos and Broms deflection curves are slightly conservative to very conservative, respectively.

Southern California

Bhushan, et al. (1978) reported the results of lateral load tests performed on drilled shafts for a transmission line. Cyclic loading was not used. The results of three tests performed at two sites will be discussed. The three piles were straight-sided and reinforced with 3 percent steel. The lateral loads were applied incrementally, and each increment was held constant for at least 40 minutes.

At both sites, the soils were silty and sandy clays of low to medium plasticity. The liquid limit was between 30 and 58 and the plasticity index was between 15 and 20. The natural water content was at or below the plastic limit, indicating that the soil was heavily overconsolidated.

The values of undrained shear strength and ε_{50} were obtained from undrained triaxial tests of intact samples. The authors reported a great deal of scatter in the results of the tests used to define the undrained strength, c. The large amount of scatter in c is common for desiccated, heavily overconsolidated soils. In the following analyses, the average c and ε_{50} values reported by the authors for each test site were used.

The data used in the analysis of Test Pile 2 are shown in Fig. 9.27. A comparison of the measured and computed results is shown in Fig. 9.28. As seen in the figure, the computed values of P_{ult} from the Broms method and from the computer are in reasonable agreement but are perhaps less than the value that would have been obtained by experiment had the pile been loaded to collapse. Because the pile was short, computations were performed by computer for the 15-ft length and for an 18-ft length. The 18-ft length resulted in a higher load but the load-deflection curves for smaller loads were identical.

The deflection curve for Test Pile 2 from the computer is in good agreement with the experiment at lighter loads but is conservative at larger loads. The deflection curves from the Broms and Poulos methods are conservative.

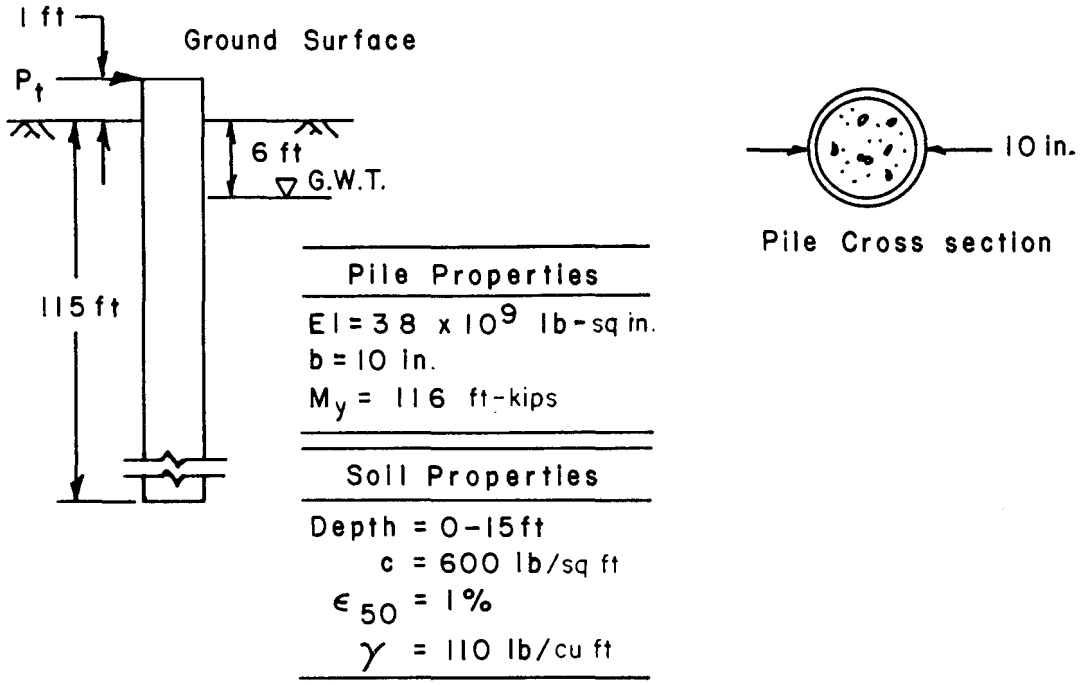

Fig. 9.25. Information for analysis of test at St. Gabriel.

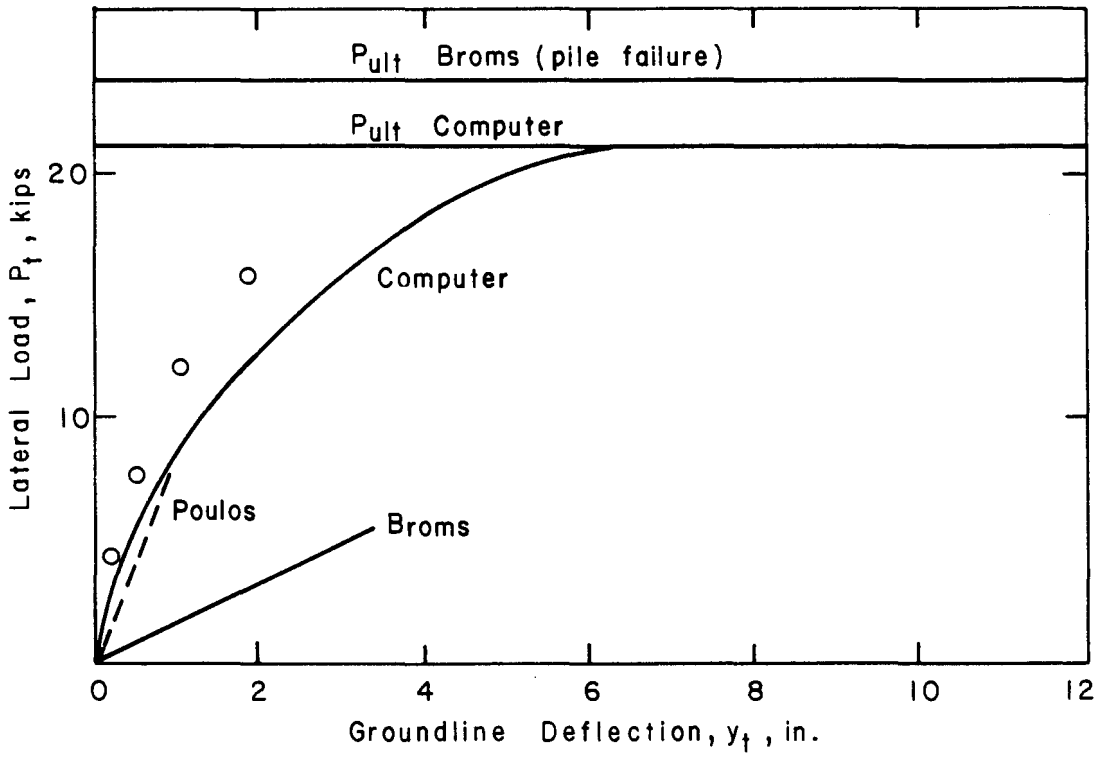

Fig. 9.26. Comparison of measured and computed results for St. Gabriel Test.

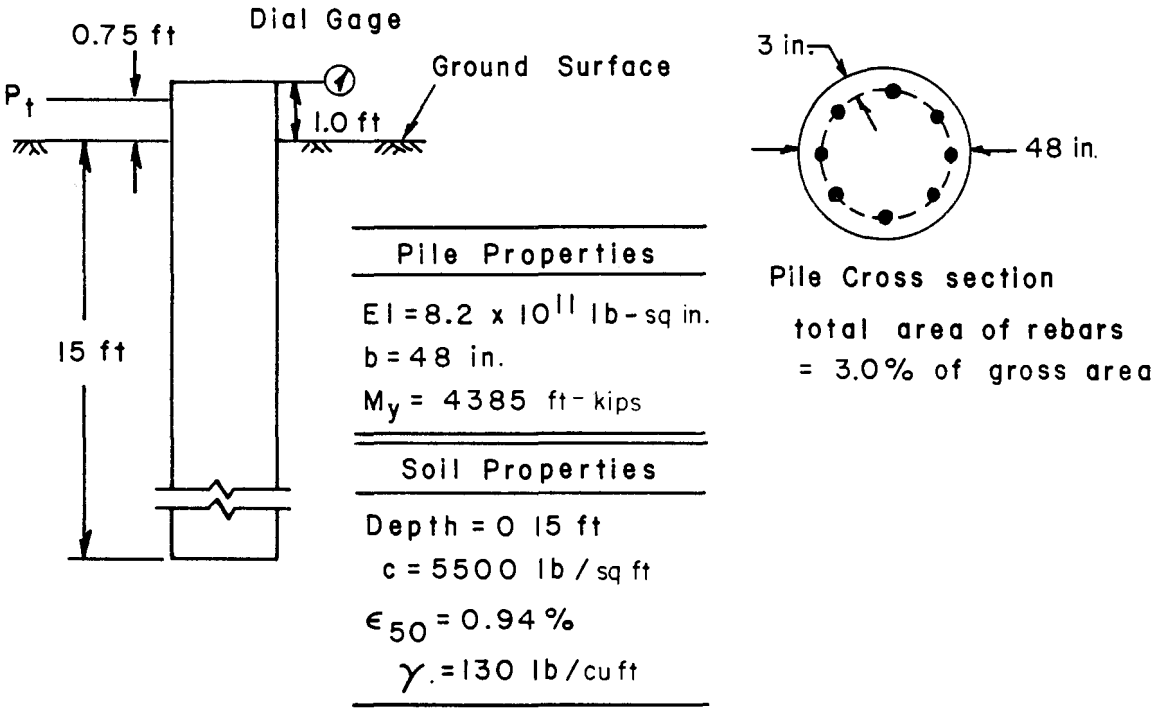

Fig. 9.27. Information for the analysis of Southern California Test Pile 2.

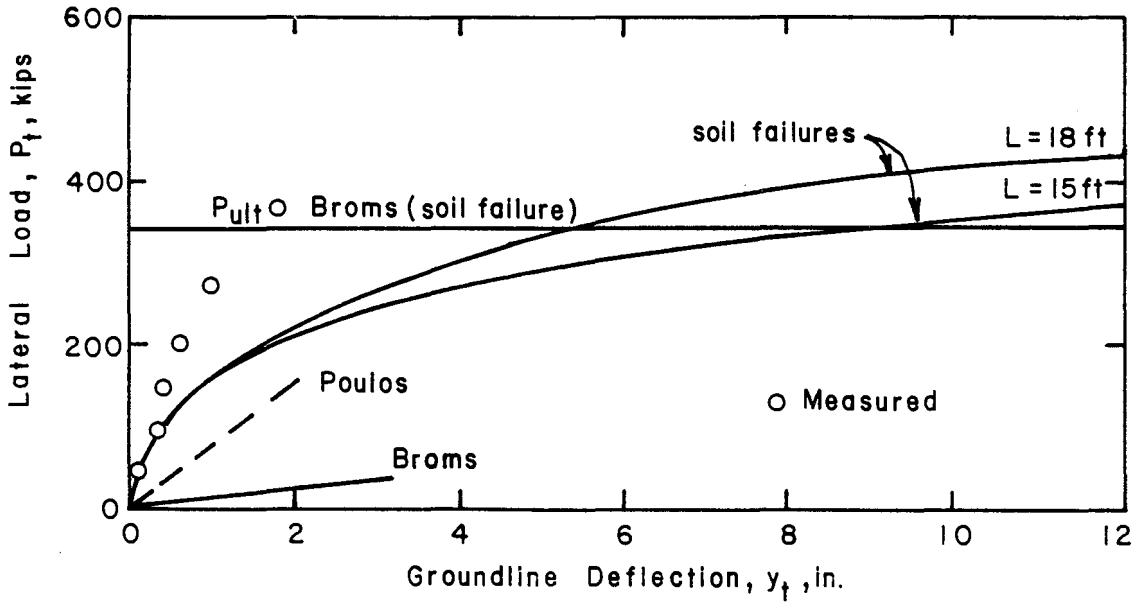

Fig. 9.28. Comparison of measured and computed results for Southern California Test Pile 2.

The data used in the analyses of Test Piles 6 and 8 are shown in Fig. 9.29. As noted, Test Pile 6 was 48 in. in diameter and Test Pile 8 was 24 in. in diameter. A comparison of the measured and computed results for Test Pile 6 is shown in Fig. 9.30. A soil failure was computed by the Broms method and by the computer. The values from both methods of analysis, even when the pile was increased in length to 20 ft in the computer analysis, are conservative.

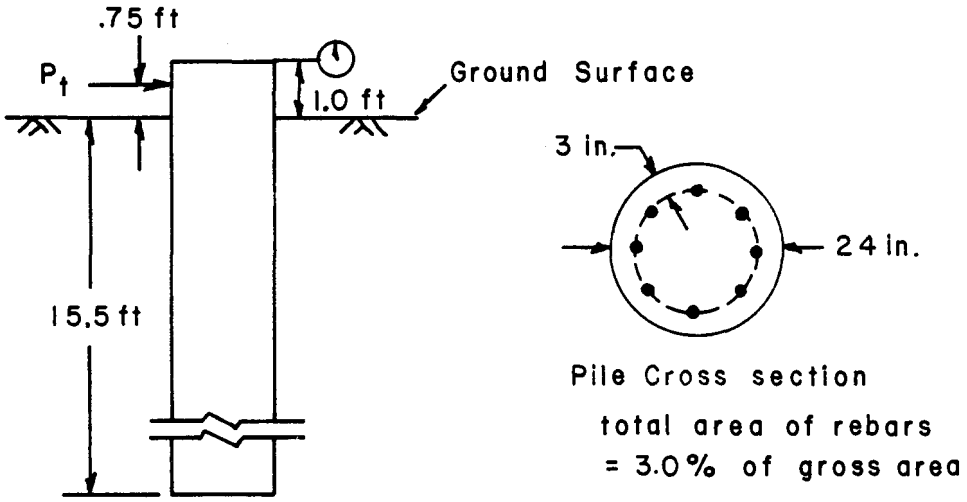

Pile Properties			
Test Pile Number	EI (lb-sq in)	b (in.)	M_y (ft-kips)
6	82×10^{11}	48	4385
8	52×10^{10}	24	503

Soil Properties
Depth = 0 - 16 ft
c = 4750 lb/sq ft
$\epsilon_{50} = 0.72\%$
γ = 130 lb/cu ft

Fig. 9.29. Information for the analysis of Southern California Test Pile 6.

The deflection curve for Test Pile 6 from the computer is in good agreement with the experiment at lighter loads but is conservative at larger loads. The deflection curves from Broms and Poulos are conservative.

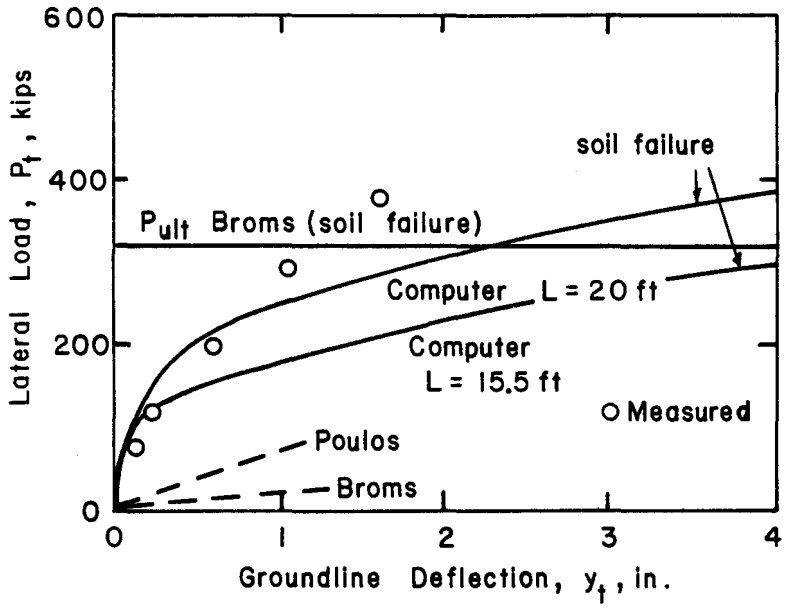

Fig. 9.30. Comparison of measured and computed results for Southern California Test Pile 6.

A comparison of the measured and computed results for Test Pile 8 is shown in Fig. 9.31. Comparatively, the results for this test are similar to those of the other two in this series. A pile failure was computed, in contrast with soil failures for the other two tests, but again the computed results are generally conservative with respect to the experiment.

It is of interest to note that if a factor of safety had been used to reduce the computed P_{ult} to obtain a service load, there would be good to excellent agreement between computed and measured deflections.

Lake Austin

The test program consisted of both short-term and cyclic tests of a free-head pile (Matlock, 1970). Water was kept above the ground surface for the entire test program. The pile was 12.75 in. in diameter, had a penetration of 42 ft, and was instrumented to measure moment along its length. The load was applied at a few inches above the mudline. The bending stiffness EI of the pile was 10.9×10^9 lb-sq in.

The clay at the site was slightly overconsolidated by desiccation and was slightly fissured. The shear strength was measured with a vane and averaged 800 lb/sq ft. The ε_{50} was 0.012 and the submerged unit weight was 50 lb/cu ft.

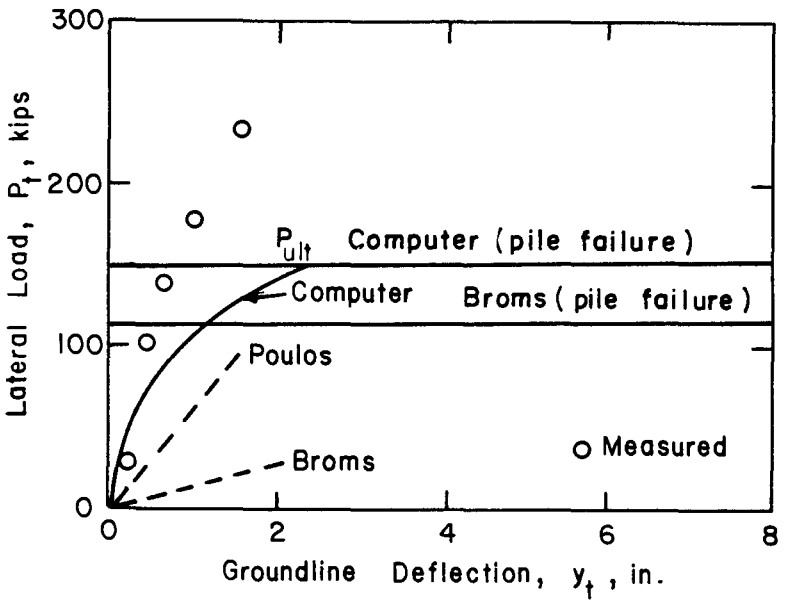

Fig. 9.31. Comparison of measured and computed results for Southern California Test Pile 8.

Figure 9.32 shows a comparison of measured and computed deflections. The results from cyclic loading are shown in Fig. 9.32a and from static loading in Fig. 9.32b. Also shown by a note in Fig. 9.32b are the computed ultimate loads by the Broms and computer methods. It can be seen that the experimental loading was stopped well below the ultimate capacity of the piles. The instrumented piles were employed at another site.

There is reasonable agreement between the deflection curves from the experiment and from the computer at the lower loads, but a considerable deviation at the higher loads. The Poulos curve fell close to the experimental curve for static loading but the Broms curve was conservative.

A comparison of the measured and computed maximum moments for the Lake Austin pile are shown in Fig. 9.33. The comparison for static loading is good but the computer under-predicts the maximum moments for cyclic loading.

Sabine

The piles used in the Lake Austin tests were pulled and re-driven at Sabine (Matlock, 1970). Static and cyclic loads were applied with the pile head free to rotate and with the pile head restrained against rotation. The restrained-head tests are not discussed herein. The point of application of the load was 12 in. above the mudline. Water was kept above the mudline throughout the testing program.

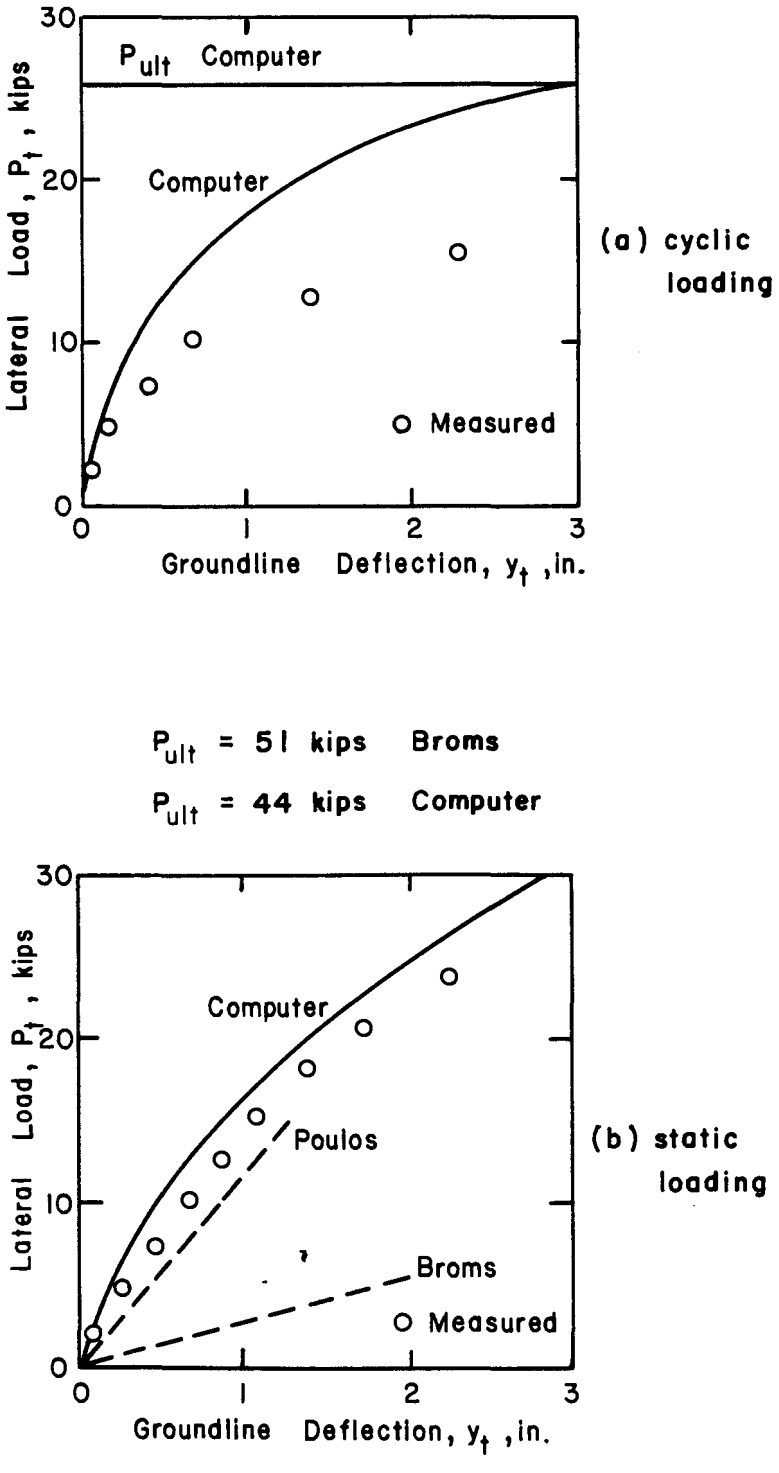

Fig. 9.32. Comparison of measured and computed deflections for Lake Austin Test.

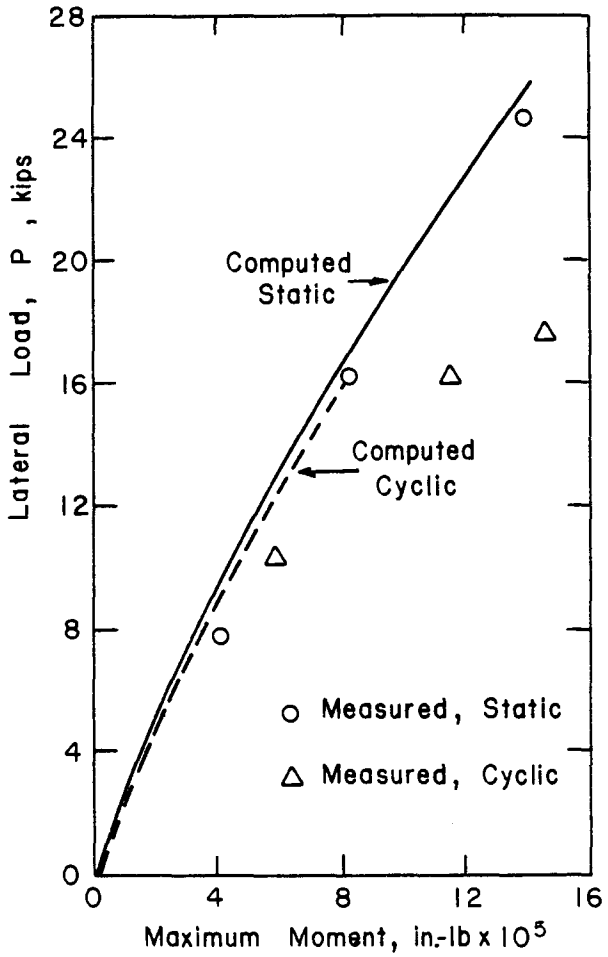

Fig. 9.33. Comparison of measured and computed maximum moments for Lake Austin Test.

The clay at the site was a slightly overconsolidated marine deposit. The undrained shear strength was about 300 lb/sq ft and the submerged unit weight was 35 lb/cu ft. The strain ε_{50} at one-half the compressive strength was 0.007.

A comparison of measured and computed deflections is shown in Fig. 9.34. The results from cyclic loading are shown in Fig. 9.34a and from static loading in Fig. 9.34b. The computed ultimate loads from the Broms method and from the computer are shown in Fig. 9.34b. There is excellent agreement between the experimental and the computed deflections for static loading. The deflections for the cylic case are under-predicted by the computer. The deflection curves from the Broms and Poulos methods, shown in Fig. 9.34b, are conservative.

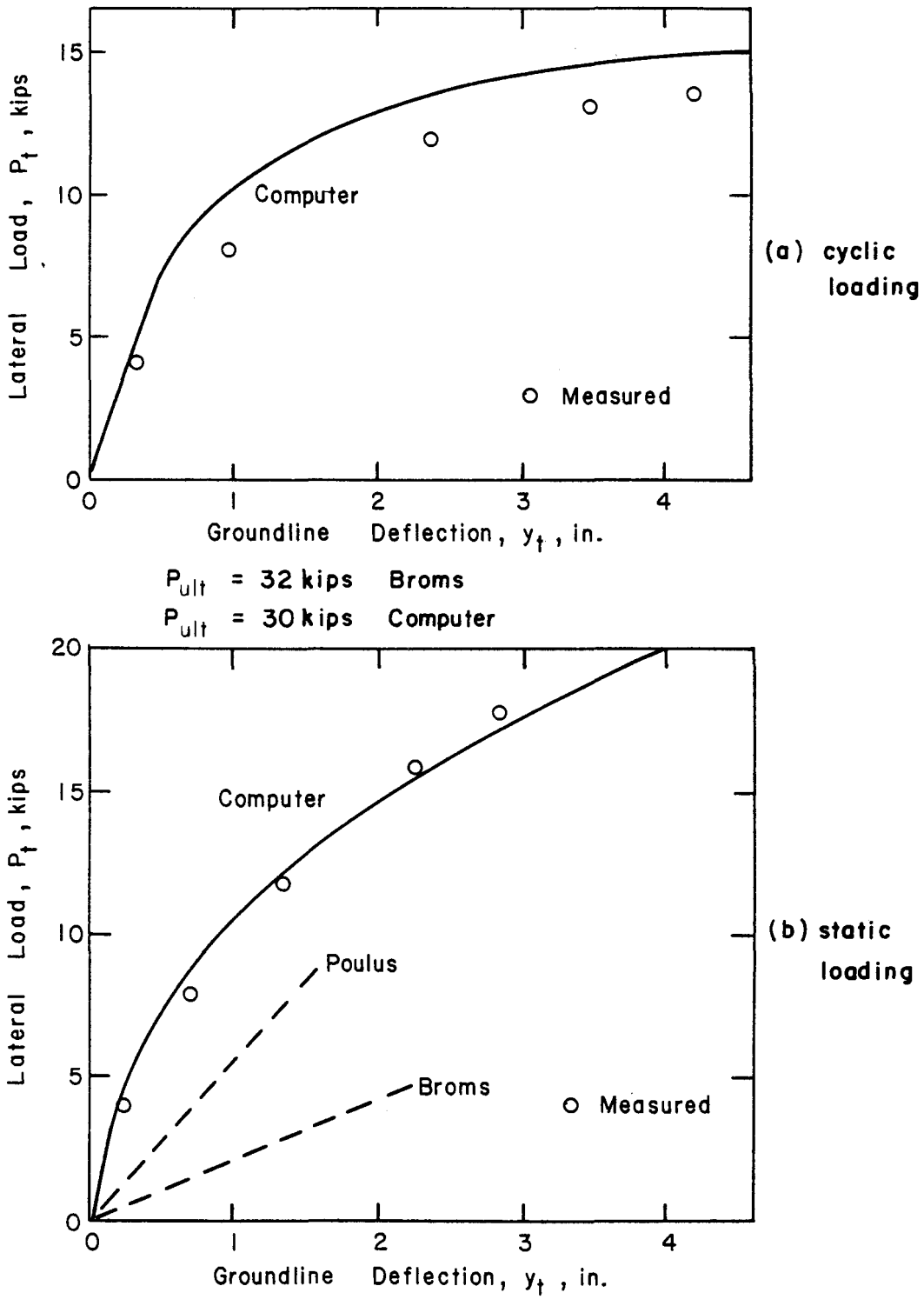

Fig. 9.34. Comparison of measured and computed deflections for Sabine Test.

Figure 9.35 shows a comparison of the measured and computed maximum moments for the Sabine tests. In both instances, the comparisons are excellent.

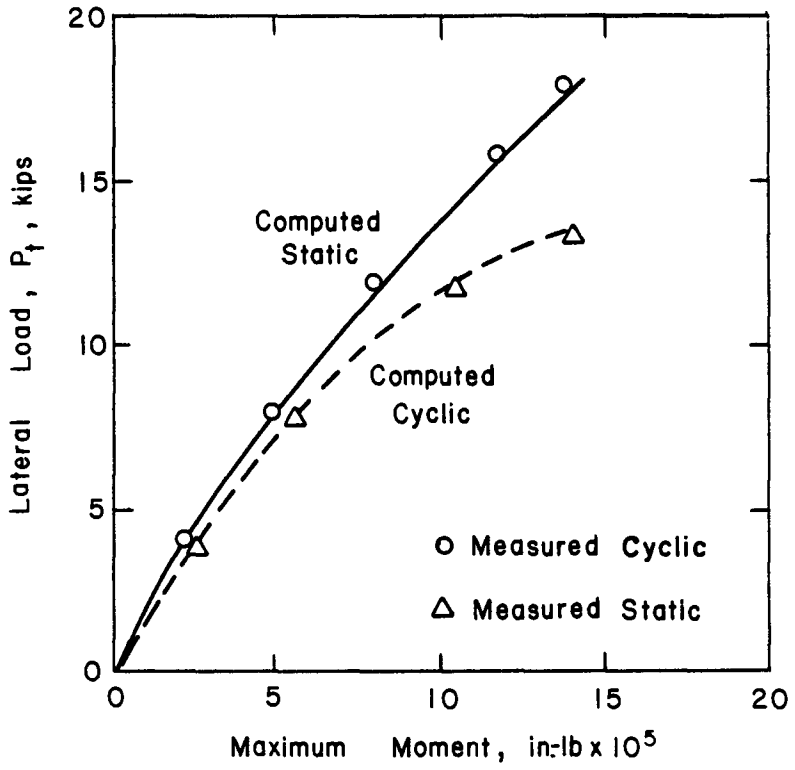

Fig. 9.35. Comparison of measured and computed maximum moments for Sabine Test.

Houston

A drilled shaft was tested at a site in Houston (Reese and Welch, 1975). The diameter of the pile was 30 in. and the penetration was 42 ft. The foundation was instrumented along its length for the measurement of bending moment. Difficulty was encountered in getting the excavation filled with concrete because of the close spacing of the reinforcing steel and there was a cavity near the top of the shaft. Field measurements indicated that the bending stiffness EI of the pile was about 1.47×10^{11} lb-sq in.

The pile head was free to rotate and a combined static-cylic loading program was employed. A given load was applied, measurements were taken, and the load was removed and re-applied a number of times. A total of 20 cycles of loading was applied at each load increment.

The soil profile consisted of 28 ft of stiff to very stiff red clay, 2 ft of interspersed silt and clay layers, and very stiff silty clay to a depth of 42 ft. The water table was at a depth of 18 ft. The undrained shear strength was determined by triaxial tests and was found to vary widely in the top 20 ft. A value of 2.2 kips/sq ft was selected for analyses. The average value of ε_{50} was 0.005, and the unit weight of the clay was 120 lb/cu ft.

A comparison of measured and computed deflections is presented in Fig. 9.36. The results from cyclic loading (10 cycles) are shown in Fig. 9.36a and from static loading in Fig. 9.36b. The computed ultimate loads from the Broms method and from the computer method are shown in Fig. 9.36b. There is good to excellent agreement between the experimental deflection curves and the results from the computer. The Broms method appears to under-estimate the ultimate load. The deflection curves from the Poulos and Broms methods are conservative.

Figure 9.37 shows the comparisons between the measured and computed maximum moments for the Houston test. The agreement is good to excellent.

Manor

Tests were performed on steel pipe piles that were 25.25 in. in diameter and with a penetration of 49 ft. The piles were instrumented along their length for the measurement of bending moment. The pile heads were unrestrained against rotation and both static and cyclic tests were performed.

An excavation about 5 ft deep was made at the site and water was ponded for several weeks prior to and during the testing. The soil was a stiff, fissured clay. The undrained shear strength was measured by triaxial tests; there was much scatter in the results but in general the shear strength increased rapidly with depth. The following depths and undrained shear strengths were used in the analyses (feet and kips/sq ft, respectively): 0, 0.4; 1.0, 1.6; 13.0, 7.0; 21.0, 7.0. The average value of ε_{50} at the site was 0.005 and the submerged unit weight of the clay was 65 lb/cu ft.

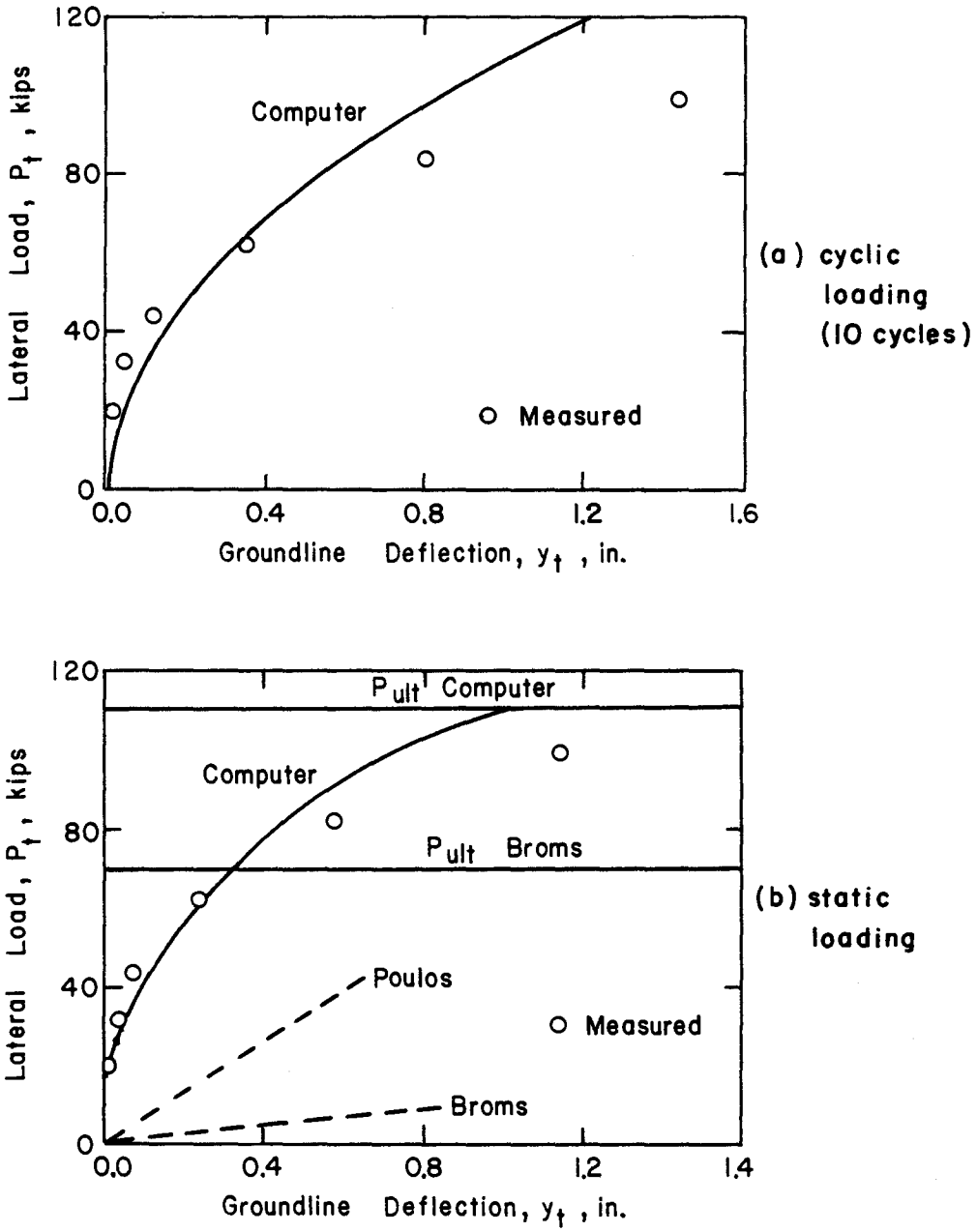

Fig. 9.36. Comparison of measured and computed deflections for Houston Test.

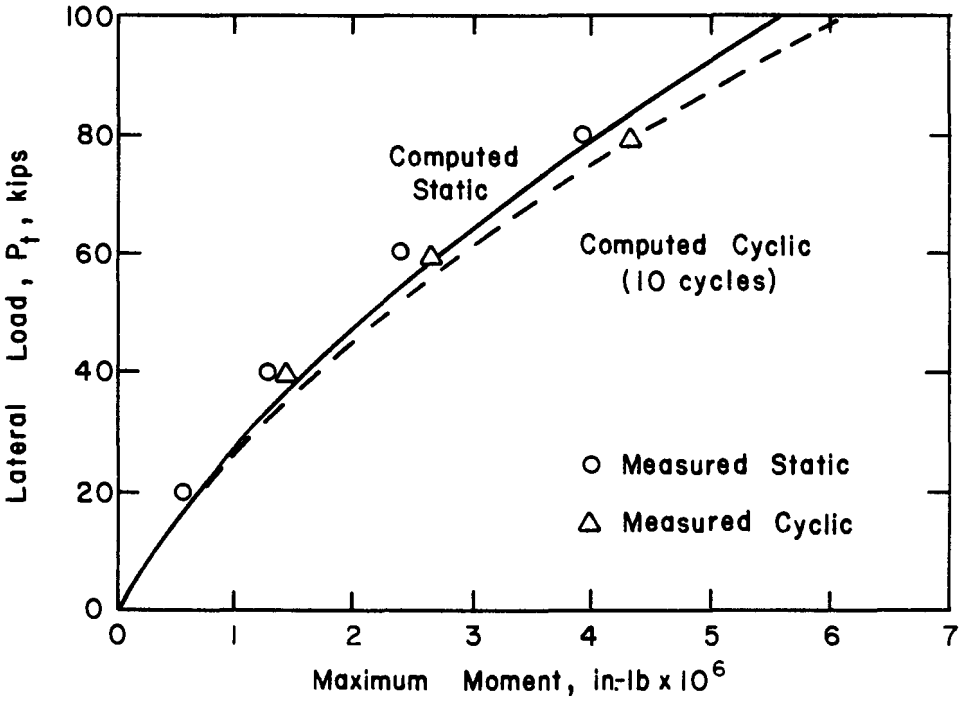

Fig. 9.37. Comparison of measured and computed maximum moments for Houston Test.

Figure 9.38 shows the comparison between the measured and computed deflections. The results from cyclic loading are shown in Fig. 9.38a and from static loading in 9.38b. The computed ultimate loads from the Broms method and from the computer method are indicated in Fig. 9.38b. There is generally good agreement between the experimental deflection curves and those from the computer. The deflection curves from the Broms and Poulos methods are conservative.

Figure 9.39 shows the comparisons between the measured and computed maximum moments for the Manor test. The agreement is good to excellent.

9.5 CASE STUDIES OF PILES IN SAND

Gill Tests

Gill (1969) reported the results of four lateral load tests performed on pipe piles. The piles were of different stiffnesses and were all embedded to a sufficient depth so that they behaved as flexible members. The pile heads were free to rotate during testing and the loads were applied statically.

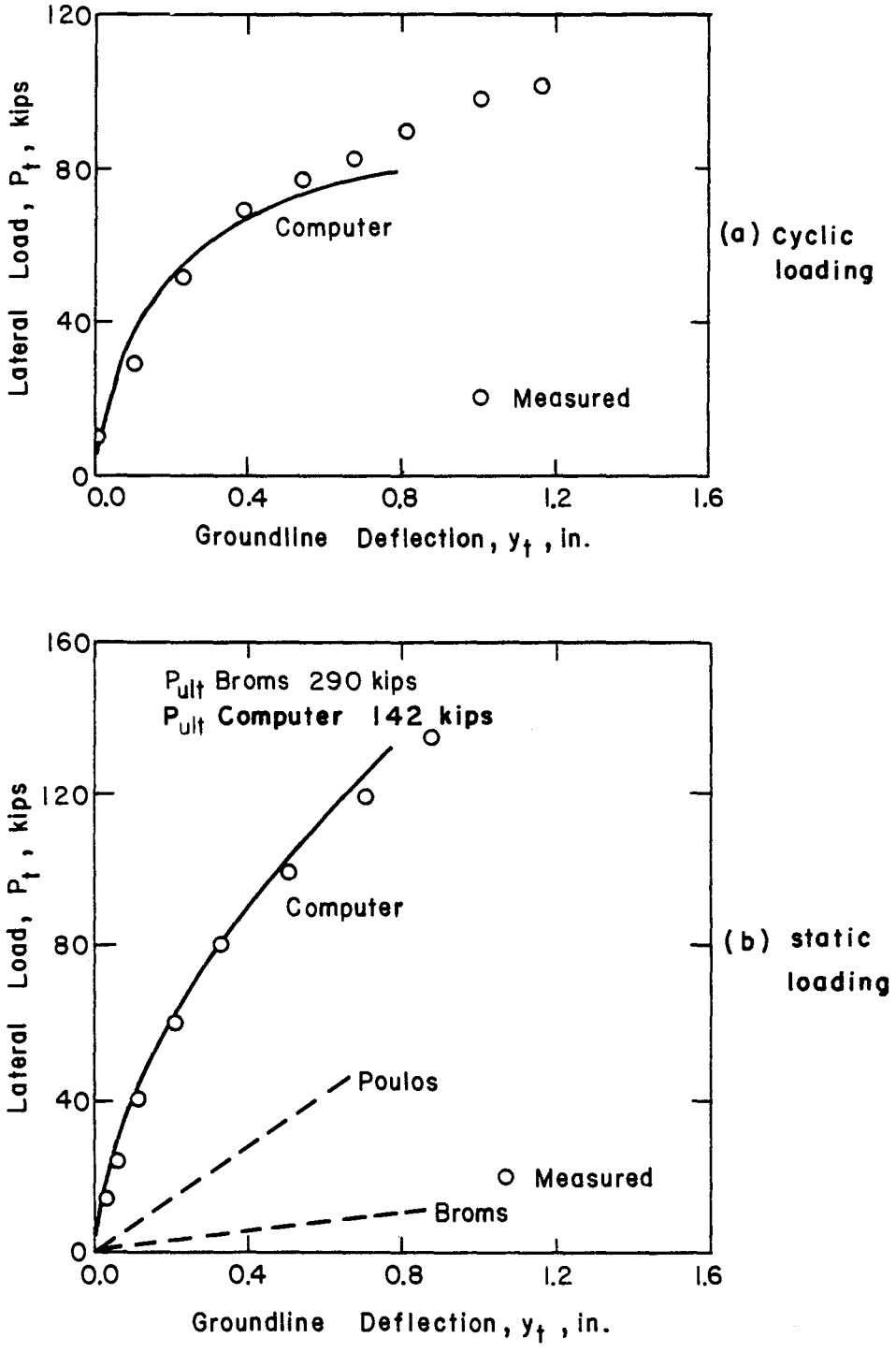

Fig. 9.38. Comparison of measured and computed deflections for Manor Test.

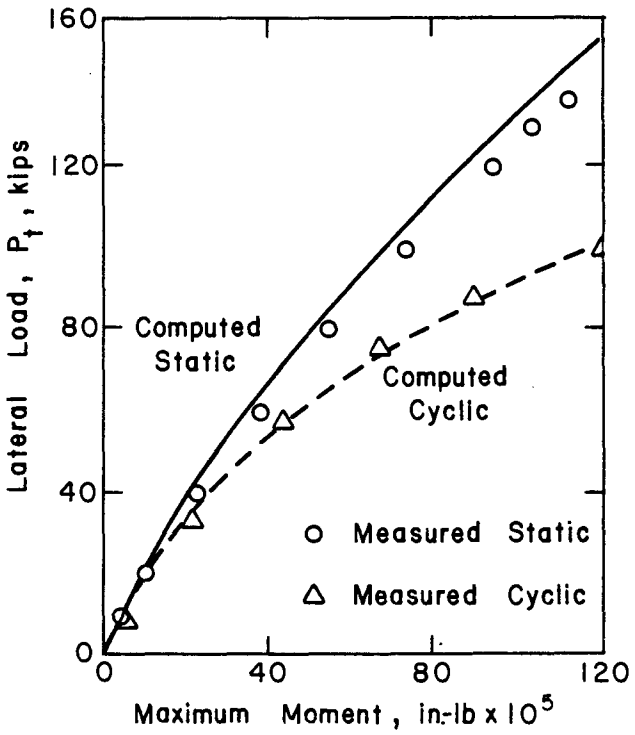

Fig. 9.39. Comparison of measured and computed moments for Manor Test.

The soil at the site was mainly an old hydraulic fill which had been placed in the 1940's (Gill, 1969). A compacted granular surface had reportedly been placed over the hydraulic fill. This compacted surface could account for the high blow count of 58 blows/ft at a depth of 2 ft, shown in Fig. 9.40. Below 2 ft, the blow count decreased rapidly until it reached 16 blows/ft at a depth of 4.5 ft. No information concerning the SPT resistance of the material was given below 4.5 ft, and it was assumed that the relative density was constant below that depth.

The data shown in Fig. 9.40 were used in the analyses and the resulting curves are shown in Figs. 9.41 through 9.44. As may be seen in the figures, the initial slopes of the curves from the computer, from Broms, and from Poulos are in good agreement and also agree reasonably well with the initial slopes of the experimental curves. The ultimate capacities obtained from the computer and from Broms are in reasonable agreement. At the larger loads the deflection curves from the computer agree well with the experiments or are somewhat conservative.

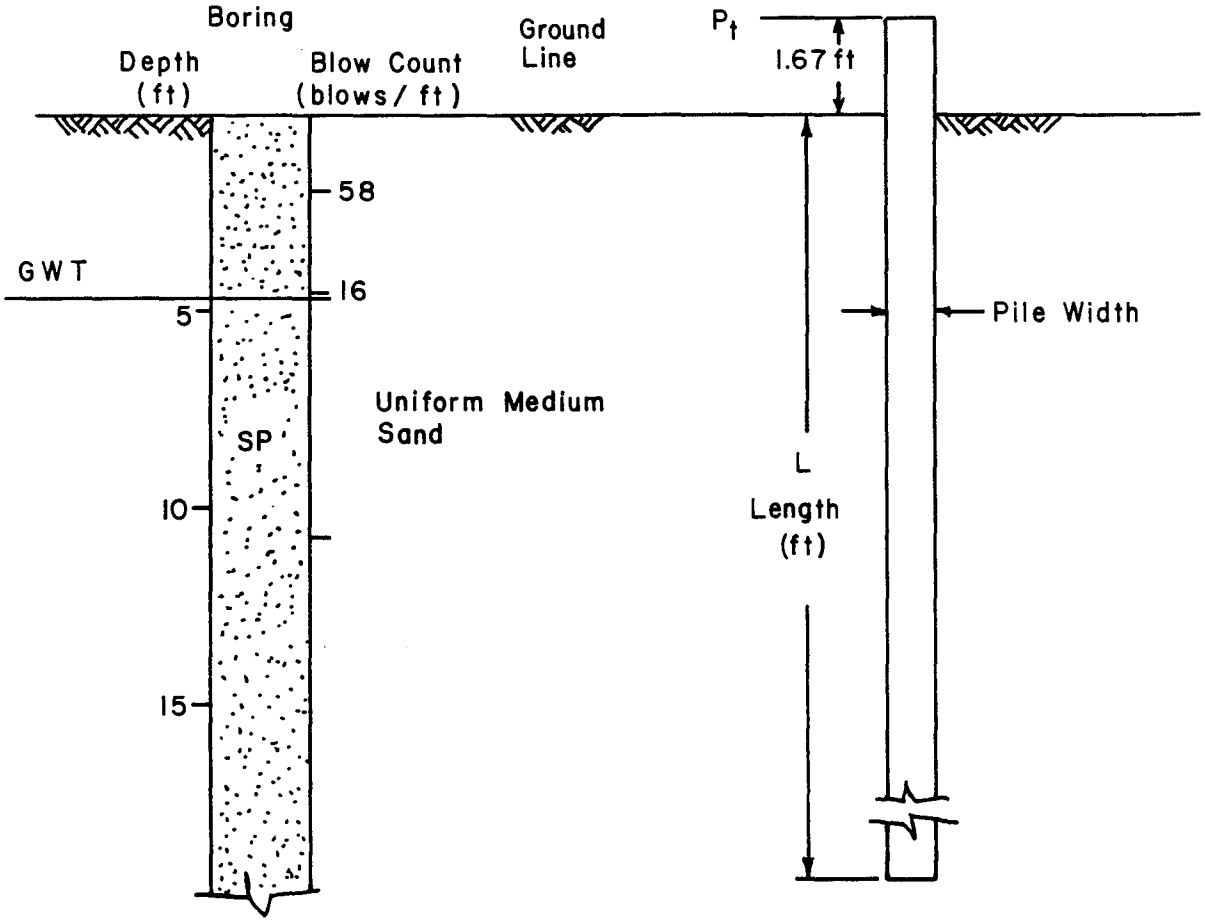

Soil Properties				
Depth	ϕ	γ (lb/cu ft)	k (lb/cu in.)	K_o
0 2	41	125	275	0.4
2 4.5	40	115	175	0.4
4.5 32	38	60	110	0.4

Pile Properties			
Test Pile Number	b (in.)	EI (lb-sq in.)	L (ft)
P9	4.75	2.17×10^8	18
P10	8.62	2.17×10^9	24
P11	12.75	7.46×10^9	30
P12	16.00	1.69×10^{10}	30

Fig. 9.40. Information for the analysis of tests in hydraulic fill.

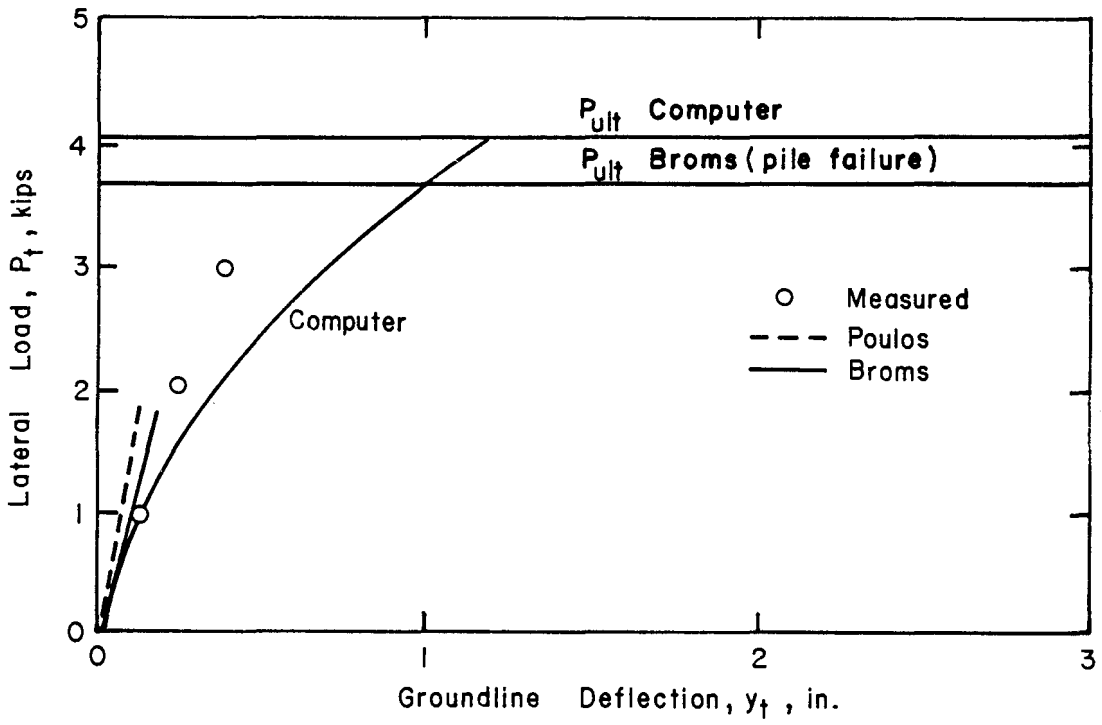

Fig. 9.41. Comparison of measured and computed results for Gill Test Pile 9.

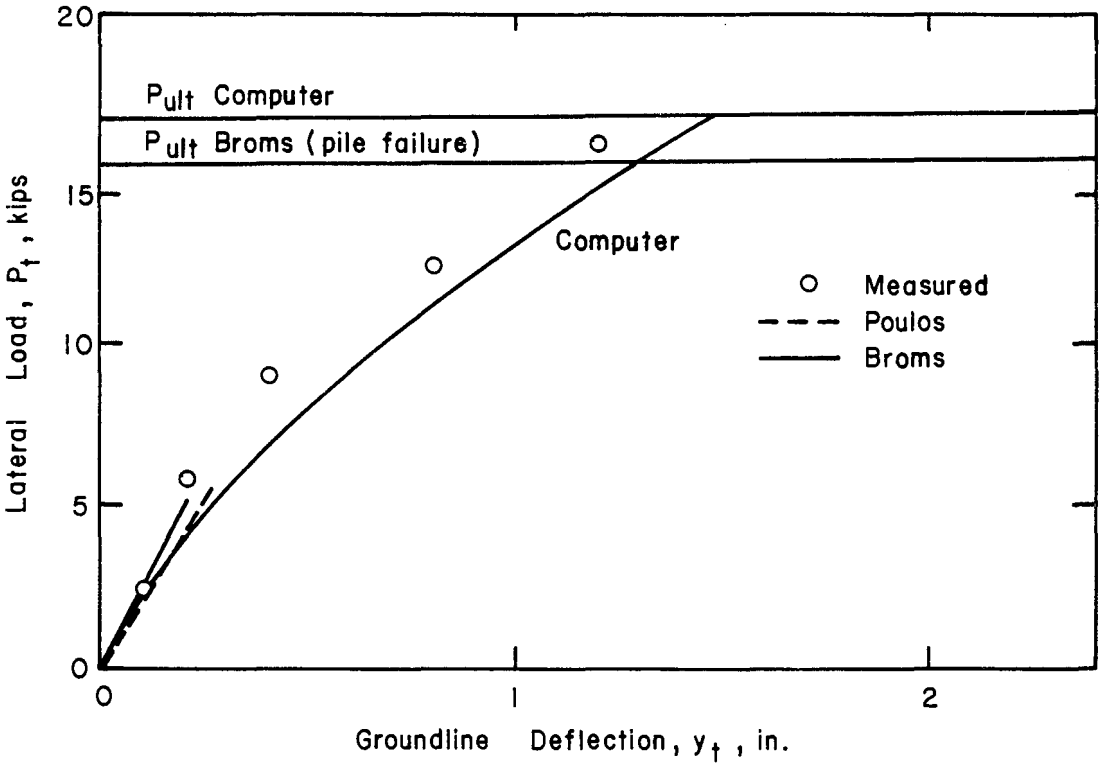

Fig. 9.42. Comparison of measured and computed results for Gill Test Pile 10.

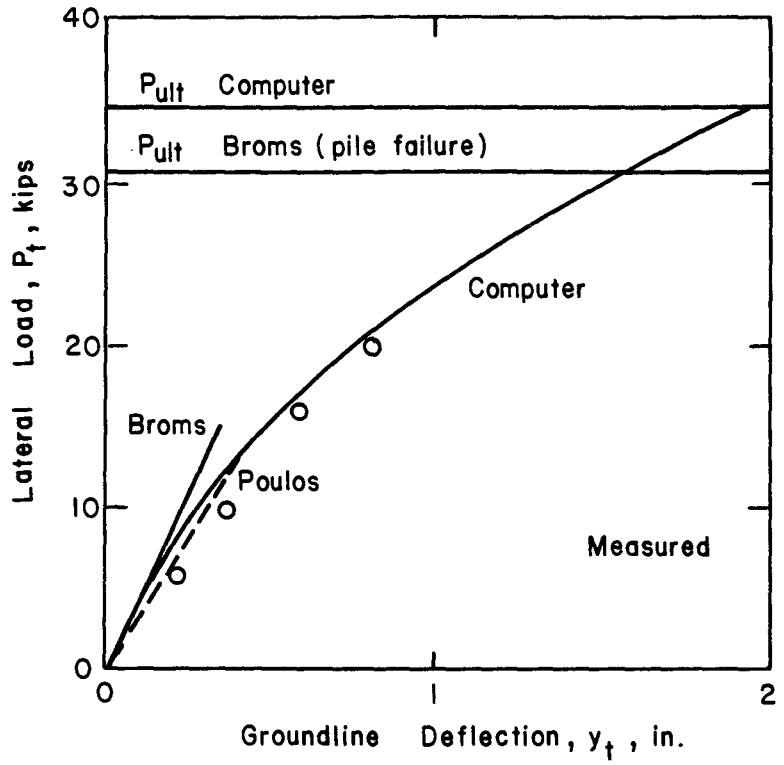

Fig. 9.43. Comparison of measured and computed results for Gill Test Pile 11.

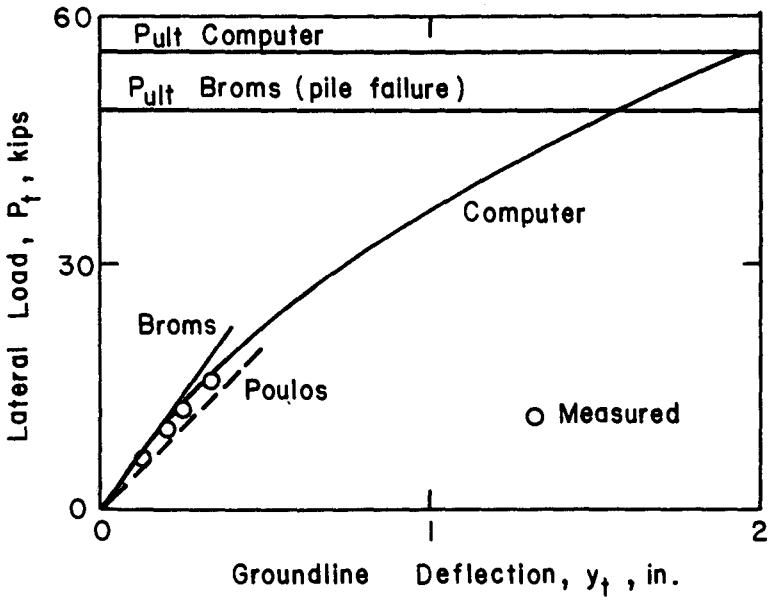

Fig. 9.44. Comparison of measured and computed results for Gill Test Pile 12.

Arkansas River

A number of lateral load tests were performed for the Corps of Engineers by Fugro and Associates at a site on the Arkansas River near Pine Bluff, Arkansas (Alizadeh and Davisson, 1970). Test Piles 2 was a pipe pile with a 16 in. outside diameter and modified by welding four steel channels (4 x 7.25) at 90 degrees apart around the exterior of the pipe. It was installed by driving. The bending stiffness of the pile was 2.44 x 10^{10} lb-sq in. and it had a penetration of 53 ft. The ultimate moment capacity M_y of the pile section was computed to be 778 ft-kips.

The pile head was free to rotate during testing and the lateral load was applied 0.1 ft above the groundline. Static loading was used in the testing program. The pile was instrumented along its length for the measurement of bending moment.

The soil conditions at the site are shown in Fig. 9.45. As may be noted, the water table was near the ground surface. The soil of primary importance with regard to lateral loading is the sand, classified as SP by the Unified method; the sand extends from the ground surface to a depth of about 22 ft.

Figure 9.46 shows the comparison between the measured and computed deflections for Test Pile 2. The computer predicts a higher P_{ult} than does Broms. The deflections from Broms and Poulos are larger than the measured deflections and the deflection curve from the computer is stiffer than either of these at lower loads. There is some indication that the sand near the ground surface was denser than assumed, which may account for some of the lack of agreement between the computer and the experiment.

The comparison between the measured and computed maximum bending moments is shown in Fig. 9.47. As may be seen, the computed results are somewhat conservative with regard to the measured values.

Test Pile 6 at the Arkansas River site was a 14BP73 steel bearing pipe that was driven into place. The pile had a bending stiffness EI of 2.15 x 10^{10} lb-sq in. and a width of 14 in. Its ultimate-moment capacity was computed to be 397 ft-kips. The penetration of the pile was 40 ft.

A comparison of the measured and computed results for Test Pile 6 is shown in Fig. 9.48. The results are similar to those for Test Pile 2 as shown in Fig. 9.46.

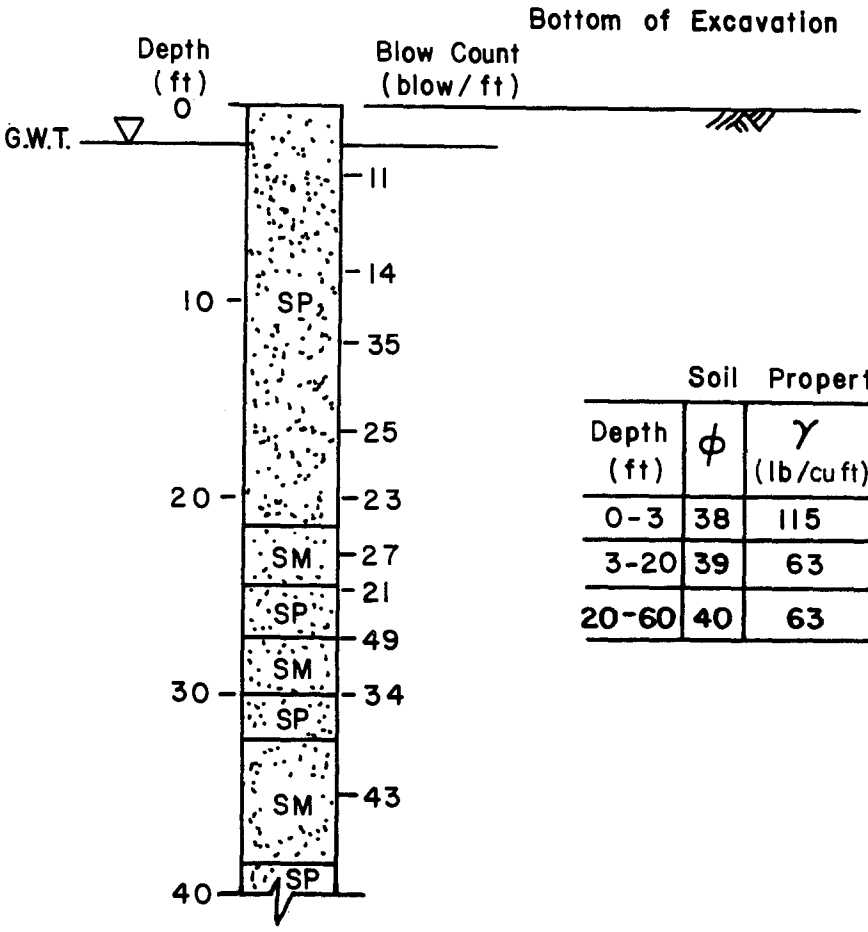

Soil Properties

Depth (ft)	ϕ	γ (lb/cu ft)	k (lb/cu in.)	K_o
0-3	38	115	160	1.0
3-20	39	63	90	1.0
20-60	40	63	90	1.0

Fig. 9.45. Soils information for analysis of tests at Arkansas River.

Florida

A load test was performed by the Florida Power and Light Company (Davis, 1977) on a 56-in. O.D. steel tube that was vibrated to a depth of 26 ft. The interior of the tube was filled with concrete and a utility pole was embedded in the upper part of the tube so that the load could be applied at 51 ft above the groundline. The bending stiffness of the pile was computed to be 1.77×10^{12} lb-sq in. in the top 4 ft and 8.8×10^{11} lb-sq in. below that. The ultimate-moment capacity of the pile was computed to be 4,630 ft-kips. The loads were applied statically.

The soil profile consisted of 13 ft of medium dense sand overlying stiff to very stiff sandy, silty clay. The water table was at a depth of 2 ft. The angle of internal friction of the sand was estimated at 38° and

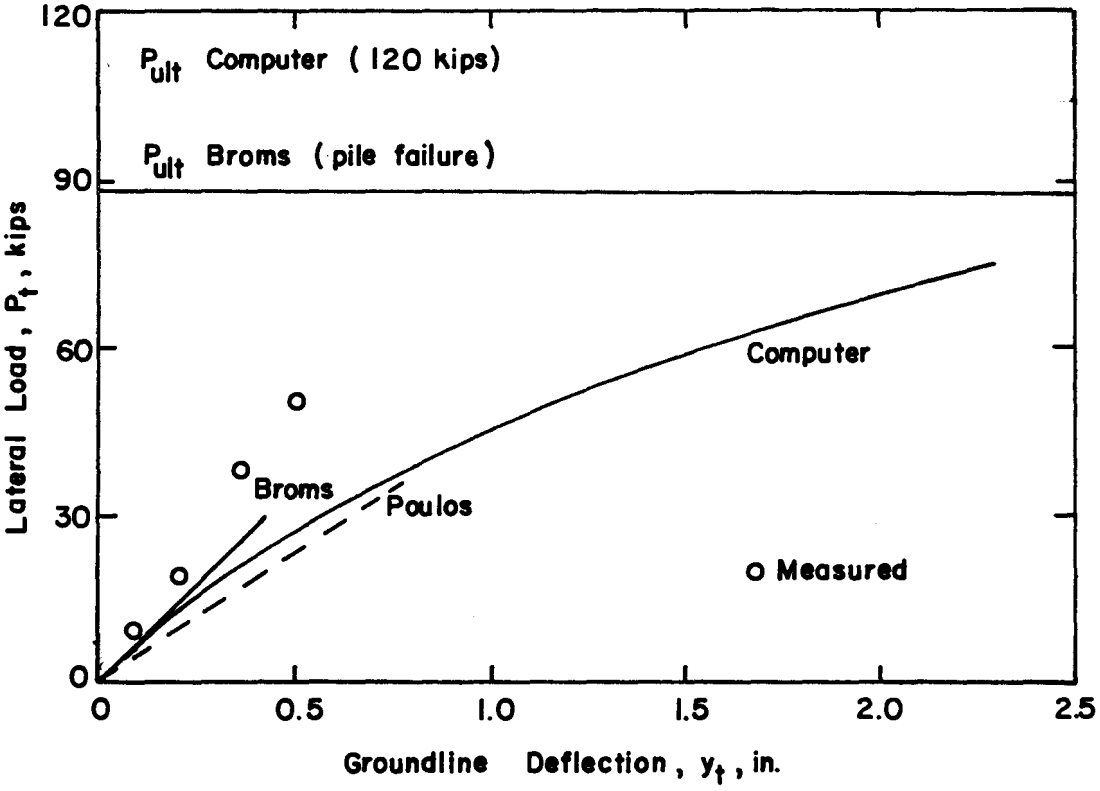

Fig. 9.46. Comparison of measured and computed deflections for Arkansas River Test Pile 2.

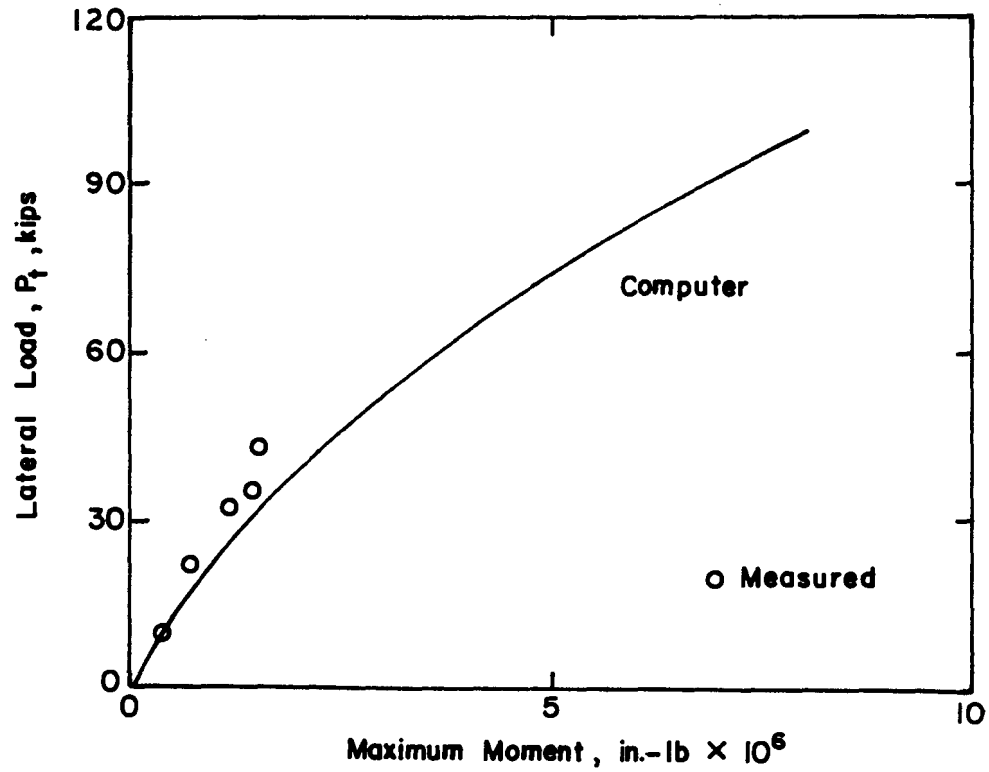

Fig. 9.47. Comparison of measured and computed maximum moments for Arkansas River Test Pile 2.

the undrained shear strength of the clay was estimated at 2.5 kips/sq ft. The total unit weight of the soil was 115 lb/cu ft and the submerged unit weight was 60 lb/cu ft.

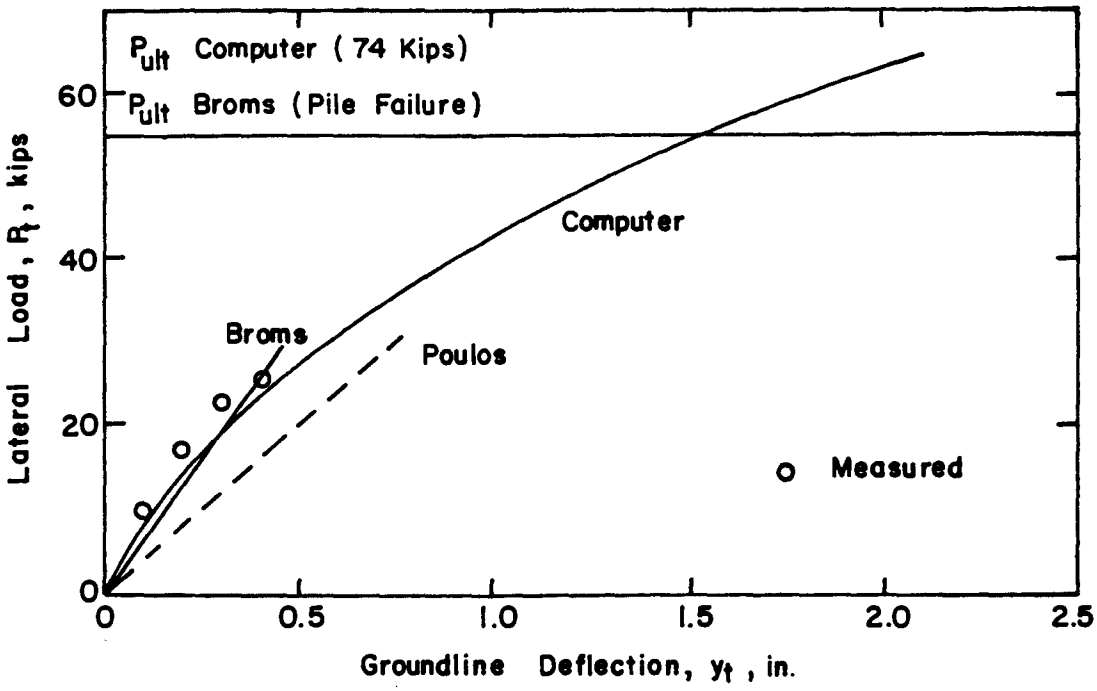

Fig. 9.48. Comparison of measured and computed results for Arkansas River Test Pile 6.

Figure 9.49 gives the comparison between the measured and computed results. The agreement between measured deflections and those from computer are in excellent agreement. The deflection curves from Broms and Poulos are conservative. The same value of of ultimate load (84 kips) was obtained from the Broms method and from the computer.

Mustang Island

Tests were performed at Mustang Island near Corpus Christi, Texas, on two 24-in. O.D. pipe piles that were instrumented along their lengths for the measurement of bending moment (Reese, et al., 1974). One of the piles was subjected to static loads and the other to cyclic loads. The pile heads were free to rotate and the loads were applied one foot above the groundline. The penetration of the piles was 69 ft.

The soil at the site consisted of clean fine sand to silty fine sand. An excavation was made at the site to a depth of about 5 ft and the natural water table was above the testing surface. A program of in situ tests and laboratory soil tests was conducted at the site. The angle of internal friction was found to be 39° and the submerged unit was 66 lb/cu ft.

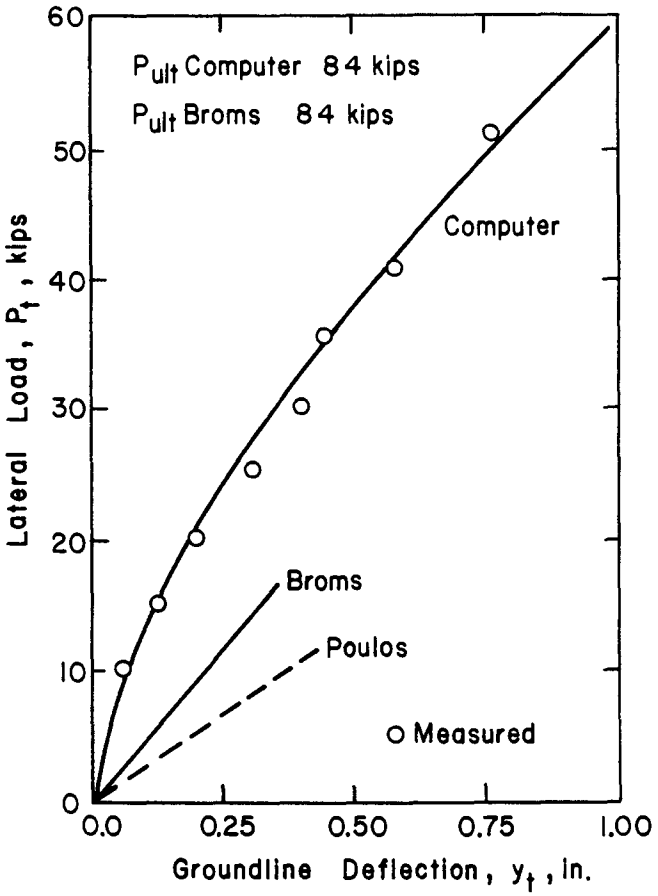

Fig. 9.49. Comparison of measured and computed results for Florida Test.

Figure 9.50 shows the comparison betweeen the measured and computed deflections. The results from cyclic loading are shown in Fig. 9.50a and from static loading in 9.50b. The computed ultimate loads from the Broms method and from the computer method are indicated in Fig. 9.50b. There is excellent agreement between the experimental deflection curves and the ones from the computer. The deflection curves from the Broms and Poulos methods are slightly conservative.

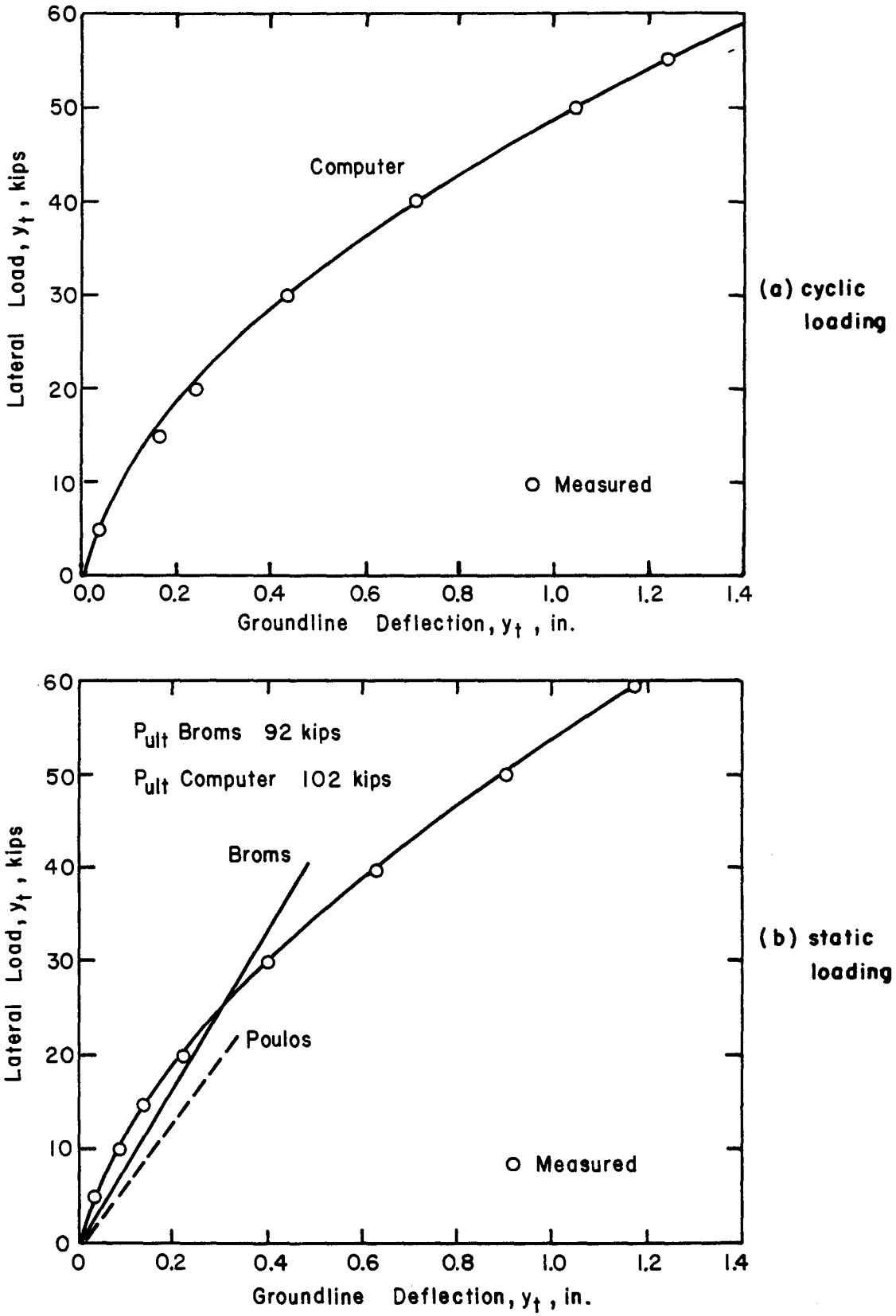

Fig. 9.50. Comparison of measured and computed deflections for Mustang Island Test.

Figure 9.51 shows the comparisons between the measured and computed maximum moments for the Mustang Island Test. The agreement is excellent.

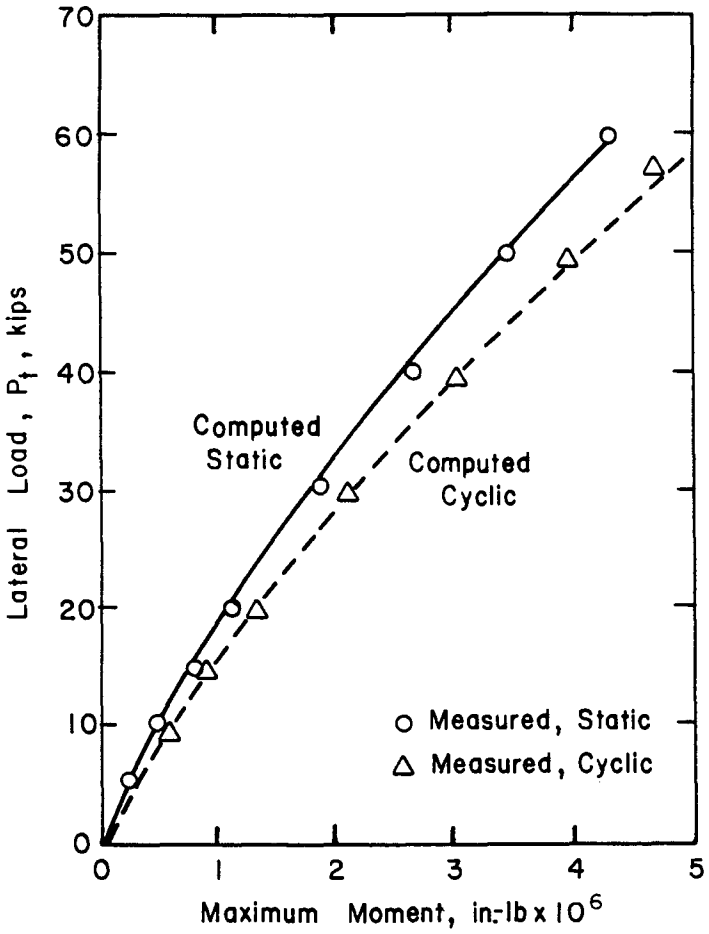

Fig. 9.51. Comparison of measured and computed maximum moments for Mustang Island Test.

9.6 COMMENTS ON RESULTS OF CASE STUDIES

The comparisons in the preceding sections show agreements between experiment and analysis that range from fair to excellent. At the present time it cannot be stated with certainty that the fair agreement is due to deficiencies in the analytical methods or to poor data from the experiments. It can be stated, however, that an excellent soil investigation is mandatory when design of piles under lateral loading is to be done. As noted earlier, the soils near the ground surface need careful attention. The construction method also needs careful control.

The computer method appears to be more versatile. Even in those cases where agreement between the results from the computer and those from experiment, the use of a factor of safety in the range of those normally used for foundation design would lead to an acceptable solution.

The reader can examine the cases that are presented and reach a decision about the factor of safety that should be employed in any particular design. On important jobs, of course, the design should be confirmed with a full-scale field load test. The test should be performed in such a way that the experimental results can be analyzed with the computer. That is, the careful measurement of load, pile-head deflection, and pile-head rotation will allow the soil response to be ascertained (Reese and Cox, 1968). The soil response so obtained can then be used in the design for different pile-head conditions or for piles of different sizes, with appropriate adjustment.

9.7 REFERENCES

Alizadeh, M., and Davisson, M. T., "Lateral Load Tests on Piles - Arkansas River Project," Journal of the Soil Mechanics and Foundation Division, American Society of Civil Engineers, Vol. 96, SM5, September 1970, pp. 1583-1604.

Bhushan, K., Haley, S. C., and Fong, P. T., "Lateral Load Tests on Drilled Piers in Stiff Clays," Preprint 3248, American Society of Civil Engineering Spring Convention and Exhibit, April 1978, 28 pp.

Capozzoli, L., "Test Pile Program at St. Gabriel, Louisiana," Louis J. Capozzoli and Associates, July 1968.

Committee of Piles Subjected to Earthquake, Architectural Institute of Japan, "Lateral Bearing Capacity and Dynamic Behavior of Pile Foundation (Loading Test of Single and Grouped Piles)," May 1965, pp. 1-69 (in Japanese).

Davis, L. H., "Tubular Steel Foundation," Test Report RD-1517, Florida Power and Light Company, Miami, Florida, 1977.

Gill, H. L., "Soil-Pile Interaction Under Lateral Loading," Conference on In-Situ Testing of Soils and Rocks, London, England, 1969, pp. 141-147.

Matlock, Hudson, "Correlations for Design of Laterally Loaded Piles in Soft Clay," Paper No. OTC 1204, Proceedings, Second Annual Offshore Technology Conference, Houston, Texas, 1970, Vol. 1, pp. 577-594.

Meyer, Barry J., "Analysis of Single Piles under Lateral Loading," Masters Thesis, University of Texas, Austin, Texas, December 1979.

Reese, Lymon C., and Cox, W. R., "Soil Behavior from Analysis of Tests of Uninstrumented Piles Under Lateral Loading," Special Technical Publication 444, American Society for Testing and Materials, Vol. 123, 1968, pp. 161-176.

Reese, Lymon C., Cox, W. R., and Koop, F. D., "Analysis of Laterally Loaded Piles in Sand," Paper No. OTC 2080, Proceedings, Sixth Annual Offshore Technology Conference, Houston, Texas, 1974, Vol. 2, pp. 473-483.

Reese, Lymon C., Cox, W. R., and Koop, F. D., "Field Testing and Analysis of Laterally Loaded Piles in Stiff Clay," Paper No. OTC 2312, Proceedings, Seventh Annual Offshore Technology Conference, Houston, Texas, 1975, Vol. 2, pp. 671-690.

Reese, Lymon C. and Welch, R. C., "Lateral Loading of Deep Foundations in Stiff Clay," Journal of the Geotechnical Engineering Division, American Society of Civil Engineers, Vol. 101, No. GT7, Proc. Paper 11456, July 1975, pp. 633-649.

Scott, Ronald F., Foundation Analysis, Prentice-Hall, Englewood Cliffs, New Jersey, 1981.

Sullivan, W. Randall, Reese, Lymon C., and Fenske, Carl W., "Unified Method for Analysis of Laterally Loaded Piles in Clay," Proceedings, Numericsl Mehtods in Offshore Piling, Institution of Civil Engineers, London, England, May 1979, pp. 107-118.

Terzaghi, Karl, "Evaluation of Coefficients of Subgrade Reaction," Geotechnique, Vol. 5, December 1955, pp. 297-326.

Terzaghi, Karl, and Peck, Ralph B., Soil Mechanics in Engineering Practice, John Wiley and Sons, Inc., New York, 1948.

9.8 EXERCISES

9.1 Do a parameter study for a 30-in. O.D. pile in sand.

9.2 Do a parameter study for a 30-in. O.D. pile in clay.

9.3 Find in the technical literature or in company files the results of a field test of a pile under lateral loading. Analyze the test according to the procedures employed in this chapter.

CHAPTER 10. ANALYSIS OF PILE GROUPS UNDER LATERAL LOADING

10.1 INTRODUCTION

There are two general problems in the analysis of pile groups: the computation of the loads coming to each pile in the group, and the determination of the efficiency of a group of closely-spaced piles. Each of these problems will be discussed in the following sections.

The methods that are presented are applicable to a pile group that is symmetrical about the line of action of the lateral load. That is, there is no twisting of the pile group so that no pile is subjected to torsion. Therefore, each pile in the group can undergo two translations and a rotation. However, the method that is presented for obtaining the distribution of loading to each pile can be extended to the general case where each pile can undergo three translations and three rotations (Reese, et al., 1970; O'Neill, et al., 1977; Bryant, 1977).

In all of the analyses presented in this section, the assumption is made that the soil does not act against the pile cap. In many instances, of course, the pile cap is cast against the soil. However, it is possible that soil can settle away from the cap and that the piles will sustain the full load. Thus, it is conservative and perhaps logical to assume that the pile cap is ineffective in carrying any load.

If the piles that support a structure are spaced far enough apart that the stress transfer between them is minimal and if the loading is shear only, the methods presented earlier in this work can be employed. Kuthy, et al. (1977) present an excellent treatment of this latter problem.

10.2 DISTRIBUTION OF LOAD TO EACH PILE IN A GROUP

The derivation of the equations presented in this section is based on the assumption that the piles are spaced far enough apart that there is no loss of efficiency; thus, the distribution of stress and deformation from a given pile to other piles in the group need not be considered. However, the method that is derived can be used with a group of closely-spaced piles but another level of iteration will be required.

Problem Statement

The problem to be solved is shown in Fig. 10.1. Three piles supporting a pile cap are shown. The piles may be of any size and placed on any

batter and may have any penetration below the groundline. The bent may be supported by any number of piles but, as noted earlier, the piles are assumed to be placed far enough apart that each is 100% efficient.

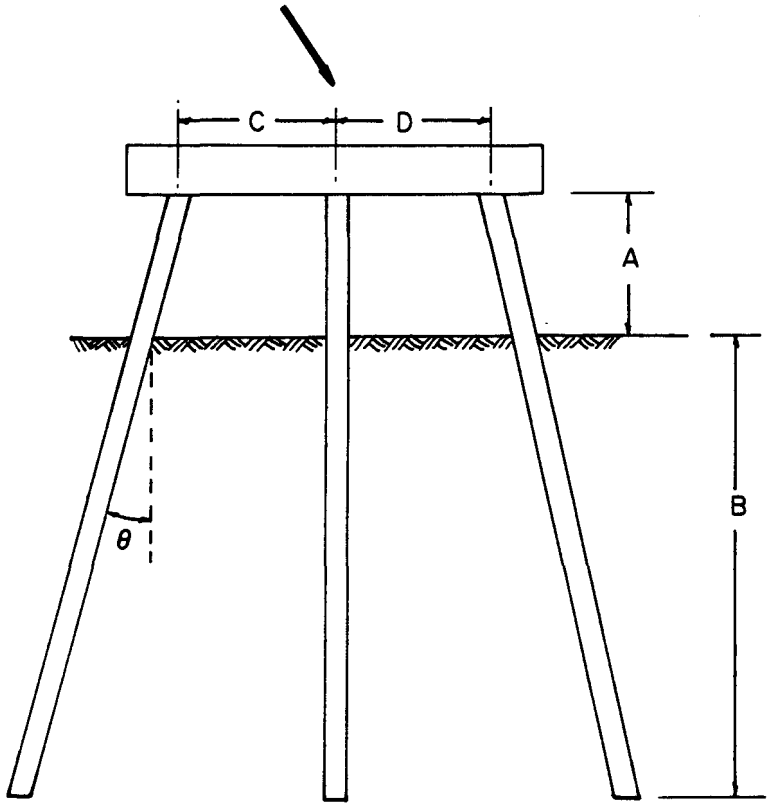

Fig. 10.1. Typical pile-supported bent.

The soil and loading may have any characteristics for which the response of a single pile may be computed.

Loading and Movement of the Structure

The derivation of the necessary equations in general form proceeds conveniently from consideration of a simplified structure such as that shown in Fig. 10.2 (Reese and Matlock, 1966; Reese, 1966). The sign conventions for the loading and for the geometry are shown. A global coordinate system, a-b, is established with reference to the structure. A coordinate system, x-y, is established for each of the piles. For convenience in deriving the equilibrium equations for solution of the problem, the a-b axes are located so that all of the coordinates of the pile heads are positive.

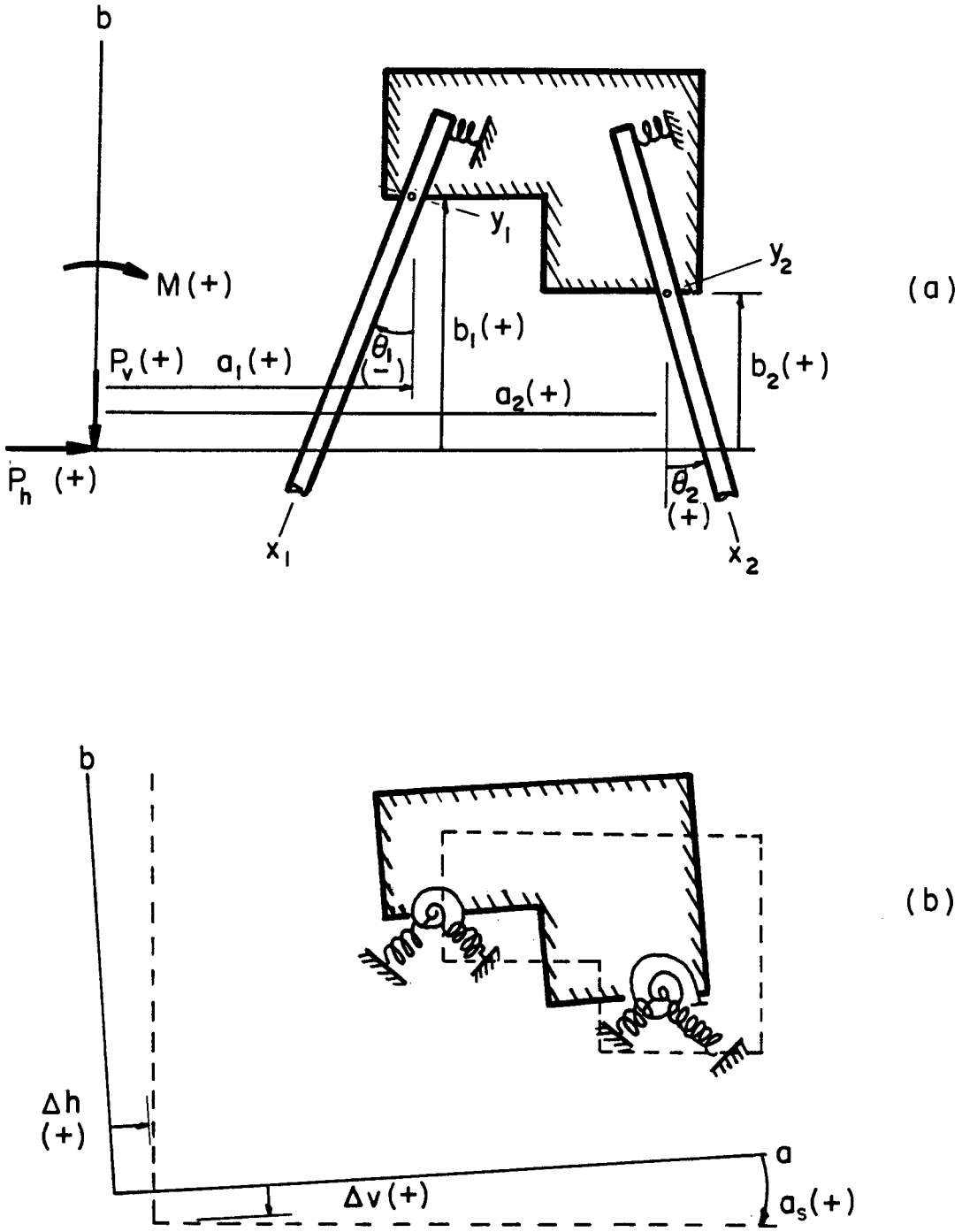

Fig. 10.2. Simplified structure showing coordinate systems and sign conventions (after Reese and Matlock).

The soil is not shown, but as shown in Fig. 10.2b, it is desirable to replace the piles with a set of "springs" (mechanisms) that represent the interaction between the piles and the supporting soil.

Movement of a Pile Head

If the global coordinate system translates horizontally Δh and vertically Δv and if the coordinate system rotates through the angle α_s, the movement of the head of each of the piles can be readily found. The angle α_s is assumed to be small in the derivation.

The movement of a pile head x_t in the direction of the axis of the pile is

$$x_t = (\Delta h + b\alpha_s) \sin \theta + (\Delta v + a\,\alpha_s) \cos \theta. \tag{10.1}$$

The movement of a pile head y_t transverse to the direction of the axis of the pile (the lateral deflection) is

$$y_t = (\Delta h + b\alpha_s) \cos \theta - (\Delta v + a\alpha_s) \sin \theta. \tag{10.2}$$

The assumption is made in deriving Eqs. 10.1 and 10.2 that the pile heads have the same relative positions in space before and after loading.

Forces and Moments

The movements computed by Eqs. 10.1 and 10.2 will generate forces and moments at the pile head. The assumption is made that curves can be developed, usually nonlinear, that give the relationship between pile-head movement and pile-head forces. A secant to a curve is obtained at the point of deflection and called the modulus of pile-head resistance. The values of the moduli, so obtained, can then be used, as shown below, to compute the components of movement of the structure. If the values of the moduli that were selected were incorrect, iterations are made until convergence is obtained.

Using sign conventions established for the single pile under lateral loading, the lateral force P_t at the pile head may be defined as follows:

$$P_t = J_y y_t. \tag{10.3}$$

If there is some rotational restraint at the pile-head, the moment is

$$M_t = -J_m y_t. \tag{10.4}$$

The moduli J_y and J_m are not single-valued functions of pile-head translation but are functions also of the rotation α_s of the structure.

If it is assumed that a compressive load causes a positive deflection along the pile axis, the axial force P_x may be defined as follows:

$$P_x = J_x x_t. \tag{10.5}$$

It is usually assumed that P_x is a single-value function of x_t.

The forces at the pile head defined in Eqs. 10.3 through 10.5 may now be resolved into vertical and horizontal components of force on the structure, as follows:

$$F_v = -(P_x \cos\theta - P_t \sin\theta) \text{ , and} \tag{10.6}$$

$$F_h = -(P_x \sin\theta + P_t \cos\theta) \text{ .} \tag{10.7}$$

The moment on the structure is

$$M_s = J_m y_t . \tag{10.8}$$

Equilibrium Equations

The equilibrium equations can now be written, as follows:

$$P_v + \Sigma F_{v_i} = 0, \tag{10.9}$$

$$P_h + \Sigma F_{h_i} = 0, \text{ and} \tag{10.10}$$

$$M + \Sigma M_{s_i} + \Sigma a_i F_{v_i} + \Sigma b_i F_{h_i} = 0. \tag{10.11}$$

The subscript i refers to values from any "i-th" pile. Using Eqs. 10.1 through 10.8, Eqs. 10.9 through 10.11 may be written in terms of the structural movements.

$$\sum \left\{ \left[J_{x_i} \cos^2\theta_i + J_{y_i} \sin^2\theta_i \right] \Delta v + \left[(J_{x_i} - J_{y_i}) \sin\theta_i \cos\theta_i \right] \Delta h + \left[a_i (J_{x_i} \cos^2\theta_i + J_{y_i} \sin^2\theta_i) + b_i (J_{x_i} - J_{y_i}) \sin\theta_i \cos\theta_i \right] \alpha_s \right\} = P_v \tag{10.12}$$

$$\sum \left\{ \left[(J_{x_i} - J_{y_i}) \sin\theta_i \cos\theta_i \right] \Delta v + \left[J_{x_i} \sin^2\theta_i + J_{y_i} \cos^2\theta_i \right] \Delta h + \left[a_i (J_{x_i} - J_{y_i}) \sin\theta_i \cos\theta_i + b_i (J_{x_i} \sin^2\theta_i + J_{y_i} \cos^2\theta_i) \right] \alpha_s \right\} = P_h \tag{10.13}$$

$$\sum \left\{ \left[J_{m_i} \sin\theta_i + a_i (J_{x_i} \cos^2\theta_i + J_{y_i} \sin^2\theta_i) + b_i (J_{x_i} - J_{y_i}) \sin\theta_i \cos\theta_i \right] \Delta v + \left[-J_{m_i} \cos\theta_i + a_i (J_{x_i} - J_{y_i}) \sin\theta_i \cos\theta_i + b_i (J_{x_i} \cos^2\theta_i + J_{y_i} \cos^2\theta_i) \right] \Delta h + \left[J_{m_i} (a_i \sin\theta_i - b_i \cos\theta_i) + (J_{x_i} \cos^2\theta_i + J_{y_i} \sin^2\theta_i) a_i^2 + (J_{x_i} \sin^2\theta_i + J_{y_i} \cos^2\theta_i) b_i^2 + 2(J_{x_i} - J_{y_i})(\sin\theta_i \cos\theta_i) a_i b_i \right] \alpha_s \right\} = M \tag{10.14}$$

Several of the terms in the above equation occur a number of times; it is convenient to define five terms as shown below.

$$A_i = J_{x_i} \cos^2 \theta_i + J_{y_i} \sin^2 \theta_i \tag{10.15}$$

$$B_i = (J_{x_i} - J_{y_i}) \sin \theta_i \cos \theta_i \tag{10.16}$$

$$C_i = J_{x_i} \sin^2 \theta_i + J_{y_i} \cos^2 \theta_i \tag{10.17}$$

$$D_i = J_{m_i} \sin \theta_i \tag{10.18}$$

$$E_i = -J_{m_i} \cos \theta_i \tag{10.19}$$

Equations 10.12 through 10.14 can be simplified by use of the above expressions. Equations 10.20 through 10.22 are the final form of the equilibrium equations.

$$\Delta v[\Sigma A_i] + \Delta h[\Sigma B_i] + \alpha_s[\Sigma a_i A_i + \Sigma b_i B_i] = P_v \tag{10.20}$$

$$\Delta v[\Sigma B_i] + \Delta h[\Sigma C_i] + \alpha_s[\Sigma a_i B_i + \Sigma b_i C_i] = P_h \tag{10.21}$$

$$\Delta v[\Sigma D_i + \Sigma a_i A_i + \Sigma b_i B_i] + \Delta h[\Sigma E_i + \Sigma a_i B_i + \Sigma b_i C_i]$$

$$+ \alpha_s[\Sigma a_i D_i + \Sigma a_i^2 A_i + \Sigma b_i E_i + \Sigma b_i^2 C_i$$

$$+ \Sigma 2a_i b_i B_i] = M \tag{10.22}$$

The equilibrium equations can be solved in any convenient way. Because of the number of operations required, it is usually convenient to use a digital computer (Awoshika, 1971; Lam, 1982).

Solution Procedure

1. Select a coordinate center and find the horizontal component, the vertical component, and the moment through and about that point.
2. Compute by some procedure (Reese, 1964; Coyle and Reese, 1966; Coyle and Sulaiman, 1967; Kraft, et al., 1981) a curve showing axial load versus axial deflection for each pile in the group. An alternate procedure is to use the results from a field load test. A typical curve is shown in Fig. 10.3a.
3. Use procedures presented earlier in this work and compute curves showing lateral load as a function of lateral

deflection and moment as a function of lateral deflection. In making these computations, attention must be paid to the effect of structural rotation on the boundary conditions at each pile head. Typical curves are shown in Figs. 10.3b and 10.3c.

4. Trial values of J_x, J_y, and J_m are estimated for each pile in the structure.
5. Equations 10.15 through 10.22 are solved for values of Δv, Δh, and α_s.
6. Pile-head movements are computed and new values of J_x, J_y, and J_m are obtained for each pile. Curves such as those shown in Fig. 10.3 are employed or a computer solution yields directly the values of the moduli.
7. Equations 10.15 through 10.22 are solved again for new values of Δv, Δh, and α_s.
8. Iteration is continued until the computed values of the structural movements agree, within a given tolerance, with the values from the previous computation.
9. The loads and moments at each pile head can then be used to compute the stresses along the length of each pile.

Example Problem

Figure 10.4 shows a pile-supported retaining wall with the piles spaced 8 ft apart. The piles are 14-in. in outside diameter with 4 No. 7 reinforcing-steel bars spaced equally. The centers of the bars are on an 8-in. circle. The yield strength of the reinforcing steel is 60 kips/sq in. and the compressive strength of the concrete is 2.67 kips/sq in. The length of the piles is 40 ft.

The backfill is a free-draining, granular soil without any fine particles. The surface of the backfill is treated to facilitate runoff and weep holes are provided so that water will not collect behind the wall.

The forces P_1, P_2, P_s, and P_w were computed as follows: 21.4, 4.6, 18.4, and 22.5 kips, respectively. The resolution of the loads at the origin of the global coordinate system resulted in the following service loads: P_v = 46 kips, P_h = 21 kips, and M = 40 ft-kips (some rounding was done).

The moment of inertia of the gross section of the pile was used in the analysis. The bending stiffness EI of the piles was computed to be

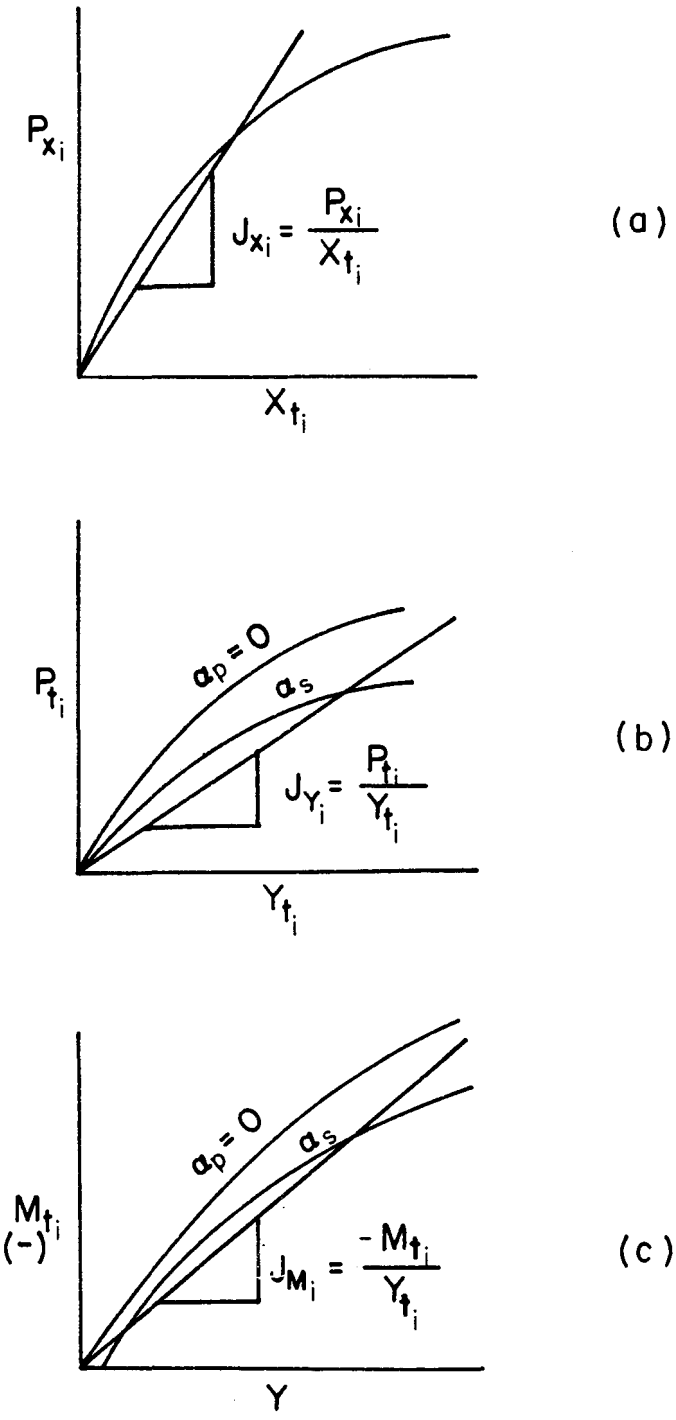

Fig. 10.3. Set of pile resistance functions for a given pile.

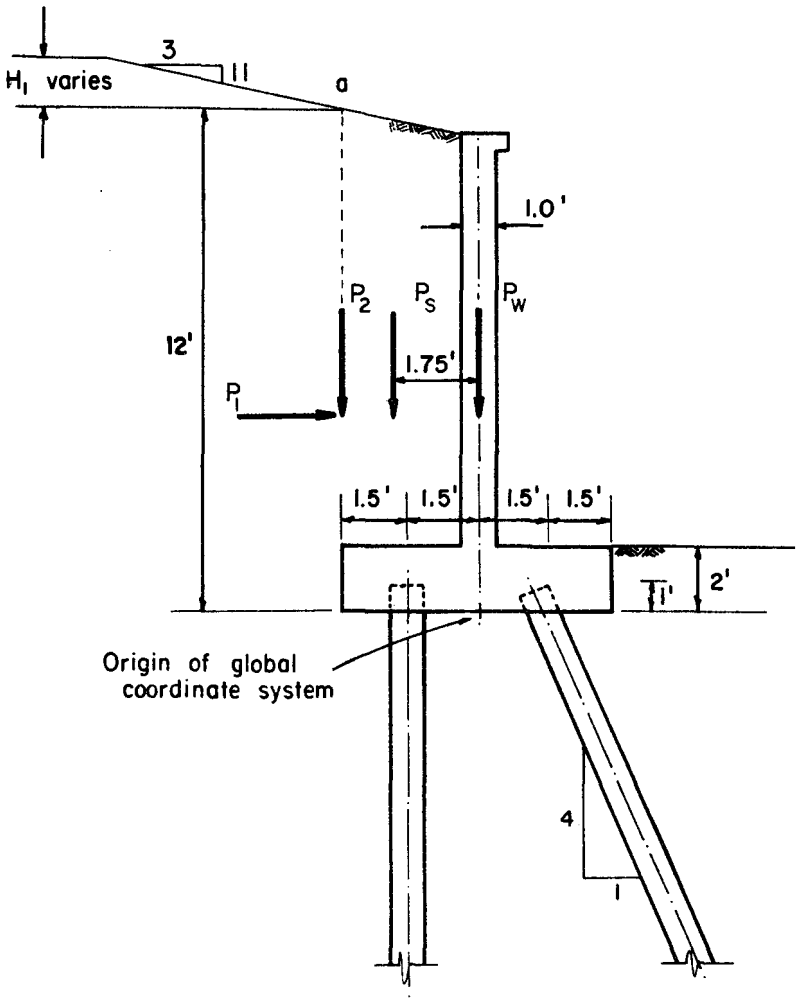

Fig. 10.4. Sketch of a pile-supported retaining wall.

5.56 x 10^9 lb-sq in. Computer Program PMEIX was run and an interaction diagram for the pile was obtained. That diagram is shown in Fig. 10.5.

A field load test was performed at the site and the ultimate axial capacity of a pile was found to be 176 kips. An analysis was made to develop a curve showing axial load versus settlement. The curve is shown in Fig. 10.6.

The subsurface soils at the site consist of silty clay. The water content in the top 10 ft averaged 20% and below 10 ft it averaged 44%. The water table was reported to be at a depth of 10 ft. There was a considerable range in the undrained shear strength of the clay and an average value of 3 kips/sq ft was used in the analysis. A value of the submerged unit weight of 46 lb/cu ft was employed and the value of ε_{50} was estimated to be 0.005.

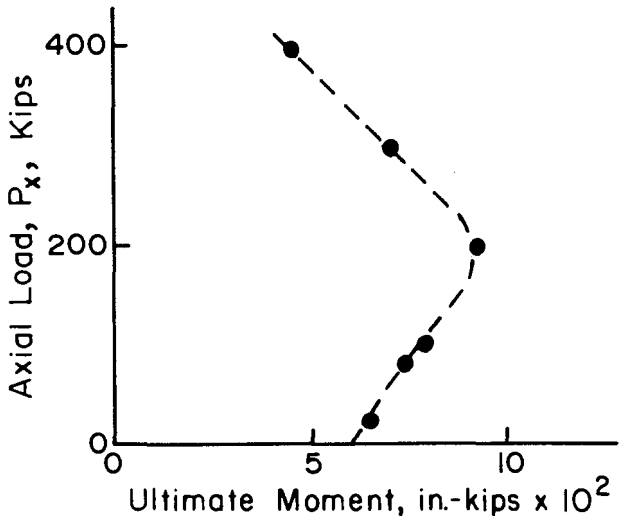

Fig. 10.5. Interaction diagram of the reinforced oncrete pile.

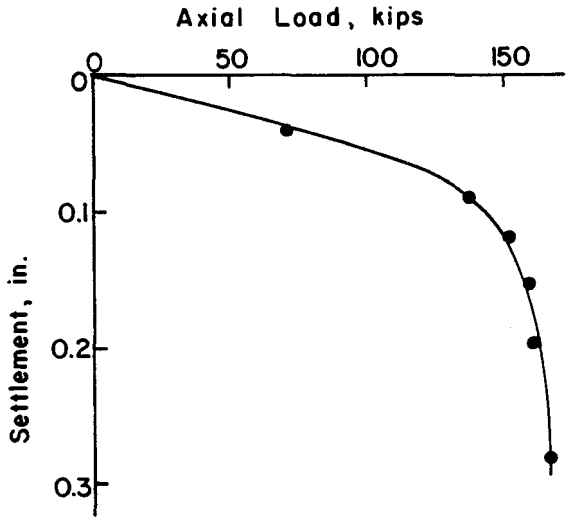

Fig. 10.6. Axial load versus settlement for reinforced concrete pile.

In making the computations, the assumptions were made that all of the load was carried by the piles with none of the load taken by passive earth pressure or by the base of the footing. It was further assumed that the pile heads were free to rotate. As noted earlier, the factor of safety

must be in the loading. Therefore, the loadings shown in Table 10.1 were used in the preliminary computations.

TABLE 10.1. VALUES OF LOADING EMPLOYED IN ANALYSES.

Case	Loads, kips		moment, ft-kips	Comment
	P_v	P_h		
1	46	21	40	service load
2	69	31.5	60	1.5 times service load
3	92	42	80	2 times service load
4	115	52.5	100	2.5 times service load

Table 10.2 shows the movements of the origin of the global coordinate system when Eqs. 10.20 through 10.22 were solved simultaneously. The loadings were such that the pile response was almost linear so only a small number of iterations were required to achieve convergence. The computed pile-head movements, loads, and moments are shown in Table 10.3.

TABLE 10.2. COMPUTED MOVEMENTS OF ORIGIN OF GLOBAL COORDINATE SYSTEM.

Case	Vertical Movement Δv	Horizontal Movement Δh	Rotation α
	inches	inches	rad
1	0.004	0.08	9×10^{-5}
2	0.005	0.12	1.4×10^{-4}
3	0.008	0.16	1.6×10^{-4}
4	0.017	0.203	8.4×10^{-4}

TABLE 10.3. COMPUTED MOVEMENTS AND LOADS AT PILE HEADS.

Case	Pile 1					Pile 2				
	x_t	y_t	P_x	P_t	M_{max}	x_t	y_t	P_x	P_t	M_{max}
	in.	in.	kips	kips	in.-kips	in.	in.	kips	kips	in.-kips
1	0.005	0.08	9.7	6.0	148	0.02	0.077	38.9	5.8	143
2	0.008	0.12	14.5	9.0	222	0.03	0.116	58.3	8.6	215
3	0.011	0.162	19.3	12.1	298	0.04	0.156	77.7	11.5	288
4	0.013	0.203	24.2	15.2	373	0.06	0.194	97.2	14.3	360

The computed loading on the piles is shown in Fig. 10.7 for Case 4. The following check is made to see that the equilibrium equations are satisfied.

$$\Sigma F_v = 24.2 + 97.2 \cos 14° - 14.3 \sin 14°$$
$$= 24.2 + 94.3 - 3.5 = 114.9 \text{ kips OK}$$
$$\Sigma F_h = 15.2 + 14.3 \cos 14° - 97.2 \sin 14°$$
$$= 15.2 + 13.9 + 23.6 = 52.7 \text{ kips OK}$$
$$\Sigma M = -(24.2)(1.5) + (97.2 \cos 14°)(1.5)$$
$$- (14.3 \sin 14°)(1.5)$$
$$= -36.3 + 141.4 - 5.2 = 99.9 \text{ ft-kips OK}$$

Thus, the retaining wall is in equilibrium. A further check can be made to see that the conditions of compatibility are satisfied. One check can be made at once. Referring to Fig. 10.6, an axial load of 97.2 kips results in an axial deflection of about 0.054 in., a value in reasonable agreement with the value in Table 10.3. Further checks on compatibility can be made by using the pile-head loadings and Computer Program COM622 to see if the computed deflections under lateral load are consistent with the values tabulated in Table 10.3.

No firm conclusions can be made concerning the adequacy of the particular design without further study. If the assumptions made in performing the analyses are appropriate, the results of the analyses show the foundation to be capable of supporting the load. As a matter of fact, the piles could probably support a wall of greater height.

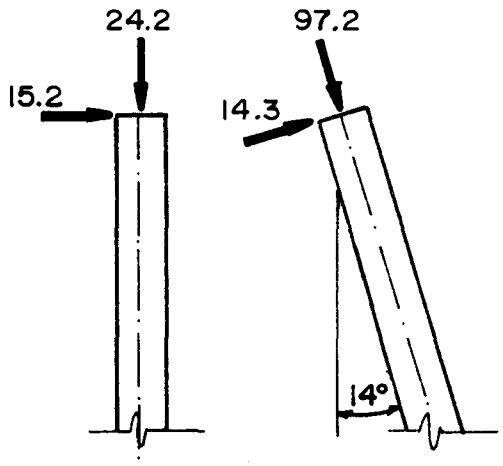

Fig. 10.7. Pile loading, Case 4.

With a multiplier of 2.5 times the service loads, the batter pile takes an axial load of 97 kips which is well short of the ultimate capacity of the pile as shown in Fig. 10.6. Figure 10.5 shows that Pile 1 should be able to sustain an ultimate moment of about 700 in-kips and under Case 4 (2.5 times the service load) the actual moment is about 373 in.-kips.

The example problem illustrates the use of the procedure. The example shows further that an the appropriate solution of a design problem probably should involve a number of computations in which the important parameters in the problem are varied through a range that represents the reasonable uncertainty.

10.3 BEHAVIOR OF A GROUP OF CLOSELY-SPACED PILES

The analysis of a group of closely-spaced piles under lateral loading can be undertaken by a number of methods, two of which will be presented herein. The most obvious problem is to take into account the effect of a single pile on others in the group. Approximate solutions have been developed (Poulos, 1971b; Banerjee and Davies, 1979) by use of the equations of elasticity; however, as demonstrated in Chapter 8, the assumption of a linear response of the soil-pile system is inadequate to deal with many problems of a pile under lateral loading.

The first method that will be presented uses a combination of the elastic method with the p-y method. The second method is the single-pile approach to group analysis.

The principal difficulty in achieving an acceptable solution to the closely-spaced group is that there have been few full-scale load tests of such groups. Such tests are expensive and difficult to carry out. Therefore, the methods that are presented here must only be used in consideration of the assumptions that underlie each of the methods.

Poulos-Focht-Koch Method

The following equation was developed by Poulos (1971a, 1971b) to obtain the deflection and load on each of the piles in a group, assuming the soil to act elastically.

$$\rho_k = \rho_F \sum_{\substack{j=1 \\ j \neq k}}^{m} (H_j \alpha_{\rho Fkj} + H_k) \qquad (10.23)$$

where

ρ_k = deflection of the k-th pile

ρ_F = the unit reference displacement of a single pile under a unit horizontal load, computed by using elastic theory

H_j = lateral load on pile j

$\alpha_{\rho Fkj}$ = the coefficent to get the influence of pile j on pile k in computing the deflection ρ (the subscript F pertains to the fixed-head case and is used here for convenience; there are also influence coefficients as shown later where shear is applied, $\alpha_{\rho Hkj}$, and where moment is applied, $\alpha_{\rho Mkj}$)

H_k = lateral load on pile k

m = number of piles in group.

If the total load on the group is H_G, then

$$H_G = \sum_{j=1}^{m} H_j. \qquad (10.24)$$

If the piles are connected to a cap such that each of the piles is caused to deflect an equal amount, the deflection ρ_k is equal to y_G, the deflection of the group. If there are m piles in the group, m + 1 equations can be formulated using Eqs. 10.23 and 10.24 and solved for the group deflection and the load H on each pile in the group.

In order to write the equations it is necessary to have the influence coefficients. Poulos has supplied a family of curves for the α-values with the curves based on a Poisson's ratio of 0.5. The curves must be entered with values of L/b, s/b, β, and K_R, where L is pile length, b is pile diameter, s is center to center spacing, β is the angle between the line through the two piles in question and the line giving the direction of the loading, and K_R is defined by the following equation.

$$K_R = \frac{EI}{E_s L^4} \tag{10.25}$$

where

E = modulus of elasticity of pile material

I = moment of inertia of pile

E_s = soil modulus

Figures 10.8 and 10.9 present Poulos curves for free-head piles that are subjected to shear and to moment, respectively. Figure 10.10 presents the Poulos curve for a fixed-head pile.

Focht and Koch (1973) have proposed modifications of the Poulos method. They suggested a revision of Eq. 10.23 as follows:

$$\rho_k = \rho_F \sum_{\substack{j=1 \\ j \neq k}}^{m} (H_j \alpha_{\rho F kj} + RH_k), \tag{10.26}$$

where

R = relative stiffness factor.

The relative stiffness factor is the ratio of the mudline deflection of a single pile computed by the p-y curve approach, y_s, to the deflection ρ computed by the Poulos method that assumes elastic soil. In both instances, the lateral load on the single pile is the total lateral load on the pile group divided by the number of piles.

Equation 10.27 is the Poulos equation for the deflection of a single pile with free head (Eq. 10.27 is identical to Eq. 7.28 except for difference in symbols).

$$\rho = I_{\rho F} \frac{H}{E_s L} + I_{\rho M} \frac{M}{E_s L^2} \tag{10.27}$$

The influence coefficients $I_{\rho H}$ and $I_{\rho M}$ may be obtained from Figs. 10.11 and 10.12, respectively.

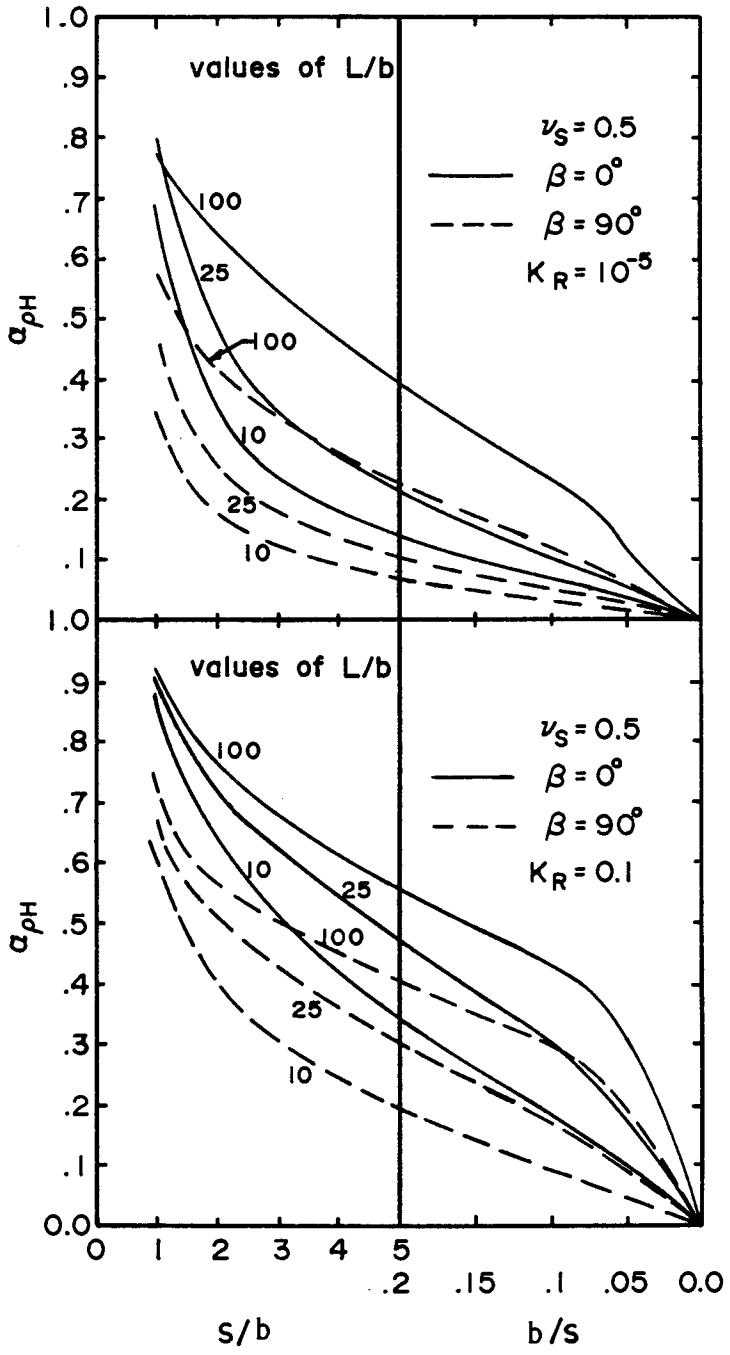

Fig. 10.8. Interaction factors $\alpha_{\rho H}$ for free-head piles subjected to horizontal load (Poulos, 1971).

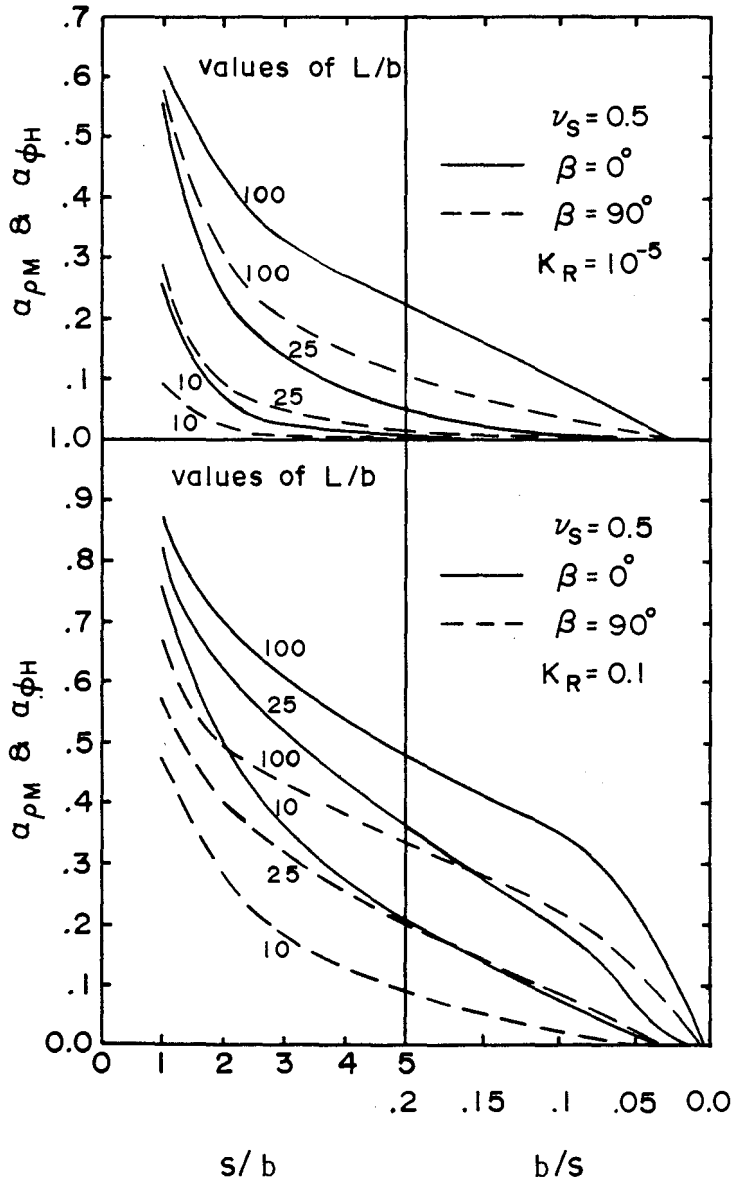

Fig. 10.9. Interaction factors $\alpha_{\rho M}$ for free-head piles subjected to moment (Poulos, 1971).

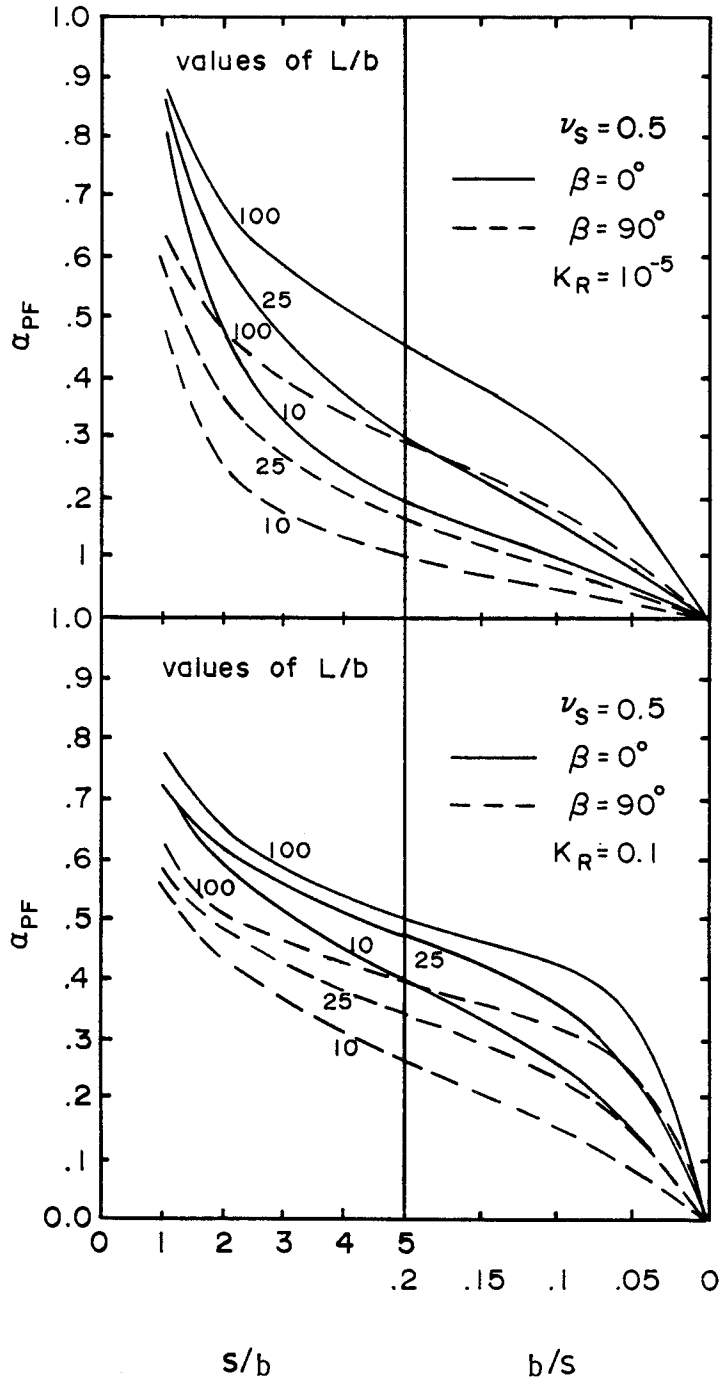

Fig. 10.10. Interaction factors $\alpha_{\rho F}$ for fixed-head pile (Poulos, 1971).

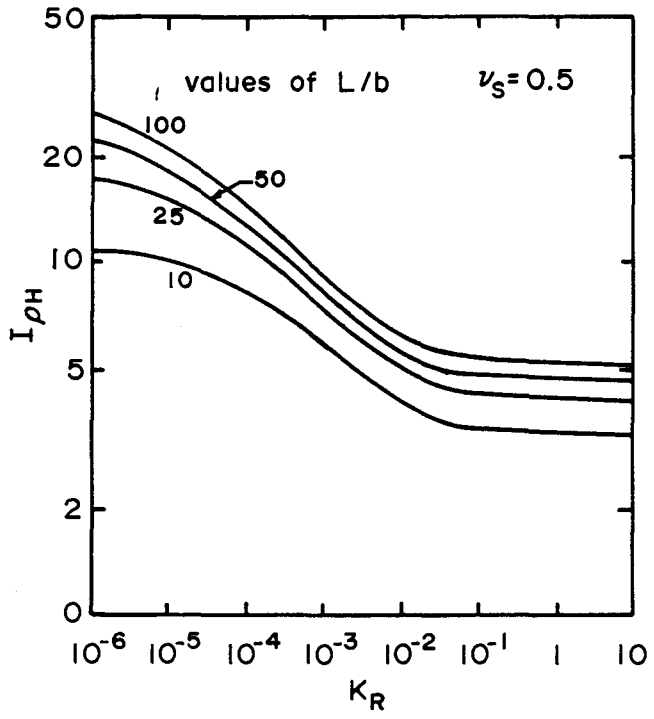

Fig. 10.11. Influence factors $I_{\rho H}$ for a free-head pile (Poulos, 1971).

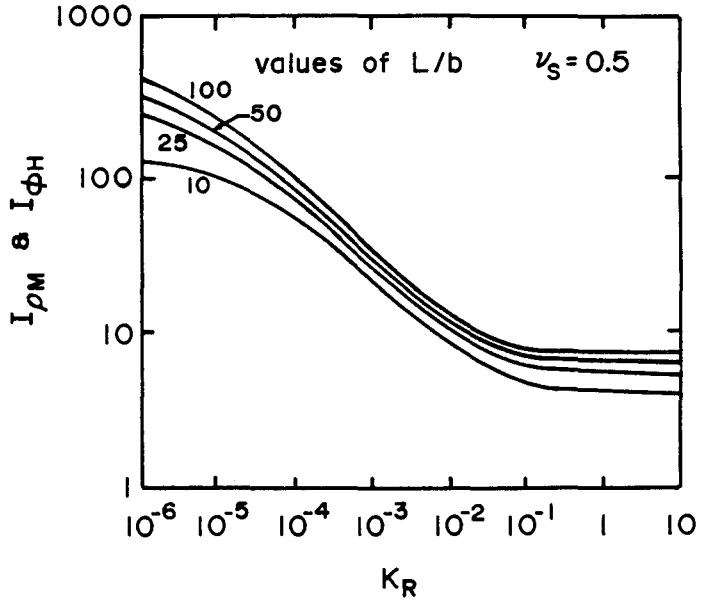

Fig. 10.12. Influence factors $I_{\rho M}$ for a free-head pile (Poulos, 1971).

Equation 10.28 is the Poulos equation for the deflection of a single pile with fixed head.

$$\rho = I_{\rho F} \frac{H}{E_s L} \tag{10.28}$$

The influence coefficients $I_{\rho F}$ may be obtained from Fig. 10.13.

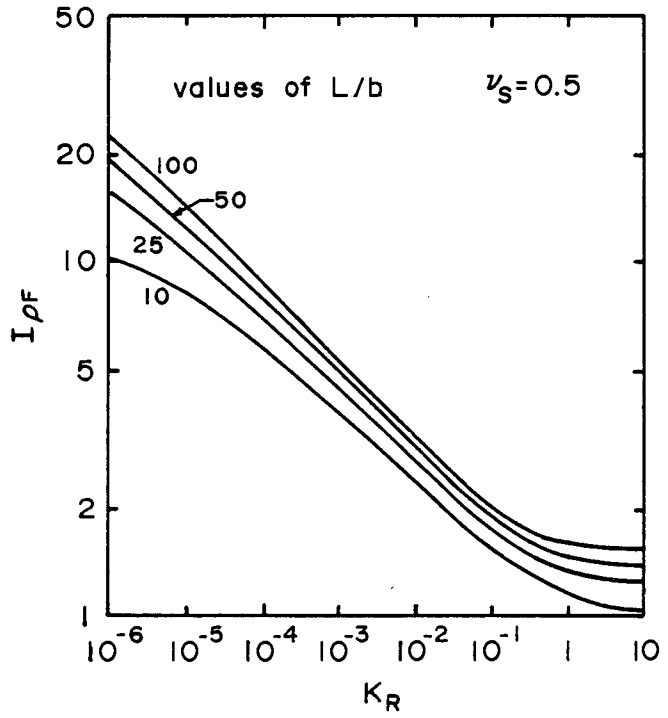

Fig. 10.13. Influence factors $I_{\rho F}$ for a fixed-head pile (Poulos, 1971).

The curves that are presented in Figs. 10.11 through 10.13 are entered with values of K_R and L/b. (Figures 10.11 through 10.13 are the same as Figs. 7.10, 7.11, and 7.14, respectively, but are repeated here for convenience.) A value of Poisson's ratio of 0.5 was used in developing all three curves.

It is important in using the Poulos equations to obtain a value of the soil modulus E_s that is as accurate as possible. It is generally agreed that the best method for determining E_s is to perform a field loading test. However, such tests are not practical in many instances for both economic and practical reasons. In the absence of such tests, some

correlations of E_s with the undrained shear strength can be used as a rough guide. The stress-strain data obtained from triaxial tests can furnish representative E_s values that are better than those obtained from correlations with the undrained shear strength. Focht and Koch state that E_s should be selected from available stress-strain-test results using a low stress level in the soil. They suggest that the value should be at least as great as the secant modulus corresponding to a stress equal to 50 percent of the strength and probably as great as the initial tangent modulus indicated by most laboratory tests.

Using Eqs. 10.24 and 10.26, a set of simultaneous equations is formulated and solved for the group deflection y_G and the lateral load on each pile in the group. The pile with the greatest load is selected for analysis by employing modified p-y curves. The p-values are modified by employing a multiplication factor to reflect the "shadowing" effect of closely-spaced piles. The y-values are modified by multiplying all of the deflections in the p-y curves by a Y-factor of 2, 3, 4 and so on. The deflection of the single pile is computed with the modified p-y curves and the Y-factor is found that gives agreement between the single-pile deflection so computed and the deflection of the pile group. With this appropriate Y-factor, the pile behavior can be computed with the modified p-y curves, completing the solution. Figure 10.14 presents the form of the solution that employs the Y-factor.

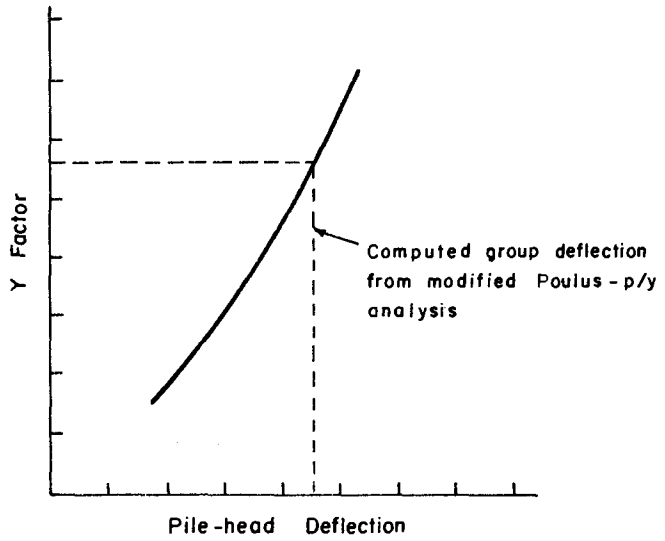

Fig. 10.14. "Y" factor influence on computed pile-head deflection.

Single-Pile Method

The single-pile method of analysis is based on the assumption that the soil contained between the piles moves with the group. Thus, the pile group with the contained soil can be treated as a single pile of large diameter.

The first step in the use of the single-pile method is to select the group to be analyzed and to ascertain the loading. A plan view of the piles at the groundline is prepared and the minimum length is found for a line that encloses the group. This length is considered to be the circumference of a pile of large diameter; thus, the length is divided by π to obtain the diameter of the imaginary pile.

The next step is to determine the stiffness of the group. For a lateral load passing through the tops of the piles, the stiffness of the group is taken as the sum of the stiffness of the individual piles. Thus, it is assumed that the deflection at the pile top is the same for each pile in the group and, further, that the deflected shape of each pile is identical. Some judgement must be used if the piles in the group have different lengths.

An analysis is made for the imaginary pile, taking into account the nature of the loading and the boundary conditions at the pile head. The shear and moment for the imaginary large-sized pile is shared by the individual piles according to the ratio of the lateral stiffness of the individual pile to that of the group.

The shear, moment, pile-head deflection, and pile-head rotation yield a unique solution for each pile in the group. As a final step, it is necessary to compare the single-pile solution to that of the group. It could possibly occur that the piles in the group could have an efficiency greater than one, in which case the single-pile solutions would control.

Example Problem

A sketch of an example problem is shown in Fig. 10.15. It is assumed that steel piles are embedded in a reinforced concrete mat in such a way that the pile heads do not rotate. The piles are 14HP89 by 40 ft long and placed so that bending is about the strong axis. The moment of inertia is 904 in.^{4} and the modulus of elasticity is 30 x 10^6 lb/sq in. The width of the section is 14.7 in. and the depth is 13.83 in.

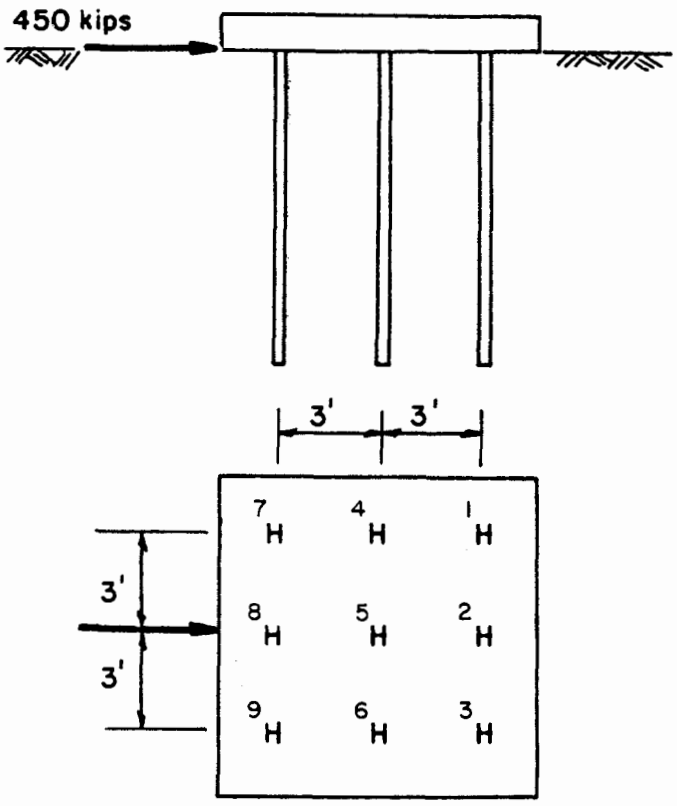

Fig. 10.15. Plan and elevation of foundation analyzed in example problem.

The soil is assumed to be a sand with an angle of internal friction of 34 degrees, the unit weight is 114 lb/cu ft, and the assumed Poulos soil modulus is 3000 lb/sq ft.

Poulos-Focht-Koch Solution

Computation of value of R:

The lateral load is 450/9 or 50 kips

Computation of ρ using Eqs. 10.25 and 10.28

$$K_R = \frac{(30 \times 10^6)(904)}{(3000)(480)^4} = 1.70 \times 10^{-4}$$

$L/b = 480/14.7 = 32.7$

$I_{\rho F} = 7.8$ (from Fig. 10.13)

$$\rho = (7.8)\frac{(50{,}000)}{(3000)(480)} = 0.27 \text{ in.}$$

$y_t = 0.35$ in. (from COM622 solution)

$R = 0.35/0.27 = 1.29.$

Computation of Poulos deflection under unit load:

$\bar{\rho}_F = 0.27/50{,}000 = 0.54 \times 10^{-5}$ in./lb.

Determination of α-values:

(Because a number of the α-values are identical, it is convenient to obtain these identical values together rather than to determine the values pile-by-pile as they are used.)

$\alpha_{1-2} = \alpha_{2-1} = \alpha_{2-3} = \alpha_{3-2} = \alpha_{4-5} = \alpha_{5-4} = \alpha_{5-6} = \alpha_{6-5} = \alpha_{7-8} = \alpha_{8-7} = \alpha_{8-9} = \alpha_{9-8}$

$\beta = 90°$, $s/b = (3)(12)/14.7 = 2.45$, $\alpha = 0.35$

(from Fig. 10.10)

(Note: the α-value was obtained by straight-line interpolation)

$\alpha_{1-3} = \alpha_{3-1} = \alpha_{4-6} = \alpha_{6-4} = \alpha_{7-9} = \alpha_{9-7}$

$\beta = 90°$, $s/b = 4.9$, $\alpha = 0.23$

$\alpha_{1-4} = \alpha_{4-1} = \alpha_{4-7} = \alpha_{7-4} = \alpha_{2-5} = \alpha_{5-2} = \alpha_{5-8} = \alpha_{8-5} = \alpha_{3-6} = \alpha_{6-3} = \alpha_{6-9} = \alpha_{9-6}$

$\beta = 0°$, $s/b = 2.45$, $\alpha = 0.53$

$\alpha_{1-7} = \alpha_{7-1} = \alpha_{2-8} = \alpha_{8-2} = \alpha_{3-9} = \alpha_{9-3}$

$\beta = 0°$, $s/b = 4.9$, $\alpha = 0.40$

$\alpha_{1-5} = \alpha_{5-1} = \alpha_{2-4} = \alpha_{4-2} = \alpha_{2-6} = \alpha_{6-2} = \alpha_{3-5} = \alpha_{5-3}$
$\alpha_{4-8} = \alpha_{8-4} = \alpha_{5-7} = \alpha_{7-5} = \alpha_{5-9} = \alpha_{9-5} = \alpha_{6-8} = \alpha_{8-6}$

$\beta = 45°$, $s/b = 3.46$, $\alpha = 0.38$

$\alpha_{1-6} = \alpha_{6-1} = \alpha_{3-4} = \alpha_{4-3} = \alpha_{4-9} = \alpha_{9-4} = \alpha_{6-7} = \alpha_{7-6}$

$\beta = 63°$, $s/b = 5.47$, $\alpha = 0.25$

$\alpha_{1-8} = \alpha_{8-1} = \alpha_{2-7} = \alpha_{7-2} = \alpha_{2-9} = \alpha_{9-2} = \alpha_{8-3} = \alpha_{3-8}$

$\beta = 26.6°$, $s/b = 5.47$, $\alpha = 0.28$

$\alpha_{1-9} = \alpha_{9-1} = \alpha_{3-7} = \alpha_{7-3}$

$\beta = 45°$, $s/b = 6.93$, $\alpha = 0.22$

Simultaneous equations:

Piles 1, 3, 7, 9 have identical equations:

$$\rho_1 = \rho_3 = \rho_7 = \rho_9$$
$$= \bar{\rho}_F [RH_1 + (\alpha_{1-3} + \alpha_{1-7} + \alpha_{1-9})H_1 + (\alpha_{1-2} + \alpha_{1-8})H_2 + (\alpha_{1-4} + \alpha_{1-6})H_4 + \alpha_{1-5}H_5]$$
$$= 0.54 \times 10^{-5}[1.29H_1 + (0.23 + 0.40 + 0.22)H_1 + (0.35 + 0.28)H_2 + (0.53 + 0.25)H_4 + 0.38H_5]$$
$$= 0.54 \times 10^{-5}[2.14H_1 + 0.63H_2 + 0.78H_4 + 0.38H_5] \qquad (A)$$

Piles 2 and 8 have identical equations:

Substitutions as shown above yield the following equation:

$$\rho_2 = \rho_8 = 0.54 \times 10^{-5}[1.26H_1 + 1.69H_2 + 0.76H_4 + 0.53H_5] \quad (B)$$

Piles 4 and 6 have identical equations:

$$\rho_4 = \rho_6 = 0.54 \times 10^{-5}[1.56H_1 + 0.76H_2 + 1.52H_4 + 0.35H_5] \quad (C)$$

Pile 5:

$$\rho_5 = 0.54 \times 10^{-5}[1.52H_1 + 1.06H_2 + 0.70H_4 + 1.29H_5] \quad (D)$$

Summation of loads:

$$4H_1 + 2H_2 + 2H_4 + H_5 = 450 \text{ kips} \quad (E)$$

Solving equations A, B, C, D, E simultaneously, noting that:

$$y_G = \rho_1 = \rho_2 = \rho_3 = \rho_4 = \rho_5 = \rho_6 = \rho_7 = \rho_8 = \rho_9$$

$H_1 = 61.9$ kips, $H_2 = 49.1$ kips, $H_4 = 40.9$ kips, $H_5 = 22.5$ kips

$y_G = 0.91$ in.

Using a computer program to solve for the moment curve in Piles 1, 3, 7, 9, the piles with the heaviest load (Sullivan and Reese, 1980):

The Y-factors of 2, 4, and 5 were employed and Fig. 10.16 was plotted.

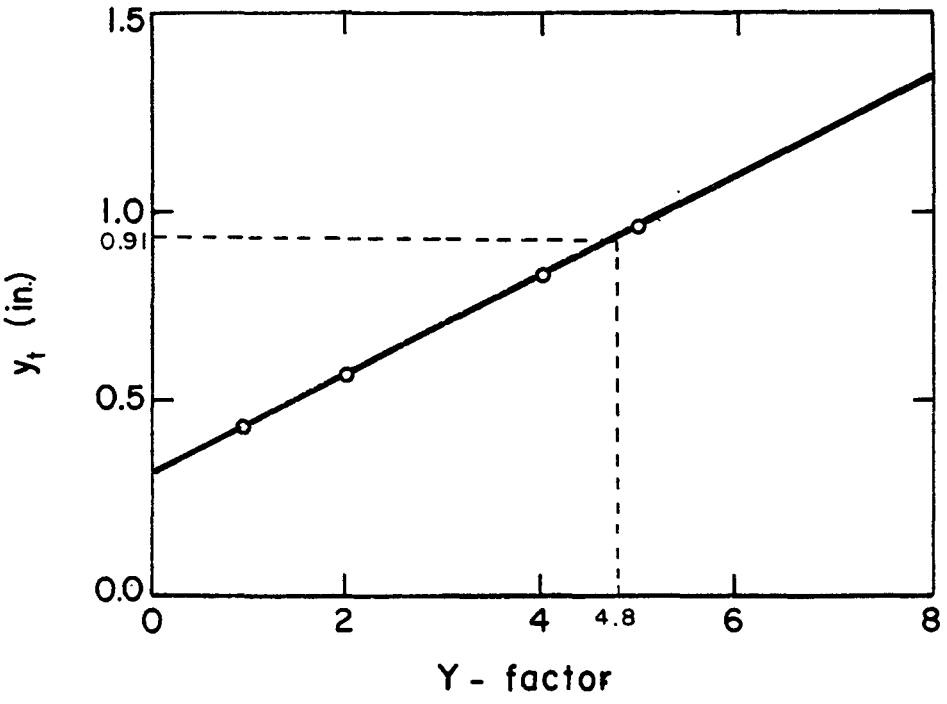

Fig. 10.16. Graphical solution for Y-factor.

As noted, a Y-factor of 4.8 yielded a deflection of 0.91. The bending moment curve corresponding to a deflecton of 0.91 is shown in Fig. 10.17. The maximum bending stress is computed as follows:

$$f = \frac{Mc}{I} = \frac{(4.4 \times 10^3)(6.915)}{904} = 33.7 \text{ kips/sq in.}$$

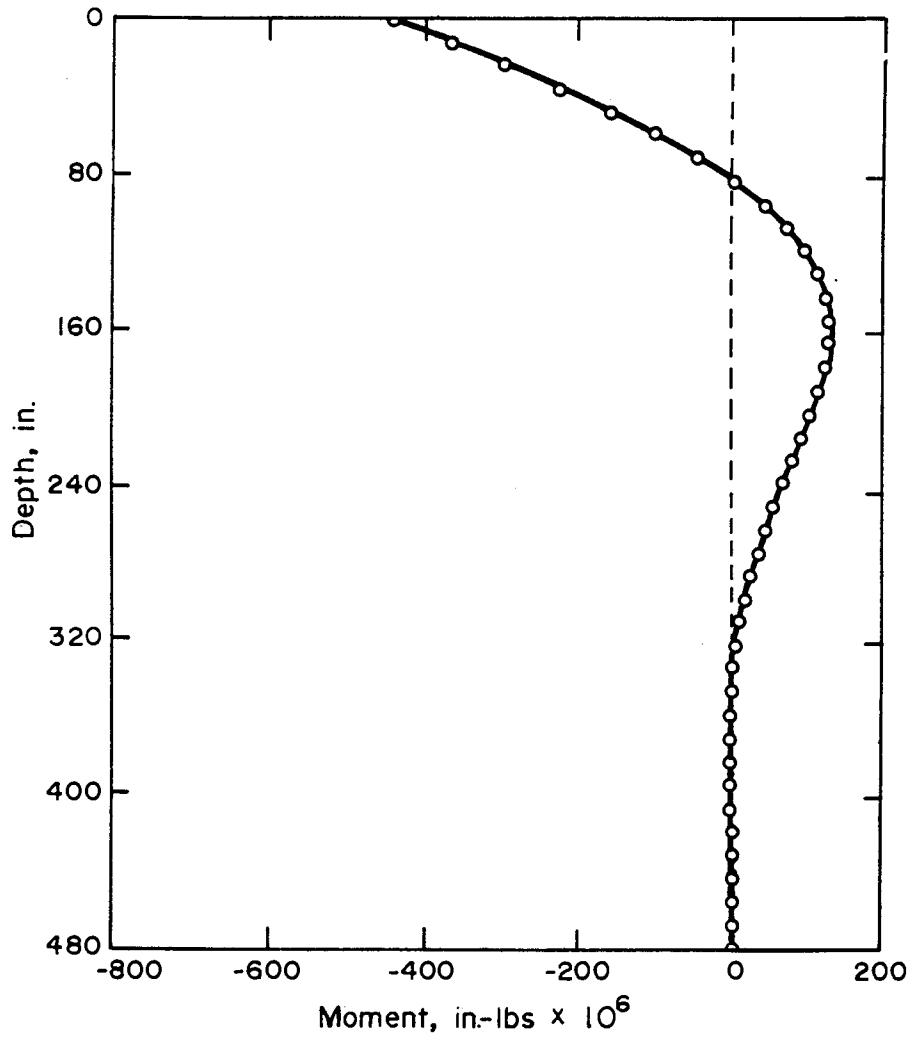

Fig. 10.17. Bending moment curve for pile with greatest load, example solution.

Solution Assuming Group Behaves as a Single Pile

The computer program was run with a pile diameter of 109 in. and a moment of inertia of 8136 in.^{4} (9 times 904). The results were as follows:

Y_t = 1.04 in.

$M_t = M_{max}$ = 3.53×10^7 in.-lb for group

= 3.92×10^6 in.-lb for single pile

Bending stress = 31.9 k/sq in.

The deflection and stress are in reasonable agreement with the previous solution.

Comment on Solution of Example Problem

For the example problem, good agreement was found between the two methods of analysis. However, that good agreement could be fortuitous. As noted earlier, there is a need for more full-scale load tests on pile groups under lateral loading. If the size of the construction project justifies, consideration should be given to a field test program prior to making final designs.

The methods demonstrated herein are recommended for preliminary studies. Studies should be done to investigate the effects on the results of changing the values of the input parameters through a range consistent with reasonable expectations. If final designs are made on the basis of results from these methods, an appropriate factor of safety should be carefully considered.

10.4 REFERENCES

Awoshika, Katsuyuki, and Reese, Lymon C., "Analysis of Foundation with Widely Spaced Batter Piles," Research Report 117-3F, Project 3-5-68-117, Center for Highway Research, University of Texas at Austin, February 1971.

Banerjee, P. K., and Davies, T. G., "Analysis of Some Reported Case Histories of Laterally Loaded Pile Groups," Proceedings, Numerical Methods in Offshore Piling, The Institution of Civil Engineers, London, May 1979, pp. 101-108.

Bryant, L. M., "Three-Dimensional Analysis of Framed Structures with Nonlinear Pile Foundations," Unpublished Dissertation, The University of Texas at Austin, 95 pages, December 1977.

Coyle, H. M., and Reese, L. C., "Load Transfer for Axially Loaded Piles in Clay," Proceedings, American Society of Civil Engineers, Vol. 92, No. SM2, March 1966, pp. 1-26.

Coyle, H. M., and Sulaiman, I. H., "Skin Friction for Steel Piles in Sand," Proceedings, American Society for Civil Engineers, Vol. 93, No. SM6, November 1967, pp. 261-278.

Focht, J. A., Jr., and Koch, K. J., "Rational Analysis of the Lateral Performance of Offshore Pile Groups," Proceedings, Fifth Annual Offshore Technology Conference, Paper No. 1896, Vol. II, Houston, 1973, pp. 701-708.

Kraft, L. M., Jr., Ray, R. P., and Kagawa, T., "Theoretical t-z Curves," Proceedings, American Society of Civil Engineers, Vol. 107, No. GT11, November 1981, pp. 1543-1561.

Kuthy, R. A., Ungerer, R. P., Renfrew, W. W., Hiss, J. G. F., Jr., and Rizzuto, I. F., "Lateral Load Capacity of Vertical Pile Groups," Research Report 47, Engineering Research and Development Bureau, New York State Department of Transportation, Albany, April 1977, 37 pages.

Lam, Philip, "Computer Program for Analysis of Widely Spaced Batter Piles," Unpublished Thesis, The University of Texas at Austin, August 1981.

O'Neill, M. W., Ghazzaly, O. I., and Ha, H. B., "Analysis of Three-Dimensional Pile Groups with Nonlinear Soil Response and Pile-Soil-Pile Interaction," Proceedings, Offshore Technology Conference, Houston, Texas, Vol. II, Paper No. 2838, pp. 245-256, 1977.

Poulos, H. G., "Behavior of Laterally Loaded Piles: I - Single Piles," Proceedings, American Society of Civil Engineers, Vol. 97, No. SM5, May 1971a, pp. 711-731.

Poulos, H. G., "Behavior of Laterally Loaded Piles: II - Pile Groups," Proceedings, American Society of Civil Engineers, Vol. 97, No. SM5, May 1971b, pp. 733-751.

Reese, Lymon C., "Load versus Settlement for an Axially Loaded Pile," Proceedings, Part II, Symposium on Bearing Capacity of Piles, Central Building Research Institute, Roorkee, February 1964, pp. 18-38.

Reese, Lymon C., "Analysis of a Bridge Foundation Supported by Batter Piles," Proceedings, Fourth Annual Symposium on Engineering Geology and Soil Engineering, Moscow, Idaho, April 1966, pp. 61-73.

Reese, Lymon C., and Matlock, Hudson, "Behavior of a Two-Dimensional Pile Group Under Inclined and Eccentric Loading," Proceedings, Offshore Exploration Conference, Long Beach, California, 1966, pp. 123-140.

Reese, Lymon C., O'Neill, M. W., and Smith, R. E., "Generalized Analysis of Pile Foundations," Proceedings, American Society of Civil Engineers, Vol. 96, No. SM1, pp. 235-250, January 1970.

Sullivan, W. Randall, and Reese, Lymon C., "Documentation of Computer Program COM624," Geotechnical Engineering Center, Department of Civil Engineering, University of Texas at Austin, February 1980.

CHAPTER 11. STEP-BY-STEP PROCEDURE FOR DESIGN

The material presented in the preceding chapters is designed for self-study. An engineer can begin with Chapter 1 with a reading schedule and read directly through the manual. The worked examples can be checked and some of the exercises can be worked out.

If such a self-study program is elected, the guidelines that follow will serve to confirm the design procedures that are suggested. The procedures that are shown below may be modified to agree with the particular preferences of the designer. However, if some time has passed since the self-study or if the designer elects merely to scan much of the material that has been presented, the step-by-step procedures may prove to be useful.

1. A structural engineer and a geotechnical engineer should work together to establish the general nature of the problem and to cooperate as solutions are developed (Chapter 1).
2. The nature, magnitude, and direction of the various loadings on the pile should be found. The service load and design load, both axial and lateral, should be established (Chapter 1). Where there is uncertainty about the magnitude of the load, an upper-bound value and a lower-bound value may be used.
3. A pile should be selected for analysis (if not already done from considerations of axial loading) and the pile-head conditions should be considered, whether fixed, free, or partially restrained (Chapters 2, 4, 5, 6, and 7). The Broms method (Chapter 7) could prove useful if lateral load only controls design.
4. A check should be made to see whether or not any of the assumptions made in deriving the differential equation are violated (Chapter 2); if so, a change in the pile make-up should be considered.
5. All of the information on the soil properties at the site should be analyzed and a soil profile should be selected for design (Chapter 3). If there is uncertainty about the soil properties, upper-bound values and lower-bound values may

be selected. The importance of the various soil parameters may be understood by reference to the first part of Chapter 9.

6. Having at hand the loading, the pile geometry, and a soil profile, p-y curves can be developed according to procedures in Chapter 3. Or if Computer Program COM624 is available, the program may be used directly in design or the soil subroutines in the program may be used to generate p-y curves, a desirable step to give a better understanding of the method of computation.
7. Computer Program PMEIX (Appendix 5) can be used to obtain the bending stiffness of a reinforced concrete pile. The bending stiffness of other kinds of piles can be obtained from handbooks or from the elementary principles of mechanics.
8. Computer Program PMEIX (Appendix 5) can be used to compute the bending moment capacity of a reinforced concrete pile. The moment capacity of other kinds of piles can be obtained from handbooks or from elementary principles of mechanics. The case studies of piles in clay and in sand in Chapter 9 can provide guidance in performing Steps 7 and 8.
9. The engineer who has not made many computations or is making only infrequent computations should use the procedures in Chapter 6 to gain familiarity with the design process and to gain some insight into the particular design being done.
10. The input for Computer Program COM622 or Computer Program COM624 can be prepared. The best estimate of the important parameters can be made for small jobs and a series of solutions performed with increasing loads until a soil failure (excessive deflection) or a pile failure (excessive bending moment) is found. Only in rare cases should a soil failure be allowed, because a small increase in the length of a pile can lead to a sharp increase in ability to carry load.
11. If the job is large and if time allows for small jobs, parameter studies can be made using the upper-bound values and lower-bound values of soil properties (and possibly other variables) to gain additional insight into the possi-

ble range in the response of the pile. The computer solutions are inexpensive and especially so if results can be read directly from the screen of a terminal.

12. As a part of using the computer program as outlined in Steps 11 and 12, checks must be made to see that an appropriate increment length and a suitable closure tolerance are being employed (Chapter 5). The number of significant figures used in the internal computations of the computer must also be satisfactory (Appendix 3).
13. From the computer solutions in Steps 10 and 11, the pile being analyzed can be judged to be satisfactory or a new pile can be selected and the steps repeated. A specific design will result, yield pile diameter (or projected width), length, and bending capacity along the length of the pile. Further, information can be gained as to the most favorable way to connect the pile head to the superstructure.
14. In performing the computer solutions as outlined in Steps 10 and 11, the engineer should make use of the methods presented in Chapters 4, 6, and 7 to make approximate solutions and to make checks on computer runs so that confidence is developed in the solution techniques.
15. If the piles occur in groups, the methods shown in Chapter 10 should be employed. In some cases it is not necessary to make the detailed analyses presented in Chapter 10, but judgement can be used in making any necessary design modifications.
16. The methods presented in Chapter 8 should be employed to see that the piles that are selected using the concepts of soil-structure interaction are adequate from the standpoint of structural behavior.
17. A design office may have the same type of pile, say a steel bearing pile, to design in many instances in the same type of soil profile, say a sand with a high water table. A computer program, COM622 or COM624, can be used to develop design charts to allow preliminary designs, or final

designs in some cases, to be made rapidly. Such design charts are demonstrated in Chapter 7.

*U.S. GOVERNMENT PRINTING OFFICE: 1986--491-810/20705

FEDERALLY COORDINATED PROGRAM (FCP) OF HIGHWAY RESEARCH, DEVELOPMENT, AND TECHNOLOGY

The Offices of Research, Development, and Technology (RD&T) of the Federal Highway Administration (FHWA) are responsible for a broad research, development, and technology transfer program. This program is accomplished using numerous methods of funding and management. The efforts include work done in-house by RD&T staff, contracts using administrative funds, and a Federal-aid program conducted by or through State highway or transportation agencies, which include the Highway Planning and Research (HP&R) program, the National Cooperative Highway Research Program (NCHRP) managed by the Transportation Research Board, and the one-half of one percent training program conducted by the National Highway Institute.

The FCP is a carefully selected group of projects, separated into broad categories, formulated to use research, development, and technology transfer resources to obtain solutions to urgent national highway problems.

The diagonal double stripe on the cover of this report represents a highway. It is color-coded to identify the FCP category to which the report's subject pertains. A red stripe indicates category 1, dark blue for category 2, light blue for category 3, brown for category 4, gray for category 5, and green for category 9.

FCP Category Descriptions

1. **Highway Design and Operation for Safety**
   Safety RD&T addresses problems associated with the responsibilities of the FHWA under the Highway Safety Act. It includes investigation of appropriate design standards, roadside hardware, traffic control devices, and collection or analysis of physical and scientific data for the formulation of improved safety regulations to better protect all motorists, bicycles, and pedestrians.

2. **Traffic Control and Management**
   Traffic RD&T is concerned with increasing the operational efficiency of existing highways by advancing technology and balancing the demand-capacity relationship through traffic management techniques such as bus and carpool preferential treatment, coordinated signal timing, motorist information, and rerouting of traffic.

3. **Highway Operations**
   This category addresses preserving the Nation's highways, natural resources, and community attributes. It includes activities in physical maintenance, traffic services for maintenance zoning, management of human resources and equipment, and identification of highway elements that affect the quality of the human environment. The goals of projects within this category are to maximize operational efficiency and safety to the traveling public while conserving resources and reducing adverse highway and traffic impacts through protections and enhancement of environmental features.

4. **Pavement Design, Construction, and Management**
   Pavement RD&T is concerned with pavement design and rehabilititation methods and procedures, construction technology, recycled highway materials, improved pavement binders, and improved pavement management. The goals will emphasize improvements to highway performance over the network's life cycle, thus extending maintenance-free operation and maximizing benefits. Specific areas of effort will include material characterizations, pavement damage predictions, methods to minimize local pavement defects, quality control specifications, long-term pavement monitoring, and life cycle cost analyses.

5. **Structural Design and Hydraulics**
   Structural RD&T is concerned with furthering the latest technological advances in structural and hydraulic designs, fabrication processes, and construction techniques to provide safe, efficient highway structures at reasonable costs. This category deals with bridge superstructures, earth structures, foundations, culverts, river mechanics, and hydraulics. In addition, it includes material aspects of structures (metal and concrete) along with their protection from corrosive or degrading environments.

9. **RD&T Management and Coordination**
   Activities in this category include fundamental work for new concepts and system characterization before the investigation reaches a point where it is incorporated within other categories of the FCP. Concepts on the feasibility of new technology for highway safety are included in this category. RD&T reports not within other FCP projects will be published as Category 9 projects.